Université Catholique de Louvain

Secteur des Sciences de la Santé, Faculté de Médecine

Institut de Recherche Expérimentale et Clinique (IREC)

Pôle de Gynécologie

Shedding light on recruitment and differentiation of human theca interna cells

Parinaz Asiabi Kohneh Shahri

February 2021

Promoter: Prof. Christiani Andrade Amorim

Co-promoter: Prof. Marie-Madeleine Dolmans

Thesis submitted with a view to obtaining a doctoral degree (PhD) in Biomedical and Pharmaceutical Science

Faculty of Medicine

Université Catholique de Louvain

Jury

President:	**Professor Etienne Marbaix**
Promoter:	**Professor Christiani Andrade Amorim**
Co-promoter:	**Professor Marie-Madeleine Dolmans**
Members:	**Professor Christophe Pierreux**
	Professor Anne des Rieux
	Professor Alessandra Camboni
External members:	**Professor Susana M. Chuva De Sousa Lopes**
	Leiden University Medical Center
	Professor Johan Smitz
	Vrije Universiteit Brussel

To the Love of My Life, Kaveh

To My Beloved Mom & Dad

To My Dear Sister, Sannaz

To My Sweet Nephew, Arnia

To My Dear Nazanin & Payman

To My Family

Acknowledgments - سپاسگزاری

This PhD has been a long and exciting journey and a truly life-changing experience for me. It would not have been possible without the support and guidance I received from so many people both inside and outside the laboratory.

I would first like to say a huge thank you to my promoter, Professor Amorim, for her motivating, positive energy, kind smile, always being there, and all the help and encouragement she gave me over these last five years. Without her guidance and constant feedback, I would not be in this position.

Special thanks to my co-promoter, Professor Dolmans, for always supporting when I needed biopsies from the operating room. Without her kind help, it would not have been possible to conduct the necessary experiments.

My gratitude to Professor Marbaix, president of my PhD committee, for his support and help obtaining human ovarian blocks from the biobank and assessing immunostained slides, not to mention our scientific discussions in his calm, patient and humble manner.

I would also like to acknowledge and thank all the other members of my PhD committee, including Professor Pierreux, Professor des Rieux, Professor Camboni, Professor Smitz, and Professor M. Chuva De Sousa Lopes, for agreeing to follow my project and giving me invaluable advice and constructive criticism, all of which contributed significantly to improving my work.

Huge thanks to all my colleagues (past and present) for making me feel so welcome in our laboratory and filling my days with smiles, encouragement, and endless support.

I am grateful to have shared an office and become friends with Janice and Emi, enjoying our professional discussions, friendly chats, and joyful lunch together with so many laughs.

Thanks to Emna for her attention to detail in our office space, enhancing the atmosphere by bringing plants and installing new frames on the walls.

I am thankful to Saeed and Arezoo for their positive vibes, smiles, and always offering me coffee and cookies, essential in our line of work.

I am grateful to Olivier for being my friend, our joyful coffee times, and all his help over the years with different techniques, especially during lockdown.

Thanks to Dolores and Sarah for their kind help and support with immunostaining experiments from A to Z.

Thanks to Deborah for her kind help facilitating administrative work.

Thanks to Dora for her warm and friendly character and all her efforts to order and receive the required materials for experiments, as well as financial issues.

Thanks to Mira for all her patience with English corrections and instruction, our friendly chats during essential coffee breaks, and her kind smile.

Thanks to Camille for all the kindness she showed me and her positive energy.

Thanks to Thu for her characteristic politeness and understanding.

Thanks to our Italian girls, Luciana, Costanza, Rossella and Alice, for creating a warm Italian environment during lunch.

Thanks to Mercedes, Chiara, Diego, Guillaume, Javier, Renan, Ellen and Ana for the lively atmosphere and making me smile.

Thanks to Clara for her hard work on our joint project over one year of her master studies.

I would also like to thank Mustapha Najimi, Joachim Ravau and Jonathan Evraerts from PEDI, Ludovic D'Auria and Zakia Nasr from CEMO, and everyone from different laboratories and departments who helped me with their advice and practical endeavors to get one step closer to my objective.

Special thanks go to my friends, Afsaneh, Amin, Marie, Salim, Walid, Maria, Adriano, Luminita, Christina, Pantea, Saeed, Nassim, Forough and Mohi, who made me feel at home and were there for me whenever I needed them.

Last, but not least, to my family:

تقدیم به کاوه عزیزم که همراه و حامی همیشگیم تو مسیر زندگی مشترکمونی، به من باور داری و همواره من رو برای پیشرفت روزافزون تشویق می‌کنی. به پاس قدردانی از قلب پر از عشق و معرفتت که برای آینده‌ی هرچه بهتر و رنگی‌تر و قشنگترمون تلاش می‌کنی.

تقدیم به مامان و بابای عزیزم که کلام از ابراز احساسم به شما قاصره. از اینکه در تمام مراحل زندگی یار و پشتیبانم بودین، من رو باور دارین و بهترین‌هارو برای سلامتی و موفقیتم فراهم کردین بی‌نهایت سپاسگزارم و نتیجه این تلاش بزرگ زندگیم که درواقع ثمره‌ی تمام فداکاری‌ها و ازخودگذشتگی‌هاتونه رو تقدیم مهربونیاتون می‌کنم.

تقدیم به سناز عزیزم، که در سراسر زندگیم با دل پاک و پرمهرت از هیچ کوششی دریغ نکردی و همواره و در همه حال همراه و کمکم بودی و هستی، با تمام وجود دوست دارم.

تقدیم به شیرینکم، فرشته‌ی دوست داشتنیم، آرنیا، که با اومدنت هم باعث خوشحالی من شدی و هم دل مامان و بابا رو گرم کردی و نذاشتی جای خالی من اونارو از پا در بیاره.

تقدیم به نازنین و پیمان عزیزم که با تکیه به شما و کمک‌های بی دریغتون تونستم پا تو دنیای جدید بذارم و فصل تازه‌ای رو تو دفتر زندگیم شروع کنم. محبت‌هاتون رو هرگز فراموش نمی‌کنم.

تقدیم به تمام کسانی که دوسم دارن و همواره خواهان موفقیت و پیروزی من هستن.

Table of contents

List of abbreviations 8

Chapter 1: The transplantable engineered ovary 13

1.1 Transplantable engineered ovary to restore fertility in cancer patients 14

1.2 Transplantable engineered ovary concept 18

1.2.1 Isolation and purging of ovarian preantral follicles to ensure TEO safety 20

1.2.2 TEO physical structure 22

1.2.3 TEO biological compounds 28

Chapter 2: Human ovary and theca cells 33

2.1 Human ovary 35

2.1.1 Human ovary development 35

2.1.2 Folliculogenesis 40

2.2 Theca cells 46

2.2.1 Origin of theca steroidogenic (interna) cells 47

2.2.2 Theca cell differentiation 53

2.2.3 Structural and matrix-related functions of the theca layer 68

2.2.4 Vascular and immune cell functions in the theca layer 69

2.2.5 Endocrine function and theca interna cells 72

2.2.6 Theca externa 76

2.3 Two-cell, two gonadotropin theory 76

2.4 Theca cell fate 80

2.4.1 Ovulation and corpus luteum formation 80

2.4.2 Follicle atresia and theca cells 87

2.5 Markers for theca interna and luteal cells in human 89

2.5.1 Aminopeptidase-N (ANPEP / CD13) 89

2.5.2 Dipeptidyl peptidase IV (DPP IV/ CD26) 89

2.5.3 NOTCH1 90

2.5.4 Adipose differentiation-related protein (ADRP) 91
Chapter 3: Personal contribution, objectives, and results 93
3.1 Assessment of the steroidogenic pathway in human follicles..... 98
3.2 Investigation of the presence of a precursor theca cell population in human ovaries 115
3.4 In vitro differentiation of human theca cells 173
Chapter 4: Conclusions and perspectives 206
4.1 Conclusions 207
4.1.1 Assessment of the steroidogenic pathway in human follicles..... 207
4.1.2 Investigation of the presence of a precursor theca cell population in human ovaries..... 209
4.1.3 In vitro differentiation of human theca cells 211
4.2 Perspectives and future research 215
4.2.1 What is the origin of theca cells in the human ovary? 215
4.2.2 Can theca cells be differentiated in the transplantable engineered ovary?..... 218
I. References 219
II. Other publications during the thesis 279
i. First-author article 281
ii. Co-authored article 290
iii. Co-authored book chapter 298

Summary

For women and prepubertal girls with cancer, fertility restoration often becomes an essential concern after disease remission. Chemo/radiotherapy treatments can be very harmful to the ovaries. It often causes loss of endocrine and reproductive functions, leading to premature menopause and emotional distress. Ovarian tissue cryopreservation and transplantation have proved to be a promising technique to restore fertility in women and prepubertal girls who need immediate cancer treatment. However, transplantation of cryopreserved ovarian tissue is not safe for patients diagnosed with cancers with a high risk of ovarian metastasis, such as leukemia, neuroblastoma, and Burkitt lymphoma, due to the possible chance of reintroducing malignant cells present in the grafted tissue. As this could lead to the recurrence of the primary disease, ovarian tissue transplantation is not advised in these patients. To provide an alternative to restore endocrine and reproductive functions in these patients, several research groups worldwide have been working on developing a transplantable engineered ovary (TEO). Different TEO prototypes have successfully demonstrated the feasibility of this strategy. Studies have reported the restoration of both endocrine and reproductive functions in a murine model with the production of healthy pups and ovarian hormones. However, developing a TEO for women has shown to be much more challenging. This is mainly due to our lack of knowledge of human ovaries.

Nevertheless, promising results have been obtained in the three main requirements to assemble a TEO: safe isolation of a large number of viable preantral follicles and TEO physical structure and biological compounds. Our group has recently optimized a good manufacturing practice procedure that safely isolates a large number of viable preantral follicles from surrounding malignant cells. Regarding the TEO physical aspect, several hydrogels have been tested to encapsulate and graft isolated follicles. Among them, fibrin was shown to be the most promising one. Finally, concerning TEO biological compounds, similar to the natural ovary, endothelial cells should be present in the TEO to promote vascularization, and stromal cells are equally necessary to synthesize extracellular matrix and bioactive factors.

Moreover, some of these cells will be recruited to differentiate into theca cells, which are essential during folliculogenesis and hormone production. While the previous studies from our group have demonstrated that grafting of isolated endothelial and stromal cells in the TEO promoted the formation of an ovarian-like tissue, with vascularization throughout the graft and synthesis of the extracellular matrix, we were not yet able to observe the differentiation of theca cells in our prototypes. Actually, due to the lack of knowledge and access to the source of theca cells, we do not have much information on the recruitment and differentiation of theca cells in human ovaries, and we cannot, therefore, predict if or how this process will occur in the TEO. Hence, my thesis's overall goal is to shed light on this intriguing cell population of the ovarian follicle. To this end, I have focused on the three following issues:

1. Investigate the steroidogenic pathway in human follicles: markers to be used in subsequent studies

This study aimed to characterize human theca cells at different stages of follicle development in relation to expression and quantification of steroidogenic enzymes (steroidogenic acute regulatory protein (StAR), cytochrome P450 11A1 (CYP11A1), cytochrome P450c17 (CYP17A1), 3-beta-hydroxysteroid dehydrogenase I (HSD3B1), and 3-beta-hydroxysteroid dehydrogenase II (HSD3B2), lipid storage marker (adipose differentiation-related protein (Perilipin-2)) and luteinizing hormone receptor levels. The follicle growth stage was considered to ascertain temporal patterns and elucidate the sequence of their expression throughout folliculogenesis in the human ovary. Our results showed a noticeable elevation in enzymes involved in the steroidogenic pathway of theca cells during folliculogenesis, evidenced by their coordinated action in area-covered and expression intensity. This study, conducted for the first time on human ovarian tissue, contributes to localizing and quantifying key steroidogenic proteins' expression at both intracellular and tissue levels. To the best of our knowledge, our study showed the specificity of the steroidogenic pathway in the human ovary for the first time. Apart from an obvious need to identify basic mechanisms of action, clarifying this cascade's workings in human tissue would promote the further advancement of theca cell differentiation experiments to support the creation of technologies to benefit females healthy and quality of life. Moreover, our findings may help unveil pathological conditions, such as androgen-secreting tumors of the ovary

and other disorders associated with theca cells in patients with polycystic ovary syndrome.

2. Searching for a population of precursor theca cells in human ovaries

While the origin of theca cells remains unclear in human ovaries, studies in animal models show different hypotheses. In mice, studies have identified a population of precursor theca cells in neonatal ovaries. These cells express glioma-associated oncogene homolog1 (GLI1), GLI3, and protein patched homolog 1 (PTCH1) protein, while differentiated theca cells express GLI1, GLI2, and LH receptor. In a cascade of events that start with the synthesis of growth differentiation factor 9 (GDF9) by the oocyte of primary follicles, these precursor theca cells are recruited and differentiated into theca cells. On the other hand, studies on cow and goat ovarian cells indicate that there are no precursor theca cells in ovaries from large animal species. Indeed, in vitro experiments have shown that under the stimuli of granulosa cells, ovarian stromal cells can easily differentiate into theca cells. In order to assess if precursor theca cells can be found in human ovaries, we decided to evaluate the hedgehog-GLI pathway by studying GDF9, Indian (IHH), desert (DHH) and sonic hedgehog (SHH), PTCH1, GLI1, GLI2, and GLI3 proteins in human fetal, prepubertal, reproductive-age and postmenopausal ovaries. Our results showed that all these proteins are expressed in granulosa and oocytes from follicles in all stages of development in fetal, prepubertal, and reproductive age ovaries.

Interestingly, they are expressed in stromal cells from reproductive age and postmenopausal ovaries as well. While we can find this pathway in human ovaries, taken into account that the majority of cells in the ovarian stroma are GLI1-positive, we find questionable that precursor

theca cells represent the large cell population in the human ovary. We hypothesize that since HH signaling regulates several processes in the cells, such as proliferation, differentiation, and fate determination, it is expected that ovarian cells express GLI proteins, including the ones that will differentiate into theca cells. Based on our findings, we can therefore conclude that either there is a subpopulation of precursor theca cells in human ovaries, but we do not know their specific markers yet, or similar to cows and goats, all ovarian stromal cells are able to differentiate into theca cells.

3. In vitro differentiation of theca cells

Considering our results in the previous study, we decided to test if, similar to other large animal species, human ovarian stromal cells can differentiate into theca cells. Isolated stromal cells from postmenopausal cortical ovarian tissue samples were in vitro cultured using four different conditions: basic medium (BM), containing DMEM-F12, knockout serum and antibiotics (G1); enriched medium (EM), composed of BM with growth factors (GFs) and hormones (G2); EM with cells seeded onto a permeable collagen membrane (G3), and EM with co-culture of stromal and granulosa cells separated by a permeable collagen membrane (G4). To confirm cell differentiation, genes and proteins involved in the theca cell steroidogenic pathway were assessed. Moreover, three other markers, CD13 (specific marker for theca interna cells), CD26, and NOTCH1 (involved in luteinization process), were used to aid cell characterization after in vitro culture. Finally, the ultrastructure of theca

cells and hormone production were assessed. Based on gene and protein expression patterns for proteins involved in the theca steroidogenic pathway, one could conclude that almost all ovarian cells can differentiate into theca cells, which would be in concordance with the studies in cow and goat stromal cells. However, the lack of CD13 immunostaining in G1 and most cells in the other groups show that after in vitro culture, the vast majority of cells become steroidogenic, but less than half of them are theca cells. Ultrastructural analysis and the presence of CD13-positive cells confirmed that the theca cell population accounted for 21%-43% of differentiated cells in G2, G3, and G4.

Interestingly, differentiation did not stop once cells were converted into theca cells: similarly to what takes place in the human ovary, this process advances until theca cell luteinization and small luteal cell senescence, as evidenced by transmission electron microscopy analysis in G3 and G4. With the help of collagen inserts in G3 and G4, which improved cell attachment and proliferation and, consequently, their communication, theca cell differentiation was faster, so small luteal cells could be detected. The addition of a granulosa cell line accelerated this process further, as older luteal cells with aggregates of luteal debris were also observed in G4. In conclusion, we showed that human theca cells could differentiate in vitro under the influence of different growth factors and hormones. Our results appear to indicate the presence of precursor theca cells in human ovaries. More interestingly, such cells remain even after menopause. We believe that this study is a great step forward in understanding theca cell ontogenesis in human ovaries.

List of abbreviations

2D: two-dimensional

3D: three-dimensional

ADAM: a disintegrin and metalloproteinase

ADAMTS1: a disintegrin and metalloproteinase with thrombospondin motifs 1

ADRP: adipose differentiation-related protein /perilipin 2

AMH: Anti-Müllerian Hormone

AML: acute myeloblastic leukemia

AR: androgen receptor

bFGF: basic fibroblast growth factor

BM: basic medium

Bmpr1: bone morphogenetic protein receptor, type 1

BMPs: bone morphogenic proteins

BRCA1: breast cancer type 1

BRCA2: breast cancer type 2

cAMP: cyclic adenosine monophosphate

CD13: aminopeptidase N

CD26: dipeptidyl peptidase-4 (DPP4)

CYP11A1: cholesterol side-chain cleavage cytochrome P450

CYP17A1: 17α-hydroxylase or cytochrome P450 17A1

DHEA: dehydroepiandrosterone

DHH: desert hedgehog

DHT: dihydrotestosterone

DLL1: delta-like protein 1

DLL4: delta-like protein 4

ECM: extracellular matrix

EGF: epidermal growth factor

EGFP: excitation and Emission of Green Fluorescent Proteins

ELISA: enzyme-linked immunosorbent assays

EM: enriched medium

ERK1/2: extracellular signal-regulated protein kinase ½

ESR1: estrogen receptor

FACS: fluorescence-activated cell sorting

FIGLA: folliculogenesis-specific basic helix-loop-helix

Foxl2: forkhead box protein L2

FSH: follicle-stimulating hormone

GDF: growth differentiation factor

GMP: good manufacturing practice

GnRH: gonadotropin-releasing-hormone

GREL: gonadal ridge epithelial-like

HCG: human chorionic gonadotropin

HDL: high-density lipoprotein

HGF: hepatocyte growth factor

HH: hedgehog

HHIP: hedgehog interacting protein

HIF1α: hypoxia-inducible factor 1-α

HPO: hypothalamus-pituitary-ovarian

HSD3B: 3-beta-hydroxysteroid dehydrogenase

HSL: hormone-sensitive lipase

IGF: insulin-like growth factor

IHC: immunohistochemistry

IHH: Indian hedgehog

IL: interleukin

IVF: in vitro fertilization

KGF: keratinocyte growth factor

KL: KIT Ligand

LDL: low-density lipoprotein

LH: luteinizing hormone

LHR: LH receptor

LIF: Leukemia inhibitory factor

MAPK: mitogen-activated protein kinase

NOTCH1: Notch homolog 1, translocation-associated (Drosophila)

PCOS: polycystic ovary syndrome

PEG: polyethylene glycol

PKA: protein kinase A

POI: premature ovarian insufficiency

PTCH1: protein patched homolog 1

PTEN: phosphatase and tensin homolog

qPCR: quantitative real-time polymerase chain reaction

RGD: Arg-Gly-Asp

SHH: sonic hedgehog

SI: staining index

SMAD: small mothers against decapentaplegic

SMO: smoothened

StAR: steroidogenic acute regulatory protein

TEM: transmission electron microscopy

TEO: transplantable engineered ovary

TGF-β: transforming growth factor beta

VCAM1: vascular cell adhesion protein 1

VEGF: vascular endothelial growth factor

Chapter 1:

The transplantable engineered ovary

1.1 Transplantable engineered ovary to restore fertility in cancer patients

Gonadotoxicity caused by chemotherapy is almost irreversible. Histologic sections of the exposed ovary to cytotoxic drugs presented a spectrum of changes ranging from decreased numbers to complete absence of follicles (Warne *et al.*, 1973). Chemotherapy and radiotherapy may severely affect ovarian reserve by damaging the primordial follicle population and reducing ovarian reserve (Fleischer *et al.*, 2011; Gracia *et al.*, 2012; Meirow *et al.*, 2010; Wallace *et al.*, 2005) (Figure 1 and Table 1). Premature ovarian insufficiency is a prominent consequence of exposure of the female gonad to chemo- and radio-therapeutic drugs (Chapman, 1982; Rivkees and Crawford, 1988; Torrealday *et al.*, 2017; Van Dorp *et al.*, 2016). As the cancer cure rate for childhood and adolescent patients has currently reached almost 80% (Lambert *et al.*, 2018; Miller *et al.*, 2016), protecting their fertility and, therefore, their future quality of life should be a major issue to be considered (Bedaiwy, 2005). The 2004 bioethics law (article L2141-11) mandates that "all patients whose medical care is likely to impair fertility, or whose fertility risks being prematurely altered, should benefit from the collection and preservation of their gametes or germinal tissues, with a view to the subsequent realization of Medically Assisted Procreation or for the preservation and restoration of their fertility" (de Lambert *et al.*, 2018).

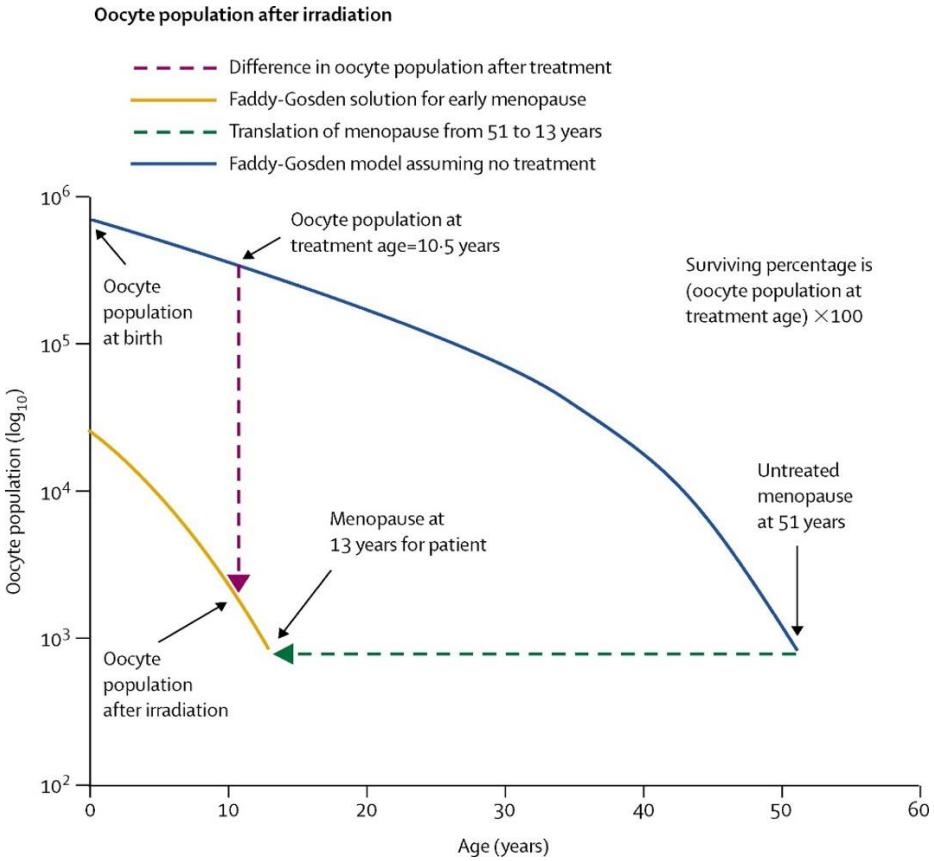


Figure 1. Faddy-Gosden model demonstrates the size of the oocyte pool from birth to menopause (estimated at 51 years). The graph shows an estimation of survived follicles for a patient treated at age 10·5 years with whole-body irradiation (14·4 Gy) who developed ovarian failure at age 13 years. *From Wallace et al. (2005).*

Table 1. Risk of subfertility after chemo- and/or radiotherapy treatment for common cancers in childhood and adolescence. *Adapted from Wallace et al. (2005).*

High risk (>80%)	Medium risk	Low risk (<20%)
Total body irradiation	Acute myeloblastic leukemia	Acute lymphoblastic leukemia
Pelvic radiotherapy	Cerebral tumor > 24 Gy	Wilms' tumor
Bone-marrow transplantation	Non-Hodgkin lymphoma	Soft-tissue sarcoma: stage I
Hodgkin's disease: treatment with alkylating-drugs	Hodgkin's lymphoma: without alkylating agents	Germinal cell tumor (no radiation)
Ewing's sarcoma: metastatic	Ewing's sarcoma: no metastases	Retinoblastoma
Soft-tissue sarcoma: stage IV (metastatic)	Osteosarcoma	Brain tumor: surgery only, cranial irradiation 24 Gy
	Neuroblastoma	
	Hepatoblastoma	

The fertility preservation technique choice depends on the patient's age, ovarian reserve, the urgency of treatment, and marital status. It should be co-decided by the reproductive endocrinologist, oncologist, the patient, her partner, and parents in case of being a child (Hyman and Tulandi, 2013). Nowadays, various fertility preservation techniques are available, such as embryo or oocyte vitrification, oophoropexy, and ovarian tissue cryopreservation. While most cancer patients can choose among these strategies, prepubertal patients and women who cannot delay the start of their chemo- or radiotherapy have to rely on ovarian tissue cryopreservation and transplantation (Donnez and Dolmans, 2017). Despite successful outcomes reported with this approach, including more than 150 live births to date (Donnez and Dolmans, 2017), it cannot be applied to all cancer survivors. Indeed, there are some types of cancer where malignant cells may be present in the ovaries,

which is a legitimate concern (Greve *et al.*, 2012; Meirow *et al.*, 2008; Rosendahl *et al.*, 2010). Dolmans *et al.* (2013) and Sonmezer, Oktay (2004) classified malignant diseases into three categories according to the risk of ovarian involvement (Table 2). Patients with leukemia, neuroblastoma ad Burkitt lymphoma were found to have the highest risk of metastasizing to the ovaries, so transplantation of ovarian tissue after disease remission is not advisable for these patients due to the possible chance of reimplanting malignant cells after cancer treatment that could cause the recurrence of the primary disease. Studies performed by our group have shown that similarly to ovarian cells and preantral follicles, malignant cells are cryoresistant and can spread in the host after the grafting procedure (Dolmans *et al.*, 2010). While ovarian tissue cryopreservation has been advised to these patients, we do not yet have alternatives to restore their fertility. In order to help these cancer survivors, our team has been working on the development of a transplantable engineered ovary (TEO).

Table 2. Risk of ovarian metastasis according to the cancer type. *Adapted from Dolmans et al. (2013).*

High risk	Leukemia
	Neuroblastoma
	Burkitt lymphoma
Moderate risk	Breast cancer stage IV
	Infiltrating lobular subtype
	Colon cancer
	Adenocarcinoma of the cervix
	Non-Hodgkin lymphoma
	Ewing sarcoma
Low risk	Breast cancer stage I-III
	Infiltrating ductal subtype
	Squamous cell carcinoma of the cervix
	Hodgkin's lymphoma
	Osteogenic carcinoma
	Nongenital rhabdomyosarcoma
	Wilms tumor

1.2 Transplantable engineered ovary concept

TEO's main goal is to replace the natural ovary, allowing the production of fertilizable mature oocytes and secretion of hormones. To assemble a functional TEO, three main requirements must be considered: (a) safe isolation of thousands of viable preantral follicles; (b) development of a

three-dimensional (3D), biodegradable and biocompatible matrix to encapsulate and transplant ovarian follicles and cells, and (c) incorporation of different cell populations present in the ovary.

TEO should be prepared with the patient's follicles and cells in order to avoid immunological rejection. In practice, once the patient is diagnosed with cancer, she would have a biopsy of her ovary removed for cryopreservation. Once in remission, the patient would have a second biopsy removed for isolation of ovarian cells. After cancer treatment, Procuring cells would guarantee that all malignant cells were destroyed, and they would not be accidentally present in the TEO. At this point, the cryopreserved tissue would be thawed for follicle isolation. Finally, isolated cells and follicles would be encapsulated by the 3D matrix, forming the TEO, which will then be transplanted to the patient (Figure 2).

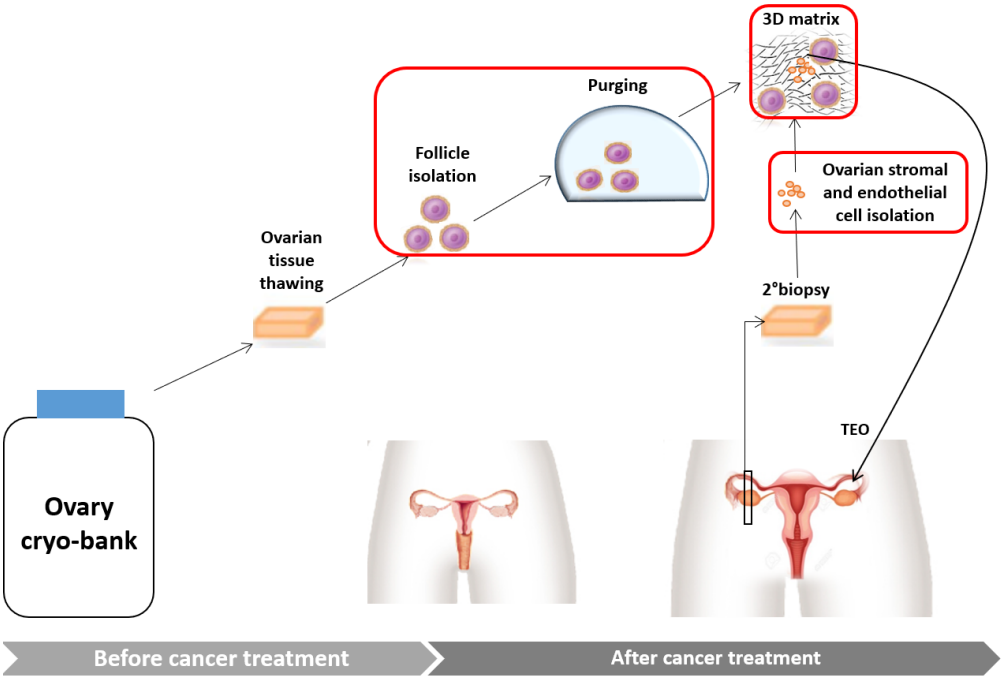


Figure 2. TEO grafting containing isolated preantral follicles from frozen-thawed ovarian tissue and isolated ovarian cells from fresh ovarian biopsies. *Drawing by M. C. Chiti.*

1.2.1 Isolation and purging of ovarian preantral follicles to ensure TEO safety

The first essential step for TEO development is the safe isolation of at least one thousand viable ovarian preantral follicles. This procedure allows the separation of intact follicles from the surrounding ovarian stroma thanks to the presence of a thin layer of the basement membrane, which serves to delimit each follicle and thereby maintain its cell composition and spherical architecture (Irving-Rodgers *et al.*, 2009). Several mechanical and or enzymatic techniques have been developed to isolate human preantral follicles from their surrounding extracellular

matrix (ECM) (Dolmans *et al.*, 2006; Lierman *et al.*, 2015; Schmidt *et al.*, 2018; Telfer *et al.*, 2008). However, due to the nature of the human ovarian cortex, where most primordial follicles reside, the better effective way of obtaining a high number of fully isolated and viable follicles is usually based on a combination of mechanical and enzymatic tissue digestion. Indeed, combining these two methods, our group has developed an isolation protocol that can be personalized according to the stiffness of the ovarian tissue sample, which in turn has shown to increase the number of isolated viable follicles (Chiti *et al.*, 2017b). It is important to consider that in young girls, the medullary layer should also be used in the isolation procedure as small preantral follicles can also be found in this inner ovarian compartment (Kristensen *et al.*, 2011).

Before contemplating clinical application, experimental studies have to provide robust evidence of TEO safety, and the first step is follicle isolation. Indeed, during isolation, it is possible that malignant cells present in the ovarian tissue are isolated together with follicles and be present in the digested suspension. Although all early-stage ovarian follicles are externally delimited by the basal lamina that physically separates them from the surrounding ovarian stroma, we cannot exclude potential contamination by cancer cells. Indeed, in experimental practice, when ovarian follicles are isolated from a suspension of digested ovarian tissue, some residual malignant cells may remain attached to the basement membrane or be inadvertently picked up along with the follicles and then grafted back to the patient. For this reason, studies were recently performed in an attempt to ascertain the safety of

the procedure (Mouloungui *et al.*, 2018; Soares *et al.*, 2015b; Soares *et al.*, 2015d). Soares *et al.* (2015b) demonstrated that despite follicle pick-up from an ovarian tissue suspension previously contaminated with a leukemia cell line being deemed unsafe, a simple follicle purging step is based on three consecutive washes in saline solution was enough to remove any contaminating cells. However, the interaction between ovarian follicles and naturally, resident leukemia cells may differ from that in artificially contaminated suspensions of isolated follicles. Therefore, our group performed a similar study using ovarian tissue from leukemia patients and demonstrated the safety of our follicle isolation procedure (Soares *et al.*, 2017).

1.2.2 TEO physical structure

For successful follicle development, contact between the oocyte and surrounding granulosa cells is essential (Murray *et al.*, 1998; Reynaud *et al.*, 2000), as disruption in the connection between these cells would lead to disharmonic growth and differentiation of somatic and germ cells (Picton and Gosden, 2000). In order to avoid failure in the metabolic link between granulosa cells and oocytes, follicles need to maintain their 3D structure (Xu *et al.*, 2006). Furthermore, follicles recruit cells and vessels to support their development that changes from around 30 μm up to 8 mm. Hence, TEO should be stiff enough to maintain follicle spherical shape and biodegradable to allow exponential growth of follicles, the formation of vessels, and proliferation of surrounding cells. With these

features in mind, different synthetic and natural polymers have been tested to develop a TEO 3D matrix (Table 3).

Table 3. Polymers were tested as the TEO matrix.

Polymer		Advantages	Disadvantages
Synthetic polymer	Polyethylene glycol (PEG)	• Biocompatible. • Degradation rate, porosity, and elasticity can be tailored. • Production in large amounts.	• Degradation products can be toxic to cells. • Organic solvents are necessary for PEG synthesis, which may trigger a negative response in the graft after transplantation.
Natural polymers	Alginate Collagen Fibrin Plasma clot Decellularized ECM	• Biocompatible. • Biodegradable. • Right environment to support cell adhesion, migration, proliferation, and differentiation.	• Insufficient mechanical strength. • Complex structure. • Not easily modified. • Control of polymer degradation rate is challenging.

1.2.2.1 Synthetic polymers used as TEO matrix

Synthetic polymers have been extensively applied in regenerative medicine, as they have several advantages (Lin *et al.*, 2015), including a long shelf life (Dhandayuthapani *et al.*, 2011). Contrarily, it is important to mention that these polymers can degrade into products that may be toxic at high concentrations for the body, such as acids, which could cause local inflammation (Seal *et al.*, 2001; Yoon and Fisher, 2009) and negatively influence the graft outcomes.

PEG is the most commonly used synthetic polymer. It is a linear-chained polymer consisting of a simple oxygen-carbon-carbon repeating unit (Yoon and Fisher, 2009). PEG can be copolymerized with other numerous polymers to create matrices with higher degradation rates or adhesion properties (Tessmar and Göpferich, 2007). PEG hydrogels, modified with vinyl sulfone groups crosslinked by Michael-type addition

(PEG-VS), was used by Kim *et al.* (2016) to investigate the survival and development of murine isolated follicles. PEG gels were modified with the adhesion tripeptide arginylglycylaspartic acid (Arg–Gly–Asp) (RGD), the most common peptide motif responsible for cell adhesion to the ECM, and protease-sensitive peptide N-[3-(2-Furyl) acryloyl]-L-leucyl-glycyl-L-prolyl-L-alanine (Leu–Gly–Pro–Ala), a synthetic substance resembling the primary structure of collagen. Primordial follicles were encapsulated and transplanted to mice, and after 30 days, lower concentrations of follicle-stimulating hormone (FSH) and antral follicles were observed. Moreover, hydrogel controlled proteolytic degradation allowed graft remodeling and neovascularization (Kim *et al.*, 2015). However, when this matrix was tested for encapsulation of isolated human preantral follicles, no follicles were found in the hydrogels after seven days of in vitro culture (Amorim, unpublished data).

1.2.2.2 Natural polymers used as TEO matrix

Natural polymers were the first tested biodegradable biomaterials in clinical settings (Nair and Laurencin, 2007). These polymers have some advantages as they are biocompatible and biodegradable and have superior interaction with cells to support cellular adhesion, migration, proliferation, and differentiation (Yoon and Fisher, 2009). Conversely, natural polymers usually lack sufficient mechanical strength, which causes difficulty in handling them due to their complex structure and is not easily modified. Additionally, they are enzymatically biodegradable,

and controlling their degradation rate is challenging (Lin *et al.*, 2015; Yoon and Fisher, 2009).

Collagen: This hydrogel has been widely used in several tissue engineering applications. It is a biocompatible natural polymer with low immunogenicity and can be used in combination with many other molecules (Parenteau-Bareil *et al.*, 2010; Ramshaw *et al.*, 2009), what makes it an attractive biomaterial for TEO construction. Moreover, the ovarian cortex is rich in collagen, and a TEO matrix made of this polymer would be similar to the native organ. Telfer *et al.* (1990) tested collagen to encapsulate and graft isolated mouse follicles, showing complete folliculogenesis and recovery of oocytes for in vitro fertilization (IVF). However, to the best of our knowledge, collagen was never used to encapsulate and transplant human isolated follicles.

Alginate: Alginate is a natural polysaccharide exhibiting excellent biocompatibility and biodegradability. It has many different applications in the field of bio- and regenerative medicine. It is easily processable for applicable three-dimensional scaffolding materials such as hydrogels, microspheres, microcapsules, sponges, foams, and fibers. Alginate-based biomaterials can be used in tissue engineering as drug delivery systems and cell carriers (Sun and Tan, 2013). Alginate has been shown to preserve the 3D structure of isolated follicles, enabling their growth in vitro (Amorim *et al.*, 2009) and in vivo (Vanacker *et al.*, 2014). While this hydrogel has successfully supported the survival and development of isolated mouse follicles after transplantation (Vanacker *et al.*, 2014), its degradation rate was very slow, which possibly had a negative impact on

vascularization inside the matrix, which was limited to the matrix periphery (Amorim, 2016).

Plasma clot: After obtaining successful results using plasma clot to graft mouse isolated follicles (Carroll and Gosden, 1993; Gosden, 1990), this hydrogel was tested for human counterparts (Dolmans *et al.*, 2007; Dolmans *et al.*, 2008). Our group showed that human preantral follicles could survive and grow up to the antral stage in plasma clots (Dolmans *et al.*, 2007; Dolmans *et al.*, 2008). Despite these promising results, this matrix is difficult to handle and has a fast degradation rate, leading to follicle loss. Moreover, their unknown composition does not allow consistent results.

Fibrin: This hydrogel is made of purified allogeneic fibrinogen and purified thrombin (Ahmed *et al.*, 2007). Fibrin formulations have been extensively used in the last decade for a variety of tissue engineering applications in adipose (Cho *et al.*, 2006), cardiovascular (Birla *et al.*, 2005; Mol *et al.*, 2005), ocular (Alaminos *et al.*, 2006; Suuronen *et al.*, 2006), muscular (Nieponice *et al.*, 2007; Rowe *et al.*, 2007), hepatic (Bruns *et al.*, 2005; Sun *et al.*, 2004), skin (Balestrini and Billiar, 2006; Hojo *et al.*, 2003), cartilage (Eyrich *et al.*, 2007; Mesa *et al.*, 2006), and bone (Chung *et al.*, 2007; Weinand *et al.*, 2006) tissues. Fibrin hydrogels are able to promote angiogenesis (Dietrich and Lelkes, 2006; Liu *et al.*, 2007), and different combinations of fibrinogen and thrombin concentrations have shown to influence the morphology and rigidity of the fibrin network, which in turn affects cell survival and proliferation (Ho *et al.*, 2006; Sese *et al.*, 2011). Unlike alginate hydrogels, the fibrin

matrix showed vascularization throughout the grafts (Vanacker *et al.*, 2014). While Smith *et al.* (2014) used higher concentrations of fibrinogen and thrombin to graft isolated murine preantral follicles inside the ovarian bursa for three weeks, other studies (Chiti *et al.*, 2017c; Chiti *et al.*, 2015; Luyckx *et al.*, 2014; Luyckx *et al.*, 2013) reported that two fibrin compositions with low concentrations of fibrinogen and thrombin showed the greatest distribution of mouse ovarian cells, follicular survival, and growth during in vitro and in vivo studies in the mouse. However, it has been shown later that a low concentration of fibrinogen and thrombin in a fibrin-based matrix might lack adequate porosity and stiffness to support primary-primordial human isolated follicles (Paulini *et al.*, 2016). In a study of isolated human follicles encapsulated into different fibrin and thrombin formulations, Chiti *et al.* (2018) suggested the concentration of 50 mg/ml fibrinogen with 50 UI/ml thrombin based on fiber thickness, porosity, and rigidity and follicle recovery rate for the fibrin-based scaffold for TEO.

Decellularized ovarian ECM: The main advantage of this matrix is that it consists entirely of ECM molecules, which are preserved in their native ultrastructural architecture. Laronda *et al.* (2015) used decellularized bovine and human ovarian tissue to graft primary mouse ovarian cells and showed after 2-4 weeks of grafting; these recellularized matrices were able to initiate puberty in ovariectomized mice. Recently, a human decellularized ovarian scaffold based on a sodium lauryl ester sulfate (SLES)-the treated process was established by (Hassanpour *et al.*, 2018). They suggest an optimized protocol that acts as a biomimicry of the

natural ovarian niche and can be an ideal scaffold to reconstruct the ovary. Another study using 0.1% of sodium dodecyl sulfate for 18-24 hours to decellularize human ovarian tissue provided decellularized ovarian ECM able to support the survival of human follicles and growth of murine follicles in vivo as well as recellularization of human ovarian stromal cells and viability of isolated human preantral follicles in co-culture in vitro (Pors *et al.*, 2019). Another strategy to take advantage of the biochemical cues of ovarian ECM is its application in the form of decellularized hydrogels, which also retain the biological activity of the original tissue and can therefore support tissue regeneration (Badylak *et al.*, 2011). Using bovine ovaries, our group developed a decellularized ovarian ECM hydrogel that supported the viability of isolated mouse follicles after ten days of *in vitro* culture (Chiti *et al.*, 2016). It remains, however, to confirm these results with grafting of isolated human follicles.

1.2.3 TEO biological compounds

Although the main players involved in TEO are isolated preantral follicles, the presence of ovarian cells is fundamental to achieving complete folliculogenesis and improving vascularization and ovarian regeneration (Figure 3).

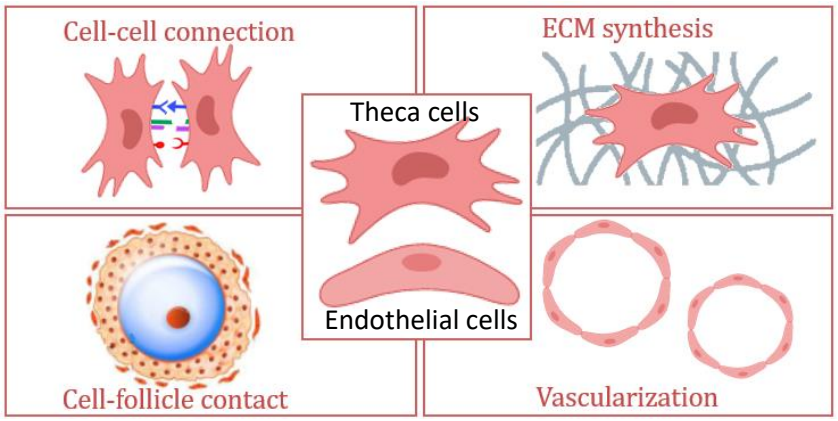


Figure 3. Isolated ovarian and endothelial cells to be added in the TEO and their role after TEO transplantation. *Drawing by C. A. Amorim.*

1.2.3.1 Endothelial cells

Similar to other engineered tissues and organs, for TEO survival, vascularization is essential to supply oxygenation and nutrients and remove metabolic waste. When follicles and or cells are grafted embedded in a 3D matrix, oxygenation occurs through simple diffusion, which may be confined by the construct (Bergmann and West, 2008). Oxygen and nutrient deprivation may lead to cellular damage and apoptosis, decreasing the TEO success rate and life span. Therefore, it is necessary to ensure fast vascularization throughout the implant to support follicle survival and development. To this end, different tissue engineering strategies can be applied. One of them is the addition of isolated endothelial cells in the TEO. Previous studies from our group showed that when stromal and endothelial cells are isolated from ovarian tissue biopsies and xenografted to immunodeficient mice,

vascularization in the 3D matrices is superior compared to transplantation of stromal cells alone (Dath *et al.*, 2011) (Figure 4).

Moreover, Soares *et al.* (2015c) demonstrated that the proportion of endothelial cells in the TEO prototype is positively correlated to vascularization rate. Comparing cells isolated from samples of the ovarian cortical or medullary layer before or after freezing and thawing procedures, these authors reported that stromal and endothelial cell isolation from fresh medulla biopsies resulted in a greater cell yield, viability, and endothelial cell number. Moreover, the transplantation of matrices containing these cells resulted in higher vascularization (Soares *et al.*, 2015c). This study suggests that ovarian biopsies containing both cortical and medullary layers are an optimal source of stromal and endothelial cells for TEO. The addition of this latter cell population is an efficient strategy to promote vascularization in the grafts without resorting to more complicated tissue engineering alternatives.

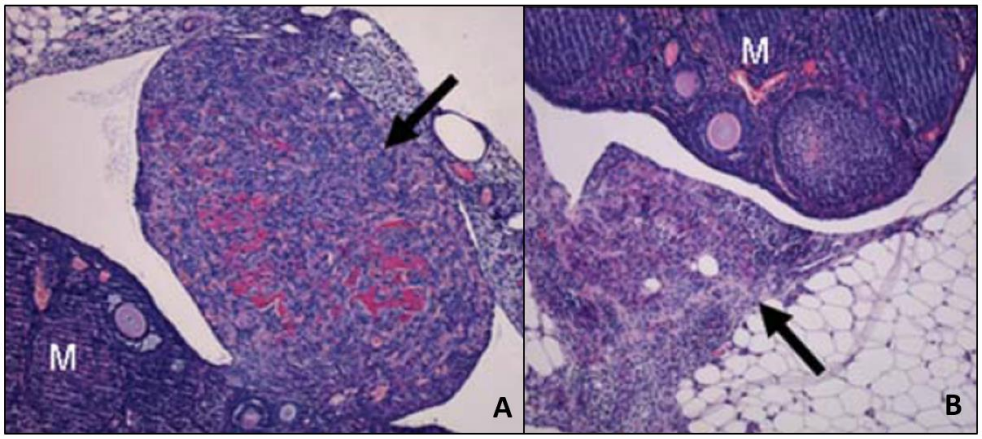


Figure 4. TEO histological representation with and without endothelial cells. (A) Plasma clot containing isolated stromal and endothelial cells with a well-organized ovary-like tissue structure and visible revascularization. (B) Plasma clot containing only stromal cells showing reduced size and low vascularization. (M) Mouse ovary. The black arrows indicate the localization of the grafted clot. *Adapted from Dath et al. (2011).*

1.2.3.2 Stromal cells

As previously mentioned, ovarian stromal cells may be retrieved from a second fresh ovarian biopsy after the patient is in cancer remission, ensuring the lack of contamination with malignant cells and avoiding the deleterious effect of freezing-thawing procedures (Keros *et al.*, 2009). On the other hand, this strategy has raised the concern of a potential negative impact of chemo- and or radiotherapy on survival and proliferation of ovarian stromal cells (Meirow *et al.*, 2007). To address this question, Soares (2015a) evaluated ovarian tissue biopsies from patients subjected to chemotherapy. Stromal cells were isolated and compared to their counterparts from healthy women who never

underwent any cancer treatment. Results showed that survival and in vitro proliferation rates were not affected by previous chemotherapy (Soares, 2015a). Therefore, we can conclude that fresh ovarian tissue obtained from patients in cancer remission may be considered a valid source of ovarian cells, without compromising their function.

Stromal cells are essential in the TEO as they have been shown to increase matrix degradation and form an ovary-like structure after grafting (Dath *et al*., 2011), creating a natural environment for follicles. Moreover, these cells play an essential role in folliculogenesis. They synthesize numerous factors that are involved in primordial-to-primary follicle transition (Knight and Glister, 2006). After activation and initial growth to the primary stage, follicles secrete factors to recruit cells from the ovarian stroma to differentiate into theca cells (Honda *et al.*, 2007; Orisaka *et al.*, 2006). Cells from theca externa and interna layers are essential during follicle development. They offer structural support to growing preantral follicles and provide androstenedione and testosterone for estrogen biosynthesis of granulosa cells. Therefore, for TEO to succeed, theca cell recruitment and differentiation should occur in the constructs. However, we do not know if ovarian cells after isolation and transplantation would have the same ability to differentiate into theca cells. There is not much information about theca cell ontogenesis in human ovaries as they only appear in fertile ovaries from the late secondary follicle stage for a specific period of time.

Chapter 2:

Human ovary and theca cells

2.1 Human ovary

Human ovaries have two main functions: support of oocyte development and secretion of hormones. Theca cells are essential to the ovary as they are part of both processes. However, despite such an important role, these cells have remained "the forgotten cell of the ovarian follicle" (Young and McNeilly, 2010). While much is known about their contribution to folliculogenesis and synthesis of sex hormones, their origin remains unclear, as well as the factors governing the recruitment and differentiation of these cells. This is possible because theca cells are more difficult to be identified, and they are less available for in vitro investigations compared to granulosa cells. Recently, a growing number of researches have been dedicated to understand these cells and unveil their origin. While theca cells emerge only after follicle activation and its initial growth, it is essential to examine the dynamics of ovary and follicle formation to perceive theca cell ontogenesis and their direct implication in folliculogenesis and fertility.

2.1.1 Human ovary development

The two ovaries are part of the female reproductive system. They are a paired intraperitoneal endocrine organ found close to the fallopian tubes within the ovarian socket in the lower left and right quadrants of the abdomen, respectively (Gibson and Mahdy, 2019). The ovaries are connected to the body wall by their suspensory ligaments. The suspensory ligament carries sympathetic and parasympathetic plexuses,

as well as the ovarian artery and vein. Inferior to the ovary is the angle of the body and the uterine tube (Gibson and Mahdy, 2019) (Figure 5).

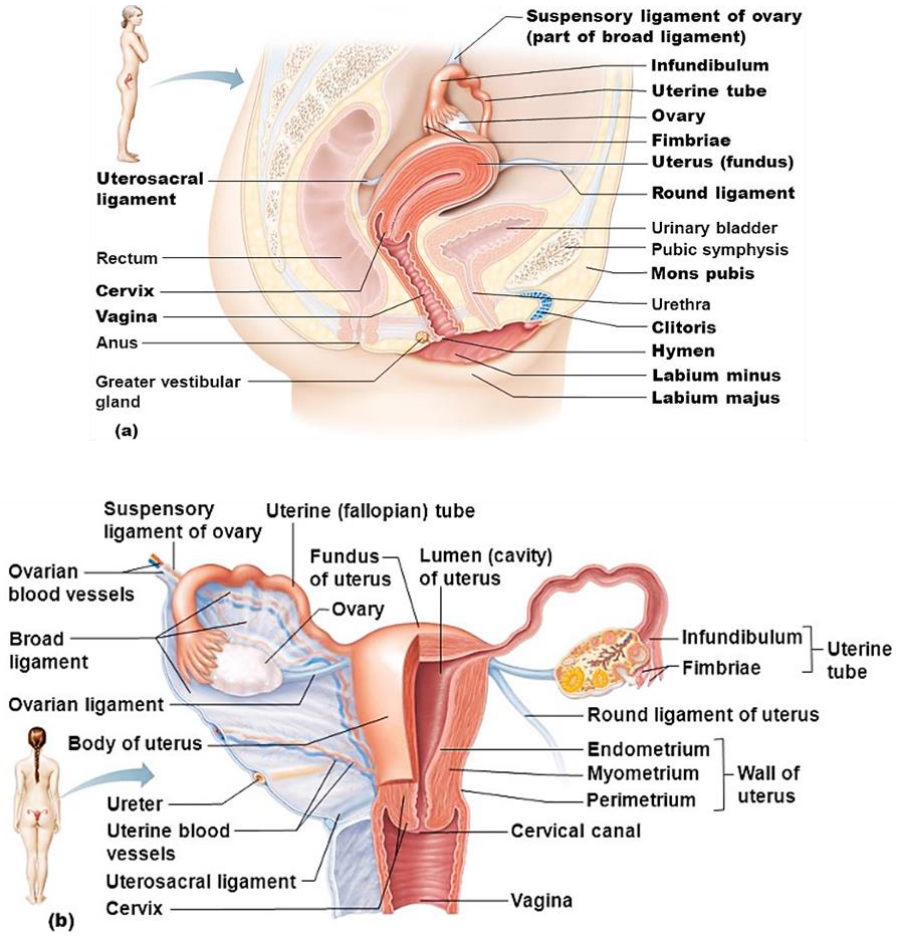


Figure 5: Female reproductive system. The main organs of the female reproductive system are located inside the pelvic cavity. *From Slide Player Website (http://slideplayer.com/slide/7334269/).*

Ovarian development initiates with differentiation and proliferation of gonadal ridge epithelial-like (GREL) cells from mesonephric epithelial cells. Initially, the ovary differentiates into the medulla, which is the central feature and has a germinal epithelium layer across the surface.

The dorsal endoderm of the yolk sac produces primordial germ cells. These cells migrate to the hindgut and then enter the female genital ridges at approximately five weeks of gestation and commence mitotic divisions. At this time, a female fetus ovary contains about 500 to 1300 primordial germ cells. Primordial germ cells proliferate and differentiate into oogonia from arrival at the developing female genital ridges until the 7th month of gestation (Freire *et al.*, 2020; Yoshino and Saito, 2019). Afterward, these oogonia undergo one of the three developmental paths of mitosis, apoptosis, or meiosis. Mitosis continues exclusively for three weeks, augmenting the cohort of oogonia to about 600,000 by nine weeks of gestation. At this moment, apoptosis, the process of programmed cell death, begins and peaks at 20 weeks of pregnancy, leading to a decrease in the primordial germ cell pool. A third process that takes place at approximately nine weeks is meiosis, which will convert oogonia into primary oocytes. The mitosis, apoptosis, and meiosis result in expanding the oogonial population to approximately 6–7 million by gestational week 20. Mitosis ceases shortly after that, whereas meiosis and apoptosis continue. As the oogonia enter the prophase of meiosis I, they are termed primary oocytes (Gago and Ginsburg, 2004).

Around the 11th and 13th week, oogonia in the deepest layers of the ovary enter the meiotic prophase (Feng *et al.*, 2014; Le Bouffant *et al.*, 2010). The stroma interpenetrates more towards the ovarian surface following spreading laterally. GREL cells undergo persistent proliferation, expansion, and invagination towards the interior of the gonads and

surround oogonia, resulting in forming ovigerous cords. GREL cells afterward give rise to the granulosa cells in follicles (Hummitzsch *et al.*, 2019). At this moment, the cords are arranged in the ovarian cortex surrounded by a basement membrane and stromal areas containing capillaries, radially orientated towards the surface of the ovary. The medulla is characterized by stromal cells, vasculature, and tubules that originated from the mesonephros. Regression of the peripartum of each germ cell cyst causes the formation of a primordial follicle, composing of an oocyte and a single layer of nourishing granulosa cells. Many germ cells are lost during this process, and thus the female is born with one to two million primordial follicles. Following a dormant period until puberty, approximately 400,000 to 500,000 primordial follicles remain in the ovary. During puberty, around 1000 follicles per month enter a path of apoptosis, resulting in follicular atresia. Usually, one or two of them complete meiosis I and initiate meiosis II just before ovulation. The rate of follicle loss increases after 35 years of age (Drummond, 2006; Hirshfield, 1997; Macklon and Fauser, 1998; Macklon and Fauser, 2001; Sun *et al.*, 2017; Yoshino and Saito, 2019) (Figures 6 and 7).

The ovaries will descend, however unlike their male counterparts, the testicles, their descent will end in the abdomen. The ovaries are attached to a strip called the gubernaculum, which also connects to the uterus and prevents the ovaries from descending lower. The proper ovarian ligament arises from the remnant of the gubernaculum (Kuyama *et al.*, 2019) (Figure 5).

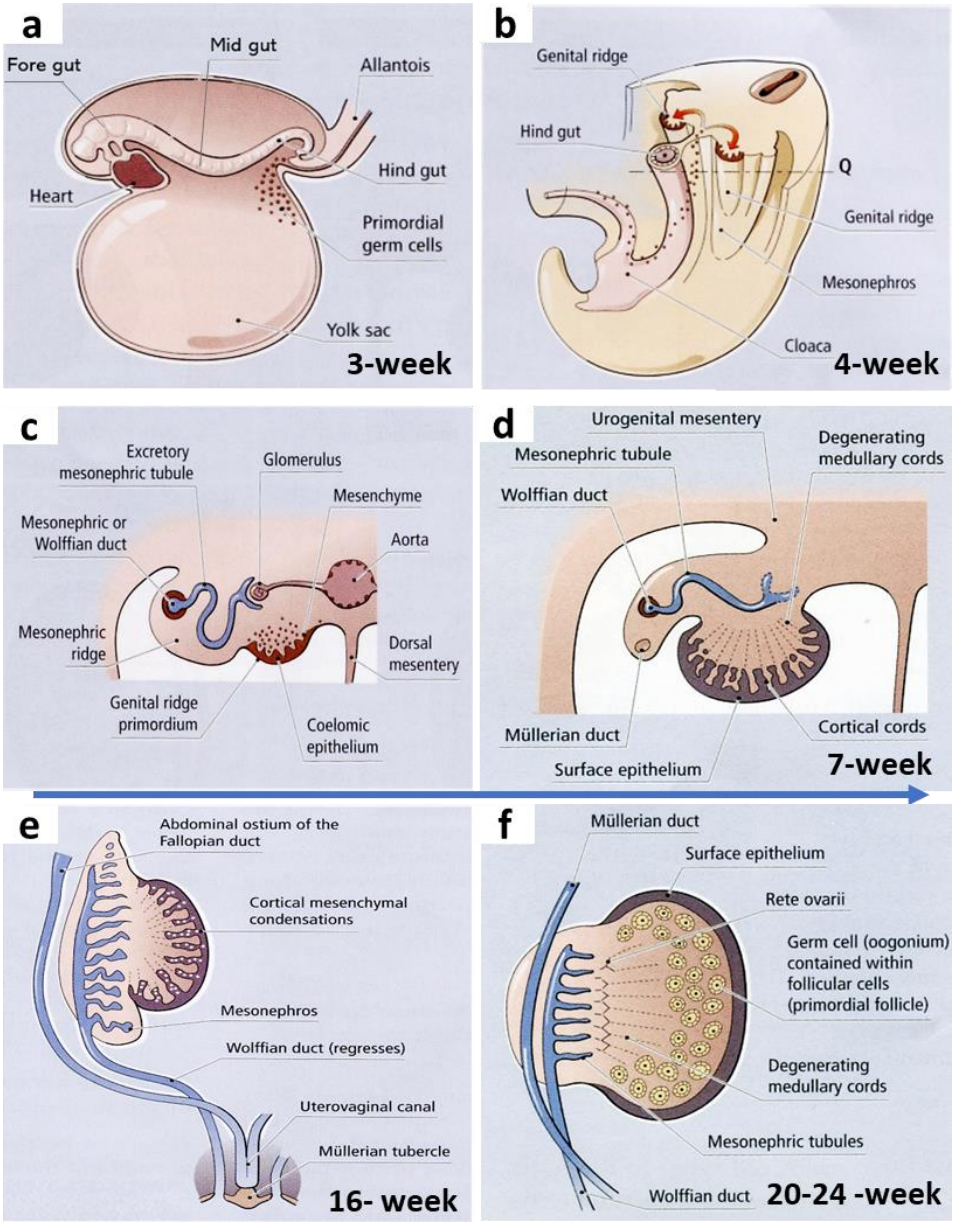


Figure 6. Embryology of the ovary. Origin and migration of primordial germ cells (a and b), the formation of basic gonad architecture (c and d), the proliferation of oogonia, and formation of syncytium (e and f). *Adapted from Sadler (2000).*

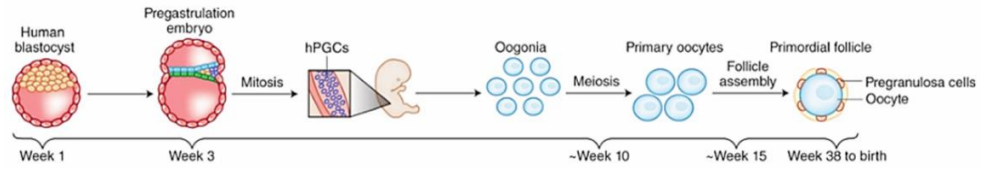


Figure 7. Oogonial development in human fetal ovaries. *Adapted from Stringer, Western (2019).*

2.1.2 Folliculogenesis

Folliculogenesis is defined as the process of activation of dormant primordial follicles followed by their development up to the preovulatory stage (Figure 8). Ovarian follicular growth starts in the peripheral cortex of the ovary, where primordial follicles are located. It takes approximately 6-12 months for a primordial follicle to grow up to the ovulatory stage (Williams and Erickson, 2012). Most of this time is spent in the pre-antral phase. Primordial follicles transition into the primary stage occurs in the late luteal phase of a cycle. It is concurrent with the change of granulosa cell shape from flattened to cuboidal and enlargement in the oocyte size. As the primary follicle grows and becomes a secondary follicle, the oocyte forms a glycoprotein; a mucoid substance called zona pellucida. It is a clear region surrounding the oocyte and separating it from the granulosa cells, which then start to express FSH receptors. As the primary follicle continues its growth, granulosa cells proliferate, increasing their number of layers around the oocyte. At this stage, follicles are called secondary and have a diameter ranging from 120 to 200 μm. At this stage, the theca layer starts to form around the follicles. While granulosa cells and oocyte remain avascular,

the follicle acquires its own blood supply, with one or two arterioles breaking up into a capillary network immediately outside the basement membrane. The theca interna develops LH receptors, and together with FSH receptors on granulosa cells, it enables the follicles to respond to the respective gonadotropins (Feher, 2012; Macklon and Fauser, 1998; Macklon and Fauser, 2001; Williams and Erickson, 2012) (Figure 8).

Further development of secondary follicles and the selection of a dominant follicle for ovulation is a gonadotropin-dependent process. FSH binds to the FSH receptors on the cell surface of the granulosa cell layer of the secondary follicle. In response to FSH stimulation, follicles continue to grow and develop an antral cavity, and at this stage, they are called tertiary or Graafian follicles. The fluid present in the antrum contains secretory materials from the growing oocyte and granulosa cells. Theca cell differentiation is a substantial step that happens at the tertiary follicle. A subpopulation of cells surrounding the growing follicle becomes mesenchymal and acquires the ultrastructural and functional characteristics typical of active steroid-secreting cells, called theca interna (Erickson *et al.*, 1985). As these changes occur, theca interna cells express the LH receptor and are called theca interstitial cells (Erickson *et al.*, 1985). There is a layer at the periphery of the theca interna layer. The cells have the ultrastructural and functional characteristics of smooth muscle cells and are concentrically arranged fusiform cells. This layer is the theca externa of the tertiary follicle (Erickson, 2000) (Figure 8).

LH binds to the LH receptors of the theca interna, leading to the production of androgens, most notably androstenedione. Androgens are aromatized by granulosa cells to produce estrogens, mainly estradiol. From now on, consequently, the estrogen levels begin to rise. Androgens are an essential requirement for the normal cyclical secretion of estradiol by granulosa cells and have an important physiological role in both preantral and antral follicle development, including granulosa cell proliferation (Drummond, 2006; Hillier, 2001; Macklon and Fauser, 1998; Macklon and Fauser, 2001; Williams and Erickson, 2012). At the late tertiary/ preovulatory stage, most of the follicles that started growth would go through atresia and apoptosis. Androgens in mature antral follicles encourage apoptosis and follicle atresia. This may be an important mechanism to ensure mono-follicular ovulation in primates, including humans (Franks and Hardy, 2018). Among those follicles, there are few who have a high rate of granulosa cell mitosis and proliferation and expressing more FSH receptors. These are antral follicles, and in response to the rise of FSH, they secrete estrogen and inhibin (Ziegler *et al.*, 2007). While most of these follicles will not develop further and show retardation in their growth rate and become atretic, usually, one antral follicle will be able to continue its growth till the preovulatory stage. The growth of this dominant follicle during the follicular/proliferative phase is about 1.5 mm per day. Around days 13-15 of the menstrual cycle and end of the follicular phase, the preovulatory follicle breaches the surface of the ovary and releases the egg/cumulus complex through a process termed ovulation (Conti and Chang, 2015; Skinner, 2018). After ovulation, the ruptured follicle

undergoes a dramatic transformation into another endocrine organ called the corpus luteum (Conti and Chang, 2015). The theca interstitial and granulosa cells become the theca lutein (paraluteal) and granulosa lutein (large luteal) cells, respectively. The corpus luteum becomes richly vascularized and serves as the site of progesterone and estradiol production during the luteal phase of the cycle. Luteinization begins shortly after the preovulatory LH surge, and if the egg is not fertilized, the corpus luteum undergoes apoptosis and formation of corpus Albicans, a process called luteolysis. During this process, there is a striking decrease in the amount of progesterone and estradiol production (Conti and Chang, 2015; Shikone *et al.*, 1996). (Figures 8 and 9).

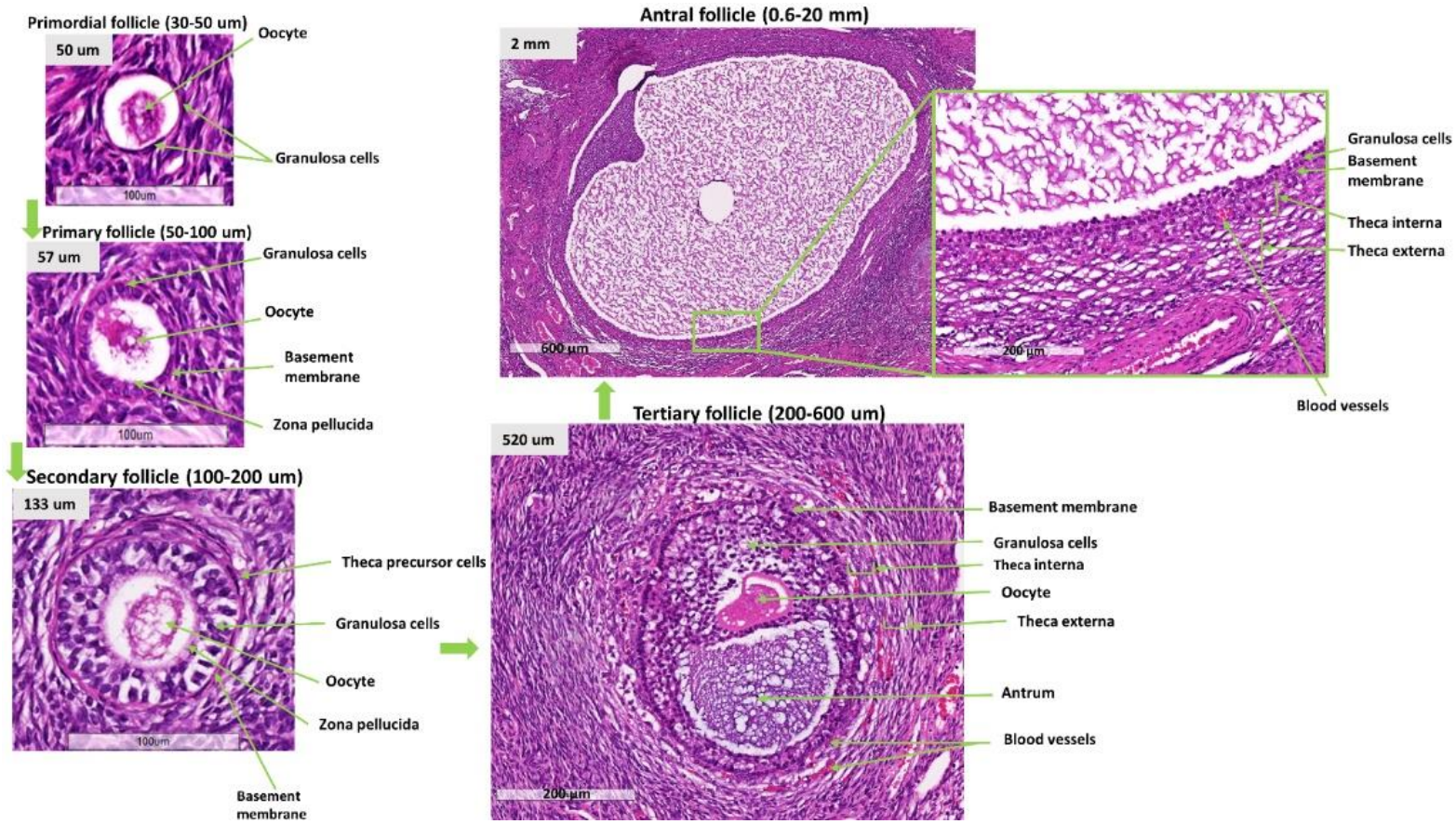


Figure 8. Classification and architecture of human ovarian follicles.

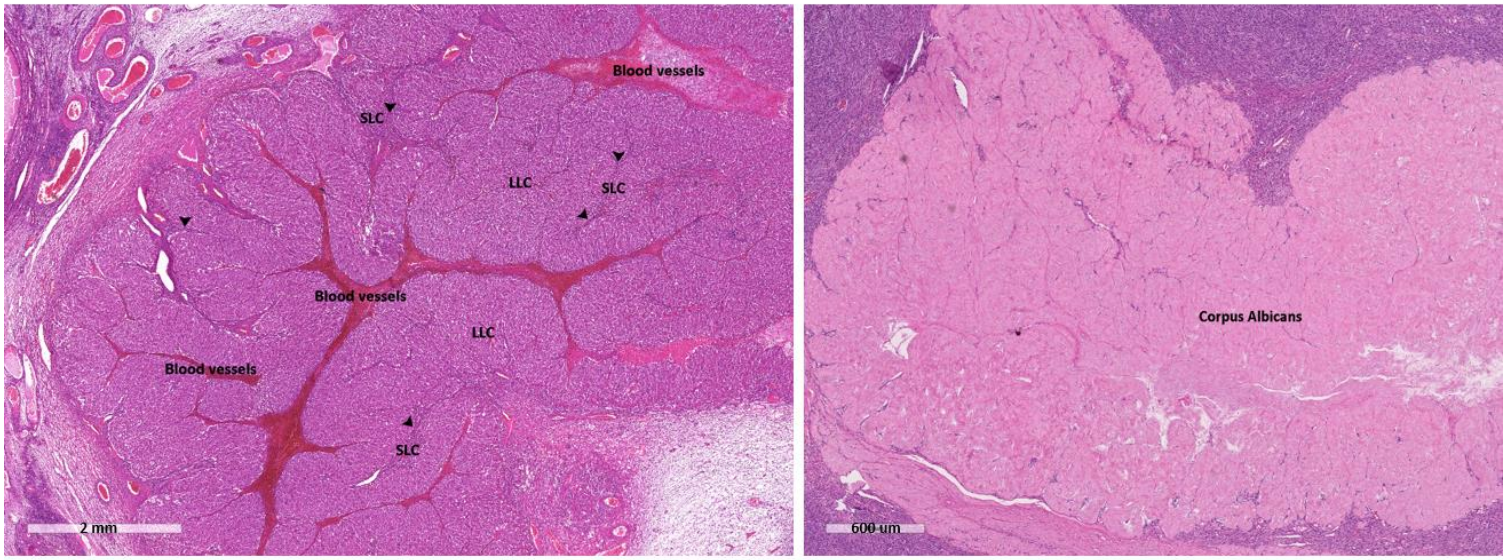


Figure 9. Human ovarian corpus luteum (left) and corpus Albicans (right). LLC: Large luteal cells, SLC: Small luteal cells (arrowhead).

2.2 Theca cells

Theca is a Latin word meaning any external case, outer covering, or sheath (Richards *et al.*, 2017). As it comes from its name, theca layer act as an envelope surrounding growing follicles in the ovary. Theca cells are considered an essential element of developing follicles located in the interfollicular stroma, close to the follicle basement membrane. The layers of theca externa and interna around ovarian follicles (Figure 10) are critical not only for supporting the structural integrity of the follicle but also for transporting nutrients to the avascular granulosa cell layers, cumulus cells, and oocyte. They are also vital for producing key endocrine regulatory factors, such as androgens (testosterone and dihydrotestosterone (DHEA)), as the substrate for granulosa cells to convert them to estrogens (Edson *et al.*, 2009). Without theca cells, follicle development would be halted, preventing hormone production and ovulation from occurring, which would not occur, leading to infertility problems.

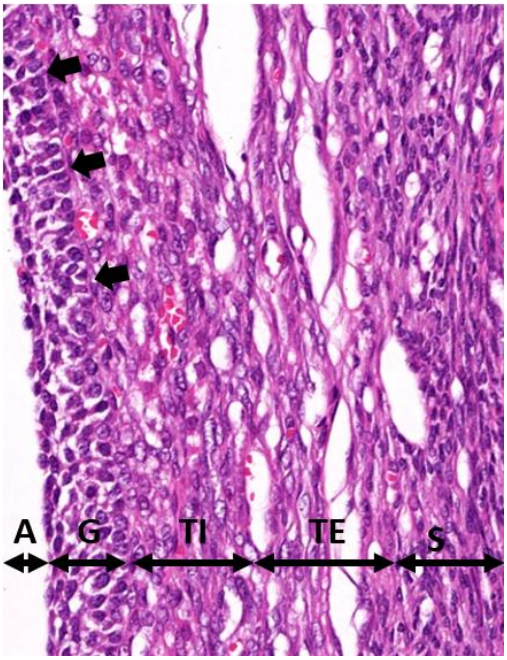


Figure 10. Wall of an antral follicle in the human ovary. This histological section shows the outer part of an antral follicle containing the antrum (A), followed by layers of mural granulosa cells (G) and basement membrane (thick arrow). In large antral follicles, it is possible to distinguish two different layers of theca cells: theca interna (TI), which is in close contact with the basement membrane and rich in endocrine-like cells; theca externa (TE), which contains fibroblasts and smooth muscle cells and merges with the ovarian stroma.

2.2.1 Origin of theca steroidogenic (interna) cells

While the origin of oocyte and granulosa cells is clear and established from the fetal stage, the origin or origins of theca cells are not yet well characterized. This could be due to the fact that theca cells appear in a short period of time during follicle development. They start to be recruited once the follicle is activated and form while the follicle

undergoes its further development from the late secondary stage till ovulation. There are few but different theories on the origin of theca cells in animal models and human, which are as follows (Table 4):

2.2.1.1 The population of theca precursor cells

Recently, a cell lineage analyses study by Liu *et al.* (2015), who traced GLI1-positive cells in *Gli1-Lac-Z* or *Gli1-CreERT2; Rosa-LSL-tdTomato* transgenic mice, reported that cells in the theca layers of growing follicles are derived from two different sources within the embryonic gonad, as follows: (1) $Gli1^+$ mesenchymal cells that migrate into the ovary from the mesonephros region and (2) $WT1^+$ stromal cells indigenous to the embryonic ovarian medullary region (Liu *et al.*, 2015). These fetal precursor cells differentiate into theca cells after birth. The $Gli1^+$ mesonephros-derived precursors become the steroidogenic androgen-producing cells within the theca interna. In contrast, the ovarian $WT1^+$ cells appear to give rise to theca fibroblasts, perivascular smooth muscle cells, and interstitial ovarian tissue (Liu *et al.*, 2015). Moreover, in this study, it was also shown that GDF9 regulates the expression of DHH and IHH in granulosa cells, and the loss of GDF9 (in)directly disrupts theca cell recruitment, proliferation, steroidogenesis, and, hence, follicle growth (Liu *et al.*, 2015).

2.2.1.2 All stromal cells can become theca cells

A study in the cow by Orisaka *et al.* (2006) demonstrated that all the ovarian stromal cells from the cortex in co-culture with granulosa cells could differentiate into theca cells acquiring LH responsiveness and expressing LH receptor and androstenedione production after 24 hours. Another study in goat has been done by Qiu *et al.* (2013). They showed the co-culture of cortical stromal cells with granulosa cells causes the LH responsiveness in stromal cells and their androgen production. These findings were also supported by Itami *et al.* (2011) study in mice using a three-dimensional follicle culture system with ovarian stromal cells. By adding FSH into the culture system, they observed follicle growth as well as the formation of the developing theca layer surrounding the follicles.

2.2.1.3 Theca stem cells

In a study by Honda *et al.* (2007), theca stem cells isolated from neonatal mouse ovaries can be stimulated to differentiate into theca cells in vitro or in vivo by transplanting into mouse host. Isolated cells from neonatal mice ovaries were in vitro cultured in a serum-free medium containing growth factors necessary for recruitment and differentiation of theca cells. The culture plate was gelatin-coated, and fibroblast-like cells were attached to it. Only floating cells were used for the secondary passage. These cells formed floating structures. In order to obtain only somatic cells with the cytological features of undifferentiated interstitial cells, three passages, totalizing 4-5 weeks, were necessary. These cell colonies stained positive for alkaline phosphatase and expressed *Ptch1* and *Gli3,*

theca cell markers, but are morphologically undifferentiated and nonsteroidogenic. The authors reported that cells after three passages in serum-free medium enriched with growth factors were theca stem cells. While the addition of serum to the media enhances theca stem cells appearance by fine lipid droplets and very low expression of *Lhr*, culturing them with granulosa cells conditioned media or co-culture with these cells induces a steroidogenic morphology (lipid droplets and smooth endoplasmic reticulum), increases expression of *Lhr* and *Gli2*, and elevates androstenedione production. Theca stem cells derived from ovaries of C57BL/6-Tg(CAG-EGFP)C14-Y01-FM131Osb mice were cultured in a serum-free medium supplemented with growth factors for seven weeks with four passages. The colonies were injected into the ovarian cortex of C57BL/6 mice, and the ovary was transplanted for 16 days in the empty ovarian bursa of another C57BL/6 female mouse host. $EGFP^+$ cells were visible in the theca interna and externa of growing follicles, showing that they were recruited by growing follicles as well as in the ovarian interstitial area (Honda *et al.*, 2007). These theca stem cells likely differentiate not only in response to IHH or DHH but also to LH and other factors derived from granulosa cells, including insulin-like growth factor (IGF), kit ligand (KL), and epidermal growth factor (EGF), as well as by intrafollicular regulatory factors, including inhibins, activins, and BMPs (Glister *et al.*, 2013; Young and McNeilly, 2010).

Adib and Valojerdi (Adib and Valojerdi, 2017) isolated theca stem cells from sheep small antral follicles (3-5 mm) and in vitro cultured them according to Honda *et al.* (2007) protocol with some modifications. The

isolated theca stem cells were cultured for seven days in DMEM-F12 supplemented with FBS and growth factors necessary for theca cell recruitment and differentiation. These cells were differentiated into theca precursor-like cells after 7 days of culture by expressing *Gli2*, *Gli3*, *Ptch1*, *Cyp17a1*, *Hsd3b*, *Lhr* and steroid hormones such as testosterone, DHEA, androstenedione, progesterone, and estradiol. The stemness nature of isolated cells were proved by the authors by culturing these cells in specialized media, showing their ability to differentiate not only into theca precursor cells but osteocyte-like cells, adipocyte-like cells and oocyte-like cells.

2.2.1.4 Mesenchymal stem cells

Dalman *et al.* (2018a) isolated human theca stem cells from the theca layer of small antral follicles (3-5mm). These cells were characterized by fluorescence-activated cell sorting (FACS) for CD29, CD44, CD73, CD90, and CD105, markers for mesenchymal stem cells (Feng-Juan *et al.*, 2014; Maleki *et al.*, 2014; Moraes, 2018). These cells are more likely to be mesenchymal stem cells. They were in vitro cultured in DMEM-F12 supplemented with EGF, basic fibroblast growth factor (bFGF), leukemia inhibitory factor (LIF), glial cell line-derived neurotrophic factor, IGF1, and KL. These cells were differentiated into human theca cells during 12 days of culture. They produced DHEA, testosterone, androstenedione, and estrogen confirmed by ELISA, expressed mRNA for *Lhr*, *Gli2*, *Ptch1*, *Cyp17a1,* and stained positive for HSD3B by blue formazan precipitates in their cytoplasm.

Mesenchymal stem cells have self-renewal and differentiation capacity into tissues of mesodermal origin. They can support hematopoiesis through release various molecules that play a crucial role in migration, homing, self-renewal, proliferation, and differentiation of hematopoietic stem cells (Aqmasheh, 2017). Up to now, there is no study on assessing the differentiation capacity of hematopoietic stem cells in the human ovary into theca cells.

Table 4: Different theories on the origin of theca interna cells in animal models and humans.

Theca cell origin	Species	Markers for theca cell origin	Markers for differentiated theca cells
Theca precursor cells	Mouse	*Gli1*-positive cells (Theca interna) *WT1*-positive cells (theca externa)	*Gli1*
All the cortical stromal cells	Cow, goat	Not mentioned	*Lhr*, *Cyp17a1*, steroid hormone production
	Mouse		Formation of the developing theca layer surrounding the follicles
Theca stem cells	Mouse: isolated from the whole ovary	Alkaline phosphatase-positive, mRNA for *Ptch1* and *Gli3*	*Lhr*, *Ptch1*, *ptch2*, *Gli2* and *Gli3*
	Sheep: Isolated from the theca layer of small antral follicles	Alkaline phosphatase-positive	*Ptch1*, *Gli2*, *Gli3*, *Cyp17A1* and *Hsd3b1*, Steroid hormone production
Mesenchymal stem cells	Human	CD29, CD44, CD73, CD90, CD105	*Lhr*, *Gli2*, *Patch1*, *Cyp17a1* and HSD3B1

According to the studies from the literature, it appears that there is a subpopulation of cells that can differentiate into theca cells. In the studies where all stromal cells were in vitro cultured (Itami *et al.*, 2011; Orisaka *et al.*, 2006; Qiu *et al.*, 2013), one could also suggest that only a subpopulation of cells differentiates into theca cells, which proliferate and produce androgens. The study using human cells performed by Dalman *et al.* (2018a) probably offers the best clue of the presence of

mesenchymal stem cells in the pool of stromal cells in the human ovary. These cells are recruited by the primary follicle, and with the paracrine and endocrine signaling pathways, they differentiate into theca interna cells.

2.2.2 Theca cell differentiation

At the primary stage, it is believed that activated follicle produces factors that recruit mesenchymal fibroblast-like cells reside in the ovarian stroma and located adjacent to the basement membrane of the primary follicles and differentiate them into theca cells (Erickson *et al.*, 1985; Honda *et al.*, 2007; Orisaka *et al.*, 2006) (Figure 11). While the exact identity and the combination of the proteins are unknown, what is known so far is not a single factor, but complex networks of signals function synergistically to result in a fully functional steroidogenic theca layer. Several factors have been studied in vitro for their effects on the recruitment and differentiation of theca cells.

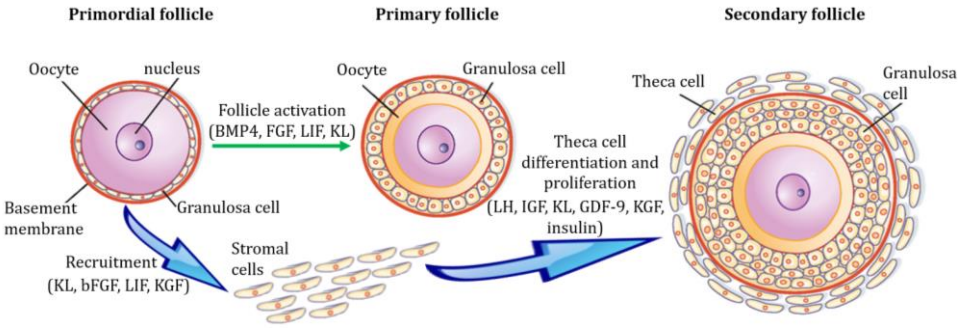


Figure 11. Schematic representation of recruitment and differentiation of theca cells in mammals. Evidence suggests that theca stem cells reside in the ovarian stroma and are recruited by factors released from follicles after they are activated. Individual factors may be responsible for recruiting these cells, whereas others may promote differentiation and proliferation. *Drawing by C. A. Amorim.*

2.2.2.1 Insulin-like growth factor (IGF)

The ovary has a comprehensive range of IGF system components. IGF receptors are found on human theca cells (Poretsky *et al.*, 1985). FSH regulates the synthesis of IGF1 in the granulosa cells (Adashi *et al.*, 1985; Hammond *et al.*, 1985; Hernandez *et al.*, 1989; Oliver *et al.*, 1989), and in vitro studies have been shown that this factor increases theca cell proliferation (Campbell *et al.*, 2006; Hillier *et al.*, 1991; Huang *et al.*, 2001; Kwintkiewicz and Giudice, 2009; Spicer and Chamberlain, 1998; Stewart *et al.*, 1995). IGF1 alone stimulates the expression of LH receptors (Magoffin and Weitsman, 1994) and acts synergistically with LH to enhance the expression of steroidogenic enzymes CYP11A1 and HSD3B, but not CYP17A1 (Magoffin and Weitsman, 1993a; Magoffin and Weitsman, 1993b; Magoffin and Weitsman, 1993c), accordingly in vitro androgen synthesis of theca cells (Hillier *et al.*, 1991). Remarkably,

human stromal tissue cultured in vitro synthesized androgens when stimulated by insulin and IGF (Barbieri *et al.*, 1984; Barbieri *et al.*, 1983). This gives additional evidence of IGF involvement in promoting theca cell differentiation (Barbieri *et al.*, 1984; Barbieri *et al.*, 1983) (Figure 11). Since IGF2 can stimulate bovine theca steroidogenesis and acts through the type 1 IGF receptors (Spicer *et al.*, 2004), it may also play important roles in theca functionality.

2.2.2.2 Kit ligand (KL)

KL, also known as stem cell factor, acts through the c-kit tyrosine kinase receptor (Besmer, 1991; Zsebo *et al.*, 1990). It is synthesized by granulosa cells and acts on differentiated theca cells, stromal cells, and oocytes, where the receptor c-kit is located (Manova *et al.*, 1993; Manova *et al.*, 1990; Motro and Bernstein, 1993; Motro *et al.*, 1991; Parrott and Skinner, 1997). Huang *et al.* (2001) showed that adding KL and IGF1 antagonists in a follicle-conditioned medium decreased the stimulatory effects of these factors on theca cell differentiation in vitro by more than 90% (Figure 12). While in rat theca cells, neither KL nor IGF1 alone cannot stimulate androstenedione production, these factors together induce androgen production, but to a lesser extent than that induced by LH. Adding KL and IGF1 together with LH showed that IGF1 acted synergistically with LH to increase androgen production, whereas KL had no added effect combined with LH. While KL alone did not affect the mRNA expression of *Cyp11a*, *Hsd3b,* and *Lhr*, it decreased *Cyp17a1* mRNA expression (Huang *et al.*, 2001) (Figure 12). IGF1 alone did not affect the

mRNA expression level of *Star* and *Cyp17a1*, whereas it increased mRNA levels of *Lhr*, *Cyp11a*, and *Hsd3b*. An increase in the expression of the mRNA levels of *Star*, *Cyp11a*, *Cyp17a1*, *Hsd3b*, and *Lhr*, due to the combination of IGF1 and KL, provides strong evidence that these factors may act synergistically to regulate theca cell differentiation into steroid-producing cells at least in the rat (Huang *et al.*, 2001). Adding KL to the in vitro culture of bovine theca and stromal cells stimulated their growth under sub-confluent conditions. However, when theca cells were grown to the confluence, KL stimulated androstenedione production (Parrott and Skinner, 1997). In contrast, KL did not affect bovine stromal cells to produce androstenedione (Parrott and Skinner, 2000), suggesting that this factor alone affects bovine theca cells once differentiated (Young and McNeilly, 2010). KL expression can also be modulated by leukemia inhibitory factor (LIF), keratinocyte growth factor (KGF), and hepatocyte growth factor (HGF) (Parrott and Skinner, 1997). KGF and HGF are produced by theca cells (Parrott and Skinner, 1997) and act on granulosa cells to produce KL, which then signals back to the theca to produce KGF and HGF in a positive feedback mechanism (Parrott and Skinner, 1998). Therefore, KL may potentially act as a final common factor in theca cell differentiation and activation (Young and McNeilly, 2010).

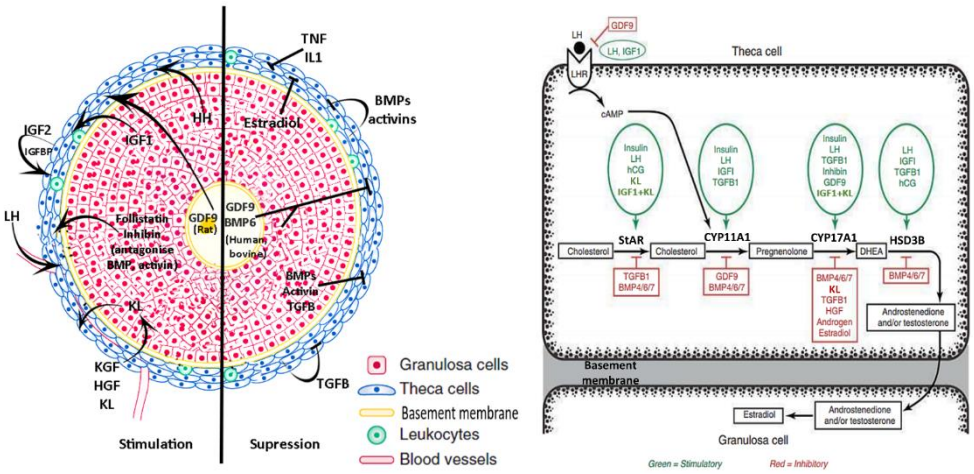


Figure 12. Steroidogenic enzymes modulation and androgen production in mammalian theca cells. The process of androgen production requires CYP11A1, CYP17A1, and HSD3B, as well as StAR. There are some differences among species as theca cells from sheep, humans, and primates principally produce androstenedione. In contrast, rodents produce testosterone as precursors for estradiol production in the neighboring granulosa cells. **(Right)** Green circles are stimulatory factors, and the inhibitory factors are listed in red boxes. BMP: bone morphogenetic protein; GDF9: growth differentiation factor 9; HGF: hepatocyte growth factor; hCG: human chorionic gonadotropin; IGF: insulin-like growth factor; KL: kit ligand; TGFβ: transforming growth factor beta. **(Left)** Factors released by oocyte, granulosa, and theca cells can modulate androgen production in theca cells in addition to external gonadotropins and insulin. Factors stimulate (green) or inhibit (red) theca cell androgen production directly and or indirectly. Specific factors have been observed to act in opposing manners, indicating species-specific differences. *Adapted from Young and McNeilly (2010).*

2.2.2.3 Basic fibroblast growth factor (bFGF)

The bFGF is expressed by primordial and primary oocytes, and granulosa cells of larger preantral follicles, and in the theca cells of rodent, bovine,

and human follicles (Berisha *et al.*, 2000; Nilsson and Skinner, 2001; Van Wezel *et al.*, 1995; Yamamoto *et al.*, 1997). It has been reported to affect somatic cell mitosis, differentiation, steroid synthesis, and apoptosis (Lavranos *et al.*, 1994; Tilly *et al.*, 1992; Vernon and Spicer, 1994). bFGF receptors have been found on the membrane of granulosa and theca cells (Schams *et al.*, 2009; Shikone *et al.*, 1992; Shimizu *et al.*, 2002).

During in vitro culture of ovarian follicles, bFGF activated primordial follicle development to the same extent as KL and promoted theca and stromal cell growth in rat and bovine experiments, respectively (Nilsson and Skinner, 2001). Therefore, it is thought that bFGF acts similarly to KL by regulating somatic cell growth (Nilsson and Skinner, 2001). While KL was not found to regulate bFGF expression, in contrast, bFGF treatment was found to increase *Kl* mRNA expression in in vitro cultured murine ovaries. These observations suggest that one of the roles of the oocyte-derived bFGF is to increase the granulosa-derived KL expression and that both are required to promote primordial to primary follicle transition optimally. This elucidates the cell-cell interactions' essential role in this network where the specific locally derived growth factors are critical to understanding the physiology of the primordial to primary follicle transition (Nilsson and Skinner, 2004).

2.2.2.4 Transforming growth factor beta (TGF-β) superfamily members

TGF-β superfamily comprises a large group of proteins, including bone morphogenetic proteins (BMPs), growth differentiation factors (GDFs), anti-Müllerian hormone (AMH; also known as Müllerian inhibiting

substance), activins, and inhibin, and play crucial roles in controlling follicular growth and development (Knight and Glister, 2006; Shimasaki *et al.*, 2004; Xia and Schneyer, 2009). They bind to their receptors and initiate phosphorylation cascades, leading to gene expression in the cell nucleus. While BMPs act through the small mothers against decapentaplegic (SMAD) 1/5/8 pathway, TGFβ/activin/GDFs act through SMAD 2/3. Members of this superfamily are involved in theca cell recruitment, proliferation, and differentiation, which may or may not interact with the gonadotropins (Table 5).

Granulosa cells are the primary ovarian source of inhibins, activins, and activin-binding protein (follistatin). In contrast, germ (oogonia, oocytes) and somatic (theca, granulosa, luteal) cells express activin receptors, signaling components, and inhibin co-receptor (betaglycan) (Knight *et al.*, 2012). Activin and inhibin play a role in follicle activation, hormone synthesis, and luteolysis (Knight and Glister, 2001). Activin promotes in vitro development of preantral follicles in the rat (Li *et al.*, 1995; Zhao *et al.*, 2001), sheep (Thomas *et al.*, 2003), and human ovarian tissue (Telfer *et al.*, 2008) by increasing FSH receptors and FSH-induced aromatization in granulosa cells and thus, is involved in promoting estradiol production (El-Hefnawy and Zeleznik, 2001; Nakamura *et al.*, 1993; Ogawa *et al.*, 2003; Park *et al.*, 2005). Moreover, since estradiol may suppress activin expression, this forms a possible interplay between activin and estrogen signaling during folliculogenesis (Kipp *et al.*, 2007). An increment in estradiol and inhibin production by putative preovulatory follicle(s) would act as a suppressor for activin production, blocking activin action

in theca cells through estradiol and inhibin. This process leads to enhancing theca cell androgen production. Therefore, inhibin is a critical factor in controlling steroid production and gonadotropin secretion (McNeilly *et al.*, 2003; McNeilly, 2001; Padmanabhan and McNeilly, 2001). Studies on in vitro culture of human isolated theca cells revealed that activin suppresses androgen and progesterone production (Hillier *et al.*, 1991; Shukovski *et al.*, 1993). Its antagonist, inhibin, enhances LH-mediated androgen production (Hillier *et al.*, 1991). Accordingly, activin directly affects theca cell steroid function and is regulated by inhibin and follistatin (Findlay, 1993; Welt *et al.*, 2002). It is shown that inhibin alone increases androgen production by human theca cells during in vitro culture and blocks the inhibitory effect of added activin (Hillier *et al.*, 1991). Inhibin might have a role in modulating hormone production through antagonizing activin and BMPs, rather than through a signal cascade of its own (Farnworth *et al.*, 2006; Wiater and Vale, 2003).

BMPs are released at particular times during folliculogenesis and function either in an autocrine or paracrine manner to modulate the growth, differentiation, and function of follicular cells. BMPs' expression patterns have been investigated in rodents, ruminants, primates, and observations suggest species-specific differences for some molecules (Shimasaki *et al.*, 2004). While BMP4 is expressed in stromal cells surrounding primordial follicles, BMP-4 and -7 are expressed in the theca layer of antral follicles (Lee *et al.*, 2004; Nilsson and Skinner, 2003; Shimasaki *et al.*, 1999). In neonatal rat ovaries, BMP-4 and -7 cause an increase in the formation of primary follicles (Nilsson and Skinner,

2003) and the percentage of growing follicles in the adult rat ovary (Lee *et al.*, 2004; Nilsson and Skinner, 2003). In humans, theca-derived tumor cells showed a reduction in androstenedione production in vitro when treated with BMP-4, and this effect was enhanced in the presence of cAMP agonists (Dooley *et al.*, 2000). Oocytes produce BMP-6, but its function appears to be different between rodents and ruminants (Glister *et al.*, 2004; Otsuka *et al.*, 2001; Shi *et al.*, 2009). Transcripts for all seven BMP/activin receptors were observed in granulosa, theca, and luteal compartments of sheep (Souza *et al.*, 2002) and cow ovaries (Kayani *et al.*, 2009). BMP-2,-4, -6, and -7 showed significantly decreased androstenedione secretion in vitro while moderately increased progesterone production and cell proliferation in ovine and bovine theca cells (Campbell *et al.*, 2006; Glister *et al.*, 2005). They also reduced *Cyp17A1* gene expression but have a lesser effect on S*tar, Cyp11A1*, and *Hsd3b* (Glister *et al.*, 2005). While BMP antagonists, follistatin, did not affect androgen production by inhibiting the BMPs (Glister *et al.*, 2005), gremlin and chordin reversed the inhibitory effects of BMP-4 and -7 respectively on androgen production in bovine theca cells (Glister *et al.*, 2005). These data point out that an intrafollicular BMP signaling pathway contributes to the negative regulation of theca androgen production and that ovarian hyperandrogenic dysfunction could result from a defective autoregulatory pathway involving theca BMP signaling (Glister *et al.*, 2005). There are many BMP mutations that lead to aberrant fertility (McNatty *et al.*, 2005), which gives the idea that these proteins may play roles in theca recruitment (Young and McNeilly, 2010).

Dong *et al.* (1996) reported that ovarian function is disrupted in mutant mice lacking GDF9, an oocyte-derived factor. Mutations in the *Gdf9* gene lead to arrested folliculogenesis at the primary stage in mice, sheep, and humans (Kovanci *et al.*, 2007; Laissue *et al.*, 2006; Nicol *et al.*, 2009; Shimasaki *et al.*, 2004). These results suggest that while GDF9 is not vital for follicle activation, it is essential for onward primary growth (Young and McNeilly, 2010), regulating function and formation of theca cells (Dong *et al.*, 1996). Theca cells are not forming in *Gdf9* null mice and Thoka sheep follicles, which indicates a role for GDF9 in regulating theca cell recruitment, differentiation, and proliferation. However, this appears to depend on the stage of follicle development (Dong *et al.*, 1996; Elvin *et al.*, 1999; Elvin *et al.*, 1999; Nicol *et al.*, 2009). In the in vitro culture of theca cells from bovine small follicles (3–6 mm), in the presence of both LH and IGF1, GDF9 increased cell numbers and dose-dependently decreased progesterone and androstenedione production. It also decreased LHR, LH-induced cAMP, and CYP11A1 expression levels without altering the expression levels of IGF1 receptors, StAR, or CYP17A1. Theca cells from small antral follicles are more responsive to GDF9 than those from their large counterparts. Theca cell proliferation rate in small antral follicles compared to those from large ones are higher, which could be related to the higher levels of GDF9 receptor, ALK5, in these cells from small follicles. In large antral and preovulatory follicles (8–22 mm), theca cells showed little or no response to GDF9 in terms of proliferation or steroid production induced by IGF1. GDF9 in small antral follicles increases theca cell proliferation and decreases their steroidogenesis while it has no effect on promoting differentiation

of these cells (Spicer *et al.*, 2008). GDF9 has important species-specific differences in increasing and decreasing theca cell androgen production (Solovyeva *et al.*, 2000) in rats and humans, respectively (Yamamoto *et al.*, 2002). GDF9 appears to affect regulating KL expression and indirectly modulating theca cell function (Dong *et al.*, 1996; Joyce *et al.*, 2000; Nilsson and Skinner, 2002; Wang and Roy, 2004). While a double knockout mouse model for *Gdf9* and inhibin shows normal morphological cells surrounding preantral follicles, these cells do not appear to have been differentiated into theca since the expression of theca cell markers, such as CYP17A1 and LHR, are absent (Wu *et al.*, 2004). These findings indicate while in the absence of GDF9, recruitment of putative theca-like cells can happen, their differentiation into theca cells will not occur (Young and McNeilly, 2010).

Both TGF-β1 and 2 are present in sheep ovarian stromal tissue and vascular systems and theca cells from the small preantral follicle stage of development onwards, but not in granulosa cells and oocytes (Juengel *et al.*, 2004). While the mRNA for the *Tgf-β1* receptor was found in stromal and vascular cells, the *Tgf-β2* receptor was found in theca cells from the preantral stage onwards through development in the surface epithelium and some stromal cells. TGF-β binding proteins affect the bioavailability of TGF-βs in tissues and are localized on the membrane of ovarian cortical stroma and theca externa layer of bovine antral follicles (Prodoehl *et al.*, 2009). TGF-β1 has species-specific effects, and while has been reported to suppress androgen synthesis in human and rat theca cells (Attia *et al.*, 2000; Fournet *et al.*, 1996), in mouse, it increases

Cyp11A1, *Cyp17A1,* and *Hsd3b* genes expression during in vitro culture (Fournet *et al.*, 1996). A study on in vitro culture of rat ovarian fragments demonstrated that TGF-β1 blocks steroidogenesis at the level of CYP17A1 (Hernandez *et al.*, 1990). Even though these results are not explicit, it appears in humans, TGF-β has a similar role as activin and BMPs in suppressing androgen production (Young and McNeilly, 2010).

Table 5: Summary of the role of TGF-β superfamily members in mammalian ovaries.

Factors	Produced by	Acts on	Function
IGF1	Granulosa cells	Theca cells	Increase theca cell differentiation and proliferation
			Stimulate expression of LH receptor
			IGF1+LH: enhance the expression of steroidogenic enzymes
		Stromal cells	IGF+insulin: induce in vitro androgen production
KL	Granulosa cells	Differentiated theca cells, stromal cells, and oocyte	KL+IGF1: regulate theca cell differentiation and androgen production
KGF	Theca cells	Granulosa cells	Produce KL
HGF			
bFGF	Oocyte of primordial and primary follicles	Granulosa cells, theca cells, and stromal cells	Mitosis, differentiation, steroid synthesis, and apoptosis
	Granulosa cells of secondary and tertiary follicles		bFGF affect KL: required to promote primordial to primary follicle transition in vitro
	Theca cells		
TGF-β members: Activin, Inhibin, BMPs, GDF9, and AMH	Pituitary glands and ovary	Oocyte, granulosa, theca, and stromal cells	Recruitment, differentiation, and proliferation of theca cells
			Follicular growth and development
Activin	Granulosa cells	Germ (oogonia, oocytes) and somatic (theca, granulosa, luteal) cells	Increase FSH receptor, and FSH-induced aromatization on granulosa cells: promoting estradiol production
Inhibin	Granulosa cells	Germ (oogonia, oocytes) and somatic (theca, granulosa, luteal) cells	Modulating hormone production by antagonizing activin and BMPs
			Activin and inhibin: play a crucial role in controlling follicular growth and development
BMPs:	Oocyte, theca, and stromal cells	Oocyte, granulosa, and theca cells	Theca cell recruitment
			Regulating androgen production
GDF9	Oocyte	Granulosa cells, theca cells, and stromal cells	Follicle activation, necessary for further primary follicle growth
			Theca cell differentiation and proliferation (stage-specific)
			affect regulating KL expression, and indirectly modulating theca cell function
TGF-β1	Stromal cells, vascular system	Theca cells	Species-specific: in vitro studies showed in human and rat suppress, while in mouse increase androgen production
TGF-β2	Stromal cells theca cells from small preantral follicles onward and surface epithelium		

2.2.2.5 Hedgehog proteins

A recent study demonstrates that the effects of GDF9 are mediated partially by the induction and activation of hedgehog (HH) signaling pathways (Liu *et al.*, 2015). Pioneering studies by Wijgerde *et al.* (2005) and others (Ren *et al.*, 2009; Ren *et al.*, 2012; Spicer *et al.*, 2009) revealed that HH signaling pathway components are expressed in mouse and bovine ovaries (Figure 13) and might impact local cell patterning as in other tissues (Holtz *et al.*, 2013). HH signaling pathway has three ligands: IHH, DHH, and Sonic hedgehog (SHH). IHH and DHH, but not SHH, are expressed selectively in granulosa cells of growing follicles and act in a paracrine way to activate the HH cell surface transmembrane receptors PTCH1 and 2 presents on the membrane of theca interna cells, fibroblasts, and or perivascular cells within the theca layer (Figure 13). PTCH receptors are a conserved 12-pass transmembrane protein that plays a negative regulatory role in the HH signaling pathway (Ingham *et al.*, 1991). In the absence of HH proteins, PTCH1 suppresses the activity of the seven-transmembrane G protein-like receptor Smoothened (SMO) (Taipale *et al.*, 2002). The presence of HH proteins inactivates the repressor actions of PTCH1 expressed in adjacent cells (Ingham and McMahon, 2001) on SMO (Di Marcotullio *et al.*, 2007; Gulino *et al.*, 2007; Taipale *et al.*, 2002) and leading the activation of the latent cytoplasmic transcription factors, glioma-associated oncogene homolog (zinc finger protein GLI1, 2 and 3) (Ingham and McMahon, 2001; Lum and Beachy, 2004), potential markers of theca precursor cells (Liu *et al.*, 2015; Russell *et al.*, 2007; Wijgerde *et al.*, 2005) (Figure 13). Activation of SMO also leads to the mRNA induction of *Ptch2,* the inhibitory factor, and

Hedgehog interacting protein (*Hhip*). This signaling pathway provides autocrine negative regulatory loops within the follicle (Holtz *et al.*, 2013). HH signaling is tightly controlled at a local level. In granulosa cells depleted from *Smad1/5* and bonemorphogenic protein receptor 1 (*Bmpr1)*, there is an increase in HH signaling pathway components (Edson *et al.*, 2010), which gives the idea that HH signaling may be suppressed in granulosa cells by BMPR1 activity. Furthermore, HH signaling in granulosa cells is modulated by forkhead box protein L2 (FOXL2), a key determinant of their fate, due to the increased expression of *Dhh* mRNA in *Foxl2* knockout mice (Garcia-Ortiz *et al.*, 2009).

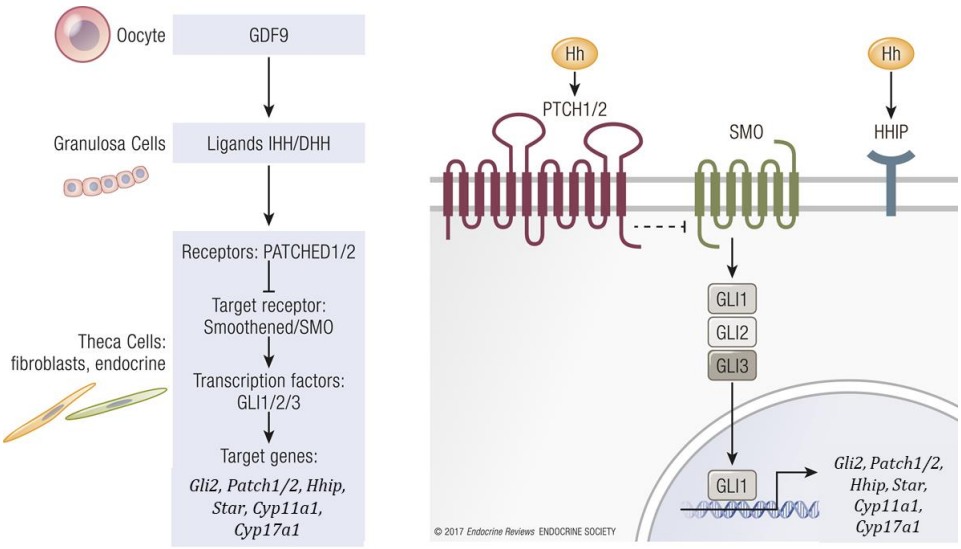


Figure 13. Schematic representation of hedgehog signaling pathway components in the ovary. GDF9, expressed by the oocyte, induces the expression of the IHH and DHH ligands in granulosa cells. These ligands bind to and activate cell surface receptors PTCH1/2 in theca cells. This activation blocks PTCH inhibition of the target receptor SMO, leading to the activation of the transcription factors GLI1, 2, or 3. These transcription factors regulate the expression of selected genes, including inhibitory feedback molecules (*Hhip* and *Ptch2*) and enzymes in the steroidogenic pathway, including *Star*, *Cyp11a1,* and *Cyp17a1*. *Adapted from Richards et al. (2017).*

2.2.3 Structural and matrix-related functions of the theca layer

The theca layer provides a substructure that preserves the follicle's spherical integrity and is mostly composed of extracellular matrix factors, including collagen, vimentin, vascular cell adhesion molecule 1 (VCAM1), laminin, fibronectin, proteoglycans, tenascin C, and fibrillins. Collagen fibers and other factors in mammalian ovarian theca and stroma compartments are evident with electron microscopy,

immunohistochemistry, picrosirius red staining, and circularly polarized light microscopy (Bagavandoss, 2014; Berkholtz *et al.*, 2006; Briley *et al.*, 2016).

Although the extracellular matrix appears highly structured, it is not stationary. The theca of growing follicles undergoes dynamic changes and contributes to follicular function and specific intraovarian niches (Irving-Rodgers *et al.*, 2010; Tingen *et al.*, 2011). Studies (Pangas *et al.*, 2003; Shea *et al.*, 2014; Woodruff and Shea, 2011) show that the rigidity of the extracellular matrix impacts not only follicle growth but also its steroidogenic potential (Kreeger *et al.*, 2005; Pangas *et al.*, 2003; West-Farrell *et al.*, 2009; Woodruff and Shea, 2011). Encapsulating mice follicles using alginate as a tissue-engineered artificial matrix provided follicles growth and fertile offspring, demonstrating that theca and granulosa cell functions and oocyte maturation are maintained (Xu *et al.*, 2006). It has been reported that small follicles in vitro cultured in the presence of stroma, containing theca cells and macrophages, grow better and survive longer than follicles cultured in the absence of stroma, indicating the dependence of the follicles on the ovarian stroma (Tingen *et al.*, 2011). Collectively, the stroma- and matrix-associated factors impact ovarian function.

2.2.4 Vascular and immune cell functions in the theca layer

The vascular network in the theca layer (Figure 14) is vital to provide nutrients for theca cells and the avascular granulosa cells, cumulus cells, and oocyte. Apart from its importance, little is known about the factors

that regulate the vascular network in the theca and stromal tissue during follicular growth and prevent the vascular invasion to the granulosa cell layers until after ovulation (Brown and Russell, 2014). Vascular endothelial growth factor (VEGF) is expressed as an essential factor in theca, and granulosa cells of late secondary follicles (Fraser, 2006), and its targeted disruption or overexpression of an antiangiogenic splice variant of VEGF in these cells leads to extreme changes in follicular development and reduced fertility (Sargent *et al.*, 2015). Hypoxia-inducible factor-1α (HIF1α) may regulate the expression of endothelin 2, a known regulator of vascular functions associated with ovulation (Bridges *et al.*, 2011; Cacioppo *et al.*, 2017). Targeted disruption of the HIF1α binding sites in mouse *Vegfa* promoter impairs vascular development and follicular growth (Feng *et al.*, 2017; Rico *et al.*, 2014). Accordingly, it seems functions of vascular components in the theca layer are regulated in part by factors from granulosa cells (Richards *et al.*, 2017).

Microarrays from bovine theca cells revealed there are minor differences in the vascular markers in theca of small and large follicles, which means the maintenance of vascular tissue is relatively stable during follicle growth (Hatzirodos *et al.*, 2017). However, VCAM1 is higher in theca of large follicles (Hatzirodos *et al.*, 2017), perhaps due to increased androgen levels (Death *et al.*, 2004; Solano *et al.*, 2011). The number of immune cells, specifically macrophages, associated with growing follicles increases during the prepubertal period in mice, and they are associated not only with apoptotic follicles but also with healthy

secondary follicles (Tingen *et al.*, 2011). The theca and stroma cells of the ovary also contain a well-developed lymphatic system (Brown and Russell, 2014), which in part, is dependent on a disintegrin and metalloproteinase (ADAM) with thrombospondin type 1 motif 1 (ADAMTS1) (Brown *et al.*, 2010). ADAMTS1 is a protease required not only for ovulation but also for other ovarian functions. Endothelins, especially endothelin 2 (Cacioppo *et al.*, 2017), play a crucial role in ovulation, presumably by regulating vasoconstriction and or smooth muscle contraction (Bridges *et al.*, 2011; Ko *et al.*, 2012). It is also a direct target of progesterone and progesterone receptor A (Sriraman *et al.*, 2010). Although more studies are needed to fully characterize what controls the vascular and lymphatic tissues and immune cell functions in the theca layer of growing follicles, it seems there are specific molecular markers that indicate the vascular tissue and immune cells associated with follicles at defined stages of growth (Nolan *et al.*, 2013).

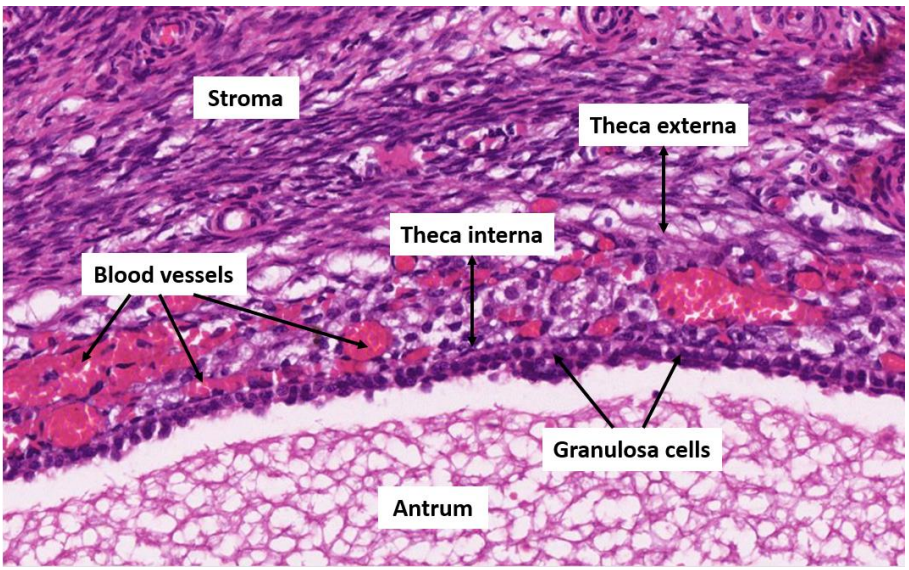


Figure 14. Vascularization in the theca layer of an antral follicle.

2.2.5 Endocrine function and theca interna cells

A particularly significant physiological event that happens in the secondary stage of follicle development is the acquisition of a blood supply with one or two arterioles, which terminate in a wreath-like network of capillaries adjacent to the basement membrane (Bassett, 1943). This allows the follicle to be directly exposed to factors circulating in the blood. As the capillaries form, dramatic changes in theca mesenchymal cells occur, and they undergo a path of theca interna cytodifferentiation. The first transition is a change from a precursor cell to one which contains LH receptors and at least one enzyme in the steroid biosynthetic pathway, such as 3-beta-hydroxysteroid dehydrogenase (HSD3B) (Magoffin and Erickson, 1982). This must be considered a significant event leading to the cytodifferentiation of a

theca interna cell, which initiates close to the theca externa and spreads inward towards the basement membrane. Together, these results suggest that the primary transition in the differentiation of theca interna cells is specified by a basic clock mechanism operating within the secondary follicle and may be triggered by the theca externa (Erickson *et al.*, 1985). The consequence of the first transition to the differentiated state is evident. By virtue of the LH receptor, the fibroblast-like precursor cell changes to one with a theca interna phenotype. This second step in the differentiation process occurs in the early tertiary follicle and converts the non steroidogenic theca interna cells to a polygonal type with the fine structure typical of active steroid synthesizing cells.

One interesting cytologic aspect of the theca interna is the presence of what appears to be subtypes of differentiated theca interna cells from animal models (Quattropani, 1973). In humans, Hiura *et al.* (1981), reported three different cell types in the theca interna of secondary follicle: fibroblast-like cells, transitional cells, and theca cells. These three cell types were always in contact with one another. The fibroblast-like cell had an elongate nucleus, well developed rough endoplasmic reticulum, Golgi apparatus, rod-shaped mitochondria with lamellar cristae, a few lipid droplets, and free ribosomes. The transitional cell, ellipsoidal in shape, contained an oval nucleus, rough endoplasmic reticulum, Golgi apparatus, lipid droplets, elongate or oval mitochondria with lamellar or tubular cristae, a relatively developed smooth endoplasmic reticulum, and lysosomes (Figure 15). The theca cells with

steroid-secreting activity are characterized by a round, oval, or somewhat undulated nucleus, rough endoplasmic reticulum, Golgi apparatus, lipid droplets, oval mitochondria with tubular or vesicular cristae, abundant smooth endoplasmic reticulum, and lysosomes (Figure 15). At the antral stage, theca cells were increased in number compared with those in the theca interna of the secondary follicle (Hiura *et al.*, 1981) (Table 6). This is expected as the follicle is growing, the number of fully differentiated steroidogenic theca cells increases to produce steroidogenic hormone substrates for granulosa cells and the follicle needs.

Table 6. The number of three cell types (fibroblast-like cells, transitional cells, and theca cells) in the theca interna of the primordial, secondary and antral follicles Hiura *et al.* (1981).

	Primordial follicles	Secondary follicles	Antral follicles
Fibroblast-like cells	100 (100%)	76 (60.3%)	88 (25.7%)
Transitional cells	0 (0%)	29 (23.0%)	103 (30.0%)
Theca cells	0 (0%)	21 (16.7%)	152 (44.3%)

Theca interna cells show the typical ultrastructural features characteristic of a steroid-secreting cell, namely numerous mitochondria with tubular or vesicular cristae, abundant agranular endoplasmic reticulum, and lipid vesicles, rough endoplasmic reticulum, Golgi apparatus, and lysosomes. These ultrastructural features correspond to the specialized biochemical characteristics of steroid-secreting cells (Figure 15).

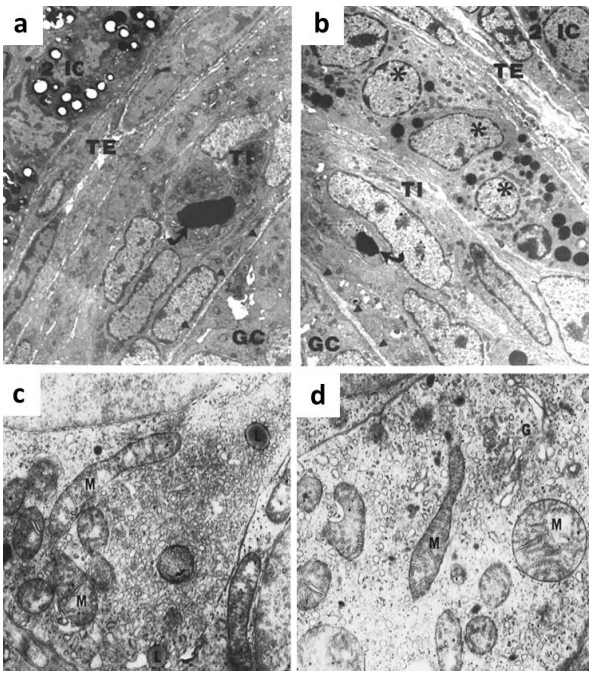


Figure 15. Electron micrographs showing the early steps in theca interna differentiation. Unspecialized fibroblast-like cells in the theca of a non-LH stimulated secondary follicle (a); LH-stimulated follicle showing some pro-theca interstitial cells transforming into polygonal steroidogenic cells (*) (b). Note that the process proceeds as a wave from the periphery to the more central regions and that the switch begins with those cells nearest the theca externa (b). Parts of the transitional cell in the theca interna of the secondary follicle. Lipid droplets (L), mitochondria (M) with lamellar or tubular cristae, and relatively well developed smooth endoplasmic reticulum are seen (c). A part of a fairly well differentiated transitional cell in the theca interna of the secondary follicle. Golgi apparatus (G), mitochondria (M) with lamellar or tubular cristae, and numerous elements of the smooth endoplasmic reticulum (d). Granulosa cells (GC): basement membrane {arrowheads): theca interna (TI): capillaries (arrow): theca externa (TE): secondary interstitial cells (2 IC). *Adapted from Hiura et al. (1981) and Erickson et al. (1985).*

2.2.6 Theca externa

Theca externa is defined as the outermost layer of the follicle. It has smooth muscle-like cells, macrophages, and fibroblasts that produce extracellular collagen to provide a supportive semi-rigid structure around the follicle. The theca externa has an elaborate vascular network to supply nutrients and oxygen to the follicle (Bulun, 2016; Richards *et al.*, 2015). The theca externa in antral follicles are innervated by autonomic nerves that seem to play an active role in their contraction (Erickson, 1995; Erickson, 2000). While the full significance of the theca externa layer is not yet well known, but the regulated contraction of these cells has been involved in the processes of both ovulation and atresia (Erickson, 2000).

2.3 Two-cell, two gonadotropin theory

The classic "two-cell, two-gonadotropin" model describes the cooperation between theca and granulosa cells to ensure the production of estradiol (the most bioactive ovarian estrogenic steroid) during the follicular phase (Edson *et al.*, 2009). The theca cells possess all of the cellular and enzymatic components required for *de novo* androgen production from circulating cholesterol. These androgens subsequently diffuse through the basement membrane and serve as substrates for the granulosa cells, which express the enzymes required to convert them to estradiol. Theca cell steroidogenesis is mainly under the control of LH, which activates the cAMP signaling pathway via a G protein-coupled receptor (Short, 1964). LH/cAMP induces the expression of the key

steroidogenic enzymes StAR (translocate cholesterol from the outer mitochondrial membrane to the inner membrane where CYP11A1 is located and performs the first step of steroidogenesis by converting cholesterol to pregnenolone. This steroid is then converted mainly to androstenedione in most species via the successive actions of CYP17A1, and HSD3B resides in the smooth endoplasmic reticulum. Androstenediones will diffuse through the basement membrane to granulosa cells, and there these androgens are then further transformed into estradiol by FSH-stimulated granulosa cells (Figure 16).

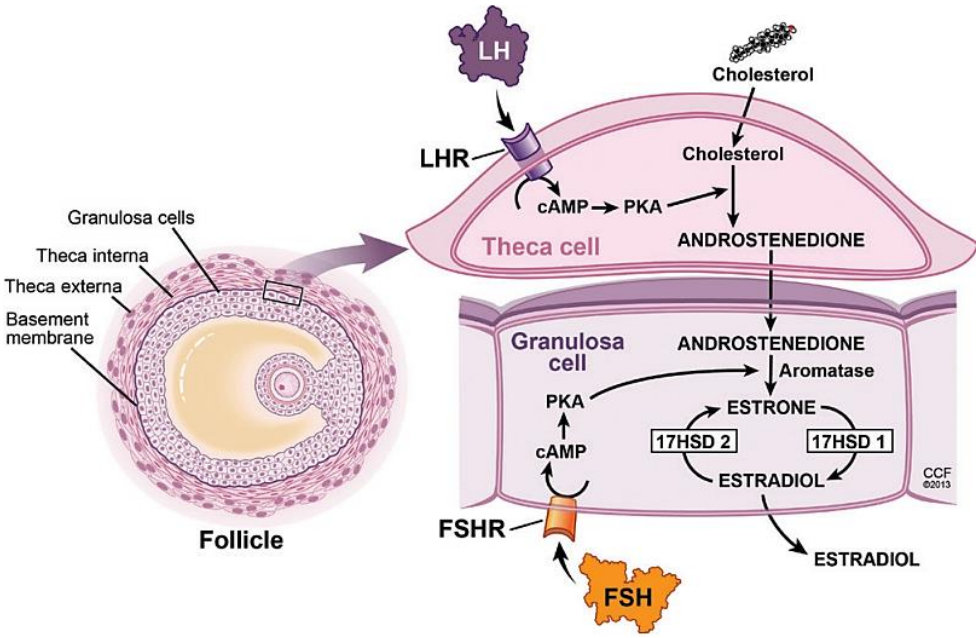


Figure 16: Schematic representation of two-cell, two-gonadotropin theory in small antral follicles in mammalian species. *From Doshi, Agarwal (2013).*

The secretion of progesterone is essential for ovulation, embryonic implantation, and the maintenance of pregnancy. The chain of events leading to progesterone secretion begins with the preovulatory LH surge. The latter stimulates the granulosa and theca cells to undergo a terminal differentiation process called luteinization, characterized by growth arrest, tissue remodeling, angiogenesis, and gene expression changes that will lead to the formation and function of the corpus luteum (Stocco *et al.*, 2007). However, our pilot study with immunohistochemistry shows there is not much but scattered expression of Ki67 in only small luteal (paraluteal) cells meaning the cellular growth is not totally arrested (Figure 17).

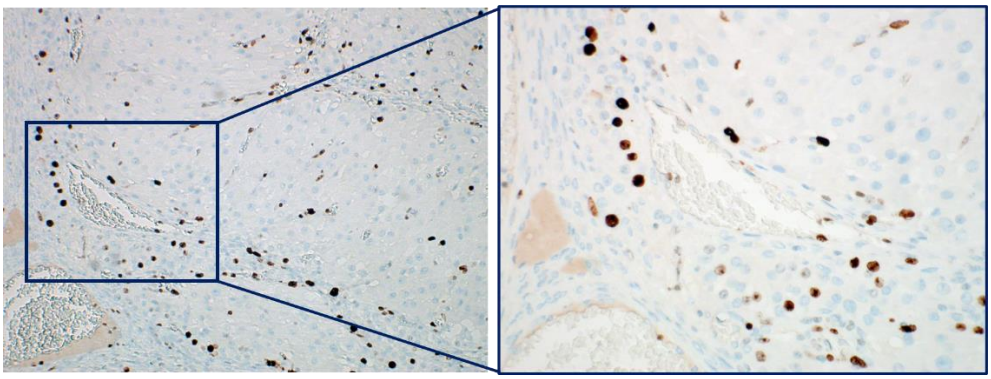


Figure 17: Ki67 immunohistochemistry in human corpus luteum.

Androgens produced by theca cells exert paracrine functions within the ovary by binding and activating the androgen receptor (AR; NR_3C_4) present in granulosa, theca, and stromal cells (Fowler *et al.*, 2011; Lenie

and Smitz, 2009; Yang and Fortune, 2006). Targeted disruption of the AR (*Nr3c4*) (Dewailly *et al.*, 2016; Sen and Hammes, 2010; Sen *et al.*, 2014) in mice in cell culture experiments and in vivo hormone treatments revealed the critical roles of androgens in follicular development (Dewailly *et al.*, 2016; Lebbe and Woodruff, 2013; Richards, 1994; Yang and Fortune, 2006). Now, it is a fact that androgens are made in small follicles and regulate the expression of FSH receptor (*Fshr*), leading to early follicle growth (Dewailly *et al.*, 2016; Sen *et al.*, 2014). Eventually, androgens with FSH promote expression of *Cyp19a1* (aromatase) (Fitzpatrick and Richards, 1991) and *Lhr* in granulosa cells of antral follicles (Hsueh *et al.*, 2015; Richards, 1994). Androgens, along with activins, also regulate the expression of connective tissue growth factor (*Ctgf*) in granulosa cells (Slee *et al.*, 2001). Moreover, androgens act in granulosa cells via AR canonical and noncanonical pathways to promote cell survival (Sen *et al.*, 2014). Recent studies in which *Ar* was selectively disrupted in theca cells of *Cyp17a1*$^{Cre+}$ mice show that loss of theca AR does not impair follicular growth or fertility (Ma *et al.*, 2017). The possible roles of androgens in the stroma, fibroblastic, immune cells within the ovary are less well characterized but appear to impact normal processes in the ovary and the ovarian phenotype of women with polycystic ovary syndrome (PCOS).

Estrogens also impact theca cell functions, as confirmed by the conditional depletion of *Esr1* in theca cells (Lee *et al.*, 2009). The mutant mice become progressively infertile and have elevated expression of *Cyp17a1*, mildly increased testosterone, and reduced levels of serum

LH. Since cystic follicles are present even with low LH, this may be related, in part, to changes in insulin signaling. It is shown that diet-induced obesity in mice leads to increased expression of theca cell *Cyp17a1* and testosterone. Conditional depletion of the insulin receptor in theca cells significantly weakens the diet-induced changes in *Cyp17a1* and androgen production and improves fertility without changes in the LH receptor (Wu *et al.*, 2014). By contrast, conditional depletion of *Pten*, a downstream regulator of insulin signaling, leads to increment expression of *Lhr*, *Star*, *Cyp17a1*, and *Cyp11a1*; androgen excess; estrous cycle disorder; and early loss of fertility. Atretic follicles are present in the ovaries of these mice rather than cystic follicles, which is the characteristic of most high androgen mouse models (Lan *et al.*, 2017). These data indicate that more severe changes occur in the follicles of these mice compared with those in mice with theca cell insulin receptor deficiency.

2.4 Theca cell fate

2.4.1 Ovulation and corpus luteum formation

Different from the events in small growing follicles, noticeable changes occur in gene expression profiles in the theca cells following LH induction during ovulation (Christenson *et al.*, 2013). One is the significant changes in the follicular vascular system following ovulation. At this time, vessels rapidly invade the granulosa cell layer and contribute to the formation of the corpus luteum (Feng *et al.*, 2017; Stocco *et al.*, 2007). Targeted disruption of mitogen-activated protein

kinases (MAPK) 1/3 and extracellular-regulated kinases ½ (ERK1/2) in granulosa cells prevents both ovulation and the invasion of vascular cells into the granulosa cell layer (Fan *et al.*, 2009). These observations provide evidence that the MAPK pathway is essential for LH induction during ovulation, and in the absence of ovulation, vascular invasion does not occur (Figure 18). Moreover, targeted disruption of genes encoding the transcription factors, CCAAT enhancer-binding proteins α and β in granulosa cells, would also block ovulation and vascular invasion (Fan *et al.*, 2011) (Figure 18). Gene expression studies on the profile of the granulosa cells of these mice demonstrate the ADAMTS1 gene, in addition to VEGF, is markedly increased during ovulation and likely contributes to the vascular invasion of the granulosa cell compartment (Fan *et al.*, 2011). Recently, LIF has been implicated as a modulator of ovulation in primates, and its function may be mediated, in part, in theca and stromal cells, as well as in granulosa cells (Murphy *et al.*, 2016; Robker and Russell, 2016). Immune cells are also required for ovulation and vascular invasion of the newly formed corpus luteum. Substantial evidence demonstrates the depletion of immune cells either by clodronate treatment (Turner *et al.*, 2011) or diphtheria toxin-mediated immune cell disruption (Care *et al.*, 2013; Cohen-Fredarow *et al.*, 2014), before ovulation, blocks corpus luteum formation. While the recruitment of immune cells is dependent on follicular expression of cytokines and chemokines such as interleukin 6 (IL-6) and chemokine (c-c motif) ligand 20 (Adams *et al.*, 2016; Al-Alem *et al.*, 2015), expression of these factors appears to rely on LH, androgens, and IL-6 (Adams *et al.*, 1991). It is thought that high levels of VCAM1 may also contribute to immune cell

recruitment (Solano *et al.*, 2011). Hyperstimulation of the murine ovary with gonadotropins leads to ovarian hyperstimulation syndrome that is associated with elevated cytokines, including IL-6, vascular changes, and immune cell invasion (Wei *et al.*, 2013).

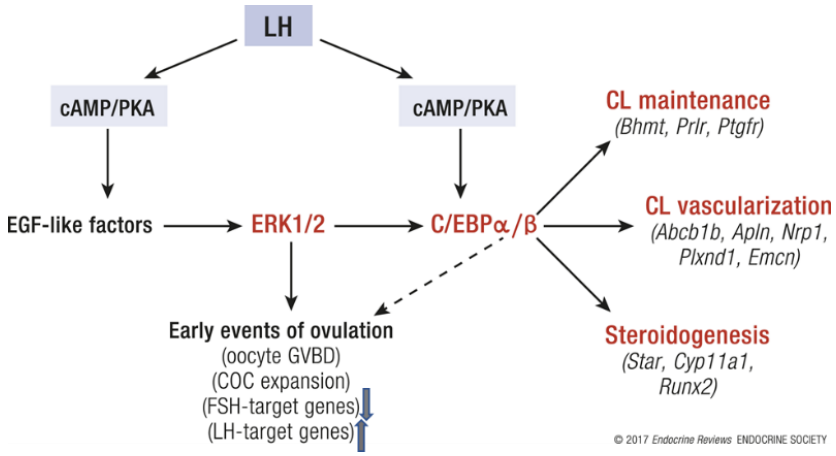


Figure 18. Schematic view of signaling events induced by the LH surge and regulate the processes of ovulation and luteinization in mammals. The LH surge induces the epidermal growth factor (EGF)–like factors (amphiregulin, epiregulin, and betacellulin) by activating the adenylyl cyclase, cyclic adenosine monophosphate (cAMP), and protein kinase A (PKA) pathway. These EGF-like factors activate the EGF receptors, leading to the activation of extracellular-regulated kinases [ERK1/2, also known as mitogen-activated protein kinase (MAPK)3/1]. These kinases, along with PKA, activate the transcription factors CAAT and enhance binding proteins α and β (C/EBPα/β). ERK1/2 is essential for activating oocyte maturation, cumulus cell oocyte complex (COC) expansion, ovulation, and the downregulation of FSH target genes such as *Cyp19a1* and *Fshr*. C/EBPα/β is essential for regulating genes associated with the formation, maintenance, and vascularization of the corpus luteum (CL) as well as steroidogenesis. *Adapted from* Richards *et al.* (2017).

After ovulation, the follicle remains and transforms into another endocrine organ, the corpus luteum. Progesterone is the major functional steroid product of the corpus luteum and is essential to prepare the endometrium for blastocyst implantation and to maintain early pregnancy (Devoto *et al.*, 2009). In most mammals, both theca and granulosa cells contribute to the formation of the corpus luteum. They morphologically develop into two appearances, small and large cells with discrete functions (Ohara *et al.*, 1987). Theca–lutein (paraluteal) cells in primates remain at the outer edge of the corpus luteum, whereas granulosa–lutein (large luteal) cells are more central (Stocco *et al.*, 2007). The small luteal cells are insulated from the theca cells, while the large luteal cells are originated from the granulosa cells (Fujiwara *et al.*, 1996). Unlike the ovarian follicle, where theca cells utilize cholesterol for de novo steroidogenesis, both the granulosa and theca-derived luteal cells have this ability in the corpus luteum. This increase in the capacity of de novo steroidogenesis leads to the greater production of progesterone by the corpus luteum compared to the follicle (LaVoie, 2017). Since de novo cholesterol synthesis is energetically expensive to cells, they may only be significant when intracellular stores are depleted. However, lipoproteins from plasma are accepted to be the primary source of cholesterol for steroidogenesis. While low-density lipoproteins (LDL) are a major source of sterol in larger mammals (Grummer and Carroll, 1988), high-density lipoprotein (HDL) is the major source in rodents (Khan *et al.*, 1985). During luteinization, while luteinized theca cells retain their progesterone production functions, major changes occur in granulosa cells. Luteinized granulosa cells gain the ability for

massive de novo steroidogenesis. This ability is caused by the upregulation of the proteins involved in the delivery of cholesterol substrate into the mitochondria, transfer the cholesterol from the outer mitochondrial membrane into the inner one, and the components of CYP11A1 complex, which reside in the inner membrane to convert cholesterol into the first steroid hormone pregnenolone (LaVoie and King, 2009). The cholesterol translocation from the outer to the inner mitochondrial membrane is believed to be the critical rate-limiting step in de novo steroidogenesis both in ovarian follicles and luteal cells. This task is accomplished by StAR protein (Clark *et al.*, 1994; Stocco and Clark, 1996). In the meantime, HSD3B abundance increases above follicular levels to convert the augmented produced pregnenolone into progesterone in the smooth endoplasmic reticulum (LaVoie, 2017) (Figure 19).

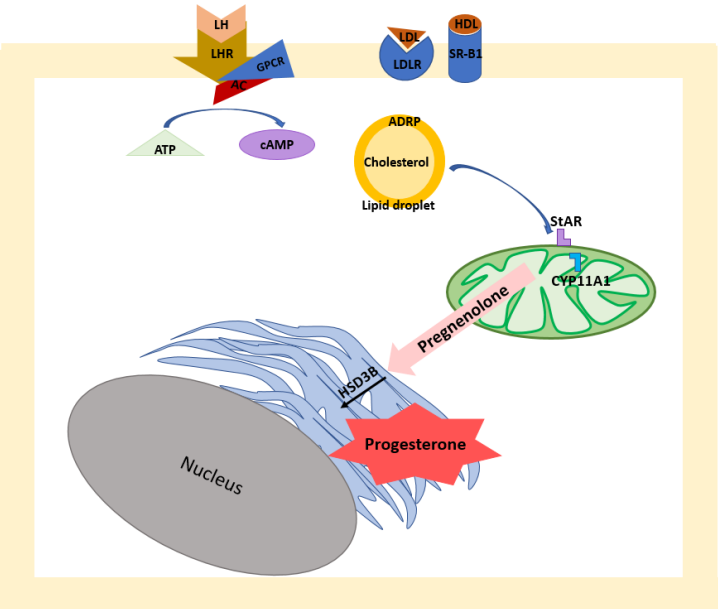


Figure 19: In the corpus luteum, luteal cells transform cholesterol into pregnenolone and produce progesterone. Cholesterol is either taken up from extracellular lipoprotein through the actions of the LDL receptor (LDL only) and scavenger receptor B1 (SR-B1, cholesteryl esters from HDL and LDL) or can be synthesized by the cell. Intracellular- and extracellular-derived cholesterol is stored as cholesteryl esters in lipid droplets. Liberated free cholesterol is transported to the outer mitochondrial membrane, where StAR will transfer cholesterol to the inner mitochondrial membrane, where CYP11A1 resides. CYP11A1 converts cholesterol to pregnenolone. Pregnenolone is converted to progesterone by the actions of HSD3B in the smooth endoplasmic reticulum.

Specific signaling cascades are modified by the terminal differentiation of theca and granulosa cells to luteal cells (Stocco *et al.*, 2007). Of particular relevance to what has been mentioned before, the HH

signaling components, *Ptch1*, *Smo*, and *Gli1*, decrease rapidly in residual tissue (containing theca) and granulosa cells following hCG administration to eCG-primed mice (Ren *et al.*, 2009). PTCH1 is also absent in the CL of adult mice (Wijgerde *et al.*, 2005). Luteal cell expression of IHH and DHH is negligible, indicating that HH signaling is terminated in luteinized granulosa cells as well (Ren *et al.*, 2009; Wijgerde *et al.*, 2005). Thus, whereas HH signaling appears to impact theca cell steroidogenic and theca *α*-smooth muscle actin–positive cells in growing follicles, these pathways do not appear to play a role in regulating steroidogenesis or vascular elements in luteal cells. Whether similar changes in HH signaling occur in primates or other species is not yet known. Also, AR is expressed in theca and granulosa cells and corpora lutea of primates, felines, and rodents (Amelkina *et al.*, 2016; Hild-Petito *et al.*, 1991; Szołtys *et al.*, 2007). Nevertheless, the functions of androgens and AR in corpora lutea are not well characterized (Richards *et al.*, 2017).

As mentioned before, luteinization begins shortly after the preovulatory LH surge, and lutein cells are fully differentiated one week after ovulation (day 21 or 22 of a 28-day menstrual cycle). If the egg is not fertilized, the corpus luteum undergoes apoptosis (Shikone *et al.*, 1996), regressing rapidly, ceasing all progesterone production, and leaving in its place a small, scar-like structure called the corpus Albicans (K.Hughes and L.Pate, 2019). In histology sections, corpus Albicans is seen as a dense connective tissue aggregate (Williams and Erickson, 2012). Degradation of the corpus luteum will cause menstruation and the beginning of a new ovulatory cycle. This process will continue each

month until the end of the female's reproductive years with the cessation of ovulatory function, termed menopause (Rojas *et al.*, 2015).

2.4.2 Follicle atresia and theca cells

Growing follicles that did not succeed in ovulating go through atresia in the ovary. In this process, granulosa cells and oocyte die, but it is believed that theca interna cells undergo marked hypertrophy. These hypertrophied cells stay in the atretic follicle region and give rise to the so-called secondary interstitial cells (Dawson and McCabe, 1951; Deanesly, 1972; Guraya and Greenwald, 1964; Kingsbury, 1939; Rennels, 1951) (Figure 20). These cells maintain their specialized ultrastructure of steroid secreting cells (Al-Mehdi, 1979; Carithers and Green, 1972; Erickson, 1983; Mori and Matsumoto, 1973) and continue to respond to LH with increased androstenedione production (Erickson, 1983; McNatty *et al.*, 1979; Rice and Savard, 1966). In this sense, secondary interstitial cells continue to exhibit properties of their precursors, the theca interna cells (Erickson *et al.*, 1985). However, there is a significant difference among these two cell populations: secondary interstitial cells are innervated (Burden, 1972; Lawrence Jr and Burden, 1976; Lawrence Jr and Burden, 1980; Neilson *et al.*, 1970; Svensson *et al.*, 1975). In vivo (Burden *et al.*, 1977; Capps *et al.*, 1978) and in vitro (Dyer and Erickson, 1985) studies on innervation of secondary interstitial cells led to the concept that precise information from the brain is transmitted directly to the ovaries via secondary interstitial cells (Erickson *et al.*, 1985). These cells are believed to be the targets of

noradrenergic innervation that control steroidogenic activity (Strauss and Williams, 2019). Unfortunately, information about secondary interstitial cells' life span and fate is not available. Only one old publication mentioned that secondary interstitial cells might incorporate into the ovarian stroma (Nicosia, 1986). The ovarian stroma contains fibroblastic cells that express some steroidogenic enzymes, even during menopause (Dupont *et al.*, 1992; Havelock *et al.*, 2005). Whether secondary interstitial cells remain in the ovary and are responsible for androgen production in menopausal stromal cells is not yet defined and needs more investigation.

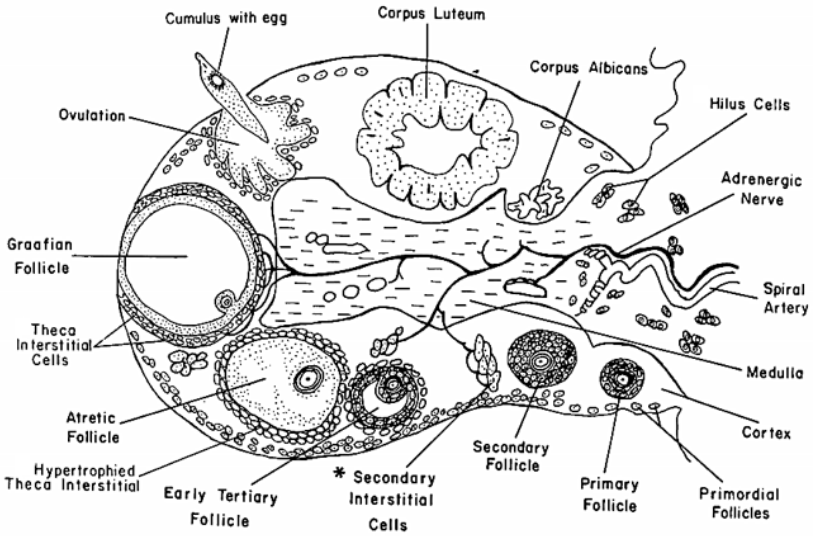


Figure 20. Location of ovarian secondary interstitial cells. Schematic figure showing the morphology and architecture of a typical mammalian ovary during the reproductive period. The secondary interstitial cells (*) are embedded in the connective tissue in the outer cortex and are innervated by adrenergic nerves. *From Erickson et al. (1985).*

2.5 Markers for theca interna and luteal cells in human

2.5.1 Aminopeptidase-N (ANPEP / CD13)

The very first study is by Fujiwara *et al.* (1992a), showing by IHC that aminopeptidase-N (CD13), a membrane-bound protein peptidase, is detected on theca interna of secondary, antral, and preovulatory follicles and corpus luteum. Since CD13 is not detected on granulosa cells, theca externa cells, and ovarian stromal cells, this could be used as a specific marker for theca interna cells (Fujiwara *et al.*, 1992a). CD13 may play an essential role in folliculogenesis (Fujiwara *et al.*, 1992a). In a recent study, using immunostaining, flow cytometry, bulk, and single-cell RNA sequencing, Man *et al.* (2020) identified CD13 (also known as ANPEP) as a surface marker for theca interna cell cluster. It is known that CD13 is involved in a wide range of physiological functions. It processes peptide hormones at the cell surface and promotes angiogenesis, growth, and cancer cells' invasive potential (Wong *et al.*, 2012). Regarding the vital function of theca cells in establishing vascular support for growing follicles, the presence of CD13 in this layer is not surprising; however, the specific expression and protein localization of CD13 in only theca interna suggests a peptidase function that is unique to these cells (Man *et al.*, 2020). As theca cells become theca lutein cells, it seems that CD13 expression decreases and the protein becomes undetectable (Figure 21).

2.5.2 Dipeptidyl peptidase IV (DPP IV/ CD26)

Dipeptidyl peptidase IV (DPP IV/ CD26) is a membrane-bound protein peptidase on granulosa cells, theca cells of growing, preovulatory and

atretic follicles, as well as corpus luteum (Fujiwara *et al.*, 1992b). The expression of CD26 becomes stronger in luteinized granulosa and theca cells by timing (Fujiwara *et al.*, 1992b). These results indicate that CD26 is a useful differentiation marker of human luteal cells (Fujiwara *et al.*, 1992b) (Figure 21).

2.5.3 NOTCH1

The NOTCH signaling pathway is active in both embryonic and postnatal ovaries and plays important roles in follicle assembly, growth, meiotic maturation, ovarian vasculogenesis, and steroid hormone production (Vanorny and Mayo, 2017). NOTCH signaling in the ovary occurs between germ and granulosa cells, between adjacent granulosa cells, and between the ovarian vasculature cells (Vanorny and Mayo, 2017). *Notch1* and *Notch4* receptors and their ligands, *Jagged-1*, *delta-like protein 1 and 4*, are expressed within luteinized theca and granulosa cells reviewed by (Vanorny and Mayo, 2017). Studies in mice on *Notch1*, *2*, *3*, and *4*, and their ligands in all the follicle stages and corpus luteum demonstrated while *Notch1* is not expressed in the ovarian stroma, oocytes, and follicular granulosa, and theca cells, it is specifically expressed in small and large luteal cells as well as endothelial cells and blood vessels (Accialini *et al.*, 2015; Hernandez *et al.*, 2011; Murta *et al.*, 2015). Suppression of NOTCH signaling by N-[N-(3,5-Difluorophenacetyl-L-alanyl)]-S-phenylglycine t-Butyl ester intrabursal injection in mouse causes a decrease in progesterone production and increase luteal cell apoptosis reviewed by (Vanorny and Mayo, 2017).

These findings suggest a novel role for the NOTCH pathway in the regulation of luteal function in response to progesterone stimulation, meaning an important relationship between the actions of progesterone and the NOTCH signaling pathway (Vanorny and Mayo, 2017).

Unlike mouse ovaries, only NOTCH1 immunostaining in the human ovary showed specific staining for endothelial cells and luteinized theca and granulosa cells (Figure 21).

2.5.4 Adipose differentiation-related protein (ADRP)

ADRP is a member of the perilipin (PLIN) protein family. It serves as lipid droplets coat proteins and organizing centers for enzymes and transporters in lipid metabolism (Brasaemle, 2007; Kimmel *et al.*, 2010; Olofsson *et al.*, 2009). The presence of both ADRP (Londos *et al.*, 1995) and hormone-sensitive lipase (HSL) (Lobo *et al.*, 2009) in the ovary suggests that LH via activation of the cAMP and the PKA signaling pathway may regulate the phosphorylation of PLINs and HSL to hydrolyze cholesteryl esters stored in the lipid droplets in luteal cells to produce substrate for progesterone synthesis (Talbott and Davis, 2017) (Figure 21).

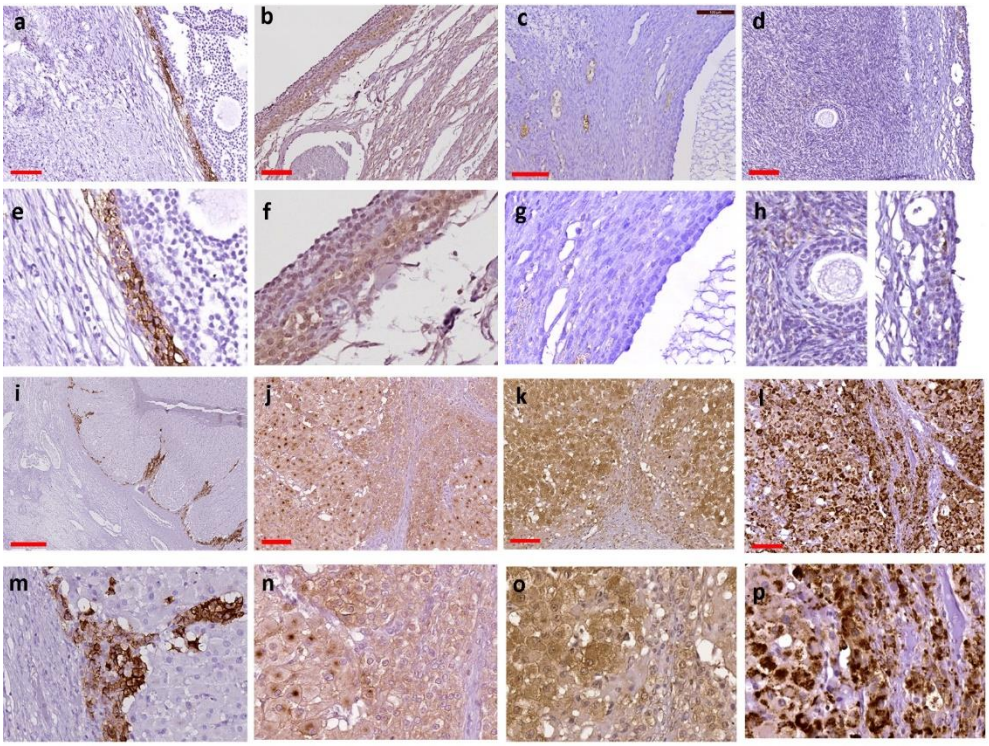


Figure 21: Immunostaining of CD13 (a, e, i, m), CD26 (b, f, j, n), NOTCH1 (c, g, k, o), and ADRP (d, h, l, p) in the antral follicles (a, b, c, d) with higher magnification (e, f, g, h) and the corpora lutea (i, j, k, l) with higher magnification (m, n, o, p). Scale bars: 100 µm (a, b, c, d, j, k, and l), 500 µm (i).

Chapter 3:

Personal contribution, objectives, and results

For cancer patients of childbearing age, fertility restoration after disease remission often becomes an important concern. For those types of cancer patients at a high risk of recurrence of the primary disease after reimplanting cryopreserved ovarian tissue, the transplantable engineered ovary can be an alternative. The transplantable engineered ovary is responsible for maintaining the original structure of follicles, ensuring proper communication between follicles and surrounding ovarian cells, preserving their interaction with the ECM, and supplying factors involved in follicular survival and development. Studies on developing the physical aspects of the transplantable engineered ovary have been investigated in our team (Amorim *et al.*, 2009; Chiti *et al.*, 2015; Chiti *et al.*, 2017c; Chiti *et al.*, 2018; Dolmans *et al.*, 2007; Dolmans *et al.*, 2008; Ouni *et al.*, 2019; Ouni *et al.*, 2019; Vanacker *et al.*, 2014; Vanacker *et al.*, 2012). Other studies in our team on biological properties proved that endothelial cells are essential to improve vascularization in grafts (Chiti *et al.*, 2015; Dath *et al.*, 2011; Luyckx *et al.*, 2014; Soares *et al.*, 2015c), and stromal cells are necessary to degrade the artificial scaffold and synthesize their own ECM (Chiti *et al.*, 2015; Luyckx *et al.*, 2014; Soares *et al.*, 2015c). One major remaining part to solve is theca cell differentiation in the transplantable engineered ovary. Even though there is little information on theca cell recruitment and differentiation, few studies in mammals suggest different hypotheses for the origin of theca cells and their ontogenesis. In mouse ovary, Honda *et al.* (2007) showed that theca progenitor cells express *Gli3* and *Ptch1* as markers, while Liu *et al.* (2015) reported that there are two origins for theca progenitor cells in mice embryonic gonads, WT1-positive mesenchymal

cells intrinsic to the ovary and GLI1-positive cells that migrate from the mesonephros into the ovary. On the other hand, in cows (Orisaka *et al.*, 2006) and goats (Qiu *et al.*, 2013), it appears that all ovarian cortical stromal cells can potentially differentiate into theca cells when in contact with granulosa cells.

Due to the lack of information regarding the theca cell population in the human ovary, my work has been focused on three principal issues:

I. **Assessment of the steroidogenic pathway in human follicles**

   Article 1

II. **Investigation of the presence of a precursor theca cell population in human ovaries**

   Article 2

III. **In vitro differentiation of human theca cells**

   Articles 3 and 4

3.1 Assessment of the steroidogenic pathway in human follicles

The association between theca and granulosa cells is pivotal to steroid biosynthesis in the ovary. During the late secondary follicle stage, theca cells form a layer around granulosa cells, and afterward, their steroidogenic function commences under the control of LH. By occupation of the LH receptor by LH, it activates the cAMP signaling pathway via a G protein-coupled receptor leading to the steroidogenic cascade in theca cells. The majority of available information on canonical follicle steroidogenesis mechanisms relates to findings from species other than humans. However, it is important to remember that interspecies differences are often reported (Nilsson and Skinner, 2001). Human pathway patterns appear to be distinct in terms of tissue expression, activity, and subcellular localization (Honda *et al.*, 2007). To the best of our knowledge, the specificity of the human steroidogenic pathway has not yet been documented in the ovary. Moreover, we do not know at which stage of follicle development, different enzymes start to be expressed in human theca cells. Apart from an obvious need to identify basic mechanisms of action, clarifying the workings of this cascade in human tissue would promote the further advancement of theca cell differentiation experiments to support the creation of new technologies, more specifically, the development of a transplantable engineered ovary. For this, we carried out a complete immunohistochemical analysis using all the steroidogenic markers that characterize theca cells, named StAR, CYP11A1, CYP17A1, HSD3B, and LH receptor. Additionally, we decided to evaluate ADRP as a marker for

lipid droplets containing esters as substrates for theca cells to produce steroidogenic hormones. We analyzed ovarian tissue from nine adult women, most (n=8) with breast cancer type 1 (BRCA1) and or breast cancer type 2 (BRCA2) mutations undergoing prophylactic bilateral oophorectomy. Pictures were taken of the theca layer of secondary, small (<3000 μm), and large (>3000 μm) antral follicles and corpora lutea at 100X magnification. By using the ImageJ software, we were able to analyze the covered surface area and expression intensity of each protein at each stage, known as the staining index. Our results demonstrated that each enzyme plays a specific and indispensable role in steroidogenesis. As biosynthesis progresses along with follicle development, enzyme levels exhibit different expression patterns, but all are increasing. This study, conducted for the first time on the human ovarian tissue, provided invaluable information to localize and quantify key steroidogenic proteins at both intracellular and tissue levels. Findings from this study may suggest new insight on pathological conditions involving the human ovary, such as androgen-secreting tumors of the ovary and other disorders associated with ovarian theca cells in patients with PCOS.

Article 1

Biology of Reproduction, 2020, 102(1), 145–155
doi:10.1093/biolre/ioz167
Research Article
Advance Access Publication Date: 28 August 2019

OXFORD

Research Article

Immunodetection and quantification of enzymatic markers in theca cells: the early process of ovarian steroidogenesis†

P. Asiabi[1,‡], E. C. R. Leonel[1,‡], E. Marbaix[2,3], M.M. Dolmans[1,4], and C.A. Amorim[1,*]

[1]Pôle de Recherche en Gynécologie, Institut de Recherche Expérimentale et Clinique, Université Catholique de Louvain, Brussels, Belgium, [2]Pathology Department, Cliniques Universitaires Saint-Luc, Brussels, Belgium, [3]Cell Biology Unit, de Duve Institute, Université Catholique de Louvain, Brussels, Belgium, and [4]Gynecology and Andrology Department, Cliniques Universitaires Saint-Luc, Brussels, Belgium

***Correspondence**: Pôle de Recherche en Gynécologie, Institut de Recherche Expérimentale et Clinique, Université Catholique de Louvain, Avenue Mounier 52, bte B1.52.02, 1200 Brussels, Belgium. Tel: +32(0)27645287; E-mail: christiani.amorim@uclouvain.be

†**Grant Support**: This study was supported by grants from the Fonds National de la Recherche Scientifique de Belgique [FNRS] (C. A. Amorim is an FRS-FNRS Research Associate; grant MIS #F4535 16 awarded to C. A. Amorim; grant 5/4/150/5 awarded to M. M. Dolmans; grant ASP-RE314 awarded to P. Asiabi) and the Fundação de Amparo à Pesquisa do Estado de São Paulo [FAPESP] (PhD grant 2016/22947–8 awarded to E. C. R. Leonel), and donations from the Ferrero family.

‡P. Asiabi and E.C.R. Leonel are joint first authors.

Received 3 April 2019; Revised 21 June 2019; Accepted 22 August 2019

Abstract

The association between theca cells (TCs) and granulosa cells is pivotal to steroid biosynthesis in the ovary. During the late secondary follicle stage, TCs form a layer around granulosa cells, after which their steroidogenic function falls under the control of luteinizing hormone (LH) that activates the cAMP signaling pathway via a G protein-coupled receptor. In addition to perilipin-2, a marker for lipid droplets containing esters as substrates for TCs to produce steroidogenic hormones, other essential proteins, like steroidogenic acute regulatory protein (StAR), cytochrome P450 11A1, cytochrome P450c17, 3 beta-hydroxysteroid dehydrogenase/delta 5 —> 4-isomerase type 1, and 3 beta-hydroxysteroid dehydrogenase/delta 5 —> 4-isomerase type 2, play a role in the cascade after luteinizing hormone–choriogonadotropic hormone receptor (LH/CG-R) occupation by LH. The aim of the present study was to assess expression levels and corresponding amounts of LH/CG-R, perilipin-2, and enzymes involved in the steroidogenic pathway of TCs based on follicle stage. Immunohistochemical analysis of each of these proteins was therefore performed on ovarian samples from nine adult women, most ($n = 8$) with BRCA1 and/or BRCA2 mutations undergoing prophylactic bilateral oophorectomy. Pictures were taken of the theca layer of secondary, small (<3000 µm), and large (>3000 µm) antral follicles and corpora lutea at 100× magnification. ImageJ software was used to analyze the surface area and expression intensity of each protein at each stage, known as the staining index. Overall, our data showed that LH/CG-R, perilipin-2, and StAR expression increased in the course of folliculogenesis and luteinization. Similarly, cytochrome P450 11A1, cytochrome P450c17, 3 beta-hydroxysteroid dehydrogenase/delta 5 —> 4-isomerase type 1, and 3 beta-hydroxysteroid dehydrogenase/delta 5 —> 4-isomerase type 2 expression were substantially elevated in TCs during folliculogenesis, evidenced by their coordinated action in

© The Author(s) 2019. Published by Oxford University Press on behalf of Society for the Study of Reproduction. All rights reserved. For permissions, please e-mail: journals.permissions@oup.com

Downloaded from https://academic.oup.com/biolreprod/article-abstract/102/1/145/5554973 by guest on 01 August 2020

terms of area covered and expression intensity. This study, conducted for the first time on human ovarian tissue, contributes to localizing and quantifying expression of key steroidogenic proteins at both intracellular and tissue levels. These findings may shed new light on pathological conditions involving the human ovary, such as androgen-secreting tumors of the ovary and other disorders associated with ovarian TCs in patients with polycystic ovary syndrome.

Summary sentence

This study, conducted for the first time on human ovarian tissue, contributes to localizing and quantifying expression of key steroidogenic proteins at both intracellular and tissue levels and may shed new light on pathological conditions involving the human ovary, such as androgen-secreting tumors of the ovary and other disorders associated with theca cells in PCOS patients.

Key words: enzyme, immunostaining, ovarian follicle, protein expression, steroid biosynthesis.

Introduction

The ovary's ability to develop and release oocytes for fertilization is closely related to its endocrine activity (estradiol and progesterone synthesis), while a network between different cell types is required for follicles to grow and develop. This system includes mainly granulosa cells (GCs) and theca cells (TCs). GCs already surround oocytes by the time of birth [1] and originate from the mesonephros, which develops from the mesoderm layer during gastrulation [2]. TCs, on the other hand, are a group of differentiated cells that start to surround follicles only after their recruitment once they reach the secondary stage.

After follicle activation and initial growth, TCs and GCs act in a synergistic way, known as the two-cell, two-gonadotropin model, to initiate production of steroid hormones in response to luteinizing hormone (LH) and follicle-stimulating hormone (FSH) (reviewed by [3, 4]). Signaling pathways involved in steroid synthesis rely on cytoplasmic factors expressed by both types of cells; TCs convert cholesterol present in blood to androstenedione and testosterone, while GCs metabolize androstenedione to estradiol [1, 5]. TCs therefore perform a remarkable function in ovarian activity and play a crucial role in steroidogenesis in association with GCs, even in in vitro systems [6].

Steroid synthesis by follicular cells is based on proteins like steroidogenic acute regulatory protein (StAR), members of the cytochrome P450 family (11A1, c17 and aromatase), and 3 beta-hydroxysteroid dehydrogenase/delta 5— > 4-isomerase types 1 and 2 (3-beta-HSD I and 3-beta-HSD II) [7]. Studies have reported expression of these proteins even before histological differentiation of the human fetal ovary occurs, as early as the 12th week of gestation [8], with levels of steroidogenic enzyme mRNA increasing in the second trimester of pregnancy [9]. Throughout this developmental phase, modifications in cytochrome P450 11A1, c17, and 3-beta-HSD II expression can already be seen [9]. However, actual steroid synthesis by TCs begins at puberty, when LH peaks become constant and receptor binding stimulates protein expression and androgen production [7]. TC steroidogenesis starts when the luteinizing hormone–choriogonadotropic hormone receptor (LH/CG-R) is occupied by LH, activating the cAMP signaling pathway via a G protein-coupled receptor. Cholesteryl esters stored in lipid droplets are substrates for androgen synthesis. Afterward, cholesteryl esters stored in lipid droplets are translocated by StAR to the inner membrane of the mitochondria, where cytochrome P450 11A1 converts it to pregnenolone, which is then converted to dehydroepiandrosterone (DHEA), androstenedione, and progesterone in the presence of cytochrome P450c17, 3-beta-HSD I, and 3-beta-HSD II in smooth endoplasmic reticulum.

The majority of available information on canonical mechanisms of follicle steroidogenesis relates to findings from species other than humans. However, it is important to bear in mind that interspecies differences are often reported [10] and human pathway patterns appear to be distinct in terms of tissue expression, activity, and subcellular localization [11]. To the best of our knowledge, the specificity of the human steroidogenic pathway has not yet been documented in the ovary. Moreover, we do not know at which stage of follicle development different enzymes start to be expressed in human TCs. Apart from an obvious need to identify basic mechanisms of action, clarifying the workings of this cascade in human tissue would promote further advancement of TC differentiation experiments to support creation of new technologies, more specifically development of a bioengineered transplantable ovary.

The aim of this study was therefore to characterize human TCs at different stages of follicle development in relation to steroidogenic enzyme expression and quantification, lipid storage markers, and LH/CG-R levels. Follicle growth stage was taken into account in order to ascertain temporal patterns and elucidate the sequence of their expression throughout folliculogenesis in the human ovary.

Materials and methods

Source of ovaries and ethical approval

Ovarian tissue samples used in this study were collected from nine adult women (age range: 35–43 years): eight patients were diagnosed with BRCA1 and/or BRCA2 mutations undergoing prophylactic bilateral salpingo-oophorectomy at Saint-Luc's University Hospital and one was bilaterally oophorectomized due to metastasis of pancreatic cancer to the left ovary (Supplementary Table 1). Each ovary was divided into fragments before fixation and dehydration and embedded in several paraffin blocks (Supplementary Table 1). Analysis of the tissue samples by the anatomical pathology department of the hospital did not reveal any modifications or anomalies in the ovaries used in our study. Each ovary contained follicles at different stages of development, as well as corpus luteum (CL). Use of human ovarian tissue was approved by the Institutional Review Board of the Université Catholique de Louvain on November 28, 2016 (IRB reference 2012/23MAR/125, registration number B403201213872).

Morphological evaluation and immunohistochemistry

Each paraffin block containing an ovarian tissue sample was serially sectioned (5-µm-thick sections) and every tenth slide was stained

Downloaded from https://academic.oup.com/biolreprod/article-abstract/102/1/145/5554973 by guest on 01 August 2020

Table 1. Antibodies and immunohistochemical protocols applied.

Antigen	Antibody type	Dilution	Incubation	Positive control
LH/CG-R (PA5–21271; ThermoFisher Scientific, Rockford, USA)	Polyclonal (rabbit)	1:1000 in TBS + 5% BSA + 2% milk	RT 1 h	Adrenal gland
Perilipin-2 (SC-377429; Santa Cruz Biotechnology, Santa Cruz, USA)	Monoclonal (mouse)	1:200 in TBS + 1% NGS + 0.1% BSA	4 °C O/N	Liver
StAR (AB133657; Abcam, Cambridge, UK)	Monoclonal (rabbit)	1:200 in TBS + 1% NGS + 0.1% BSA	4 °C O/N	Testes and placenta
Cytochrome P450 11A1 (HPA016436; Sigma Aldrich/Merck, Darmstadt, Germany)	Polyclonal (rabbit)	1:1000 in TBS + 10% NGS + 1% BSA	4 °C O/N	Testes
Cytochrome P450c17 (ORB5948; Biorbyt, Cambridge, UK)	Polyclonal (rabbit)	1:200 in TBS + 2.5% BSA + 1% milk	4 °C O/N	Adrenal gland
3-beta-HSD I (AB55268; Abcam, Cambridge, UK)	Monoclonal (mouse)	1:100 in TBS + 1% NGS + 0.1% BSA	4 °C O/N	Placenta
3-beta-HSD II (GTX102813; Genetex, San Antonio, USA)	Polyclonal (rabbit)	1:500 in TBS + 1% NGS + 0.1% BSA	4 °C O/N	Placenta

TBS: tris-buffered saline; BSA: bovine serum albumin; RT: room temperature; NGS: normal goat serum; O/N: overnight.

with hematoxylin and eosin (Merck, Darmstadt, Germany) for morphological analysis, follicle and CL localization, and measurement. The remaining slides (Superfrost Plus, Menzel-Glaser, Braunschweig, Germany) were kept for immunostaining (Supplementary Table 1).

Immunohistochemical investigations were carried out using an indirect peroxidase method with a specific antibody for each of the seven selected proteins (Table 1). Briefly, after paraffin removal and rehydration, endogenous peroxidase activity was blocked by incubating the sections for 30 minutes in 3% H_2O_2. Antigen retrieval was performed in Tris EDTA buffer, pH 9.0, for 20 minutes at 96 °C for LH/CG-R and cytochrome P450c17, or citrate buffer, pH 6.0, for 75 minutes at 98 °C for the remaining antigens. Endogenous biotins were blocked only in the LH/CG-R protocol using an avidin-biotin kit (Vector, Burlingame, USA). Nonspecific binding was avoided by incubating sections in Tris-buffered saline with 5% bovine serum albumin (BSA) and 2% milk for LH/CG-R and cytochrome P450c17 or Tris-buffered saline with 10% normal goat serum (NGS) and 1% BSA for the rest. After incubation with primary antibody for 60 minutes for LH/CG-R and overnight for the other antibodies (see Table 1), the sections were incubated for a further 60 minutes at room temperature with secondary antibody: polyclonal goat anti-rabbit biotinylated immunoglobulin (Dako, USA) followed by streptavidin/horseradish peroxidase (HRP) for LH/CG-R, EnVision anti-mouse (Dako, USA) for perilipin-2 and 3-beta-HSD I, and EnVision anti-rabbit (Dako, USA) for StAR, cytochrome P450 11A1, cytochrome P450c17, and 3-beta-HSD II. The primary antibody was omitted in negative controls, and a mixture of FLEX universal negative controls was added for rabbit or mouse antibodies (Dako, USA). Sections were stained with a solution of diaminobenzidine (DAB) (Vector, Burlingame, USA) and counterstained with hematoxylin, before being dehydrated again and mounted for light microscopy analysis.

Follicle classification

Follicles were analyzed at different stages. Since the aim of this work was to elucidate and describe expression of steroidogenic proteins in TCs and luteal cells only, follicles at primordial and primary stages were not taken into account. Follicles were evaluated and classified as follows: *secondary follicles* with two or more cuboidal GC layers but no antrum; *small antral follicles* with an antrum but measuring less than 3 mm in diameter; and *large antral follicles* with an antrum and measuring more than 3 mm in diameter. Antral follicles with no GC layers or showing substantial apoptosis were excluded from the analysis. Regarding CL, no classification was made according to developmental stage.

Digitization and image analysis

The slides were analyzed by light microscopy (Nikon Eclipse, Tokyo, Japan) and digitized using a camera acquisition system (Leica DFC450, Leica Application Suite VA) at 100-fold magnification. The whole area of extension of secondary follicles was captured, so the total number of images taken of individual follicles at this stage ranged from 1 to 4, depending on their size. Antral follicles (small antral and preovulatory) required 6 images for adequate representation, with the exception of earlier stages of small antral follicles, which could be fully accommodated in fewer than 6 images. To ensure that the inner layers of the theca interna were investigated and in order to standardize the capture process for small antral and preovulatory follicles, one layer of GCs was included, delimiting the boundaries of the picture, as shown in Figure 1. This standardization also enabled TC layer localization and identification of the area to be studied. Concerning CL, 6 images were taken of the boundaries of the structures and evaluated in their entirety.

Analysis was undertaken using ImageJ software (version 1.52a, Wayne Rasband, NIH, USA). Irrespective of the number of images obtained, all underwent evaluation and mean values for each were taken into consideration. Regions of interest (containing only TCs in case of follicles) were delineated manually. For CL, entire images were assessed, since small (paraluteal) and large luteal cells were intermingled. If present, folds, bubbles, and artifacts were delimited and excluded prior to analysis by ImageJ. Color deconvolution was applied using hematoxylin and DAB vectors of the software to isolate DAB staining from tissue counterstaining. DAB staining was

Downloaded from https://academic.oup.com/biolreprod/article-abstract/102/1/145/5554973 by guest on 01 August 2020

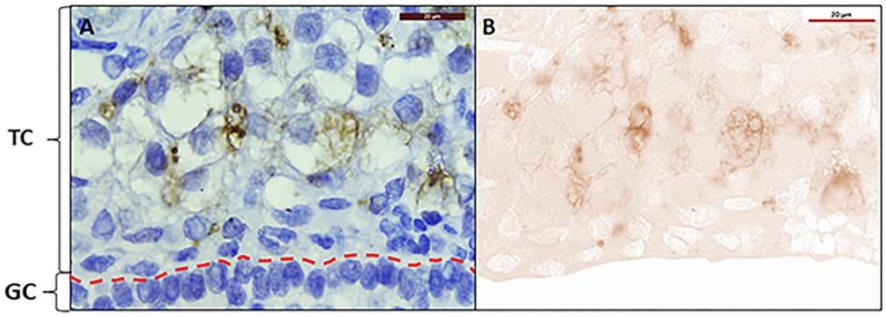


Figure 1. Photomicrograph showing the protocol used to analyze images. Each picture of small and large antral follicles was taken in such a way that one layer of GCs could be identified (shown here by a dashed red line). The area containing only TCs was then selected by the software tool for quantification analysis (A). After selection of the area of interest, deconvolution was applied and the DAB-stained area and its intensity were quantified (B). Bar: 20 µm. GC: granulosa cell; TC: theca cell.

then detected using Rényi's entropy thresholding method (chosen according to stained versus non-stained tissue areas) and stained areas were measured. The same parameters were applied to all slides. Results were expressed for each follicle/CL as a staining index (SI) following the formula:

$$\text{annotation proportion} \times \text{percentage of stained area} \times \text{staining intensity.}$$

where the annotation proportion is the percentage of delineated area in each picture of each individual follicle ($n = 1$ to 6 images per follicle or CL), the percentage of stained area is calculated as (stained area/tissue area) × 100, and staining intensity as (255 − mean intensity of stained pixels).

Statistical analysis

Statistical analysis was conducted using GraphPad Prism 5.0 software (GraphPad Software, Inc., CA, USA). For each immunohistochemical and antibody assay, the mean index obtained from all follicles in a given category was taken into account. Quantitative analysis was based on nonparametric (Kruskal-Wallis) evaluation of differences between the relevant developmental stages of follicles, followed by Dunn's multiple comparison tests. A P-value <0.05 was considered significant.

Results

The number of follicles and CL evaluated by category varied between patients and proteins and is detailed in Table 2. Proteins were mostly present in TCs, but sometimes they were also expressed by other ovarian cells, such as GCs, oocytes, or stromal cells. Expression patterns of each analyzed protein are described below and summarized in Tables 3 and 4 and Figures 5 and 6. Information on the stage of the menstrual cycle at the time of bilateral salpingo-oophorectomy was not recorded.

Expression patterns of different proteins in ovarian tissue

LH/CG-R. LH/CG-R was present in both cortical and medullary regions of the ovaries (Figure 2A and a). There were areas of focal staining in stromal cells (Figure 3C), where patterns of expression were usually cytoplasmic, but sometimes nuclear (Figure 3D). TCs showed intense immunostaining, making it easy to differentiate the TC layer from the surrounding stroma, even if some LH/CG-R-positive stromal cells were occasionally found. GCs and oocytes were negative for LH/CG-R. While CL exhibited widespread positive areas, staining intensity in these structures was not as strong as observed for other proteins. LH/CG-R expression in TCs was not significantly different between secondary, small, and large antral follicles or CL ($P < 0.2919$) but showed a tendency toward increasing patterns with follicle development and CL formation (Figure 5, LH/CG-R, and Figure 6A-1 to A-4).

Perilipin-2. Perilipin-2 was immunolabeled to investigate levels of lipid storage droplets in the cytoplasm of follicular cells at different developmental stages. This protein was only expressed in ovarian cortex, where weak staining was observed in bands of stromal cells. Some foci of darker perilipin-2 staining were identified in stroma surrounding follicle nests.

Despite some perilipin-2 expression in stromal fibroblasts, TC (from secondary follicles on) and luteal cell staining were much more intense than stromal staining (Figure 2B and b). In TCs, perilipin-2 expression was present in the cytoplasm (Figure 3H), limited to a thin theca interna layer (Figure 3G), but it was highly expressed throughout the whole cytoplasm of small circular luteal cells (Figure 6B-4). The cytoplasm of stromal cells was also perilipin-2–positive in areas surrounding CL. Perilipin-2 showed increasing expression patterns and was statistically significant in TCs of large antral follicles ($P < 0.01$) and CL ($P < 0.001$) versus secondary follicles, and in CL ($P < 0.05$) versus small antral follicles (Figure 5, perilipin-2, and Figure 6B-1 to B-4).

StAR. Once cholesterol reaches the outer mitochondrial membrane, it is translocated to the inner membrane by StAR. StAR was immunolabeled in the cytoplasm of some TCs, but with no nuclear staining. Secondary and small antral follicles showed low levels of immunostaining for StAR (Figure 6C-1 and C-2 respectively), and large antral follicles (Figure 6C-3) somewhat minimal expression of this protein, limited to two or three inner layers of the theca interna (Figure 2c).

Downloaded from https://academic.oup.com/biolreprod/article-abstract/102/1/145/5554973 by guest on 01 August 2020

Table 2. Total number of follicles and corpora lutea analyzed for each protein.

Follicle category	Proteins						
	LH/CG-R	Perilipin-2	StAR	Cytochrome P450 11A1	Cytochrome P450c17	3-beta-HSD I	3-beta-HSD II
Secondary	12	13	18	17	12	15	10
Small antral	11	11	10	10	11	10	7
Large antral	19	16	17	15	17	14	14
Corpus luteum	7	7	5	5	4	4	7
Total	49	47	50	47	44	43	38

Table 3. Expression of proteins in cells from different ovarian tissue compartments.

	From follicle compartments						From ovarian stroma	
	TC from different stages of follicle development							
	Secondary	Small antral	Large antral	CL	GC	Oocyte	Cortex	Medulla
LH/CG-R	+	+	+	+	−	−	+	+
Perilipin-2	+/−	+	+	+	−	−	−	+
StAR	+/−	+/−	+	+	+	+	−	−
Cytochrome P450 11A1	+/−	+	+	+	+	−	−	+
Cytochrome P450c17	+	+	+	+	−	−	−	−
3-beta-HSD I	+	+	+	+	+	+	+	+
3-beta-HSD II	+	+	+	+	+	+	+	+

(−) no structure analyzed showed immunostained cell; (+/−) some structures with and some without immunostained cells; (+) all structures showed immunostained cells.

Table 4. Mean standard error of the SI of each protein of interest calculated for each follicle stage, including corpus luteum.

Protein	Secondary		Small antral		Large antral		Corpus luteum	
LH/CG-R	83.25	42.85[a]	23.02	6.20[a]	110.57	43.14[a]	2441.49	2351.74[a]
Perilipin-2	9.15	4.41[a]	72.86	29.00[a,b]	438.74	359.22[b,c]	1349.71	413.70[c]
StAR	12.57	8.24[a]	192.48	38.10[b]	225.96	54.45[b]	473.62	203.02[b]
Cytochrome P450 11A1	59.54	30.55[a]	499.80	114.89[b]	313.17	44.56[b]	1594.20	924.01[b]
Cytochrome P450c17	136.42	41.17[a]	426.24	94.32[b]	460.31	82.37[b]	556.42	233.23[a,b]
3-beta-HSD I	241.81	69.24[a]	634.95	136.15[a]	505.69	64.90[a]	816.63	288.82[a]
3-beta-HSD II	102.38	68.05[a]	167.08	42.02[a,b]	236.97	70.13[b,c]	344.79	144.50[c]

Different superscript letters in the same row represent significant differences ($P < 0.05$) between the follicle categories. Values are divided by 1000.

It is important to point out that the TC layer was not consistently immunostained throughout the entire follicle (Figure 3K). GCs were StAR-negative, apart from those in the largest preovulatory follicle analyzed, which showed positive staining in their cytoplasm (Figure 3L). StAR expression was significantly elevated in TCs of small and large antral follicles ($P < 0.001$) and CL ($P < 0.01$) compared to TCs in secondary follicles (Figure 5, StAR, and Figure 6C-1 to C-4).

Cytochrome P450 11A1. Cytochrome P450 11A1 is located in the inner leaflet of the mitochondria and achieves the first step of steroidogenesis by converting cholesterol to pregnenolone. There were a few scattered foci of stromal cells in the cortex, showing enhanced cytoplasmic immunostaining for cytochrome P450 11A1 around the nucleus (Figure 4C). On the whole, no staining was observed in oocytes or GCs, and not all secondary follicles showed cytochrome P450 11A1-positive TCs. However, all TCs from small and large antral follicles were immunolabeled for cytochrome P450 11A1 (Figure 2D and d). In preovulatory follicles, only the cytoplasm of the inner theca interna layer was immunostained, but a few follicles also showed some expression in the cytoplasm and nucleus of GCs (Figure 4D). Cytochrome P450 11A1 expression was statistically higher in TCs of small ($P < 0.001$) and large ($P < 0.01$) antral follicles and CL ($P < 0.001$) than in TCs of secondary follicles (Figure 5, cytochrome P450 11A1, and Figure 6D-1 to D-4).

Cytochrome P450c17. Cytochrome P450c17 and 3-beta-HSD I and 3-beta-HSD II are located in smooth endoplasmic reticulum and convert this steroid mainly to androstenedione in most species. When detected, cytochrome P450c17 was specifically expressed in the cytoplasm of TCs (Figure 2E and e), starting as early as the secondary follicle stage (Figure 6E-1). The theca interna layer expressing this protein was very well delimited, but thin in some preovulatory

Downloaded from https://academic.oup.com/biolreprod/article-abstract/102/1/145/5554973 by guest on 01 August 2020

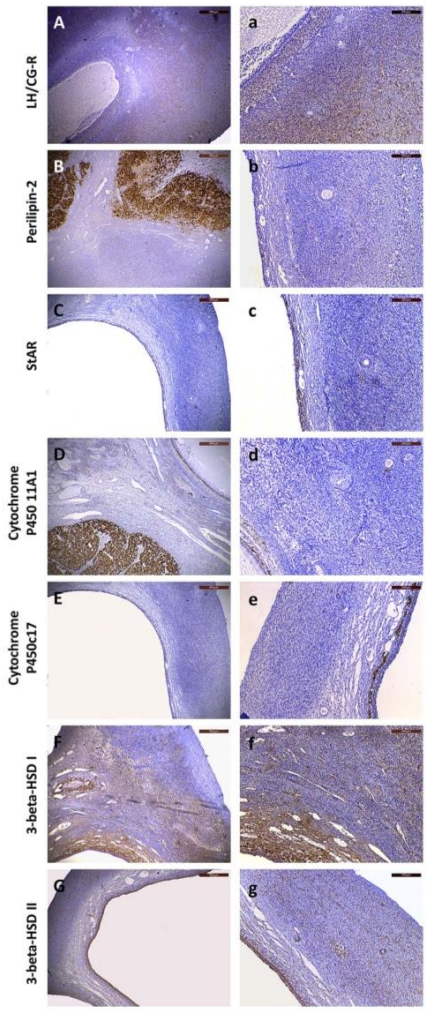


Figure 2. Lower magnification photomicrographs of human ovary immunostained with LH/CG-R (A and a), perilipin-2 (B and b), StAR (C and c), cytochrome P450 11A1 (D and d), cytochrome P450c17 (E and e), 3-beta-HSD I (F and f), and 3-beta-HSD II (G and g). Capital letters represent 4× magnified photomicrographs (bar: 500 μm) and small letters 10× magnified images (bar: 200 μm).

follicles (Figure 4G). Since no immunolabeling was observed in other ovarian cells (Figure 2E and e), this marker can be considered specific to TCs and luteal cells. Often, cytochrome P450c17 was only expressed in the external layer of CL structures, where former TCs were present (Figure 4H), while central luteal cells, previously GCs, showed no immunostaining. Cytochrome P450c17 was not encountered at advanced CL stages, which were usually identified by cells with very small nuclei and a vacuolated cytoplasm, but exhibited increasing expression patterns in TCs of small ($P < 0.05$) and large ($P < 0.05$) antral follicles and CL (Figure 6E-1 to E-4), which were statistically significant.

3-beta-HSD I. Modest quantities of progesterone can be produced in TCs of growing follicles via conversion of pregnenolone by 3-beta-HSD I and 3-beta-HSD II. In CL, down-regulation of cytochrome P450c17 allows pregnenolone to be converted to progesterone by these two isozymes, instead of DHEA. In this study, 3-beta-HSD I showed the strongest immunostaining among stromal cells, with numerous positive foci in extensive stromal areas of both the cortex and medulla (Figure 2F and f and Figure 4K). Very strong labeling was identified in the cytoplasm and nuclei of oocytes and GCs (Figure 6F-1). TCs in secondary, small, and large antral follicles also displayed 3-beta-HSD I immunostaining (Figure 6F-1, to F-3). Interestingly, preovulatory follicles exhibited a thin layer of TCs devoid of any immunolabeling, directly in contact with the basal lamina, while outer TC layers showed strong immunostaining in both the cytoplasm and nucleus of TCs (Figure 4L). Statistically significant expression patterns of 3-beta-HSD I were observed in TCs of secondary follicles versus small ($P < 0.05$) and large ($P < 0.05$) antral follicles and CL ($P < 0.05$) (Figure 5, 3-beta-HSD I, and Figure 6F-1 to F-4).

3-beta-HSD II. In general, stromal cell staining was widespread, as with 3-beta-HSD I, and secondary follicles showed 3-beta-HSD II-immunostained TCs and GCs (Figure 4O and Figure 6G-1). No distinction was apparent between the extent of TC and stromal cell expression at this stage (Figure 6G-1). Small and large antral follicles both showed the presence of this protein in the cytoplasm and sometimes nuclei of TCs (Figure 6G-2 and G-3). Cytoplasmic staining was also constant in GCs in all follicles. In CL, immunolabeling appeared as small dots scattered throughout the cytoplasm (Figure 4P and Figure 6G-4). Expression of 3-beta-HSD II in TCs of follicles and CL showed a tendency to increase from the secondary to the small antral follicle stage and was significantly higher in TCs of large antral follicles ($P < 0.05$) than in TCs of secondary follicles (Figure 5, 3-beta-HSD II).

Quantification of protein expression: staining index

Means and standard errors of the SI calculated for each follicle stage and each protein are reported in Table 4. While all proteins showed increasing expression patterns during follicle development and CL formation, perilipin-2 (Figure 5, perilipin, and Figure 6B-1 to B-4), StAR (Figure 5, StAR, and Figure 6C-1 to C-4), cytochrome P450 11A1 (Figure 5, cytochrome P450 11A1, and Figure 6D-1 to D-4), cytochrome P450c17 (Figure 5, cytochrome P450c17, and Figure 6E-1 to E-4), and 3-beta-HSD II (Figure 5, 3-beta-HSD II, and Figure 6F-1 to F-4) exhibited significant increases in the SI from secondary follicles to the CL stage. On the other hand, the SI of LH/CG-R (Figure 5, LH/CG-R, and Figure 6A-1 to A-4) and 3-beta-HSD I (Figure 5, 3-beta-HSD I, and Figure 6G-1 to G-4) did not differ statistically between follicle stages or in CL.

Discussion

Looking to uncover new data on human TCs, we evaluated proteins related to steroidogenesis in follicles at different stages of develop-

Downloaded from https://academic.oup.com/biolreprod/article-abstract/102/1/145/5554973 by guest on 01 August 2020

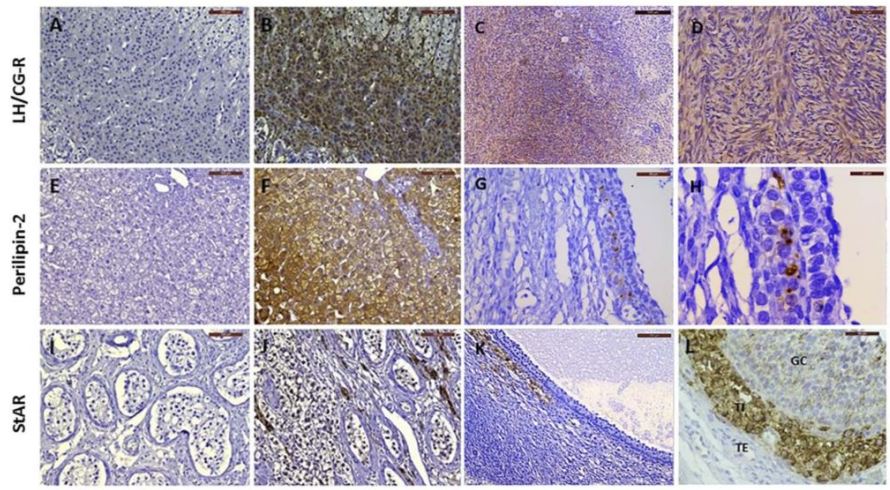


Figure 3. Photomicrographs of controls highlighting immunohistochemical patterns of LH/CG-R, perilipin-2, and StAR in ovarian tissue. Negative and positive controls for each protein respectively: adrenal gland (A and B), liver (E and F), and testes (I and J). LH/CG-R showed focal staining on the cortex (C), with cytoplasmic and nuclear staining in fibroblasts (D). Perilipin-2 was present in a thin theca interna layer (G) as faint dots in the cytoplasm (H). Some small antral follicles displayed focal expression of StAR in the theca layer (K), and a few preovulatory follicles showed some immunolabeling in GCs (L). Bars: 20 µm in H; 50 µm in G and D; 100 µm in A, B, E, F, I, J, and K; and 200 µm in C. GC: granulosa cell; TI: theca interna; TE: theca externa.

ment. While steroidogenic proteins are expressed in secondary follicles, they show different patterns of expression in growing follicles. Moreover, other ovarian compartments also express most of these proteins, like cytochrome P450 11A1, 3-beta-HSD I, and 3-beta-HSD II, but cytochrome P450c17 is the only protein expressed exclusively by TCs. While information on serum levels of sex steroids and menstrual cycle data may have aided interpretation of our results, taken together, these findings nevertheless add meaningful insights into the characterization of human ovarian tissue protein expression.

Steroidogenesis is coordinated by LH, and when it binds to its receptor LHR, TCs start intensifying their expression of steroidogenic protein-encoding genes [12, 13]. Previous studies have claimed that LH/CG-R localization is exclusively membranous [14], but the plasma membrane is internalized in coated vesicles, revealing cytoplasmic immunolabeling of this protein [15, 16], as evidenced in the present study already at the secondary stage (Figure 6A-1). Takao et al. [16] also reported expression of LH/CG-R in secondary human follicles and small antral follicles. Its identification in preantral follicles suggests it may be a promoter of follicle development, as it is involved in the first steps of androgen biosynthesis. In CL, LH/CG-R staining decreases considerably across the luteal lifespan, becoming almost undetectable in regressing CL [16]. In the present study, it was not possible to determine CL age, but levels of LH/CG-R staining indicate that the majority of evaluated structures were in the infancy of their development.

Perilipin-2 is a lipid droplet-specific marker for identification of metabolically active cells [17]. Its functions in intracellular lipid droplet structuring and fatty acid transportation have already been described [18]. According to Talbott and Davis [19], LH regulates perilipin-2 phosphorylation via a cAMP signaling pathway, releasing the necessary substrate for steroidogenesis. Our results show abundant expression of perilipin-2 in CL (Figure 6B-4), which is consistent with CL function. Moreover, it correlates with Talbott and Davis's study [19] in bovine CL. These authors showed that bovine luteal tissue contains predominantly perilipin-2 and perilipin-3 lipid droplet coating proteins, as well as 3-beta-HSD I, cytochrome P450 11A1, and StAR [19].

StAR may confer acute [20] steroidogenic properties to previously non-steroidogenic cells, and it is the first protein to play an actual role in cholesterol cleavage [21]. Its expression is mediated by protein kinases A and C, and its regulation occurs in a tissue-, stimulus-, and species-specific manner [22]. Expression of StAR mRNA in human ovaries was previously reported only in TCs of preovulatory follicles and luteal cells [23] by in situ hybridization [23]. However, this protein was sometimes found to be expressed in TCs of secondary and small antral follicles in the present study (Figure 6C-1 and C-2). It was also detected in GCs of some antral follicles. These follicles were nevertheless at very advanced stages, so it is possible that StAR expression was triggered by the start of the luteinization process, since GCs are not able to synthesize hormones directly from cholesterol [3]. Indeed, StAR is not expressed in GCs until the LH surge takes place [23]. Cytoplasmic immunohistochemical localization of StAR in the current study (Figure 6, C-1 to C-4) could not determine exactly where in the mitochondria it resides, since such identification would require ultrastructural analysis. However, it is known that StAR promotes steroidogenesis only when present in the outer mitochondrial membrane and loses its functionality when in the mitochondrial matrix [24].

Cytochrome P450 enzymes involved in steroidogenesis bind to the membranes of either mitochondria (11A1) or endoplasmic

Downloaded from https://academic.oup.com/biolreprod/article-abstract/102/1/145/5554973 by guest on 01 August 2020

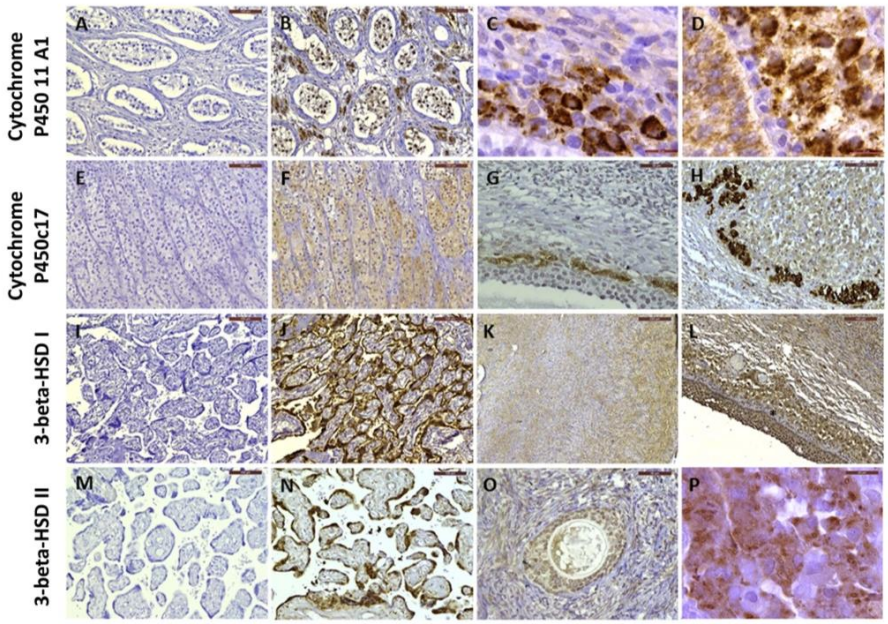


Figure 4. Photomicrographs of controls highlighting immunohistochemical patterns of cytochrome P450 11A1, cytochrome P450c17, 3-beta-HSD I, and 3-beta-HSD II in ovarian tissue. Negative and positive controls for each protein respectively: testes (A and B), adrenal gland (E and F), and placenta (I, J, M, and N). Cytochrome P450 11A1 showed strong perinuclear cytoplasmic staining (C), while GC staining was present only in some preovulatory follicles (D). The theca interna layer expressing cytochrome P450c17 was very well delimited (G), and considerably stronger staining was detected in the outer CL layer, suggesting the presence of paraluteal cells (H). 3-beta-HSD I was the protein showing the highest expression throughout stromal cells (K). GCs and oocytes were also 3-beta-HSD I immunostained, while preovulatory follicles exhibited a thin layer of TCs unstained for 3-beta-HSD I (asterisk) directly between the basal lamina and the immunolabeled theca interna layer (L). A secondary follicle can be seen with 3-beta-HSD II immunostaining in GCs and the oocyte (O), with patterns of luteal cell expression visible in the cytoplasm (P). Bars: 20 µm in C, D and P; 50 µm in G and O; 100 µm in A, B, E, F, H, I, J, L, M, and N; and 200 µm in K. GC: granulosa cell; CL: corpus luteum; TC: theca cell.

reticulum (c17) [11]. Cytochrome P450 11A1 is known to be a factor that promotes chronic steroidogenic activity and is implicated in the first cleavage step of biosynthesis [11] under the control of the cAMP signaling pathway [25]. Our findings in human ovarian tissue are inconsistent with results in rats, where cytochrome P450 11A1 was only found to be present at later follicle stages (Figure 6D-2 and D-3) [26], but corroborate observations of peak expression levels in luteal cells (Figure 6D-4), as reported in cynomolgus moneys [27]. This suggests that in human CL, as in bovine CL [19], higher levels of cytochrome P450 11A1 are probably needed for progesterone synthesis.

Cytochrome P450c17 was localized in the perinuclear cytoplasm (Figure 6E-1 to E-4), confirming its exclusive association with endoplasmic reticulum [28, 29]. It hydroxylates pregnenolone or progesterone and then cleaves C17-20 bonds to produce DHEA and androstenedione [11]. This protein was expressed in both TCs and paraluteal cells, but GCs do not express it [11] unless they are luteinized [30].

Both 3-beta-HSD I and 3-beta-HSD II are responsible for steroid reduction and oxidation. They are membrane-bound proteins distributed throughout the endoplasmic reticulum and in cristae of some TC mitochondria [11, 28], but their function and classification may be species specific [31]. Indeed, 3-beta-HSD allows synthesis of steroid hormones. It was previously claimed that human 3-beta-HSD I mRNA is only expressed in placenta, breast, and skin [32], but this protein was identified throughout ovarian tissue in the present study (Figure 6F-1 to F-4). Expression of 3-beta-HSD I and 3-beta-HSD II has also been reported in TCs and GCs of growing follicles in both human [33] (Figure 6F-1 to F-4; G-1 to G-4) and mouse [28] ovaries.

When assessing expression levels, a similar increase was encountered in StAR, cytochrome P450 11A1 and cytochrome P450c17 intensity during the process of folliculogenesis, but in luteinized cells, the SI was three times higher for cytochrome P450 11A1 than for StAR or cytochrome P450c17 (Figure 5). This was expected, since luteal cells are presumed to convert cholesterol directly to progesterone solely by the action of cytochrome P450 11A1 and 3-beta-HSD II [34]. However, the increase in 3-beta-HSD II expression was not as dramatic as that of cytochrome P450 11A1 when comparing CL and preovulatory follicles, which may be due to the

Downloaded from https://academic.oup.com/biolreprod/article-abstract/102/1/145/5554973 by guest on 01 August 2020

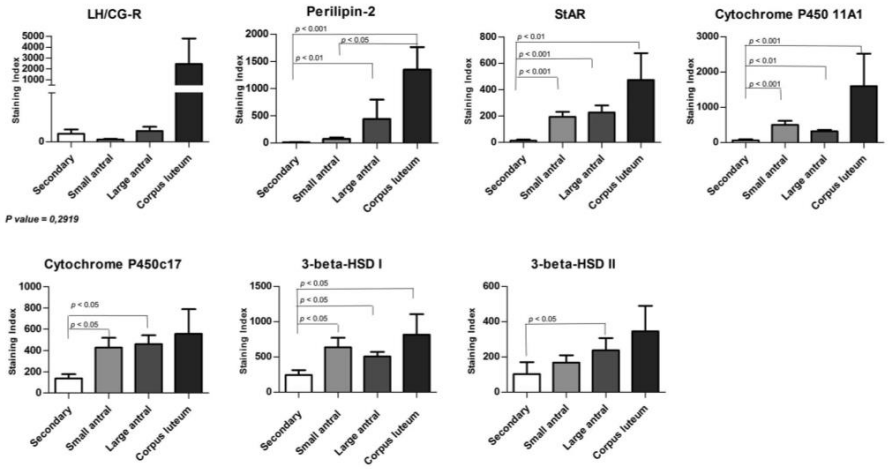


Figure 5. Immunostaining quantification of different proteins at each follicle stage expressed as mean standard error. Each graph corresponds to every enzyme involved in TC steroidogenesis. The Y axis represents the SI, and the X axis represents different stages of follicle development and CL. Lines between follicle stages and CL indicate statistically significant differences according to both the Kruskal-Wallis test and Dunn's multiple comparison test. Values are divided by 1000. TC: theca cell; SI: staining index; CL: corpus luteum.

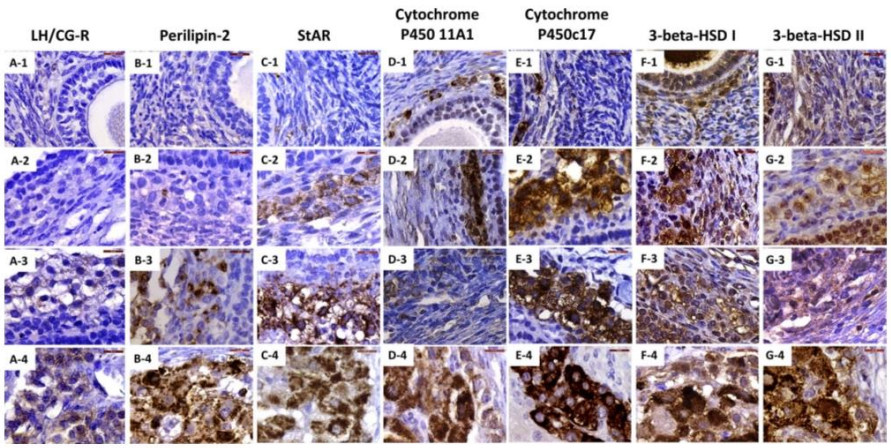


Figure 6. Representative images of secondary, small, and large antral follicles and CL. Note the differences between the intensity and area of each protein: LH/CG-R (A), perilipin-2 (B), StAR (C), cytochrome P450 11A1 (D), cytochrome P450c17 (E), 3-beta-HSD I (F), and 3-beta-HSD II (G). Secondary (1), small antral (2), and large antral (3) follicles and CL (4). Measurement bars: 20 μm. CL: corpus luteum.

fact that the 3-beta-HSD II SI was already high in preovulatory follicles.

Although follicles are self-sufficient structures in terms of steroidogenesis [35], it is not their exclusive role, as signs of steroidogenesis have also been reported in undifferentiated stromal cells [12], which could increase in pathological cases [36, 37]. Indeed, enzymes like 3-beta-HSD I and 3-beta-HSD II are widely expressed throughout the ovarian stroma, as demonstrated in our study (Figure 2F, f and G, g). While the ovaries used in our study appeared healthy, it is important to bear in mind that the patients

Downloaded from https://academic.oup.com/biolreprod/article-abstract/102/1/145/5554973 by guest on 01 August 2020

were positive for BRCA1 and/or BRCA2 mutations and one of them had metastasis of pancreatic cancer. Northern blot and quantitative real-time polymerase chain reaction analyses have shown that cytochrome P450 11A1, cytochrome P450c17, and 3-beta-HSD II mRNA levels are higher in polycystic ovary syndrome (PCOS) cells than in their counterparts from healthy ovaries, while levels of StAR mRNA do not differ between PCOS cells and normal TCs [7], suggesting that StAR content does not vary significantly according to cell synthetic capacity.

In conclusion, each enzyme plays a specific and indispensable role in steroidogenesis, and silencing those genes that encode them diminishes steroid synthesis [38, 39]. As biosynthesis progresses along with follicle development, enzyme levels exhibit different expression patterns that have been detailed in the present work. On the whole, cytochrome P450 11A1, cytochrome P450c17, and 3-beta-HSD show substantially stronger expression in TCs during folliculogenesis, evidenced by both area covered and immunostaining intensity. Other proteins that are important in steroid biosynthesis are LH/CG-R, perilipin-2, and StAR, whose expression also increases in the course of folliculogenesis and luteinization. Our findings are fundamental and may facilitate studies on pathological conditions affecting the human ovary, as well as the design and development of a bioengineered transplantable ovary.

Supplementary data

Supplementary data are available at *BIOLRE* online.

Acknowledgments

The authors thank Mira Hryniuk for reviewing the English language of the manuscript, Dolores Gonzalez and Olivier Van Kerk for their technical assistance, and Dr. Caroline Bouzin (Imaging Platform from UCLouvain's Institute of Experimental and Clinical Research) for support with the analysis of data.

Authors' roles

P. Asiabi and E. C. R. Leonel: study design, experimental procedures, analysis, interpretation of data, and manuscript preparation. E. Marbaix: tissue supply and manuscript preparation. M.M. Dolmans: manuscript preparation and revision. C. A. Amorim: experimental design, experimental procedures, interpretation of results, and manuscript revision.

Conflict of interest

None of the authors has any competing interests to declare in relation to the topic.

References

1. Edson MA, Nagaraja AK, Matzuk MM. The mammalian ovary from genesis to revelation. *Endocr Rev* 2009; **30**:624–712.
2. Kinder SJ, Tsang TE, Quinlan GA, Hadjantonakis AK, Nagy A, Tam PP. The orderly allocation of mesodermal cells to the extraembryonic structures and the anteroposterior axis during gastrulation of the mouse embryo. *Development* 1999; **126**:4691–4701.
3. Hillier SG, Whitelaw PF, Smyth CD. Follicular oestrogen synthesis: The 'two-cell, two-gonadotrophin' model revisited. *Mol Cell Endocrinol* 1994; **100**:51–54.
4. Ryan KJ, Petro Z, Kaiser J. Steroid formation by isolated and recombined ovarian granulosa and thecal cells. *J Clin Endocrinol Metab* 1968; **28**:355–358.
5. Magoffin DA. Ovarian theca cell. *Int J Biochem Cell Biol* 2005; **37**:1344–1349.
6. Honda A, Hirose M, Hara K, Matoba S, Inoue K, Miki H, Hiura H, Kanatsu-Shinohara M, Kanai Y, Kono T, Shinohara T, Ogura A. Isolation, characterization, and in vitro and in vivo differentiation of putative thecal stem cells. *Proc Natl Acad Sci* 2007; **104**:12389–12394.
7. Wickenheisser JK, Nelson-DeGrave VL, McAllister JM. Human ovarian theca cells in culture. *Trends Endocrinol Metab* 2006; **17**:65–71.
8. George FW, Wilson JD. Conversion of androgen to estrogen by the human fetal ovary. *J Clin Endocrinol Metab* 1978; **47**:550–555.
9. Fowler PA, Anderson RA, Saunders PT, Kinnell H, Mason JI, Evans DB, Bhattacharya S, Flannigan S, Franks S, Monteiro A, O'Shaughnessy PJ. Development of steroid signaling pathways during primordial follicle formation in the human fetal ovary. *J Clin Endocrinol Metab* 2011; **96**:1754–1762.
10. Havelock JC, Rainey WE, Carr BR. Ovarian granulosa cell lines. *Mol Cell Endocrinol* 2004; **228**:67–78.
11. Payne AH, Hales DB. Overview of steroidogenic enzymes in the pathway from cholesterol to active steroid hormones. *Endocr Rev* 2004; **25**:947–970.
12. McNatty KP, Makris A, Degrazia C, Rapin O, Ryan KJ. The production of progesterone, androgens, and estrogens by granulosa cells, thecal tissue, and stromal tissue from human ovaries in vitro. *J Clin Endocrinol Metab* 1979; **49**:687–699.
13. Zhang G, Garmey JC, Veldhuis JD. Interactive stimulation by luteinizing hormone and insulin of the Steroidogenic acute regulatory (StAR) protein and 17α-hydroxylase/17, 20-Lyase (CYP17) genes in porcine theca cells. *Endocrinology* 2000; **141**:2735–2742.
14. Davis JS. Mechanisms of hormone action: Luteinizing hormone receptors and second-messenger pathways. *Curr Opin Obstet Gynecol* 1994; **6**:254–261.
15. Ghinea N, Hai MV, Groyer-Picard M-T, Houllier A, Schoëvaërt D, Milgrom E. Pathways of internalization of the hCG/LH receptor: Immunoelectron microscopic studies in Leydig cells and transfected L-cells. *J Cell Biol* 1992; **118**:1347–1358.
16. Takao Y, Honda T, Ueda M, Hattori N, Yamada S, Maeda M, Fujiwara H, Mori T, Wimalasena J. Immunohistochemical localization of the LH/HCG receptor in human ovary: HCG enhances cell surface expression of LH/HCG receptor on luteinizing granulosa cells in vitro. *Mol Hum Reprod* 1997; **3**:569–578.
17. Straub BK, Gyoengyoesi B, Koenig M, Hashani M, Pawella LM, Herpel E, Mueller W, Macher-Goeppinger S, Heid H, Schirmacher P. Adipophilin/perilipin-2 as a lipid droplet-specific marker for metabolically active cells and diseases associated with metabolic dysregulation. *Histopathology* 2013; **62**:617–631.
18. Gao J, Serrero G. Adipose differentiation related protein (ADRP) expressed in transfected COS-7 cells selectively stimulates long chain fatty acid uptake. *J Biol Chem* 1999; **274**:16825–16830.
19. Talbott H, Lipid Droplets DJS. Metabolic pathways regulate steroidogenesis in the corpus luteum. In: Meidan R (ed.), *The Life Cycle of the Corpus Luteum*. Cham: Springer International Publishing; 2017: 57–78.
20. Duarte A, Castillo AF, Podestá EJ, Poderoso C. Mitochondrial fusion and ERK activity regulate steroidogenic acute regulatory protein localization in mitochondria. *PLoS One* 2014; **9**:e100387.
21. Lin D, Sugawara T, Strauss J, Clark B, Stocco D, Saenger P, Rogol A, Miller W. Role of steroidogenic acute regulatory protein in adrenal and gonadal steroidogenesis. *Science* 1995; **267**:1828–1831.
22. Manna PR, Stetson CL, Slominski AT, Pruitt K. Role of the steroidogenic acute regulatory protein in health and disease. *Endocrine* 2016; **51**: 7–21.

Downloaded from https://academic.oup.com/biolreprod/article-abstract/102/1/145/5554973 by guest on 01 August 2020

23. Kiriakidou M, Mcallister JM, Sugawara T, Strauss J 3rd. Expression of steroidogenic acute regulatory protein (StAR) in the human ovary. *J Clin Endocrinol Metab* 1996; **81**:4122–4128.
24. Miller WL. Mechanism of StAR's regulation of mitochondrial cholesterol import. *Mol Cell Endocrinol* 2007; **265-266**:46–50.
25. Guo C, Hu M-C, Chung B-C. Transcriptional regulation of CYP11A1. *J Biomed Sci* 2003; **10**:593–598.
26. Oonk RB, Parker KL, Gibson JL, Richards JS. Rat cholesterol side-chain cleavage cytochrome P-450 (P-450scc) gene. Structure and regulation by cAMP in vitro. *J Biol Chem* 1990; **265**:22392–22401.
27. Ravindranath N, Little-Ihrig L, Benyo DF, Zeleznik AJ. Role of luteinizing hormone in the expression of cholesterol side-chain cleavage cytochrome P450 and 3 beta-hydroxysteroid dehydrogenase, delta 5-4 isomerase messenger ribonucleic acids in the primate corpus luteum. *Endocrinology* 1992; **131**:2064–2070.
28. Pelletier G, Li S, Tremblay Y, Belanger A, Labrie F. Immunoelectron microscopic localization of three key steroidogenic enzymes (cytochrome P450 (scc), 3 beta-hydroxysteroid dehydrogenase and cytochrome P450 (c17)) in rat adrenal cortex and gonads. *J Endocrinol* 2001; **171**: 373–383.
29. Tamura T, Kitawaki J, Yamamoto T, Osawa Y, Kominami S, Takemori S, Okada H. Immunohistochemical localization of 17α-hydroxylase/C17–20 lyase and aromatase cytochrome P-450 in the human ovary during the menstrual cycle. *J Endocrinol* 1992; **135**:589–NP.
30. Morán FM, VandeVoort CA, Overstreet JW, Lasley BL, Conley AJ. Molecular target of endocrine disruption in human luteinizing granulosa cells by 2,3,7,8-tetrachlorodibenzo-p-dioxin: Inhibition of estradiol secretion due to decreased 17α-hydroxylase/17,20-Lyase cytochrome P450 expression. *Endocrinology* 2003; **144**: 467–473.
31. Abbaszade IG, Clarke TR, Park CH, Payne AH. The mouse 3 beta-hydroxysteroid dehydrogenase multigene family includes two functionally distinct groups of proteins. *Mol Endocrinol* 1995; **9**: 1214–1222.
32. Eric R. Structure and expression of a new complementary DNA encoding the almost exclusive 3β-hydroxysteroid dehydrogenase/Δ5-Δ4-isomerase in human adrenals and gonads. *Mol Endocrinol* 1991; **5**:1147–1157.
33. Breitenecker G, Friedrich F, Kemeter P. Further investigations on the maturation and degeneration of human ovarian follicles and their oocytes. *Fertil Steril* 1978; **29**:336–341.
34. Christenson LK, Devoto L. Cholesterol transport and steroidogenesis by the corpus luteum. *Reprod Biol Endocrinol* 2003; **1**:90–90.
35. Young JM, McNeilly AS. Theca: The forgotten cell of the ovarian follicle. *Reproduction* 2010; **140**:489–504.
36. Blanco LZ Jr, Kuhn E, Morrison JC, Bahadirli-Talbott A, Smith-Sehdev A, Kurman RJ. Steroid hormone synthesis by the ovarian stroma surrounding epithelial ovarian tumors: A potential mechanism in ovarian tumorigenesis. *Mod Pathol* 2017; **30**:563.
37. Nagamani M, Urban RJ. Increased expression of messenger ribonucleic acid encoding cytochrome P450 cholesterol side-chain cleavage and P450 17α-hydroxylase enzymes in ovarian hyperthecosis. *Fertil Steril* 1999; **71**:328–333.
38. Li Y, X-y L, L-n W, Y-l X, Yang X, H-g S, Yang Z-H. Study of RNA interference inhibiting rat ovarian androgen biosynthesis by depressing 17alpha-hydroxylase/17, 20-lyase activity in vivo. *Reprod Biol Endocrinol* 2009; **7**:73.
39. Huang C-CJ, Shih M-CM, Hsu N-C, Chien Y, B-c C. Fetal glucocorticoid synthesis is required for development of Fetal adrenal medulla and hypothalamus feedback suppression. *Endocrinology* 2012; **153**:4749–4756.

Downloaded from https://academic.oup.com/biolreprod/article-abstract/102/1/145/5554973 by guest on 01 August 2020

Supplementary Table 1. Ovarian tissue used in this study.

Patient	Reason for oophorectomy	Ovaries used in this study	Number of sections	
			H&E	IHC
1	BRCA1 mutation. Prophylactic oophorectomy	Left: 1 fragment	1st and 10th section	2nd to 8th section
2	BRCA1 mutation. Prophylactic oophorectomy	Right: 1 fragment	1st and 10th section	2nd to 8th section
3	BRCA1 and BRCA2 mutations. Prophylactic oophorectomy	Left: 1 fragment	1st and 10th section	2nd to 8th section
4	BRCA1 mutation. Prophylactic oophorectomy	Right: 1 fragment	1st and 10th section	2nd to 8th section
5	Oophorectomy: metastasis of pancreatic cancer to the left ovary. Right ovary normal	Right: 1 fragment	1st and 10th section	2nd to 8th section
6	BRCA2 mutation. Prophylactic oophorectomy	Left: 1 fragment Right: 1 fragment	1st and 10th section from each block	2nd to 8th section from each block
7	BRCA1 mutation. Prophylactic oophorectomy	Left: 1 fragment	1st and 10th section	2nd to 8th section
8	BRCA2 mutation. Prophylactic oophorectomy	Left: 2 fragments Right: 1 fragment	1st and 10th section from each block	2nd to 8th section from each block
9	BRCA1 mutation. Prophylactic oophorectomy	Right: 1 fragment	1st and 10th section	2nd to 8th section

H&E: hematoxylin and eosin; IHC: immunohistochemistry.

3.2 Investigation of the presence of a precursor theca cell population in human ovaries

From the studies in mice, it is believed that there is a population of precursor theca cells in the ovary, which will differentiate into theca cells under the influence of granulosa cells and oocytes from growing follicles. Liu *et al.* (2015) demonstrated that *Gli1* is the marker for (progenitor) theca steroidogenic cells in this species. They showed that the recruitment of theca cells starts with GDF9, the oocyte-derived factor, and its function on granulosa cells to express IHH and DHH to activate their downstream target, GLI1, through PTCH1 receptor in theca cells. In another study in mouse, Honda *et al.* (2007) reported precursor theca cells would express Gli3 and Patch1 as specific markers, while differentiated steroidogenic theca cells would express *Lhr*, *Gli2,* and *Patch2*. Since GLI1, 2, and 3 regulate expression of enzymes involved in the steroidogenic pathway of theca cells, such as CYP11A1 and CYP17A1, and the vital role of theca cells for follicle development and steroidogenesis, finding the source of these cells in human ovaries and their recruitment pathway is indispensable. Thus, for this purpose, the current study was performed to assess theca cell recruitment pathway and GLI1, 2, and 3 presence time point in the human fetus, prepubertal, reproductive-aged, and menopause ovaries by performing IHC against GDF9, IHH, DHH, SHH, PTCH1, GLI1, GLI2, and GLI3 and qPCR on *Gdf9*, *Ihh* and *Gli1, Gli2* and *Gli3* mRNA. To the best of our knowledge, this is the first study investigating the presence of the precursor theca cell population in human ovaries and the process of theca cell recruitment based on findings reported in the mouse model. Our results show all of

the GDF9-HH-GLI proteins were expressed in primordial follicles of fetal, prepubertal, and reproductive-age human ovaries and stromal cells of reproductive-age and postmenopausal ovaries. Intriguingly, *Gdf9*, *Ihh, and Gli3* mRNA, but not *Gli1 and 2,* were detected in postmenopausal ovaries. Moreover, our findings propose that GLI1-, 2- and 3-positive cells might be involved in the steroidogenesis of ovarian cells as a general marker rather than a specific marker for precursor theca cells, as observed in mice.

Article 2

Journal of Assisted Reproduction and Genetics

New insights into the GDF9-Hedgehog-GLI signaling pathway in human ovaries: from fetus to postmenopause Running title: GDF9-Hedgehog-GLI signaling in human ovaries

--Manuscript Draft--

Manuscript Number:	
Full Title:	New insights into the GDF9-Hedgehog-GLI signaling pathway in human ovaries: from fetus to postmenopause Running title: GDF9-Hedgehog-GLI signaling in human ovaries
Article Type:	Original Article
Keywords:	Growth differentiation factor 9, Hedgehog ligands, PTCH1 receptor, precursor theca cells, glioma-associated oncogene homolog 1, 2 and 3
Corresponding Author:	Christiani Andrade Amorim, V.M.D., M.Sc., Ph.D. Unviersite catholique de Louvain Brussels, BELGIUM
Corresponding Author Secondary Information:	
Corresponding Author's Institution:	Unviersite catholique de Louvain
Corresponding Author's Secondary Institution:	
First Author:	Parinaz Asiabi, MSc
First Author Secondary Information:	
Order of Authors:	Parinaz Asiabi, MSc
	Clara David, MSc
	Alessandra Camboni, MD, PhD
	Etienne Marbaix, MD, PhD
	Marie-Madeleine Dolmans, MD, PhD
	Christiani Andrade Amorim, V.M.D., M.Sc., Ph.D.

New insights into the GDF9-Hedgehog-GLI signaling pathway in human ovaries: from fetus to postmenopause

Running title: GDF9-Hedgehog-GLI signaling in human ovaries

Parinaz Asiabi[1] , Clara David[1] , Alessandra Camboni[1] , Etienne. Marbaix[2] , Marie-Madeleine Dolmans[1,3], Christiani A. Amorim[1,*]

[1]Pôle de Recherche en Gynécologie, Institut de Recherche Expérimentale et Clinique, Université Catholique de Louvain, 1200 Brussels, Belgium

[3]Pathology Department, Cliniques Universitaires Saint-Luc, Brussels, Belgium

[2]Gynecology and Andrology Department, Cliniques Universitaires Saint-Luc, 1200 Brussels, Belgium

***Corresponding author:**

Pôle de Recherche en Gynécologie

Institut de Recherche Expérimentale et Clinique

Université Catholique de Louvain

Avenue Mounier 52, bte B1.52.02, 1200 Brussels, Belgium

E-mail: christiani.amorim@uclouvain.be

Tel: +32 (0)2 764 5287

Introduction:

While orchestrated communication between the pituitary gland and the ovary is needed for reproduction in mammals, successful follicle growth and ovulation requirehighly elaborate communication between the oocyte and its surrounding granulosa and theca cells. Any flaw in this process can have dire consequences on female reproductive health and fertility [1-3].

Theca cells play a crucial role in successful folliculogenesis by providing structural support and producing androstenedione as a substrate for granulosa cells to convert into estradiol [4]. Despite the importance of theca cells, their origin in the ovary has not been positively identified. There are studies in neonatal mouse ovaries showing that precursor theca cells can be detected by glioma-associated oncogene homolog 1 (GLI1) [3], GLI3 and protein patched homolog 1 (PTCH1) [5]. Cells positive for these markers differentiate into theca interna cells (TICs) in the presence of Hedgehog (HH) ligands synthesized by granulosa cells. Differentiated TICs express GLI1 [3], GLI2, PTCH2 and luteinizing hormone receptor (LHR) [5]. For this process to occur, the HH pathway is activated in granulosa cells by secreted growth differentiation factor 9 (GDF9) expressed by oocytes [3]. Indeed, it has been reported that in

mutant mice lacking GDF9, the TIC layer fails to develop, causing follicle development arrest at preantral stages [6, 3]. GDF9 has been shown to mediate induction and activation of the HH signaling pathway in granulosa cells [3].

HH proteins are responsible for lineage specification in many organs [7], particularly mouse follicles, but HH ligands, Desert Hedgehog (DHH) and Indian Hedgehog (IHH) produced by granulosa cells are involved in recruitment of TICs from the ovarian stroma [8, 9]. Moreover, DHH and IHH deletion studies indicate that they are implicated in regulating the differentiation and steroidogenic capacity of endocrine cells, including TICs, partly by modulating expression of Sf-1/Nr5a1 and steroidogenic enzymes like cytochrome P450 family 11 subfamily A member 1 (Cyp11a1) and cytochrome P450 17A1 (Cyp17a1) [3, 10, 11].

In mammalian ovarian follicles, the HH signaling pathway is activated by stoichiometric binding of HH ligands in granulosa cells to their receptor PTCH1 [12-14] on theca cells and their precursors [9, 3]. PTCH1 is a conserved 12-pass transmembrane protein receptor that plays an obligate negative regulatory role in the HH signaling pathway [15]. In the absence of HH proteins, PTCH1 suppresses constitutive activity inthe seven-transmembrane G protein-like Smoothened (SMO) receptor [16].

The presence of HH proteins inactivates the action of PTCH1 in adjacent cells [17] by removing PTCH1 inhibition on SMO activity [16, 18, 19]. This leads to activation of latent cytoplasmic transcription factors, namely zinc finger proteins GLI1, 2 and 3 [17, 20], in (precursor) theca, interstitial/fibroblast, and/or perivascular cells within the theca layer [9, 21]. These transcription factors regulate expression of selected genes, such as enzymes involved in the steroidogenic pathway of TICs, including Cyp11a1 and Cyp17a1 [9, 10].

Due to a lack of knowledge on the origin of TICs in human ovaries, the goal of this study was to investigate the GDF9-HH-GLI pathway in human ovaries and assess whether GLI1 and 3 and PTCH1 are specific markers for precursor TICs, as has been demonstrated in mice [3, 5]. To this end, we analyzed expression of proteins and genes involved in the GDF9-HH-GLI pathway in fetal, prepubertal, reproductive-age and postmenopausal human ovaries.

Materials and methods:

Collection of human ovarian samples

Use of human ovarian cortex was approved by the Institutional Review Board of the Université Catholique de Louvain on May 13, 2019 (IRB reference 2012/23MAR/125, registration number B403201213872). Thanks to collaboration between UCLouvain's Gynecology Research Unit (GYNE) and the Anatomic Pathology Department of Saint-Luc's Hospital, we were able to study human ovarian biopsies obtained from the biobank of the Cliniques Universitaires Saint-Luc (BB190044). Samples from fetal, prepubertal, reproductive-age and postmenopausal ovaries were fixed in 4% formaldehyde and embedded in paraffin (Table 1). It is important to emphasize that none of the samples showed alterations or anomalies. Apart from menopausal tissue, all ovaries contained follicles at different stages of development, as well as corpora lutea.

Table I: Number of used paraffin block samples and their age range.

	Fetal	Prepubertal	Fertile	Menopausal
Age range	14-39 weeks	Newborn to 6 years	35-43 years	68-91 years
Number of samples	9	9	15	8

Histological and immunohistochemical analyses

Excised biopsies were fixed in 4% paraformaldehyde (VWR, Leuven, Belgium) for 24 hours, before being directly dehydrated and embedded in paraffin. Paraffin blocks were serially sectioned (5-µm-thick sections) (Microtome HM325, Thermo Fisher Scientific, Merelbeke, Belgium) and every tenth section was stained with hematoxylin and eosin (Merck, Darmstadt, Germany) for morphological analysis, while the remaining sections (Superfrost Plus, Menzel-Glaser, Braunschweig, Germany) were kept for immunohistochemistry (IHC). Follicles were classified according to their stage of development as follows:

Type 1 - Resting primordial follicles containing a single layer of flattened granulosa cells

Type 2 - Primary follicles with one layer of cuboidal granulosa cells

Type 3 - Secondary follicles with two layers of granulosa cells

Type 4 - Secondary follicles with three or more layers of granulosa cells and the start of theca cell layer formation

Type 5 - Small antral follicles (less than 6 mm in diameter)

Type 6 - Large antral follicles (more than 6 mm in diameter)

IHC analysis was performed with GDF9, IHH, DHH, Sonic Hedgehog (SHH), PTCH1, GLI1, GLI2 and GLI3 antibodies on consecutive tissue sections using an indirect peroxidase method concurrently for all ages. Information on primary antibodies, their dilution and incubation time, and details about the different steps of IHC for each antibody are provided in Supplementary Table 1.

Briefly, tissue sections were deparaffinized and rehydrated, followed by endogenous peroxidase inhibition using hydrogen peroxide. Apart from GDF9, antigen retrieval was done in a water bath at 96°C for 20 minutes or 98°C for 75 minutes, depending on the antibody. Nonspecific protein inhibition was performed using Tris-buffered saline (TBS), 3% non-fat milk, 7.5% bovine serum albumin, 1.5% Tween 20 and 3% human immunoglobulins (Igs), before incubation with primary antibody. Secondary antibody incubation (60 minutes) with EnVision anti-mouse (Dako, USA) for PTCH1 and GLI1, and EnVision anti-rabbit (Dako, USA) for GDF9, IHH, DHH, SHH, GLI2 and GLI3 followed by streptavidin/horseradish peroxidase (HRP), was accomplished after overnight incubation with primary antibody. For negative controls, ovarian tissue and the same tissue used for positive controls were treated similarly, but without any primary antibody., Diaminobenzidine

(DAB, Vector, Burlingame, USA) was used to stain the sections, followed by counterstaining with hematoxylin, dehydration in isopropanol and mounting for further analyses.

Scanning and image analyses

Stained sections were digitized with an SCN400 slide scanner (Leica Biosystems, Wetzlar, Germany) at X20 magnification. Using ImageJ software (version 1.52a, Wayne Rasband, NIH, USA), regions of interest (ovarian cortex containing follicles) were delineated and captured manually. In each group (fetal, prepubertal, reproductive-age and postmenopausal), the total number of immunostained follicles for all proteins of interest was counted in all sections. Follicles were considered positive when staining was detected in the cytoplasm or nucleus of oocytes, granulosa and or theca cells. We finally identified all positive follicles at every stage of development in each age group and for each protein (Tables 2-4). All ovarian tissue sections were scored for intensity of staining in oocytes and granulosa, theca and stromal cells. Relative intensities of staining were scored as follows: -, no staining; +, moderate staining; or ++, strong staining.

Protein extraction

The Qproteome FFPE kit (Qiagen, Hilden, Germany) was used to extract proteins from formalin-fixed paraffin-embedded (FFPE) tissue (fetal: n=4; prepubertal: n=3; fertile: n=4; postmenopausal: n=2; positive controls: n=5). Positive controls were the same samples as used for IHC (Supplementary Table 1). Extraction was achieved according to the kit datasheet. Briefly, the first step involves deparaffinization, where tissue sections (10-15 µm thickness) are successively incubated for 10 minutes at room temperature (RT) in xylene and 100%, 96% and 70% ethanol. After incubation, the supernatant is carefully removed and the pellet is retained. Once the paraffin has been removed, tissue sections undergo an incubation step for protein extraction. Samples are incubated in 100 µl extraction buffer (EXB + ß-mercaptoethanol) and undergo a first heating treatment using a heating block at 100°C for 20 minutes. This allows formalin crosslinking to be reversed. The second heating step is performed in a thermomixer at 80°C, with agitation at 750 rpm for 2 hours to ensure the highest protein solubilization. After centrifugation at 14000 g at 4°C, extracted proteins were recovered from the supernatant. Protein quantification was then carried out using the Qubit 4

fluorometer (Thermo Fisher Scientific) and protein assay kit (Thermo Fisher Scientific).

Western blotting

Two polyacrylamide gel formulations (10% and 6% acrylamide) were used to detect proteins of low (GDF9, IHH and SHH) and high (PTCH1, GLI1, GLI2 and GLI3) molecular weight respectively. Two different molecular weight markers (ladders) appropriate for proteins with small (PageRulerTM prestained protein ladder, 10-180 kDa, Thermo Fisher Scientific) and large (HiMarkTM prestained protein standard, 31-460 kDa, Thermo Fisher Scientific) molecular mass were used. Seven microliters of FFPE proteins extracted from each sample (around 30 µg/ml) were mixed with 2.5 µl fresh Laemmli sample buffer (100 µl β-mercaptoethanol in 900 µl buffer) and placed on a heated plate at 95°C for 5 minutes, before loading into the gel wells next to the loaded ladder. Mmigration of proteins based on size occurs first at 120 V for 10 minutes, then at 150 V for at least 40 minutes until the blue marker reaches the bottom limit of the gel. Since proteins need to be accessible for antibody detection, they are transferred from the gel to a polyvinylidene difluoride (PVDF) membrane at 100 V for 1 hour. Before incubating with

primary antibody, a blocking step is required to inhibit interactions between the membrane and the primary antibody. For this, the membrane is incubated in 5% blocking solution (5 g non-fat dried milk in TBS-T 1X [100 ml TBS + 100 µl 100% Tween 20]) for 1 hour at RT. It is then incubated with the primary antibody (overnight at 4°C with gentle agitation) against the protein of interest diluted in 0.5% of the previous blocking solution. After 3 rinses (5 minutes each) in TBS-T to remove the unbound primary antibody, the membrane is incubated (1 hour at RT with gentle agitation) with the secondary antibody (goat anti-mouse Ig [115-035-062, Jackson ImmunoReserch, Pennsylvania, USA] or goat anti-rabbit Ig [111-035-144, Jackson ImmunoReaserch, Pennsylvania, USA]) diluted in 0.5% of the blocking solution. The secondary antibody is linked to a peroxidase (HRP) to ensure clear identification of the protein of interest on the membrane, allowing its detection through a chemiluminescent reaction using SuperSignal West Pico Plus Chemiluminescent Substrate (35477, Thermo Fisher Scientific). This is based on a substrate present in the kit, which recognizes HRP inthe secondary antibody and produces light that can be visualized using Fusion software (Vilber Lourmat, Collégien, France).

RNA extraction and cDNA synthesis

Five human control ovarian tissue samples (age range: 52-79 years; mean age: 63.8) were frozen in Tissue-Tek® O.C.T.™ compound (Sakura, Zoeterwoude, Netherlands) and cut into 5µm sections with the Thermo Scientific Microm HM560 Cryostat-Series (Thermo Fisher Scientific). Tissue processing was performed as previously described [22]. Briefly, fragments were placed in lysing matrix Z tubes (MP Biomedicals, Ohio, USA) containing 2 mm yttria-stabilized zirconium beads with 600 µl RLT Plus buffer from the AllPrep DNA/RNA Micro kit (Qiagen) with 1% β-mercaptoethanol (Sigma-Aldrich, Steinheim, Germany). Samples were lysed by bead beating for two 30-second cycles at 6 m/s in FastPrep lysing matrix Z tubes. A cooling step on ice (40-second cycles) was performed between the two bead beatings. Tubes containing the lysates were then centrifuged for 3 minutes at 14000 g. Supernatant was collected and RNA extracted according to the manufacturer's instructions. Isolated RNA concentrations were measured using the Qubit 4 fluorometer and Qubit RNA broad range assay kit (Thermo Fisher Scientific). The QuantiTect whole transcriptome kit (Qiagen) was used to synthesize and amplify cDNA from 20 ng of isolated RNA. Synthesized cDNA concentrations were measured using the Qubit

fluorometer and Qubit dsDNA broad range assay kit (Thermo Fisher Scientific).

Quantitative real-time polymerase chain reaction (qPCR)

mRNA expression of Gdf9, Ihh, Gli1, Gli2 and Gli3 was investigated by quantitative real-time PCR using TaqMan probes for Gdf9 (Hs03986126-s1), Ihh (Hs00745531-s1), Gli1 (Hs00171790-m1), Gli2 (Hs01119974-m1) and Gli3 (Hs00609233-m1). Rplp0 (Hs99999902-m1) and B2M (Hs00187842_m1) served as housekeeping genes. cDNA from 10 fertile human ovaries was used as positive controls for Gli1 (data not shown) and cDNA from two individual hepatocyte samples were used as control for Gli1, Gli2 and Gli3 (data not shown). A total of 1 µl primer, 7 µl pyrogen, DNAse and RNAse-free diethyl pyrocarbonate (DEPC) water (Invitrogen, Thermo Fisher Scientific), 10 µl TaqMan Gene Expression Master Mix (Thermo Fisher Scientific) and 2 µl cDNA (50 ng/µl) was added to each well. Target genes were analyzed in duplicate for each sample.. Standard cycling conditions were applied as recommended by the manufacturer. Thermal cycling and fluorescence detection were performed using the StepOnePlus real-time PCR system (Applied Biosystems, California, USA).

Results

Immunohistochemistry

Ovaries from 14- and 33-week-old fetuses were quite different from each other. In the youngest fetal ovaries (14 weeks), the cell population was a mixture of stromal cells and oogonia (Fig. 1a). At around 17 weeks, some oocytes were observed in addition to oogonia in fetal ovaries (Fig. 1b). From approximately week 22 onwards, primordial follicles are known to emerge, and primary oocytes are surrounded by one layer of follicular cells, which will later form granulosa cells (Fig. 1c). Fetal ovaries at 33 weeks (Fig. 1d) contain the pool of primordial follicles that a girl will be born with. In our tissue samples from newborns to 2-year-old girls, the number of primordial follicles was still high and up to 150 follicles were counted in each ovarian section (Fig. 2-a). By the age of 6 years, the ovarian reserve had already declined (Fig. 2b). It is interesting to note that in the prepubertal group, additional follicle stages (type 2, type 3 and type 4) appeared in the stroma (Fig. 2c).

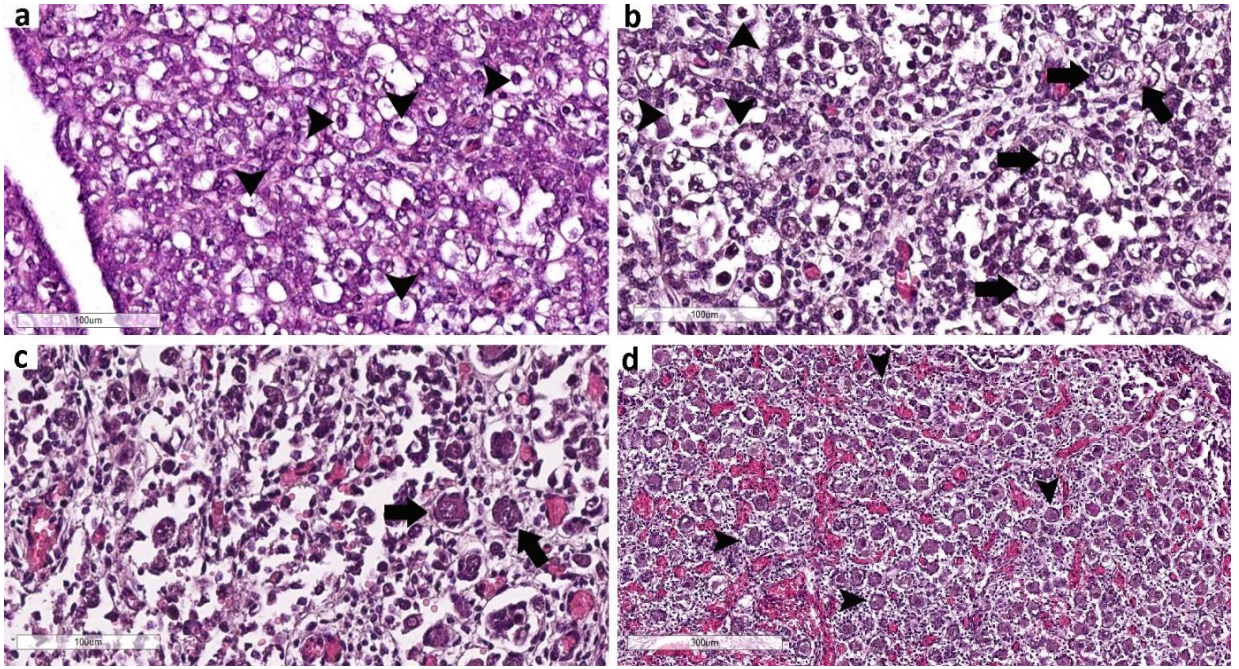


Figure 1. Histological sections of fetal ovaries at different time points of gestation. At around 14 weeks, oogonia (arrowhead) are visible (a). At around 17 weeks, oocytes (arrow) can be observed (b). At around 22 weeks, type 1 follicles (arrow) are found in the ovaries (c). At around 33 weeks (d), the ovary contains many type 1 follicles (arrow). Scale bar: 100 μm (a, b and c), 300 μm (d).

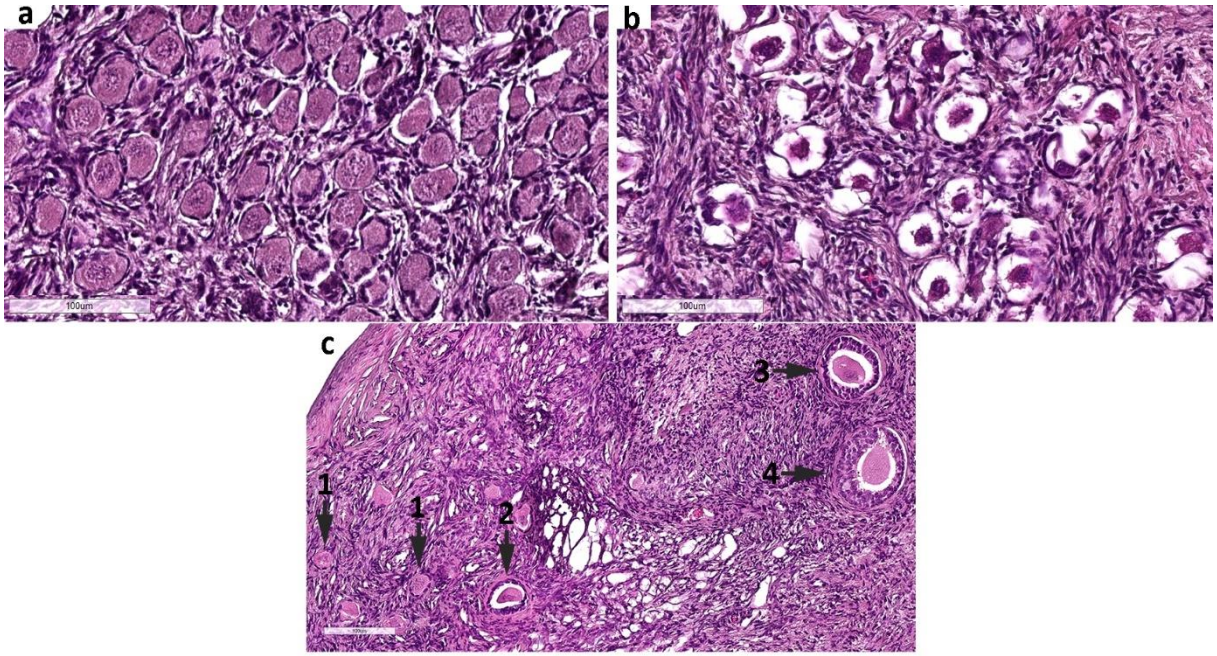


Figure 2. Histological sections of prepubertal ovaries at around the time of birth age 6. Abundant population of type 1 follicles in a newborn girl (a). Decrease in the number of type 1 follicles in the ovary of a 6-year-old girl (b). Presence of type 2, 3 and 4 follicles in addition to type 1 (shown by arrow) in the ovary of a 6-year-old girl (c). Scale bar: 100 µm

Immunohistochemical analysis of follicles in fetal ovaries revealed expression of GDF9, IHH, DHH, SHH, PTCH1, GLI1, GLI2 and GLI3 in the oocyte cytoplasm (Table 2; Fig. 3 - 10). All members of the HH family were also strongly expressed in the cytoplasm of follicular/granulosa cells (Fig. 3 - 10). Stromal cells were positive for IHH, DHH, SHH and PTCH1 only in their cytoplasm, and for GLI1, GLI2 and GLI3 in the cytoplasm and sometimes in the nucleus (Table 2; Fig. 3 - 10).

Table II: Immunostaining patterns of the GDF9-HH-GLI pathway in follicles and stromal cells in fetal ovaries.

Protein	Follicle type (n)	Oocytes		Granulosa cells		Stromal cells	
		Nucleus	Cytoplasm	Nucleus	Cytoplasm	Nucleus	Cytoplasm
GDF9	1 (426)	-	+	-	-	-	-
	2 (198)	-	+	-	-		
IHH	1 (879)	-	+	-	++	-	++
	2 (12)	-	+	-	++		
DHH	1 (780)	-	++	-	++	-	++
	2 (11)	-	+	-	++		
SHH	1 (1304)	-	++	-	+/++	-	++
	2 (17)	-	++	-	++		
PTCH1	1 (804)	-	+	-	-	-	-/+
	2 (24)	-	+	-	+		
GLI1	1 (1051)	-/++	-/++	-/++	-/++	-/++	+/++
	2 (51)	++	++	++	++		
GLI2	1 (117)	-/++	++	-/++	-/++	-/++	-/++
	2 (0)	°	°	°	°		
GLI3	1 (623)	-/+	+	+	++	-/+	+/++
	2 (0)	°	°	°	°		

Staining scored as follows: -, no staining observed; +, moderate staining; ++, strong staining. ° No type 2 follicles found on the slides.

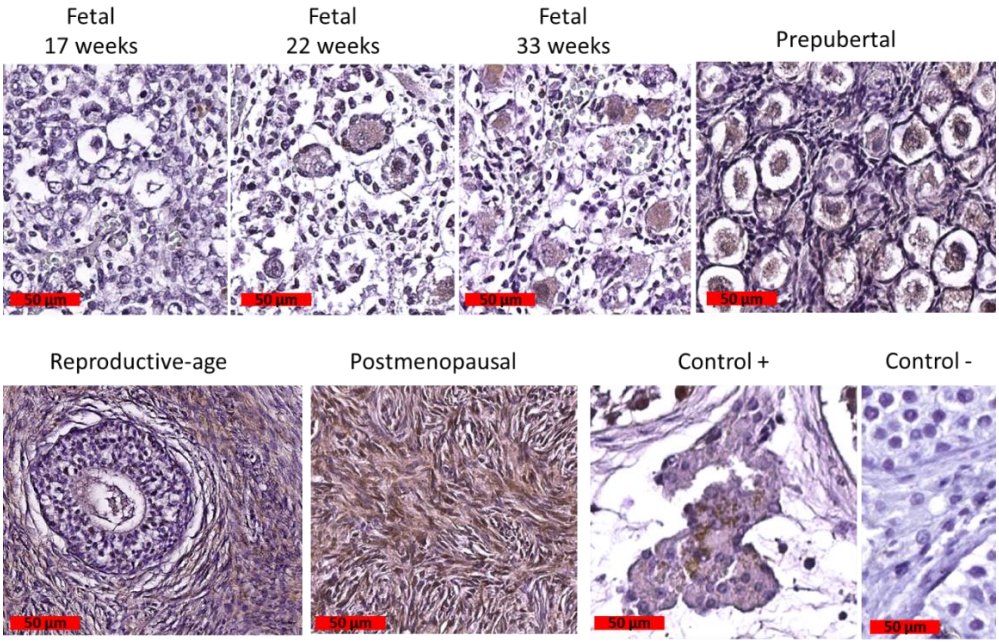


Figure 3. Immunohistochemical staining of GDF9 in fetal, prepubertal, reproductive-age and postmenopausal ovaries. No staining for GDF9 in a 17-week-old fetal ovary; GDF9 cytoplasmic staining in oocytes from type 1 follicles in 22- and 33-week-old fetal ovaries; GDF9 cytoplasmic staining in oocytes from type 1 follicles and stromal cells in prepubertal ovaries; GDF9 cytoplasmic staining in oocytes from type 1, 2, 3 and 4 follicles and stromal cells in reproductive-age ovaries and the theca interna and externa of type 5 and 6 follicles; GDF9 cytoplasmic expression in postmenopausal ovarian stromal cells; testes as positive and negative controls for GDF-9.

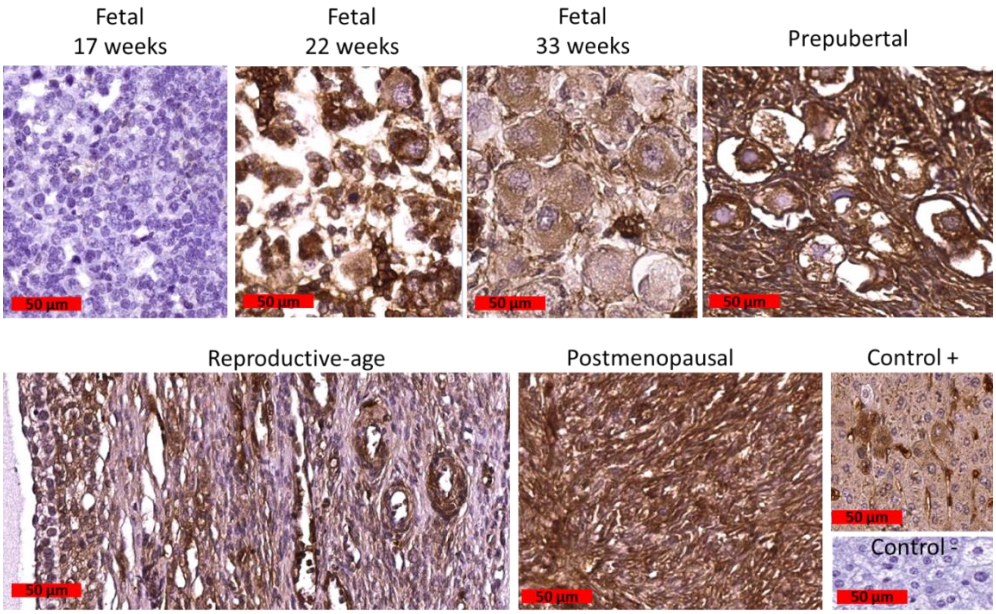


Figure 4. Immunohistochemical staining of IHH in fetal, prepubertal, reproductive-age and postmenopausal ovaries. No staining for IHH in the ovary of a 17-week-old fetus; IHH cytoplasmic staining of oocytes, granulosa and stromal cells in 22- and 33-week-old fetuses and prepubertal ovaries; IHH cytoplasmic staining in oocytes, granulosa, theca interna and externa and stromal cells in reproductive-age ovaries; IHH cytoplasmic staining in postmenopausal ovarian stromal cells; liver as positive and negative controls for IHH.

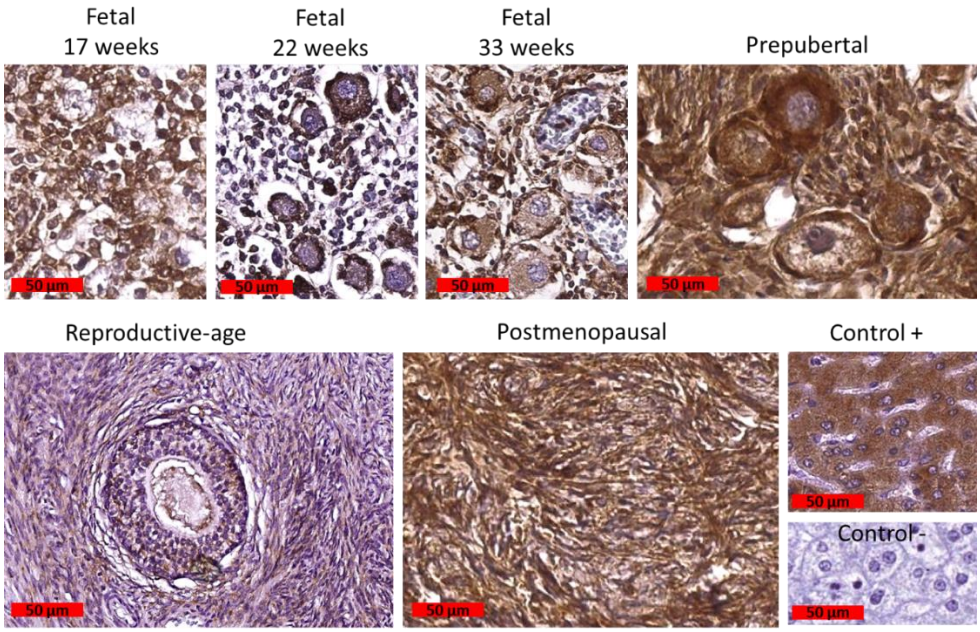


Figure 5. Immunohistochemical staining of DHH in fetal, prepubertal, reproductive-age and postmenopausal ovaries. DHH cytoplasmic staining of ovarian cells and oocyte in fetal and prepubertal ovaries; DHH cytoplasmic staining of oocytes, granulosa, theca interna and externa and stromal cells in reproductive-age ovaries; DHH cytoplasmic staining in postmenopausal ovarian stromal cells; liver as positive and negative controls for DHH.

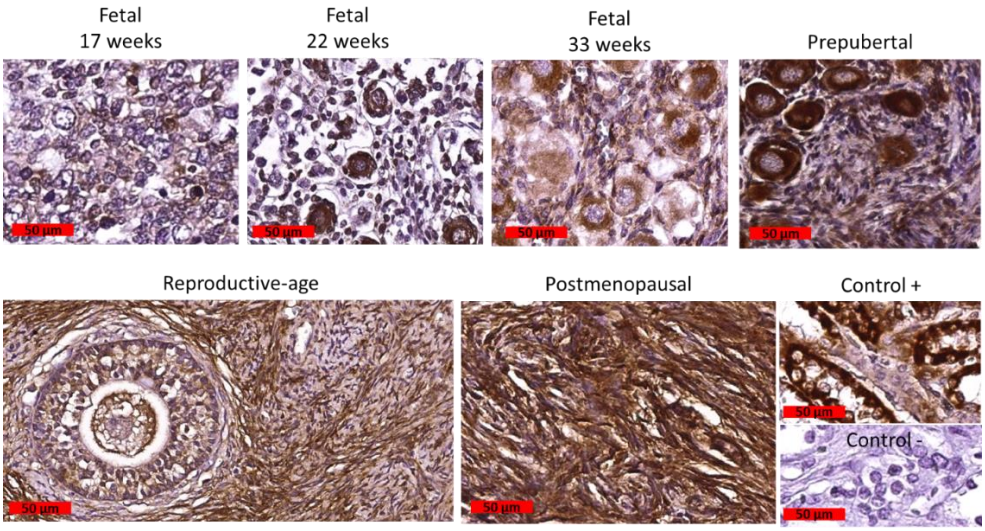


Figure 6. Immunohistochemical staining of SHH in fetal, prepubertal, reproductive-age and postmenopausal ovaries. SHH cytoplasmic staining of stromal cells and oocytes in fetal and prepubertal ovaries; SHH cytoplasmic staining of oocytes, granulosa, theca interna and externa and stromal cells in reproductive-age ovaries; SHH cytoplasmic staining in postmenopausal ovarian stromal cells; kidney as positive and negative controls for SHH.

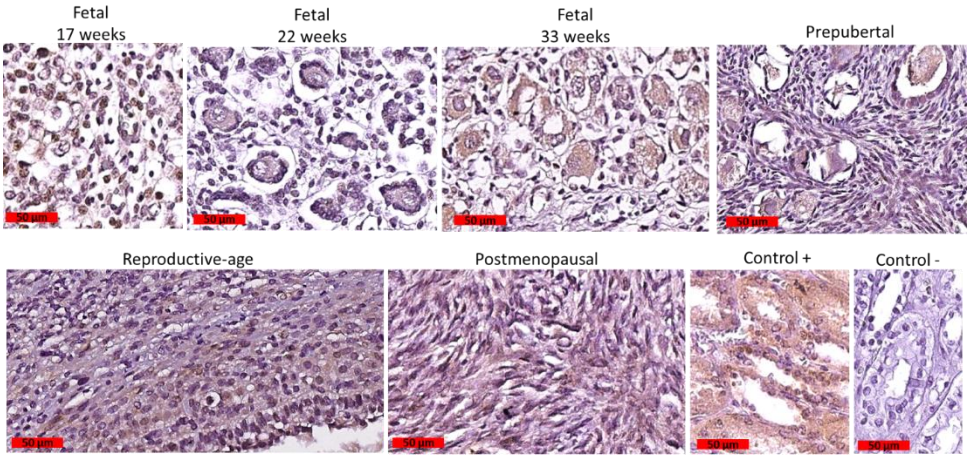


Figure 7. Immunohistochemical staining of PTCH1 in fetal, prepubertal, reproductive-age and postmenopausal ovaries. PTCH1 cytoplasmic staining of oogonia and ovarian cells of 17-week-old fetal ovary; PATCH1 cytoplasmic staining of oocytes and some ovarian cells in 22- and 33-week-old fetal ovaries; PATCH1 cytoplasmic staining in oocytes and some stromal cells in prepubertal ovaries; PATCH1 cytoplasmic staining of oocyte, granulosa cells, theca interna and externa and stromal cells in reproductive-age ovaries; PATCH1 cytoplasmic staining in postmenopausal ovarian stromal cells; kidney as positive and negative controls for PATCH1.

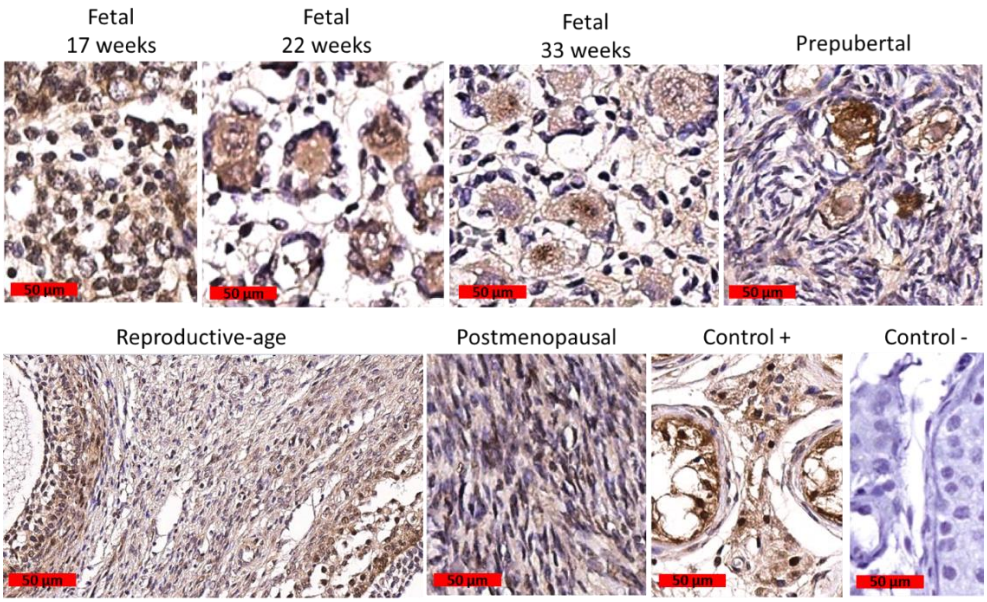


Figure 8. Immunohistochemical staining of GLI1 in fetal, prepubertal, reproductive-age and postmenopausal ovaries. GLI1 cytoplasmic and nuclear staining of oogonia and ovarian cells of 17-week-old fetal ovary; GLI1 cytoplasmic and nuclear staining of oocytes in 22- and 33-week-old fetal ovaries;GLI1 cytoplasmic and nuclear staining of oocytes and cytoplasmic staining of ovarian stromal cells in prepubertal ovaries; GLI1 cytoplasmic and nuclear staining of oocytes, theca interna and theca externa, and cytoplasmic staining of granulosa cells and ovarian stromal cells in reproductive-age ovaries; GLI1 week cytoplasmic staining in some postmenopausal ovarian stromal cells; testes as positive and negative controls for GLI1.

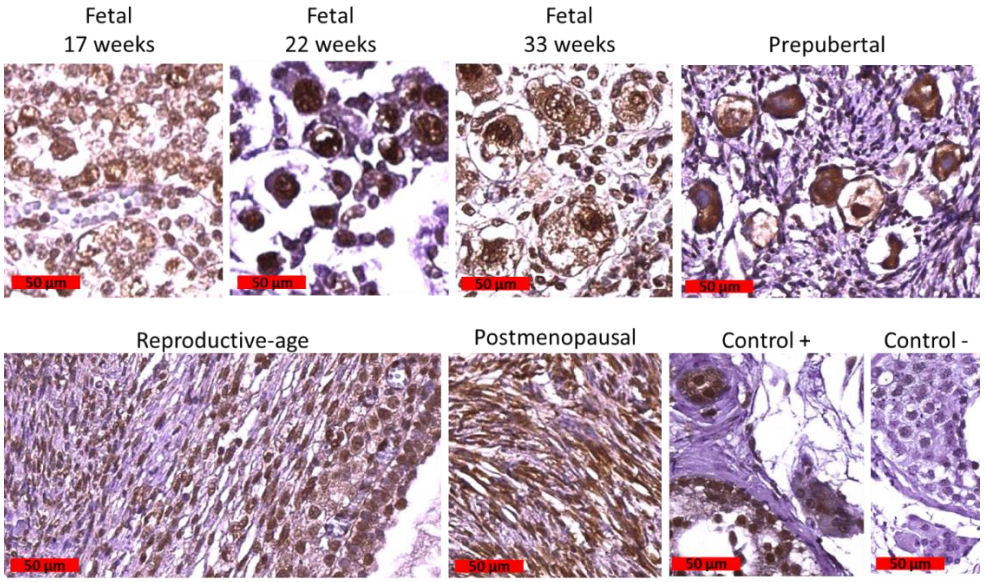


Figure 9. Immunohistochemical staining of GLI2 in fetal, prepubertal, reproductive-age and postmenopausal ovaries. GLI2 cytoplasmic and nuclear staining of oocytes, ovarian and granulosa cells in fetal ovaries; GLI2 cytoplasmic staining of oocytes and granulosa cells in prepubertal ovaries; GLI2 cytoplasmic and nuclear staining of oocytes, granulosa cells, theca interna and externa and ovarian stromal cells of reproductive-age ovaries; GLI2 cytoplasmic and nuclear staining of postmenopausal ovarian stromal cells; testes as positive and negative controls for GLI2.

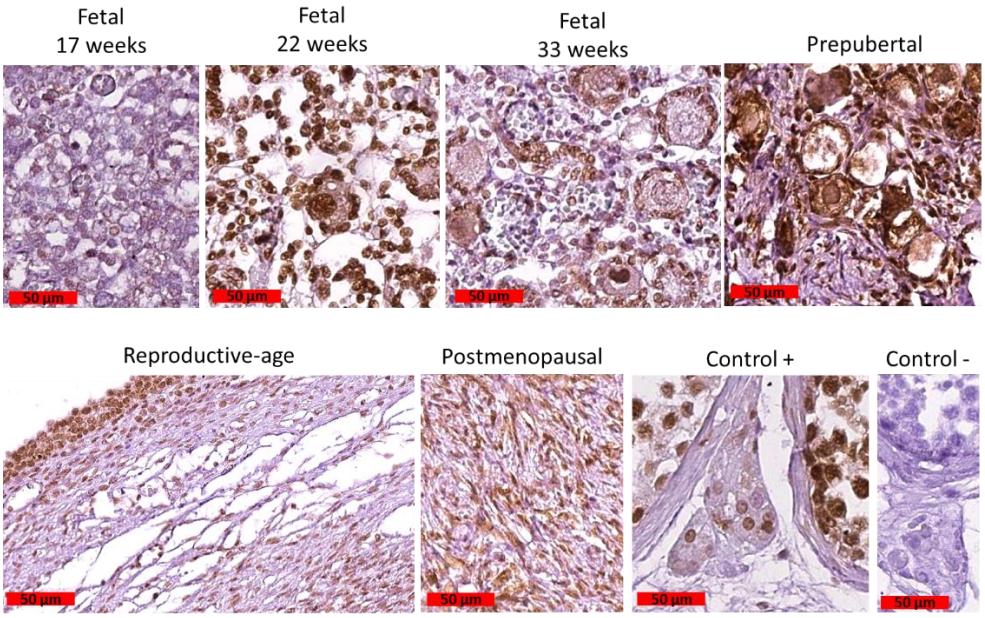


Figure 10. Immunohistochemical staining of GLI3 in fetal, prepubertal, reproductive-age and postmenopausal ovaries. GLI3 cytoplasmic staining of some ovarian cells in 17-week-old fetal ovary, GLI3 nuclear and cytoplasmic staining of oocytes and almost all the ovarian cells in 22-week-old fetal ovaries, GLI3 cytoplasmic and nuclear staining of oocytes, granulosa cells and most of the ovarian cells in 33-week-old fetal and prepubertal ovaries; GLI3 cytoplasmic staining of oocytes, cytoplasmic and nuclear staining of granulosa and stromal cells and nuclear staining of theca interna and externa of reproductive-age ovaries; GLI3 cytoplasmic and nuclear staining of postmenopausal ovarian stromal cells; testes as positive and negative controls for GLI3.

In ovaries from newborn to 6-year-old girls, GDF9 staining was specific to the oocyte cytoplasm (Table 3; Fig. 3). HH ligands (IHH, DHH and SHH) were expressed in oocytes and the granulosa cell cytoplasm in type 1 to 3 follicles, showing moderate to strong staining (Table 3; Fig. 4 - 6). As in fetal ovaries, there was weak staining for PTCH1 receptor in the cytoplasm of oocytes and granulosa cells from type 1 to 3 follicles (Table 3; Fig. 7). It is important to note that GDF9, IHH, DHH and PTCH1 expression were not possible to assess in type 4 follicles, as they were not detected in sections used for protein staining. Transcription factors GLI1, GLI2 and GLI3 showed positive nuclear and/or cytosolic staining in oocytes and granulosa cells in type 1 to 4 follicles (Table 3; Fig. 8 - 10). Only type 4 follicles contained a layer of theca cells, which did not stain any protein involved in the studied pathway. Stromal cells exhibited immunostaining for all markers except GDF9, but their nuclei expressed only GLI1, GLI2 and GLI3 (Table 3; Fig. 8 - 10).

Table III: Immunostaining patterns of the GDF9-HH-GLI pathway in follicles and stromal cells in prepubertal ovaries.

Protein	Follicle type (n)	Oocytes		Granulosa cells		Theca cells		Stromal cells	
		Nucleus	Cytoplasm	Nucleus	Cytoplasm	Nucleus	Cytoplasm	Nucleus	Cytoplasm
GDF9	1 (1360)	-	+/++	-	-	°	°	-	-/+
	2 (50)	-	+/++	-	-	°	°		
	3 (3)	-	+	-	-	°	°		
	4 (0)	°°	°°	°°	°°	°°	°°		
IHH	1 (1477)	-	+/++	-	++	°	°	-	+
	2 (102)	-	+	-	++	°	°		
	3 (3)	-	++	-	++	°	°		
	4 (0)	°°	°°	°°	°°	°°	°°		
DHH	1 (1360)	-	+/++	-	++	°	°	-	++
	2 (50)	-	+/++	-	++	°	°		
	3 (3)		+	-	++	°	°		
	4 (0)	°°	°°	°°	°°	°°	°°		
SHH	1 (3962)	-	++	-	++	°	°	-	-/++
	2 (34)	-	++	-	++	°	°		
	3 (2)	-	++	-	++	°	°		
	4 (2)	-	+	-	+	-	-		
PTCH1	1 (2096)	-	+	-	+	°	°	-	-/+
	2 (39)	-	+	-	+	°	°		
	3 (1)	-	+	-	+	°	°		
	4 (0)	°°	°°	°°	°°	°°	°°		
GLI1	1 (2114)	-/++	-/+	-/++	-/++	°	°	-/+	-/+
	2 (77)	-/++	-/+	-/++	-/++	°	°		
	3 (2)	-	+	++	+	°	°		
	4 (2)	-	+	++	+	-	-		
GLI2	1 (2957)	-/++	++	++	++	°	°	-/+	-/+
	2 (35)	-/++	++	++	++	°	°		
	3 (4)	-/++	+/++	-/++	-/++	°	°		
	4 (3)	++	++	++	++	-	-		
GLI3	1 (2396)	-/+	+	-/+	+	°	°	++	++
	2(79)	-/+	+	-/+	+	°	°		
	3 (4)	+	+	+	+	°	°		
	4 (1)	-	+	++	+	-	-		

Staining scored as follows: -, no staining observed; +, moderate staining; ++, strong staining. ° Type 1 to 3 follicles not yet surrounded by a theca layer. °° No type 4 follicles found on the slides.

In reproductive-age subjects, follicles continue their growth up to the final stages of development. There were fewer primordial follicles in the fertile group compared to prepubertal girls, but type 5 and 6 follicles were identified. At this stage of development, the cortex and medulla can be easily distinguished from each other and the majority of follicles are located in the cortex. IHC in reproductive-age ovaries showed cytoplasmic expression of GDF9 in oocytes of type 1 to 4 follicles, and granulosa and theca cells of type 5 and 6 follicles, at the same moderate intensity (Table 4; Fig. 3). Staining for HH ligands was observed in the cytoplasm of both oocytes and granulosa cells for type 1 to 6 follicles (Table 4; Fig. 4 - 6). Type 5 follicles were not detected on slides used for GDF9, IHH, DHH and SHH staining, but PTCH1 expression was seen in the oocyte cytoplasm of type 1 to 5 follicles. On the other hand, PTCH1 displayed immunostaining in the cytoplasm of granulosa cells in type 1 to 6 follicles (Table 4; Fig. 7). Theca cells in type 5 and type 6 follicles showed moderate PTCH1 expression in their cytoplasm (Table 4; Fig. 7), but those in type 4 and 6 follicles showed moderate to strong cytoplasmic staining for HH ligands (Table 4; Fig. 4 - 6). GLI1, GLI2 and GLI3 were expressed in oocytes, granulosa and theca cells at most stages of follicle development (Table 4; Fig. 8 - 10). However, GLI3 was less

expressed than other isoforms. Unexpectedly, stromal cells exhibited moderate to strong expression of GDF9 in their cytoplasm, which showed immunostaining for HH ligands and PTCH1 too. All studied GLI proteins were also stained at varying intensities in the cytoplasm and/or nucleus of stromal cells (Table 4; Fig. 3 - 10).

Table IV: Immunostaining patterns of the GDF9-HH-GLI pathway in follicles and stromal cells in reproductive-age ovaries.

Protein	Follicle type (n)	Oocyte		Granulosa cells		Theca cells		Stromal cells	
		Nucleus	Cytoplasm	Nucleus	Cytoplasm	Nucleus	Cytoplasm	Nucleus	Cytoplasm
GDF9	1 (170)	-	+	-	-	°	°	-	+/++
	2 (89)	-	+	-	-	°	°		
	3 (4)	-	+	-	-	°	°		
	4 (3)	-	+	-	+	-	+		
	5 (0)	°°	°°	°°	°°	°°	°°		
	6 (11)	-	-	-	+	-	+		
IHH	1 (69)	-	+	-	-	°	°	-	+/++
	2 (55)	-	+	-	++	°	°		
	3 (7)	-	+	-	+	°	°		
	4 (1)	-	-	-	++	-	+		
	5 (0)	°°	°°	°°	°°	°°	°°		
	6 (14)	-	-	-	-/+	-	++		
DHH	1 (143)	-	+	-	-	°	°	-	++
	2 (75)	-	+	-	++	°	°		
	3 (13)	-	+	-	++	°	°		
	4 (7)	-	+	-	++	_	+		
	5 (0)	°°	°°	°°	°°	°°	°°		
	6 (18)	-	-	-	++	-	+		
SHH	1 (89)	-	++	-	++	°	°	-	++
	2 (55)	-	++	-	++	°	°		
	3 (10)	-	+	-	++	°	°		
	4 (3)	-	+	-	+	_	++		
	5 (0)	°°	°°	°°	°°	°°	°°		
	6 (7)	-	-	-	+/++	-	++		

PTCH 1	1 (94)	-	++	-	+	°	°	-	+
	2 (48)	-	+	-	+	°	°		
	3 (8)	-	+	-	++	°	°		
	4 (0)	°°	°°	°°	°°	°°	°°		
	5 (2)	-	+	-	-/+	-	++		
	6 (9)	-	-	-	+	-	++		
GLI1	1 (85)	++	+	+	+	°	°	-/++	-/++
	2 (102)	++	+	++	++	°	°		
	3 (20)	++	+	++	++	°	°		
	4 (4)	++	+	++	+	++	++		
	5 (3)	+	+	++	+	++	++		
	6 (13)	-	-	++	++	++	++		
GLI2	1 (92)	-/++	++	++	++	°	°	-/++	-/+
	2 (104)	-/++	+	-/+/++	-/+/++	°	°		
	3 (10)	++	+	++	+	°	°		
	4 (6)	++	+	++	+	++	-		
	5 (0)	°°	°°	°°	°°	°°	°°		
	6 (12)	-	-	++	+	++	+		
GLI3	1 (101)	-	+	++	++	°	°	-/++	-/++
	2 (92)	-	+/++	+	+	°	°		
	3 (9)	+	+/++	+	+	°	°		
	4 (3)	+	+	++	+	-	-		
	5 (2)	-	-	+/++	+	+	-		
	6 (7)	-	-	+/++	-/+	-/+	-		

Since there are no follicles in postmenopausal ovaries, we focused our analysis on the stromal cell population. In the postmenopausal group, we investigated the entire stroma, as in all other groups. Like reproductive-age ovaries, stromal cells from their menopausal counterparts showed different intensities of staining for GDF9 (Table 5; Fig. 3). GDF9 expression was localized in the cytoplasm of stromal cells and its intensity differed from one patient to another (Table 5). IHH, DHH and

SHH were also detected in the same cell compartment (Table 5). Weak cytosolic PTCH1 expression was observed and GLI1, GLI2 and GLI3 showed different staining intensity in the nucleus and cytoplasm of stromal cells (Table 5; Fig. 3 - 10).

Table V: Localization and staining intensity patterns of GDF9, IHH, DHH, SHH, PTCH1, GLI1, GLI2 and GLI3 in stromal cells in postmenopausal ovaries.

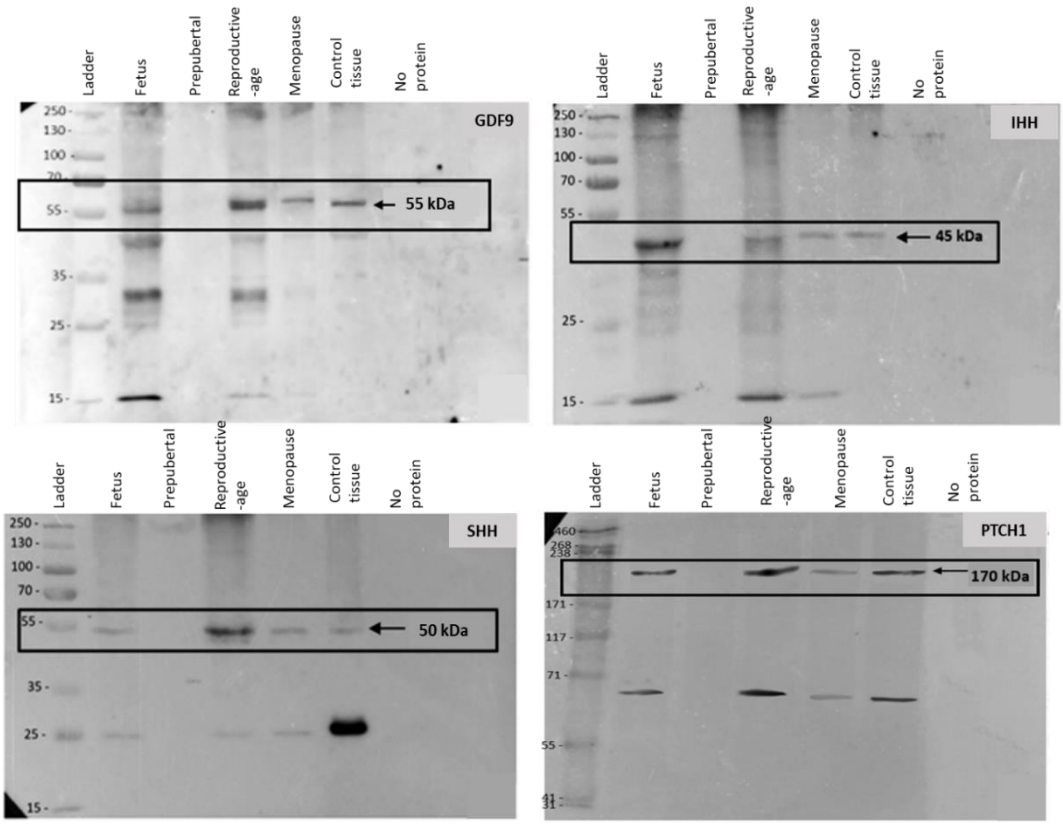
Protein	Stromal cells	
	Nucleus	Cytoplasm
GDF-9	-	-/+/++
IHH	-	++
DHH	-	++
SHH	-	++
PTCH1	-	+
GLI1	-	-/+
GLI2	++	-/+
GLI3	-/+	-/+

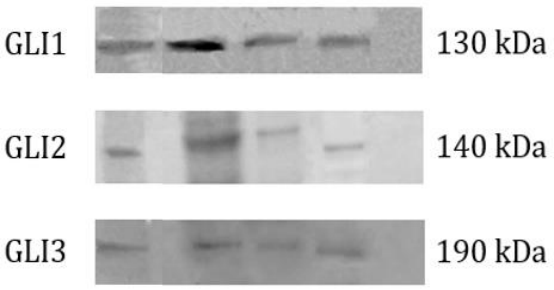
Western blot

In order to confirm our findings, we performed western blotting on the same proteins extracted from the same paraffin blocks previously used in IHC analyses. It is, however, important to stress that we encountered some complications while implementing this technique. Since ovarian tissue from prepubertal girls was encapsulated in agarose prior to paraffin embedding and this procedure affects protein extraction, we had to exclude this group from our western blot study.

Results were compared with datasheets for commercial antibodies, and positive tissue controls were the same as those used for IHC. For all proteins except DHH, whose antibody was not compatible, western blotting was carried out on lysates of fetal, prepubertal, reproductive-age and postmenopausal ovarian tissue samples, as well as positive controls (Fig. 11).

a)


Ladder
Fetus
Prepubertal
Reproductive -age
Menopause
Control tissue
No protein
GDF9
55 kDa
IHH
45 kDa
SHH
50 kDa
PTCH1
170 kDa


GLI1
130 kDa
GLI2
140 kDa
GLI3
190 kDa

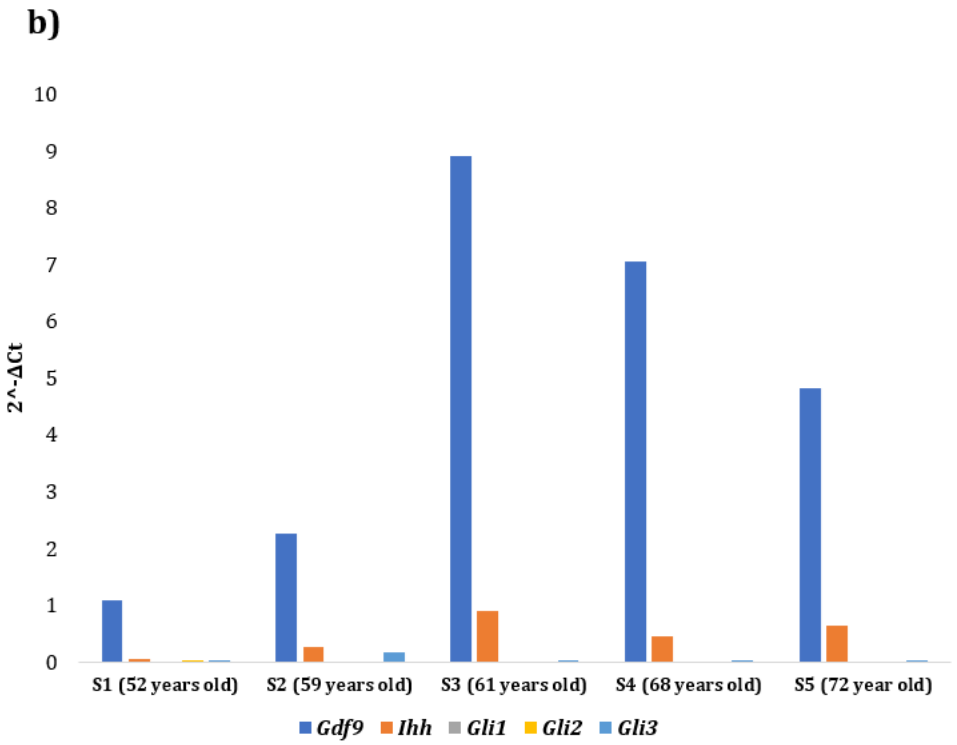


Figure 11. Western blot and Ct values from qPCR analysis. Western blotting of the same antibodies as used for immunohistochemistry (a). Ct values were obtained from qPCR for *Gdf9*, *Ihh*, *Gli1*, *Gli2 and Gli3* in stromal cells of postmenopausal ovaries.

Quantitative real-time PCR

To confirm our IHC and western blot findings in key proteins in postmenopausal ovaries, we performed quantitative real-time PCR to assess the presence of mRNA for Gdf9, Ihh, Gli1, Gli2 and Gli3 in postmenopausal ovarian tissue, despite the lack of a follicle population.

Surprisingly, our results revealed the presence of mRNA for Gdf9 (mean Ct value=22.8), Ihh (mean Ct value=26.2), and Gli3 (mean Ct value=31.9) in stromal cells from all five postmenopausal ovaries, Gli2 (Ct value=35.4) in one of the five postmenopausal ovaries, but no mRNA transcripts for Gli1 in any of the samples (Fig. 11).

Discussion

Theca cell recruitment remains an elusive process in human ovaries. Although there are some studies indicating that it occurs under the influence of different factors expressed by oocytes and granulosa cells of growing follicles [reviewed by 23], only a few hypothesize on the origin of these cells. It has been postulated that in mice, stromal cells surrounding follicles are those recruited for further differentiation [9, 24, 25]. More recently, studies in large animal models suggest that all stromal cells, not only those close to follicles, have the ability to differentiate into theca cells [26, 27]. However, we have demonstrated that while most human stromal cells can differentiate into steroidogenic cells in vitro, only a small proportion of them can actually become theca- and luteal-like cells [28]. This has led us to speculate that, just like in

mouse ovaries [3, 5], there is a population of precursor theca cells in their human counterparts. In pursuit of this theory, we assessed the GDF9-HH-GLI pathway in human fetal, prepubertal, reproductive-age and postmenopausal ovaries, as this pathway has been shown to be fundamental to recruiting precursor theca cells expressing Gli1 as a marker [3]. Our results revealed that this pathway originates from primordial follicles during the fetal period of life, and not from the primary stage after birth, as in mouse ovaries [29, 11, 30]. Based on our findings, GLI1, GLI2 and GLI3 proteins do not appear to be specific markers for precursor theca cells in human ovaries. First, they are not confined to a specific population of cells, as they are expressed in oocytes and granulosa cells as well as the stroma and not limited to precursor theca cells in ovarian stroma and differentiated steroidogenic theca cells, as in mice. Furthermore, expression of GLI1, 2 and 3 is not limited to a specific ovary age, as these proteins are expressed in 17-week-old fetal ovaries as long as the ovary continues to grow and follicles start to appear and develop. Finally, stromal cells from postmenopausal ovaries go on expressing GLI proteins, despite the absence of follicles.

The role of HH signaling in the vertebrate ovary has been investigated using in situ hybridization and IHC in murine [9, 21] and bovine [31]

samples. A study in mice indicated that the HH and PTCH1 response system may also function in an autocrine manner in granulosa cells [21]. It has been reported by Spicer et al. [31] that Ptch1 mRNA levels in theca cells were lower in cattle with double ovulation as opposed to single. This suggests that in bovines, decreased Ptch1 expression might be involved in the development of multiple dominant follicles [32]. Moreover, the GDF9-HH-GLI pathway may differ between mammals. For instance, Spicer et al. [31] speculated that differences might exist in terms of hormonal regulation of the HH system between monotocous (cattle) and polytocous (rodents) species. In mammals, HH signaling is a key factor in communication between cellular compartments (gonads, Sertoli cells in testes and granulosa cells in ovaries) involved in gametogenesis and steroidogenesis [9, 10].

While our findings indicate that GLI proteins are not specific markers to identify precursor theca cells in human ovaries, based on GDF9, IHH, DHH, SHH, PTCH1, GLI1, GLI2 and GLI3 expression patterns, we can postulate that the GDF9-HH-GLI pathway may well play a different role in human ovaries. Our results show expression of the GDF9 protein at all follicle stages, including primordial (type 1). GDF9 is crucial to regulating and promoting follicle growth and oocyte development by

predominantly acting on supporting granulosa cells via paracrine signaling [33]. Like Sun et al. [34], we also observed GDF9 expression in human fetal, prepubertal and reproductive-age ovaries. Interestingly, our IHC results from reproductive-age and postmenopausal ovaries showed GDF9 expression in the cytoplasm of stromal cells. Intrigued by this finding, we performed qPCR analysis on samples of postmenopausal ovaries (52-79 years of age), which confirmed the presence of Gdf9 mRNA in this cell population. To the best of our knowledge, there are no studies explaining this GDF9 mRNA and protein expression, which is typically associated with folliculogenesis in human ovarian stroma.

Amino acid sequences of IHH, DHH and SHH are highly similar and all three members of the HH family can evoke similar mechanistic responses through the PTCH1 receptor in vitro and in vivo [35, 36]. It has been reported that IHH and DHH are co-expressed in adult mouse ovaries [37, 31]. In mice, HH proteins are expressed in granulosa cells of primary to antral follicles [21]. Our results in humans show that IHH, DHH and SHH are expressed in the cytoplasm of oocytes and granulosa cells of primordial (type 1) to antral (type 6) follicles, as well as stromal cells. Again, we did not expect this finding, so to confirm the presence of these ligands in stromal cells, we performed qPCR on Ihh in

postmenopausal ovaries (52-79 years of age), which revealed Ihh mRNA expression in this cell population. As reported in previous studies on mouse ovaries [9, 3], GDF9 is required to trigger the HH pathway in follicles. Perhaps the presence of GDF9 in stromal cells of postmenopausal human ovaries might be the reason for Ihh mRNA and protein expression. IHH and DHH start to be expressed in murine granulosa cells on day 4 after birth, when some primordial follicles have already been activated to grow to the primary stage [21]. The SHH expression pattern in mice is different from that of IHH and DHH. Levels are higher in mouse ovaries at birth, decrease by day 4, then return to higher values in prepubertal ovaries, before declining in adult mice [21]. Unlike in mouse ovaries, we observed IHH, DHH and SHH expression in oocytes and the granulosa cell cytoplasm at all human follicle stages. IHH and DHH were more extensively expressed in primordial and primary follicles in prepubertal tissue, which could have been due to the higher expression of GDF9 by oocytes of primordial-primary follicles in this phase of life. Although SHH expression increases from fetal to reproductive age, our results show that SHH levels are lower than IHH and DHH during the fetal and prepubertal period. According to deletion studies in mice, IHH and DHH are involved in governing the

differentiation and steroidogenic capacity of adrenal, theca and Leydig cells by regulating steroidogenic enzymes [3, 11]. These results are consistent with our findings on HH expression in reproductive-age and postmenopausal ovaries. Indeed, stromal cells in reproductive-age [38-41] and postmenopausal [42-45] human ovaries exhibit steroidogenic activity.

Our results on PTCH1 expression in oocytes of primordial follicles in humans differ from those of Wijgerde et al. [9], which showed that PTCH1 only appears at the primary stage of follicles in mice. On the other hand, PTCH1 expression in granulosa and theca cells from human reproductive-age ovaries is in line with what was previously reported in bovine [31] and mouse [21] follicles. The presence of PTCH1 in stromal cells could be due to the presence of previously needed markers to trigger the HH pathway in human ovaries. In mouse ovaries, Wijgerde et al. [9] reported low background mRNA levels for the Ptch1 gene over the whole ovary, while expression of this target gene was clearly upregulated in cells surrounding follicles. PTCH1 is a key component of the HH signaling pathway, which controls cell fate during development [46]. Expression of PTCH1 in the cytoplasm of oocytes was the same as previously observed in mouse follicles [21]. As reported by Wijgerde et

al. [9] oocytes are probably exposed to IHH and DHH from surrounding granulosa cells, and express the PTCH1 receptor but lack the SMO signal transducer. That is why even in the presence of the PTCH1 receptor, the HH pathway is not complete and there is no steroidogenic activity in oocytes [9]. It has been shown that although granulosa cells from antral follicles in mice produce DHH and IHH ligands, their targets, PTCH1, SMO, GLI1, GLI2, and GLI3, reside in theca, granulosa and stromal cells [21, 9]. While our results indicate that HH ligands, PTCH1, GLI1, GLI2 and GLI3 initiate their expression in fetal ovaries of humans, in mice, the HH pathway is presumably inactive because of the absence of DHH, PTCH1, GLI1, and GLI2 expression [29, 11], which are only activated in adult mouse ovaries [30]. The presence of GLI1, 2 and 3 proteins and Gli3 mRNA, and absence of Gli1 and 2 mRNA in postmenopausal ovaries might be due to the lifetime of the protein and high degradation rate of mRNA, as well as a difference in the course of steroidogenesis in postmenopausal compared to reproductive-age ovaries. Human postmenopausal ovaries have a unique pattern of steroidogenic enzyme expression that favors Δ5 steroid formation over Δ4 steroid formation [45]. The presence of three different GLI proteins in vertebrates as opposed to one Ci ortholog in Drosophila points to more complex

responses within target fields. Therefore, cellular responses to HH signaling might not just depend on levels of ligand exposure, but also particular Gli gene expression [17].

Based on the known role of the HH signaling pathway in cell proliferation, survival and differentiation [47] as well as our findings, we hypothesize that HH proteins could be involved in human gonadal development and function, as in Drosophila [17, 48, 49, 47]. Furthermore, due to the nature of the ovary as a super-dynamic organ and its role in steroidogenesis and follicle development, it makes sense that HH proteins and their downstream targets are expressed at all ages in the human ovary. Our results also indicate that unlike in mice, GLI is expressed at all human ovary ages and could be involved in steroidogenesis as a general rather than specific marker of theca cells.

A recently published study by Fan et al. [50] suggests that NME2, APOD, APOC1, MEST, WFDC1, MATN2, PTCH1 and ACTA2 are markers of precursor theca cells in human ovaries. While immunostaining patterns of PTCH1 in the current study do not confirm this protein as a marker of precursor theca cells, these apparently contradictory findings nevertheless underline the fact that the human ovary is complex and

subtle, and that the roles of all these proteins with different lifetimes require further investigation to achieve some clarity.

Because HH proteins are involved in theca interna steroidogenesis [9, 31], and considering the role of the theca interna in the pathology of polycystic ovary disease, it might also be important to assess HH signaling pathways in the pathogenesis of polycystic ovaries. Our findings on the GDF9-HH-GLI pathway provide a basis for future investigations into human ovaries. They could be applied to define cell-specific responses to GDF9-HH-GLI signaling in human follicles and stromal cells, determining how this pathway modulates follicle development and steroidogenic function in ovaries from the fetal to the postmenopausal stage.

Authors' roles

P. A.: study design, experimental procedures, analysis, interpretation of data and manuscript preparation. C. D.: experimental procedures and analysis. M. M. D.: manuscript revision. E. M: tissue supply, analysis of IHC staining and manuscript revision. A. C.: tissue supply. C. A. A.:

experimental design, experimental procedures, interpretation of results and manuscript revision.

Acknowledgements

We are grateful to Mira Hryniuk, BA, for reviewing the English language of the manuscript, and Dolores Gonzalez and Olivier Van Kerk for their technical assistance.

Funding

This study was supported by grants from the Fonds National de la Recherche Scientifique de Belgique (FNRS) (C. A. Amorim is an FRS-FNRS Research Associate; grant MIS #F4535 16 awarded to C. A. Amorim; grant PDR T.0077.14 and grant 5/4/150/5 awarded to M. M. Dolmans; grant ASP-RE314 awarded to P. Asiabi) and the Fondation Contre le Cancer (grant 2018-042 awarded to A. Camboni).

Conflict of interest

The authors declare no conflict of interest.

References

1. Edson MA, Nagaraja AK, Matzuk MM. The Mammalian Ovary from Genesis to Revelation. Endocrine Reviews. 2009;30(6):624-712. doi:10.1210/er.2009-0012.

2. Matzuk MM, Lamb DJ. The biology of infertility: research advances and clinical challenges. Nature Medicine. 2008;14(11):1197-213. doi:10.1038/nm.f.1895.

3. Liu C, Peng J, Matzuk MM, Yao HH-C. Lineage specification of ovarian theca cells requires multicellular interactions via oocyte and granulosa cells. Nature communications. 2015;6(1):1-11.

4. Lapointe E, Boerboom D. WNT signaling and the regulation of ovarian steroidogenesis. Frontiers in bioscience (Scholar edition). 2011;3:276-85.

5. Honda A, Hirose M, Hara K, Matoba S, Inoue K, Miki H et al. Isolation, characterization, and in vitro and in vivo differentiation of putative thecal stem cells. PNAS. 2007;104(30):12389-94.

6. Dong J, Albertini DF, Nishimori K, Kumar TR, Lu N, Matzuk MM. Growth differentiation factor-9 is required during early ovarian folliculogenesis. Nature. 1996;383(6600):531-5.

7. Varjosalo M, Taipale J. Hedgehog: functions and mechanisms. Genes & development. 2008;22(18):2454-72.

8. Liu C-F, Liu C, Yao HH-C. Building pathways for ovary organogenesis in the mouse embryo. Current topics in developmental biology. Elsevier; 2010. p. 263-90.

9. Wijgerde M, Ooms M, Hoogerbrugge JW, Grootegoed JA. Hedgehog signaling in mouse ovary: Indian hedgehog and desert hedgehog from granulosa cells induce target gene expression in developing theca cells. Endocrinology. 2005;146(8):3558-66.

10. Richards JS, Ren YA, Candelaria N, Adams JE, Rajkovic A. Ovarian follicular theca cell recruitment, differentiation, and impact on fertility: 2017 update. Endocrine reviews. 2017;39(1):1-20.

11. Yao HH-C, Whoriskey W, Capel B. Desert Hedgehog/Patched 1 signaling specifies fetal Leydig cell fate in testis organogenesis. Genes & development. 2002;16(11):1433-40.

12. Marion G, Gier H, Choudary J. Micromorphology of the bovine ovarian follicular system. Journal of Animal Science. 1968;27(2):451-65.

13. Stone DM, Hynes M, Armanini M, Swanson TA, Gu Q, Johnson RL et al. The tumour-suppressor gene patched encodes a candidate receptor for Sonic hedgehog. Nature 1996;384(6605):129-34.

14. Fuse N, Maiti T, Wang B, Porter JA, Hall TMT, Leahy DJ et al. Sonic hedgehog protein signals not as a hydrolytic enzyme but as an apparent ligand for patched. Proceedings of the National Academy of Sciences 1999;96(20):10992-9.

15. Ingham P, Taylor A, Nakano Y. Role of the Drosophila patched gene in positional signalling. Nature 1991;353(6340):184-7.

16. Taipale J, Cooper M, Maiti T, Beachy P. Patched acts catalytically to suppress the activity of Smoothened. Nature 2002;418(6900):892-6.

17. Ingham PW, McMahon AP. Hedgehog signaling in animal development: paradigms and principles. Genes & development. 2001;15(23):3059-87.

18. Gulino A, Di Marcotullio L, Ferretti E, De Smaele E, Screpanti I. Hedgehog signaling pathway in neural development and disease. Psychoneuroendocrinology 2007;32:S52-S6.

19. Di Marcotullio L, Ferretti E, Greco A, De Smaele E, Screpanti I, Gulino A. Multiple ubiquitin-dependent processing pathways regulate hedgehog/gli signaling: implications for cell development and tumorigenesis. Cell cycle. 2007;6(4):390-3.

20. Lum L, Beachy PA. The Hedgehog response network: sensors, switches, and routers. Science 2004;304(5678):1755-9.

21. Russell MC, Cowan RG, Harman RM, Walker AL, Quirk SM. The hedgehog signaling pathway in the mouse ovary. Biology of reproduction. 2007;77(2):226-36.

22. Asiabi P, Ambroise J, Giachini C, Coccia ME, Bearzatto B, Chiti MC et al. Assessing and validating housekeeping genes in normal, cancerous, and polycystic human ovaries. Journal of Assisted Reproduction and Genetics 2020;37:2545-2553.

23. Young J, McNeilly AS. Theca: the forgotten cell of the ovarian follicle. Reproduction. 2010;140(4):489-504.

24. Magoffin DA. Ovarian theca cell. The international journal of biochemistry & cell biology. 2005;37(7):1344-9.

25. Magoffin DA, Magarelli PC. Preantral follicles stimulate luteinizing hormone independent differentiation of ovarian theca-interstitial cells by an intrafollicular paracrine mechanism. Endocrine reviews. 1995;3(2):107-12.

26. Orisaka M, Tajima K, Mizutani T, Miyamoto K, Tsang BK, Fukuda S et al. Granulosa cells promote differentiation of cortical stromal cells into theca cells in the bovine ovary. Biology of reproduction. 2006;75(5):734-40.

27. Qiu M, Quan F, Han C, Wu B, Liu J, Yang Z et al. Effects of granulosa cells on steroidogenesis, proliferation and apoptosis of stromal cells and theca cells derived from the goat ovary. The Journal of steroid biochemistry and molecular biology. 2013;138:325-33.

28. Asiabi P, Dolmans MM, Ambroise J, Camboni A, Amorim CA. In vitro differentiation of theca cells from ovarian cells isolated from postmenopausal women. Human Reproduction. 2020; https://doi.org/10.1093/humrep/deaa246

29. Bitgood MJ, McMahon AP. Hedgehog and Bmp genes are coexpressed at many diverse sites of cell-cell interaction in the mouse embryo. DEVELOPMENTAL BIOLOGY-ACADEMIC PRESS-. 1995;172:126-.

30. Huang CCJ, Yao HHC. Diverse functions of Hedgehog signaling in formation and physiology of steroidogenic organs. Molecular Reproduction and Development: Incorporating Gamete Research. 2010;77(6):489-96.

31. Spicer LJ, Sudo S, Aad PY, Wang LS, Chun S-Y, Ben-Shlomo I et al. The hedgehog-patched signaling pathway and function in the mammalian ovary: a novel role for hedgehog proteins in stimulating proliferation and steroidogenesis of theca cells. Reproduction. 2009;138(2):329-39.

32. Aad PY, Spicer LJ, Echternkamp SE. The Hedgehog System in Ovarian Follicles of Cattle Selected for Twin Ovulations and Births: Evidence of a Link Between the IGF and Hedgehog Systems. Oxford University Press; 2008.

33. Otsuka F, McTavish KJ, Shimasaki S. Integral role of GDF-9 and BMP-15 in ovarian function. Molecular reproduction and development. 2011;78(1):9-21.

34. Sun R, Lei L, Cheng L, Jin Z, Zu S, Shan Z et al. Expression of GDF-9, BMP-15 and their receptors in mammalian ovary follicles. Journal of molecular histology 2010;41(6):325-32. doi:https://doi.org/10.1007/s10735-010-9294-2.

35. Echelard Y, Epstein DJ, St-Jacques B, Shen L, Mohler J, McMahon JA et al. Sonic hedgehog, a member of a family of putative signaling molecules, is implicated in the regulation of CNS polarity. Cell. 1993;75(7):1417-30.

36. Bitgood MJ, Shen L, McMahon AP. Sertoli cell signaling by Desert hedgehog regulates the male germline. Current biology. 1996;6(3):298-304.

37. Van Den Brink GR, Bleuming SA, Hardwick JC, Schepman BL, Offerhaus GJ, Keller JJ et al. Indian Hedgehog is an antagonist of Wnt signaling in colonic epithelial cell differentiation. Nature genetics. 2004;36(3):277-82.

38. Parikh G, Varadinova M, Suwandhi P, Araki T, Rosenwaks Z, Poretsky L et al. Vitamin D regulates steroidogenesis and insulin-like growth factor binding protein-1 (IGFBP-1) production in human ovarian cells. Hormone metabolic research. 2010;42(10):754-7.

39. Qiu M, Quan F, Han C, Wu B, Liu J, Yang Z et al. Effects of granulosa cells on steroidogenesis, proliferation and apoptosis of stromal cells and theca cells derived from the goat ovary. The Journal of steroid biochemistry molecular Biology Reports. 2013;138:325-33.

40. Channing CP. Steroidogenesis and morphology of human ovarian cell types in tissue culture. Journal of Endocrinology. 1969;45(2):297-NP.

41. Qiu M, Liu J, Han C, Wu B, Yang Z, Su F et al. The influence of ovarian stromal/theca cells during in vitro culture on steroidogenesis, proliferation and apoptosis of granulosa cells derived from the goat ovary. Reproduction in domestic animals. 2014;49(1):170-6.

42. Fogle RH, Stanczyk FZ, Zhang X, Paulson RJ. Ovarian androgen production in postmenopausal women. The Journal of Clinical Endocrinology Metabolism. 2007;92(8):3040-3.

43. Couzinet B, Meduri G, Lecce MG, Young J, Brailly S, Loosfelt H et al. The postmenopausal ovary is not a major androgen-producing gland. Journal of Clinical Endocrinology Metabolism. 2001;86(10):5060-6.

44. Dupont E, Labrie F, Luu-The V, Pelletier G. Immunocytochemical localization of 3 beta-hydroxysteroid dehydrogenase/delta 5-delta 4-isomerase in human ovary. The Journal of Clinical Endocrinology Metabolism. 1992;74(5):994-8.

45. Havelock JC, Rainey WE, Bradshaw KD, Carr BR. The postmenopausal ovary displays a unique pattern of steroidogenic enzyme expression. Human Reproduction. 2005;21(1):309-17.

46. Hammerschmidt M, Brook A, McMahon AP. The world according to bedgebog. Trends in Genetics. 1997;13(1):14-21.

47. Walterhouse DO, Lamm ML, Villavicencio E, Iannaccone PM. Emerging roles for hedgehog-patched-Gli signal transduction in reproduction. Biology of reproduction. 2003;69(1):8-14.

48. Nüsslein-Volhard C, Wieschaus E. Mutations affecting segment number and polarity in Drosophila. Nature. 1980;287(5785):795-801.

49. McMahon AP, Ingham PW, Tabin CJ. 1 Developmental roles and clinical significance of Hedgehog signaling. Current Topics in Developmental Biology 2003;53:1-114.

50. Fan X, Bialecka M, Moustakas I, Lam E, Torrens-Juaneda V, Borggreven N et al. Single-cell reconstruction of follicular remodeling in the human adult ovary. Nature communications. 2019;10(1):1-13.

3.4 In vitro differentiation of human theca cells

Investigation of the main cell populations in the ovarian cortex is an important step before assessing the ability of ovarian cells to differentiate into theca cells. To this end, cells from the ovarian cortex were isolated mechanically with tissue chopper and enzymatically with Liberase DH at 37°C for 75 minutes. Characterization of isolated human ovarian cells was assessed by immunohistochemical staining for vimentin (a marker for mesenchymal cells), CD31 (a marker for endothelial cells), and inhibin-α (a marker for granulosa cells). Our findings showed that most cells (around 80-90%) found in the human ovarian cortex are stromal cells.

While the origin of theca cells in human ovaries remains unknown, recent studies identified a population of theca stem cells surrounding small antral follicles (Dalman *et al.*, 2018a; Dalman *et al.*, 2018b). In vitro culture of these cells using specific conditions showed that these cells could be differentiated into precursor theca cells as well as adipocyte-, osteocyte-, chondrocyte-, and oocyte-like cells (Dalman *et al.*, 2018a; Dalman *et al.*, 2018b). However, our aim in the transplantable engineered ovary is to restore fertility in patients who underwent chemo-radiotherapy. Ovaries from these women are similar to postmenopause counterparts, i.e., devoid of follicles and, consequently, their surrounding theca cells and theca stem cells (Meirow and Nugent, 2001; Spears *et al.*, 2019). Based on studies in cow and goat models that reported the in vitro differentiation of theca cells from stromal cells (Qiu *et al.*, 2013), we hypothesized that similar to these large animal species,

humans stromal cells could differentiate into theca cells. To this end, we have isolated stromal cells from the cortical ovarian biopsies of menopause women and in vitro cultured using a medium enriched with growth factors that are supposed to influence theca cell differentiation in the ovary. Our results show significant changes in expression patterns of genes involved in the steroidogenic pathway as well as their protein expression, indicating that 21 - 43% of ovarian cells were able to differentiate into theca-like cells. This was also supported by cell ultrastructure and the presence of DHEA and progesterone in the medium. In conclusion, our results show that theca cell differentiation in human ovaries is not similar to the process described in other animal models. Our exciting findings shed light on theca cell differentiation in human ovaries, suggesting the presence of a subpopulation of theca stem cells that remains in the ovary throughout a woman's life.

Article 3

DOI: 10.21451/1984-3143-AR2018-0140

Anim. Reprod., v.16, n.1, p.39-44, Jan./Mar. 2019

Isolation and characterization of the human ovarian cell population for transplantation into an artificial ovary

Parinaz Asiabi Kohneh Shahri, Maria Costanza Chiti, Christiani A. Amorim[§]

Pôle de Recherche en Gynécologie, Institut de Recherche Expérimentale et Clinique, Université Catholique de Louvain, Brussels, Belgium.

Abstract

To support survival and growth of follicles, the transplantable artificial ovary should mimic the original organ, offering a physical (3D matrix) and biological support (cells). In order to replicate the ovarian cell populations, the aim of this study is to assess the proportions of stromal and endothelial cells in the ovarian cortex. To this end, ovarian biopsies were obtained from six women (mean age: 49 years). The epithelial layer and medulla were carefully removed. The cortex was finely minced and enzymatically digested and the isolated cells were fixed. For cell characterization, immunostaining for CD31 (for endothelial cells) and inhibin-α (for granulosa cells) was performed. Positive cells in each staining were counted and the proportion of the different cell populations was estimated from the total number of isolated cells. Since there is no specific marker for ovarian stromal cells, we estimated the proportion of these cells by performing a vimentin immunostaining and subtracting the proportions of CD31- and inhibin-α-positive cells. Immunostaining showed that 84% of isolated cells were vimentin-positive. From this pool, 3% were endothelial cells and 1% granulosa cells. Consequently, the population of ovarian stromal cells was 80%. In conclusion, our findings show that stromal cells represent the larger population of cells in the human ovarian cortex. While this ensures follicle survival and development in a normal ovary, we believe that the low proportion of endothelial cells could have a negative impact on the angiogenesis in the artificial ovary after the first days of transplantation.

Keywords: artificial ovary, cell isolation, endothelial cells, stromal cells.

Introduction

The goal of a transplantable artificial ovary (TAO) is to mimic the natural ovary in order to support follicle survival and development and consequently restore fertility in cancer patients (Amorim and Shikanov, 2016). To do so, it should comply with two requirements: it must have a 3D physical structure for the isolated follicles (Amorim *et al*., 2009; Luyckx *et al*., 2013, 2014; Chiti *et al*., 2015) and some biological features, such as cell populations for angiogenesis, the synthesis of an extracellular matrix, and the formation of an ovary-like structure (Dath *et al*., 2011; Soares *et al*., 2015; Chiti *et al*., 2017b).

In order to develop a suitable supporting matrix for human isolated follicles, different polymers have been used in our in vivo studies (Dolmans *et al*., 2007; Paulini *et al*., 2016; Chiti *et al*., 2018). Among all these studies, fibrin formulations with high concentrations of fibrinogen and thrombin were found to be the best choice for supporting follicle survival after xenotransplantation (Paulini *et al*., 2016; Chiti *et al*., 2017a, 2018). This is probably because their ultrastructure and rigidity resemble the human ovarian cortex (Paulini *et al*., 2016; Chiti *et al*., 2018).

Ovarian cells may also provide structural support in a TAO. Additionally, they are necessary because they show a complex bidirectional paracrine signaling with follicles (Tagler *et al*., 2011) and are responsible for vascularization in the ovarian tissue, which is also fundamental for follicle survival and development (Dath *et al*., 2011; Luyckx *et al*., 2014; Chiti *et al*., 2015). Dath *et al*. (2011) have demonstrated that when isolated human stromal and endothelial cells are grafted together, a well-organized and fully vascularized stromal structure was observed already after one week of xenografting in the murine ovarian bursa. Moreover, higher matrix degradation and formation of tissue that resembles the ovarian cortex were also observed. Contrarily, grafts without endothelial cells were smaller and poorly vascularized (Dath *et al*., 2011). Later, Soares *et al*. (2015), a study of xenografting of isolated human ovarian stromal and endothelial cells, led us to believe in a positive correlation between the number of grafted endothelial cells and vessel area after transplantation. Interestingly, Chiti *et al*. (2017b) also pointed out another positive correlation, this time between vessel area and follicle survival. If these hypotheses prove to be correct, we can presume that in order to improve follicle survival in a TAO, we should encapsulate a significant number of isolated endothelial cells.

Our studies mentioned above have confirmed the significant role of grafting isolated ovarian cells, but, more important, they have also indicated that the number of endothelial cells seems to have an influence on the graft outcome. This led us to question our approach, described in Paulini *et al*. (2016), which was the grafting of 50,000 isolated human ovarian cells without taking into consideration the number of endothelial cells. Indeed, we do not know the proportions of stromal and endothelial cells in the human ovarian cortex soon after isolation. In order to answer this question, the aim of our study was to estimate the different cell populations obtained after the isolation procedure using biopsies of the human ovarian cortex.

[§]Corresponding author: christiani.amorim@uclouvain.be

Received: November 27, 2018
Accepted: January 15, 2019

Copyright © The Author(s). Published by CBRA. This is an Open Access article under the Creative Commons Attribution License (CC BY 4.0 license)

Methods

Ethics

Use of human ovarian tissue was approved by the Institutional Review Board of the Université Catholique de Louvain on June 2, 2014 (IRB reference 2012/23MAR/125, registration number B403201213872). Use of human granulosa cells from aspirated antral follicles was approved by the Institutional Review Board of the Université Catholique de Louvain on January 12, 2015 (IRB reference 2014/16DEC/597, registration number B403201213872).

Collection and dissection of ovarian tissue

After obtaining informed consent, fragments of ovarian tissue were collected from eight patients (mean age: 49 years) undergoing laparoscopic surgery for benign gynecological diseases. Ovarian biopsies were kept in DMEM + Glutamax™-I (Dulbecco's Modified Eagle Medium, Gibco, Paisley, UK) in an ice box while transferring from the hospital to the laboratory (less than 10 minutes). The medullary part of the tissue was removed with the help of scissors and the epithelial layer was carefully peeled with forceps.

Cell isolation procedure

The ovarian cortex was minced into small pieces with the help of a tissue chopper (McIlwain Tissue Chopper, Mickle Laboratory, Guildford, UK) adjusted to 0.5 mm. Next, tissue fragments were incubated in 10 ml Dulbecco's phosphate-buffered saline (D-PBS; BioWhittaker, Verviers, Belgium) containing 1 mg/ml collagenase type IA (Sigma, St Louis, USA). Collagenase digestion was performed in a water bath at 37°C for 45 minutes with gentle agitation and pipetted every 15 minutes. The enzymatic digestion step was halted by adding a similar volume of PBS, 10% heat-inactivated fetal bovine serum, and 1% Antibiotics-Antimycotic (Gibco). The cell suspension was then filtered through sterilized 80- and 11-µm nylon net filters (Millipore, Overijse, Belgium). The filtered solution was subsequently centrifuged at 180g for five minutes and the pellet resuspended in D-PBS and fixed for cytospin slides.

Preparation of cytospin slides

Cytospin slides were prepared using Superfrost Plus slides (Menzel-Glaser, Braunschweig, Germany) and a Thermo Electron Cytospin 2 centrifuge (Fisher Scientific, Brussels, Belgium) operating at 700 rpm for five minutes. Each cytospin slide contained approximately 50,000 cells.

Characterization of the ovarian cell population

Characterization of human isolated ovarian cells was assessed by immunohistochemical staining for 1) vimentin (mouse anti-human vimentin, clone V9, M072501-2, Dako, Heverlee, Belgium), 2) CD31 (mouse anti-human CD31, M0823, Dako) and 3) inhibin-α (MCA 951, Oxford Bio-Innovation, Langford Lane, UK) performed on cytospin slides.

Vimentin is a cytoskeleton protein mainly expressed in the cytoplasm of cells of mesenchymal origin, and strongly expressed in ovarian stromal connective tissue (Czernobilsky *et al*., 1985). CD31/platelet endothelial cell adhesion molecule-1 (PECAM-1) immunostaining is mainly expressed on the human endothelial cells (Ensminger *et al*., 2002). Inhibin was assessed as a marker of granulosa cells (Dolmans *et al*., 2007). It has two forms, A and B, having the same α-sub unit but different β- subunits. The inhibin α-sub unit mainly expresses in all the granulosa cells of follicles at all stages of development (Bristol *et al*., 2004).

Cytospin slides with isolated ovarian cells were first rehydrated and permeabilized by immersing the slides in 0.05 M Tris-buffered saline (TBS 0.05M, pH 7.4) with 20% Triton X100 (Merck, Darmstadt, Germany). After blocking endogenous peroxidase activity with 0.3% H_2O_2 diluted in demineralized water, a demasking step was performed for 75 minutes at 98°C with 0.01 M citrate buffer. To block the non-specific antigen sites, slides were incubated with 0.05 M TBS, 10% normal goat serum and 1% bovine serum albumin for 30 minutes. Then the slides were incubated overnight at 4°C with primary antibodies: mouse anti-human vimentin (1:200), mouse anti-human CD31 (1:100) or mouse anti-human inhibin-α (1:100). Finally, slides were incubated with goat anti-mouse secondary antibodies conjugated to peroxidase (K4001, Dako) for one hour at 4°C. Diaminobenzidine was used as a chromogen (K3468, Dako). The slides were then counterstained with hematoxylin and mounted with DPX neutral mounting medium (Prosan, Merelbeke, Belgium).

Negative control was stained with universal mouse negative control (N1698, Dako). Ovarian mesenchymal cells, isolated granulosa cells from human antral follicles, and human umbilical vein endothelial cells were used as positive controls for vimentin, inhibin-α and CD31, respectively. Pictures of four different areas in each slide were taken under the microscope (X200 magnification; Zeiss, Munich, Germany). In each area, 100 cells were counted and classified as positive (cells stained in brown) or negative (cells stained in blue). Proportions of endothelial and granulosa cells were calculated and used to estimate the population of ovarian stromal cells.

Statistical analysis

Comparisons of proportions of cells that were either positive or negative for vimentin, inhibin-α and CD31 were made using the chi-square test. Values of $P < 0.05$ were considered statistically significant.

Results

Characterization of the cell populations after isolation

Characterization of ovarian isolated cells was assessed with immunostaining with anti-human vimentin, CD31 and inhibin-α antibodies on cytospin slides (Fig. 1) prepared after cell isolation. Cell counting revealed 84% vimentin-positive cells (70-95% range), 3% CD31-positive cells (2-4%) and 1% inhibin-α-positive cells (0-2%). Table 1 shows the proportion of positive cells in each immunostaining in every patient. Considering that CD31- and inhibin-α-positive cells were also vimentin-positive, we can calculate the population of ovarian stromal cells by subtracting the proportion of these cells from the total proportion of vimentin-positive cells. Consequently, the proportion of ovarian stromal cells was estimated at 80%. Statistical analysis showed that the proportion of ovarian stromal cells was significantly higher than the proportions of granulosa and endothelial cells ($P < 0.001$). Moreover, granulosa cell population was statistically lower than that of endothelial cells ($P < 0.001$).

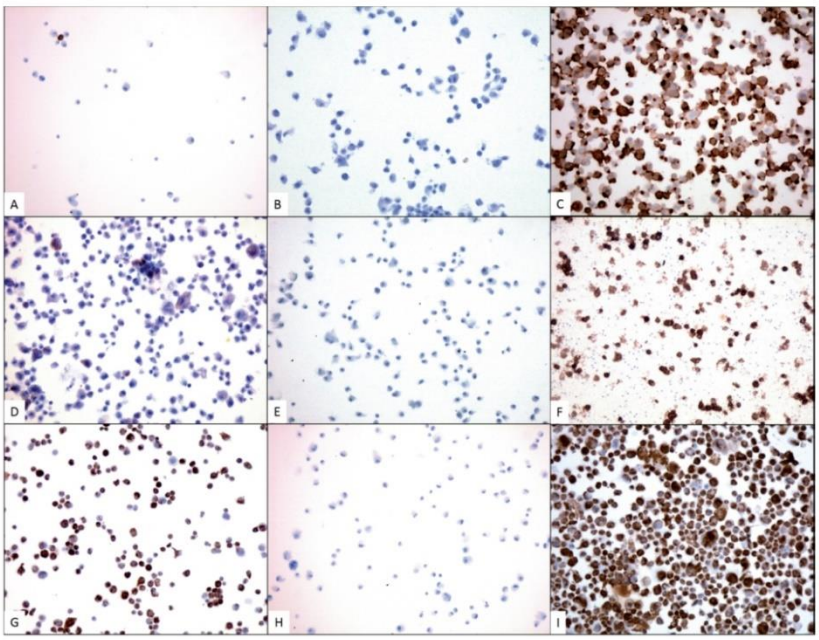


Figure 1. Immunostaining characterization of isolated human ovarian cells. Immunohistochemical staining (cells in brown) for CD31 (A), inhibin-α (D) and vimentin (G) and negative (B, E, H) controls. Commercially obtained HUVEC (C), granulosa (F) and ovarian mesenchymal cells (I) were used as positive controls for these three markers. All pictures are taken at X100 magnification.

Table 1. Proportion of vimentin-, CD31- and inhibin-α-positive cells in human ovarian cortex after cell isolation.

Patient	Age (years)	Vimentin-positive cells (%)	Inhibin-α-positive cells (%)	CD31-positive cells (%)
1	52	70	2	3
2	57	95	2	3
3	42	70	0	2
4	45	75	1	4
5	43	80	0	3
6	51	95	0	4

Discussion

In TAO conception, in order to avoid inadvertent contamination of malignant cells, ovarian cells should be isolated from the remained ovary that went through chemo- or radiotherapy (Amorim, 2016). Since ovaries of patients after cancer treatment are atrophic and devoid of follicles, just like ovaries of menopausal women (Sklar *et al*., 2005; Overbeek *et al*., 2011), we decided to use ovaries of older patients in order to have an ovarian cortex similar to that of cancer survivors. While we predicted isolating a low number of granulosa cells due to the significant decrease in follicle population, we did not expect such a low proportion of isolated endothelial cells.

To assess the role of endothelial cells in matrix vascularization, our previous studies identified this cell population using CD34 immunostaining (Dath *et al*., 2011; Soares *et al*., 2015). Our findings showed a proportion of approximately 16% of CD34-positive cells soon after isolation (Dath *et al*., 2011; Soares *et al*., 2015). While a higher proportion (18%) was reported in younger patients (34-49 years) (Soares *et al*., 2015), it does not seem statistically different from the percentage (14%) found in older women (42-78 years) (Dath *et al*., 2011). Independently of age, the percentage of CD34-positive cells reported in our previous studies was significantly higher than the proportion of CD31-positive cells found in this experiment. Since both CD31 and CD34 are markers for endothelial cells, we were surprised by such a discrepancy in our results. However, there are some possible explanations for the difference. For instance, it could be due to the fact that endothelial cells in different vessel types may express endothelial cell antigens heterogeneously (Pusztaszeri *et al*., 2006). Haber *et al.* (2015) reported that endothelial cells were only variably immunoreactive for CD31, while immunoreactivity for CD34 was more intense. Moreover, CD34 is expressed not only by endothelial cells, but also hematopoietic stem cells (Pusztaszeri *et al*., 2006). Unlike in our previous studies (Dath *et al*., 2011; Soares *et al*., 2015), in this present experiment we decided to assess CD31-positive cells because this transmembrane glycoprotein is a cell adhesion molecule with proangiogenic activity and has been shown to play an important role in angiogenesis (DeLisser *et al*., 1997; Zhou *et al*., 1999; Van Eyck *et al*., 2009), which is a necessary process after artificial ovary transplantation.

It is very likely that such a low proportion of CD31-positive cells after ovarian tissue dissociation is not enough to ensure rapid angiogenesis after grafting of the artificial ovary, which could negatively affect follicle survival and growth. In this case, an alternative could be increasing the number of CD31-positive cells by taking a biopsy that also contains the medullary part of the ovary. Indeed, Soares *et al.* (2015) showed that isolating endothelial cells from the ovarian medulla almost doubled the number of these cells compared to the ovarian cortex. In turn, this significantly increased the vessel area after transplantation of fibrin clots (Soares *et al*., 2015). It would be therefore important to devise a study to correlate the number of grafted isolated endothelial cells to artificial ovary vascularization and follicle survival after the first days of transplantation; for instance, a study where an artificial ovary prototype containing different proportions of endothelial cells associated with isolated human preantral follicles, stromal cells and lithium phthalocyanine (LiPc) crystals (Van Eyck *et al*., 2009; Manavella *et al*., 2018a) would be grafted into SCID mice. LiPc is very useful for in vitro and in vivo electron paramagnetic resonance oximetry because it is an oxygen-sensitive probe (Liu *et al*., 1993). Indeed, we already used LiPc to assess oxygenation in human ovarian tissue after xenotransplantation (Van Eyck *et al*., 2009; Manavella *et al*., 2018b).

While isolating endothelial cells from the medulla of the remaining ovary could be a promising strategy for improving artificial ovary vascularization, for some cancer patients this may not be possible, as the ovary may become too atrophic after chemo-radiotherapy, or as both ovaries were removed. For them, an alternative could be the use of adipose tissue-derived stem cells. Manavella *et al*. (2018a,b) showed that adipose tissue-derived stem cells increases follicle survival by enhancing vascularization in xenografted frozen-thawed human ovarian tissue. They obtained a significantly higher pO_2 level in the adipose tissue-derived stem cells encapsulated in fibrin matrix with the ovarian tissue group compared to the ovarian tissue alone without adipose tissue-derived stem cells after seven days of xenografting. Interestingly, the total CD34-positive vessel area on day seven was greater in the human ovarian tissue xenografted with adipose tissue-derived stem cells.

In conclusion, our findings confirm that the majority of cells found in the human ovarian cortex are stromal cells. While this ensures follicle survival and development in a normal ovary, we believe that in the artificial ovary, the low proportion of endothelial cells could have a negative impact on angiogenesis and consequently on follicle development after the first days of transplantation. In order to overcome this issue, we suggest isolating endothelial cells from the ovarian medulla (Soares *et al*., 2015) and including them in the TAO. This alternative could improve angiogenesis in TAO. However, our first step is to determine the right number of endothelial cells to be encapsulated in the artificial ovary.

Conflict of interest

None of the authors have any competing interests to declare in relation to this subject.

Acknowledgements

The authors thank Mira Hryniuk, BA, for reviewing the English language of the manuscript, and Dolores Gonzalez and Olivier Van Kerk for their technical assistance. They would also like to acknowledge all patients who donated ovarian tissue for research.

Funding sources

This study was supported by grants from the Fonds National de la Recherche Scientifique de Belgique (FNRS) awarded to C.A. Amorim as a research associate for the FRS-FNRS and P. Asiabi (Aspirant grant).

References

Amorim CA. 2016. Artificial ovary. In Suzuki, N and Donnez, J (Ed.). Gonadal tissue cryopreservation in fertility preservation. Tokyo, Japan: Springer. pp. 175-192.

Amorim CA, Van Langendonckt A, David A, Dolmans MM, Donnez J. 2009. Survival of human pre-antral follicles after cryopreservation of ovarian tissue, follicular isolation and in vitro culture in a calcium alginate matrix. *Hum Reprod*, 24:92-99.

Amorim CA, Shikanov A. 2016. The artificial ovary: current status and future perspectives. *Future Oncol,* 12:2323-2332.

Bristol SK, Woodruff TK. 2004. Follicle-restricted compartmentalization of transforming growth factor β superfamily ligands in the feline ovary. *Biol Reprod*, 70:846-859.

Chiti M, Dolmans MM, Orellana R, Soares M, Paulini F, Donnez J, Amorim CA. 2015. Influence of follicle stage on artificial ovary outcome using fibrin as a matrix. *Hum Reprod*, 31:427-435.

Chiti MC, Dolmans MM, Donnez J, Amorim CA. 2017a. Fibrin in reproductive tissue engineering: a review on its application as a biomaterial for fertility preservation. *Ann Biomed Eng*, 45:1650-1663.

Chiti MC, Dolmans MM, Lucci C, Paulini F, Donnez J, Amorim CA. 2017b. Further insights into the impact of mouse follicle stage on graft outcome in an artificial ovary environment. *Mol Hum Reprod*, 23:381-392.

Chiti MC, Dolmans MM, Mortiaux L, Zhuge F, Ouni E, Shahri PAK, Van Ruymbeke E, Champagne SD, Donnez J, Amorim CA. 2018. A novel fibrin-based artificial ovary prototype resembling human ovarian tissue in terms of architecture and rigidity. *J Assist Reprod Genet*, 35:41-48.

Czernobilsky B, Moll R, Levy R, Franke W. 1985. Co-expression of cytokeratin and vimentin filaments in mesothelial, granulosa and rete ovarii cells of the human ovary. *Eur J Cell Biol*, 37:175-190.

Dath C, Dethy A, Van Langendonckt A, Van Eyck AS, Amorim CA, Luyckx V, Donnez J, Dolmans MM. 2011. Endothelial cells are essential for ovarian stromal tissue restructuring after xenotransplantation of isolated ovarian stromal cells. *Hum Reprod*, 26:1431-1439.

DeLisser HM, Christofidou-Solomidou M, Strieter RM, Burdick MD, Robinson CS, Wexler RS, Kerr JS, Garlanda C, Merwin JR, MAdri JA, Albelda SM. 1997. Involvement of endothelial PECAM-1/CD31 in angiogenesis. *Am J Pathol*, 151:671-677.

Dolmans MM, Martinez-Madrid B, Gadisseux E, Guiot Y, Yuan WY, Torre A, Camboni A, Van Langendonckt A, Donnez J. 2007. Short-term transplantation of isolated human ovarian follicles and cortical tissue into nude mice. *Reproduction*, 134:253-262.

Ensminger SM, Spriewald BM, Steger U, Duncan GS, Morris PJ, Mak TW, Wood KJ. 2002. PECAM-1 (CD31) expression on donor endothelial cells attenuates transplant arteriosclerosis in aortic allografts. *J Heart Lung Transplant*, 21:164-165.

Haber MA, Iranmahboob A, Thomas C, Liu M, Najjar A, Zagzag D. 2015. ERG is a novel and reliable marker for endothelial cells in central nervous system tumors. *Clin Neuropathol*, 34:117-127.

Liu KJ, Gast P, Moussavi M, Norby SW, Vahidi N, Walczak T, Wu M, Swartz HM. 1993. Lithium phthalocyanine: a probe for electron paramagnetic resonance oximetry in viable biological systems. *Proc Natl Acad Sci U S A*, 90:5438-5442.

Luyckx V, Dolmans MM, Vanacker J, Scalercio SR, Donnez J, Amorim CA. 2013. First step in developing a 3D biodegradable fibrin scaffold for an artificial ovary. *J Ovarian Res*, 6:83.

Luyckx V, Dolmans M-M, Vanacker J, Legat C, Moya CF, Donnez J, Amorim CA. 2014. A new step toward the artificial ovary: survival and proliferation of isolated murine follicles after autologous transplantation in a fibrin scaffold. *Fertil Steril*, 101:1149-1156.

Manavella DD, Cacciottola L, Desmet CM, Jordan BF, Donnez J, Amorim CA, Dolmans MM. 2018a. Adipose tissue-derived stem cells in a fibrin implant enhance neovascularization in a peritoneal grafting site: a potential way to improve ovarian tissue transplantation. *Hum Reprod*, 33:270-279.

Manavella DD, Cacciottola L, Pommé S, Desmet CM, Jordan BF, Donnez J, Amorim CA, Dolmans MM. 2018b. Two-step transplantation with adipose tissue-derived stem cells increases follicle survival by enhancing vascularization in xenografted frozen–thawed human ovarian tissue. *Hum Reprod*, 33:1107-1116.

Overbeek A, van den Berg MH, van Leeuwen FE, Kaspers GJL, Kremer LCM, Lambalk CB, van Dulmen-den Boreder E. 2011. Chemotherapy-related late adverse effects on ovarian function in female survivors of childhood cancer and cancer in the reproductive age. *Cochrane Database Syst Rev*, 6:CD009127.

Paulini F, Vilela JM, Chiti MC, Donnez J, Jadoul P, Dolmans MM, Amorim CA. 2016. Survival and growth of human preantral follicles after cryopreservation of ovarian tissue, follicle isolation and short-term xenografting. *Reprod Biomed Online*, 33:425-432.

Pusztaszeri MP, Seelentag W, Bosman FT. 2006. Immunohistochemical expression of endothelial markers CD31, CD34, von Willebrand factor, and Fli-1 in normal human tissues. *J Histochem Cytochem*, 54:385-395.

Sklar C. 2005. Maintenance of ovarian function and risk of premature menopause related to cancer treatment. *J Natl Cancer Inst Monogr*, 2005(34):25-27.

Soares M, Sahrari K, Chiti MC, Amorim CA, Ambroise J, Donnez J, Dolmans MM. 2015. The best source of isolated stromal cells for the artificial ovary:

medulla or cortex, cryopreserved or fresh? *Hum Reprod*, 30:1589-1598.

Tagler DJ, Shea LD, Woodruff TK. 2011. Contributions of ovarian stromal cells to follicle culture. In Donnez, J and Kim, SS (Ed.). Principles and practice of fertility preservation. Cambridge, UK: University Press. pp.409-420.

Van Eyck AS, Jordan BF, Gallez B, Heilier JF, Van Langendonckt A, Donnez J. 2009. Electron paramagnetic resonance as a tool to evaluate human ovarian tissue reoxygenation after xenografting. *Fertil Steril*, 92:374-381.

Zhou Z, Christofidou-Solomidou M, Garlanda C, DeLisser HM. 1999. Antibody against murine PECAM-1 inhibits tumor angiogenesis in mice. *Angiogenesis*, 3:181-188.

Article 4

Human Reproduction, Vol.35, No.12, pp. 2793–2807, 2020
Advance Access Publication on December 1, 2020 doi:10.1093/humrep/deaa246

human reproduction **ORIGINAL ARTICLE** ***Reproductive Biology***

In vitro differentiation of theca cells from ovarian cells isolated from postmenopausal women

P. Asiabi[1], M.M. Dolmans[1,2], J. Ambroise[3], A. Camboni[1], and C.A. Amorim[1,*]

[1]Pôle de Recherche en Gynécologie, Institut de Recherche Expérimentale et Clinique, Université Catholique de Louvain, Brussels, Belgium [2]Gynecology and Andrology Department, Cliniques Universitaires Saint-Luc, Brussels, Belgium [3]Centre de Technologies Moléculaires Appliquées, Institut de Recherche Expérimentale et Clinique, Université Catholique de Louvain, Brussels, Belgium

*Correspondence address. Pôle de Recherche en Gynécologie, Institut de Recherche Expérimentale et Clinique, Université Catholique de Louvain, Avenue Mounier 52, bte B1.52.02, 1200 Brussels, Belgium. Tel: +32-(0)2-764-5287; E-mail: christiani.amorim@uclouvain.be

Submitted on May 5, 2020; resubmitted on July 22, 2020; editorial decision on August 25, 2020

STUDY QUESTION: Can human theca cells (TCs) be differentiated *in vitro*?

SUMMARY ANSWER: It is possible to differentiate human TCs *in vitro* using a medium supplemented with growth factors and hormones.

WHAT IS KNOWN ALREADY: There are very few studies on the origin of TCs in mammalian ovaries. Precursor TCs have been described in neonatal mice ovaries, which can differentiate into TCs under the influence of factors from oocytes and granulosa cells (GCs). On the other hand, studies in large animal models have reported that stromal cells (SCs) isolated from the cortical ovarian layer can also differentiate into TCs.

STUDY DESIGN, SIZE, DURATION: After obtaining informed consent, ovarian biopsies were taken from eight menopausal women (53–74 years of age) undergoing laparoscopic surgery for gynecologic disease not related to the ovaries. SCs were isolated from the ovarian cortex and *in vitro* cultured for 8 days in basic medium (BM) (G1), enriched with growth factors, FSH and LH in plastic (G2) or collagen substrate without (G3) or with (G4) a GC line.

PARTICIPANTS/MATERIALS, SETTING, METHODS: To confirm TC differentiation, relative mRNA levels for LH receptor (*Lhr*), steroidogenic acute regulatory protein (*Star*), cholesterol side-chain cleavage enzyme (*Cyp11a1*), cytochrome P450 17A1 (*Cyp17a1*), hydroxy-delta-5-steroid dehydrogenase, 3 beta- and steroid delta-isomerase 1 (*Hsd3b1*) and hydroxy-delta-5-steroid dehydrogenase, 3 beta- and steroid delta-isomerase 2 (*Hsd3b2*) were assessed. Immunohistochemistry was also performed for their protein detection and a specific marker was identified for TCs (aminopeptidase-N, CD13), as were markers for theca and small luteal cells (dipeptidyl peptidase IV (CD26) and Notch homolog 1, translocation-associated (NOTCH1)). Finally, we analyzed cell ultrastructure before (Day 0) and after *in vitro* culture (Day 8), and dehydroepiandrosterone (DHEA) and progesterone levels in the medium using transmission electron microscopy (TEM) and ELISA, respectively.

MAIN RESULTS AND THE ROLE OF CHANCE: Results obtained from qPCR showed a significant increase ($P < 0.05$) in mRNA levels of *Lhr* in F2 (floating cells in G2) and G4, *Cyp17a1* in G1 and F1 (floating cells in G1) and *Hsd3b2* in G1, G2, G3 and G4. Immunohistochemistry confirmed expression of each enzyme involved in the steroidogenic pathway at the protein stage. However, apart from G1, all other groups exhibited a significant ($P < 0.05$) rise in the number of CD13-positive cells. There was also a significant increase ($P < 0.05$) in NOTCH1-positive cells in G3 and G4. Ultrastructure analyses by TEM showed a distinct difference between groups and also versus Day 0. A linear trend with time revealed a significant gain ($q < 0.001$) in DHEA concentrations in the medium during the culture period in G1, G2, G3 and G4. It also demonstrated a statistical increase ($q < 0.001$) in G2, G3 and G4 groups, but G1 remained the same throughout culture in terms of progesterone levels.

LARGE SCALE DATA: N/A

LIMITATIONS, REASONS FOR CAUTION: Shorter periods of *in vitro* culture (e.g. 2, 4 and 6 days) could have led to increased concentrations of differentiated TCs in G2, G3 and G4. In addition, a group of cells cultured in BM and accompanied by COV434 cells would be necessary to understand their role in the differentiation process. Finally, while our results demonstrate that TCs can be differentiated *in vitro* from cells isolated from the cortical layer of postmenopausal ovaries, we do not know if these cells are differentiated

© The Author(s) 2020. Published by Oxford University Press on behalf of European Society of Human Reproduction and Embryology. All rights reserved.
For permissions, please email: journals.permissions@oup.com

Downloaded from https://academic.oup.com/humrep/article/35/12/2793/6015748 by Universite catholique de louvain user on 11 January 2021

from a subpopulation of precursor TCs present in ovarian cortex or ovarian SCs in general. It is therefore necessary to identify specific markers for precursor TCs in human ovaries to understand the origin of these cells.

WIDER IMPLICATIONS OF THE FINDINGS: This is a promising step toward understanding TC ontogenesis in the human ovary. Moreover, *in vitro*-generated human TCs can be used for studies on drug screening, as well as to understand TC-associated pathologies, such as androgen-secreting tumors and polycystic ovary syndrome.

STUDY FUNDING/COMPETING INTEREST(S): This study was supported by grants from the Fonds National de la Recherche Scientifique de Belgique (FNRS) (C.A.A. is an FRS-FNRS Research Associate; grant MIS #F4535 16 awarded to C.A.A.; grant 5/4/150/5 awarded to M.M.D.; grant ASP-RE314 awarded to P.A.) and Foundation Against Cancer (grant 2018-042 awarded to A.C.). The authors declare no competing interests.

Key words: progenitor theca cells / human ovary / stromal cells / theca cells / cell differentiation / luteal cells

Introduction

While theca cells (TCs) play a pivotal role in follicle development and production of female steroids, they have never been studied as comprehensively as granulosa cells (GCs). Indeed, Young and McNeilly (2010) called them 'the forgotten cells of the ovarian follicle'. The theca compartment is formed during the early stages of follicle growth, surrounding the outer part of the basement membrane. It is divided into two specific layers, namely theca interna cells (TICs), which synthesize steroid hormones together with GCs, and theca externa cells, which are important during ovulation (Edson *et al.*, 2009). Recently, recruitment and differentiation of TCs were investigated in different animal models (Vitt *et al.*, 2000; Orisaka *et al.*, 2006; Honda *et al.*, 2007; Itami *et al.*, 2011; Qiu *et al.*, 2013; Liu *et al.*, 2015; Adib and Valojerdi, 2017). In mice, a subpopulation of cells known as progenitor TCs was reported to differentiate into TCs (Honda *et al.*, 2007). On the other hand, in goats and cows, studies revealed that TCs can be converted from ovarian cortical stromal cells (SCs) (Orisaka *et al.*, 2006; Qiu *et al.*, 2013, 2014). In both cases, the differentiation process was shown to be regulated by factors secreted by GCs and the oocyte (Orisaka *et al.*, 2006; Honda *et al.*, 2007; Itami *et al.*, 2011; Qiu *et al.*, 2013).

In human ovaries, TC ontogeny remains unclear. Dalman *et al.* (2018a,b) described a population of theca stem cells in the theca layer of small antral follicles that has the ability to differentiate into progenitor TCs, as well as adipocyte-, osteocyte-, chondrocyte- and oocyte-like cells. Similarly to Adib and Valojerdi (2017), Dalman *et al.* (2018a,b) collected these cells from small antral follicles, but we do not know if human TCs originate from these stem cells.

In the present study, we identified a population of TCs after *in vitro* culture of cells isolated from the cortical layer of postmenopausal human ovaries. In order to obtain TCs, we attempted to mimic the *in vivo* differentiation process by employing different growth factors (Honda *et al.*, 2007; Liu *et al.*, 2015) and adding companion GCs (Orisaka *et al.*, 2006; Qiu *et al.*, 2013). The resulting TCs closely resembled their ovarian counterparts when investigated by immunohistochemical, ultrastructural and functional analyses.

Materials and methods

Source of ovaries and ethical approval

Ovarian biopsies were taken from eight menopausal women (53–74 years of age) undergoing laparoscopic surgery for gynecologic disease not related to the ovaries, after obtaining informed consent. None of the patients were under hormone replacement therapy. Use of human ovarian tissue was approved by the Institutional Review Board of the Université Catholique de Louvain on 13 May 2019 (IRB reference 2012/23MAR/125, registration number B403201213872). The biopsies were immediately transported on ice to the laboratory in Dulbecco's modified Eagle's medium/Ham's nutrient mixture F-12 with 1% (v/v) l-alanyl-l-glutamine (DMEM/F-12 (1:1) (1X) + GlutaMAX-I; Gibco, Thermo Fisher Scientific, Merelbeke, Belgium). Once in the laboratory, the medullary part of the tissue was removed with scissors and the epithelial layer was carefully peeled off using atraumatic forceps.

SC isolation

Fragments of ovarian cortex were digested using Liberase DH (Sigma-Aldrich, Bornem, Belgium) and DNase I (Roche Diagnostics, Brussels, Belgium), as previously described (Chiti *et al.*, 2017). The resulting cell suspension was halted by adding a similar volume of Dulbecco's phosphate-buffered saline (DPBS, Gibco, Paisley, UK) supplemented with 10% (v/v) heat-inactivated fetal bovine serum (FBS, Gibco, New York, USA) and 1% (v/v) antibiotic and antimycotic (Anti-Anti; Gibco, Bleiswijk, Netherlands). The cell suspension was then filtered through sterilized 80- and 30-µm nylon net filters (Millipore, Overijse, Belgium) (Soares *et al.*, 2015). The obtained solution was centrifuged at 1200 *g* for 10 min and the pellet was resuspended in DPBS plus 10% FBS for cell counting. A small proportion of isolated SCs (20%) from each ovarian biopsy were divided into two parts: (i) 15% were immediately fixed in 4% paraformaldehyde (VWR, Leuven, Belgium) for immunohistochemical analysis; (ii) 5% were snap-frozen for qPCR analysis. The rest was frozen for further *in vitro* culture.

Freezing and thawing of SC suspensions

The remaining 80% of SCs were centrifuged at 1200 *g* for 10 min and the pellet was resuspended in 1 ml DMEM/F12 supplemented with 20% FBS, 1% Anti-Anti and 10% dimethyl sulfoxide (Sigma-Aldrich). The cryovials were loaded into a Mr. Frosty™ freezing container (Thermo Fisher Scientific) and transferred to a −80°C freezer. After 24 h, cryovials were removed from the container and stored at −80°C till needed.

Once cells had been collected from eight patients, they were thawed for *in vitro* culture. For this, cryovials were kept for 2 min at 37 °C in a bead bath (Lab Armor, Cornelius, USA) and then the cell

Downloaded from https://academic.oup.com/humrep/article/35/12/2793/6015748 by Universite catholique de louvain user on 11 January 2021

suspension was transferred to 9 ml DMEM/F12. The diluted suspension was centrifuged at 1200 *g* for 10 min and supernatant was carefully removed. The remaining cell pellet was suspended in basic medium (BM) containing DMEM/F12 supplemented with 10% KnockOut™ serum replacement (KSR; Gibco) and 1% Anti-Anti. A total of 10 000 SCs were immediately fixed in 2.5% glutaraldehyde (Agar Scientific, Stansted, UK) in 0.1 M sodium cacodylate buffer (sodium salt trihydrate, 98% pure, Acros Organics, Thermo Fisher Scientific) for ultrastructural evaluation. Another group of 100 000 SCs were fixed in 4% paraformaldehyde for immunohistochemical analysis and 15 000 were snap-frozen for qPCR analysis. The remaining cells were divided into groups of 6×10^4 cells for *in vitro* culture.

SCs in *in vitro* culture

Since it was not possible to collect enough GCs from IVF patients, we replaced them by COV434 cells (ECACC 07071909; Culture Collections, Salisbury, UK) (Havelock *et al.*, 2004), which have been described as the best candidate to substitute GCs in follicle developmental studies (Zhang *et al.*, 2000). In order to mimic the follicle basement membrane that separates GCs from TCs, we used atelocollagen permeable inserts (Koken Co., Tokyo, Japan), as described by Orisaka *et al.* (2006).

Isolated SCs were cultured with or without COV434 cells using either BM or enriched medium (EM) (Supplementary Table SI) and seeded directly onto plastic or permeable atelocollagen inserts.

In total, four groups were created (Fig. 1):

G1—SCs in BM, seeded directly onto plastic dishes.

G2—SCs in EM, seeded directly onto plastic dishes.

G3—SCs in EM, seeded onto atelocollagen inserts.

G4—SCs co-cultured with 1.8×10^5 COV434 cells. In this group, COV434 cells were seeded onto one side of the atelocollagen inserts and, after 24 h of incubation at 37 °C with 5% CO_2, the inserts were inverted and the SCs were seeded onto the other side (Orisaka *et al.*, 2006).

For G1 and G2, 700 µl medium was added to the wells, while for G3 and G4, 300 µl medium was placed in the inserts and 400 µl in the wells. Half of the medium was changed every second day. For G4, half of the medium in the well (in direct contact with COV434 cells) and half from the insert (in direct contact with SCs) were separately collected and kept for analysis. Retrieved media were frozen at −20 °C for hormone measurement.

Cells were cultured for 8 days at 37 °C with 5% CO_2. It is important to note that in G1 and G2, apart from proliferating attached fibroblast-like cells, floating spheroid structures were also formed. They were removed from the wells when the medium was changed and, to avoid losing them, the medium was centrifuged at 1200 *g* for 10 min to collect the spheroids in the bottom of the tube and return them to their original dishes.

At the end of culture, the media were removed and frozen, and the SCs were detached using Accutase™ (Sigma-Aldrich). Cells were then counted and apportioned for qPCR (15% SCs), ultrastructural analysis (45% SCs) and immunohistochemistry (40% SCs).

RNA isolation and cDNA synthesis

SCs were snap-frozen before and after *in vitro* culture. They were treated with AllPrep DNA/RNA Micro Kit (Qiagen, Hilden, Germany) as described in the data sheet provided. In brief, cells were lysed with the Buffer RLT Plus supplied with the kit, passed through the DNA column, and then the liquid part was mixed with 70% ethanol following different centrifugation and washing steps in order to obtain purified RNA. To synthesize and amplify cDNA from a small RNA yield, the QuantiTect Whole Transcriptome Kit (Qiagen) was used. A gel electrophoresis method was applied to ensure the presence of synthesized cDNA.

qPCR analysis

To determine whether SCs are able to differentiate into TICs, relative mRNA levels for LH receptor (*Lhr*), steroidogenic acute regulatory protein (*Star*), cytochrome P450 17A1 (*Cyp11a1*), steroid 17-alpha-hydroxylase/17,20 lyase (*Cyp17a1*) and 3 beta hydroxysteroid dehydrogenase/delta 5–>4-isomerase types 1 (*Hsd3b1*) and 2 (*Hsd3b2*) were assessed in snap-frozen cells before and after *in vitro* culture. To this end, we used TaqMan probes (Applied Biosystems, Waltham, USA) for genes of interest (Supplementary Table SII), as well as the TaqMan Gene Expression Master Mix (Applied Biosystems) and diethyl pyrocarbonate-treated water (Thermo Fisher Scientific). To select the best housekeeping gene(s), samples from four different *in vitro* culture groups were loaded onto precoated TaqMan Array Human Endogenous Control Plates (Thermo Fisher Scientific) and qPCR was performed. Average expression stability of the investigated housekeeping genes was analyzed using the geNorm method in R, version 3.5.3.

Immunohistochemical analysis

Cytospin slides were prepared using isolated SCs fixed in paraformaldehyde before and after *in vitro* culture (G1 and G2), Superfrost Plus slides (Menzel-Glaser, Braunschweig, Germany) and a Thermo Electron Cytospin 2 centrifuge (Fisher Scientific, Brussels, Belgium) operating at 700 rpm for 5 min. Each cytospin slide contained approximately 30 000 cells.

Since we analyzed floating spheroid structures separately from attached cells, we named them F1 (and attached cells, G1) and F2 (and attached cells, G2). F1, F2, G3 and G4 were first fixed in 4% paraformaldehyde for 40 min at room temperature and then centrifuged at 1200 *g* for 10 min. After removing the supernatant, spheroid structures or cells were embedded in 30 µl of 2% UltraPure™ agarose (Invitrogen, Thermo Fisher Scientific) and centrifuged immediately at 14 000 *g* for 1 min to combine the spheroid structures/cells with the agarose. After solidification, the agarose mixture was dehydrated and embedded in paraffin. Five-µm-thick tissue sections were then placed on Superfrost Plus slides for immunohistochemical processing. The following markers were selected to assess SC differentiation into TCs: LHR, STAR, CYP11A1, CYP17A1, HSD3B1 and HSD3B2. We also added specific markers for TCs and small luteal cells: perilipin-2 (adipose differentiation-related protein (ADRP)), neurogenic locus notch homolog protein 1 (NOTCH1), aminopeptidase-N (CD13) and dipeptidyl peptidase IV (CD26) (Supplementary Table SIII).

Cytospin and paraffin-free slides were subjected to blocking of endogenous peroxidase activity by incubation in 3% H_2O_2 for 30 min. Antigen retrieval steps, antibody dilutions, incubation conditions and positive controls are summarized in Supplementary Table SIII. The primary antibody was omitted in negative controls and a mixture of

Downloaded from https://academic.oup.com/humrep/article/35/12/2793/6015748 by Universite catholique de louvain user on 11 January 2021

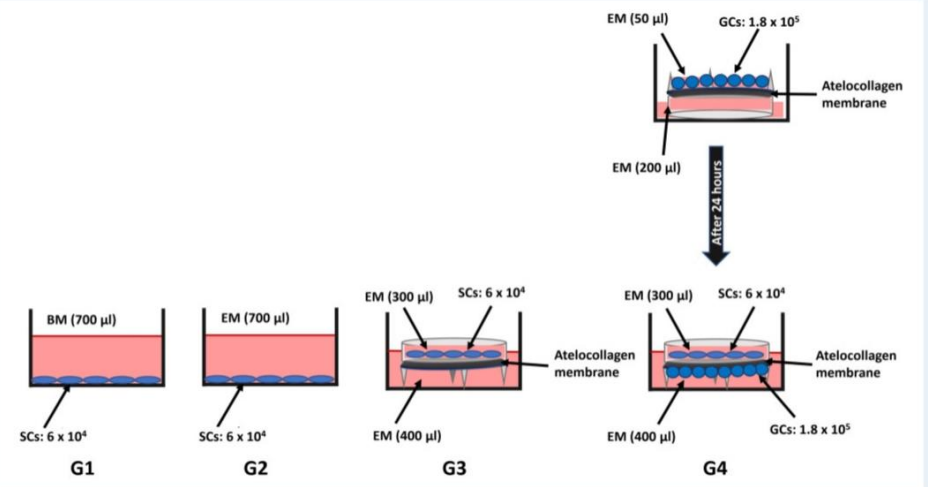


Figure 1. Schematic representation of the *in vitro* culture groups. G1: 6×10^4 SCs in basic medium (BM) containing DMEM-F12 supplemented with KSR and antibiotics, seeded directly onto a plastic dish. G2: 6×10^4 stromal cells (SCs) in enriched medium (EM) containing BM supplemented with growth factors, FSH and LH, seeded directly onto a plastic dish. G3: 6×10^4 SCs in EM seeded onto a permeable atelocollagen membrane. G4: 6×10^4 SCs in EM seeded onto the top of a permeable atelocollagen membrane in co-culture with 1.8×10^5 COV434 cells on the other side of the membrane.

FLEX universal negative control antibodies for rabbit or mouse was added (Dako, Glostrup, Denmark). Sections were stained with a solution of diaminobenzidine (Vector, Burlingame, USA), counterstained with hematoxylin, and mounted for light microscopy (Nikon Eclipse, Tokyo, Japan) analysis. Slides were visualized at 40× magnification and positive cells for each protein were counted by two independent observers.

Ultrastructural analysis

Cells fixed in glutaraldehyde before and after *in vitro* culture were washed in 0.2 M sodium cacodylate buffer (pH 7.4) and placed in 1% osmic acid (2% osmium tetraoxide solution, Carl Roth, Karlsruhe, Germany) and 0.1 M sodium cacodylate buffer solution for 1 hour. After a series of dehydration steps with ethanol, the cells were embedded in resin (Eponate 12, Ted Pella Inc., Redding, USA) and cut into 80-nm ultra-thin sections (Ultrotome III, LKB Company, Bromma, Sweden) using a diamond knife (Ultra 45°, Diatome Diamond Knives, Hatfield, USA). Ultra-thin sections were placed on a copper/rhodium grid (21-9M0300, Micro to Nano, Haarlem, the Netherlands). Samples were then contrasted with 2% uranyl acetate (Spi Supplies, West Chester, USA) in water, Reynold's lead nitrate (Millipore) and tris sodium citrate (VWR).

Hormone assays

Frozen media from each *in vitro* culture group were thawed for ELISA analysis at different time points (D2, D4, D6 and D8). Dehydroepiandrosterone (DHEA) and progesterone secreted by differentiated cells were measured using DHEA ELISA (ADI901093, Enzo Life Sciences BVBA, Farmingdale, USA) and progesterone ELISA (ADI900011, Enzo Life Sciences) kits.

Statistical analyses

All statistical analyses were performed using R, version 3.6.1. Because a number of genes (or proteins) were simultaneously assessed and multiple comparisons were carried out, *P*-values were adjusted for multiple testing using the Benjamini–Hochberg method to control the false discovery rate.

- qPCR: All transcriptomic data were analyzed using R, version 3.6.1. Before qPCR data analysis, the most stable housekeeping genes were selected from the dedicated dataset using the geNorm algorithm (Vandesompele *et al.*, 2002) implemented in the NormqPCR Bioconductor package. All undetected values were processed using the 'non-detects' Bioconductor package and imputed accordingly using an algorithm based on an expectation–maximization approach. Expression levels of each gene were then normalized according to the selected housekeeping genes by computing ΔCT values. The

Downloaded from https://academic.oup.com/humrep/article/35/12/2793/6015748 by Universite catholique de louvain user on 11 January 2021

Limma Bioconductor package was used to determine ΔΔCT values and associated *P*-values of each gene. This process was undertaken for each comparison and respective results were displayed in volcano plots.

- ELISA (DHEA and progesterone): For each element of interest, DHEA and progesterone levels were analyzed using linear mixed-effects models. Logarithmic transformation was applied to both DHEA and progesterone in order to normalize data distribution. In each model, the patient effect was assumed to follow normal distribution and was therefore defined as a random effect, while time was introduced as a fixed effect.
- Immunohistochemistry: Protein expression after *in vitro* culture was compared with D0 values using linear regression models.

Results

SCs isolated from ovarian tissue easily adhered to both plastic and permeable inserts after one day of *in vitro* culture. However, after two days, their appearance changed in G1 and G2, and spheroid structures started forming and floating in the medium (Fig. 2). It has been previously demonstrated that GCs and TCs cultured in serum-free conditions, reaggregate into multicellular clumps during *in vitro* culture, which indicates cell–cell or cell–extracellular matrix interactions (Yamada *et al.*, 1999; Yang and Xiong, 2012; Hatzirodos *et al.*, 2017). On Day 4, some fibroblast-like cells remained strongly attached to the plastic surface in G1 (Fig. 2), while almost all spheroid structures were detached from the bottom of the dish in G2 (Fig. 2). These structures continued to increase in diameter and became larger in G2 than in G1, with some measuring around 300 µm (Fig. 2). Conversely, cells in G3 and G4 remained adherent to the membrane throughout the *in vitro* culture period (Fig. 2). They exhibited typical fibroblast morphology and, after 8 days, entirely covered the inserts (Fig. 2).

Quantitative real-time polymerase chain reaction (qPCR)

Volcano plots of qPCR results from isolated SCs before and after *in vitro* culture revealed very different gene expression patterns for enzymes involved in the steroidogenic pathway of TICs, and special markers for TICs, such as *Lhr* and *Cyp17a1* (Fig. 3). In G1 (n = 5), a significant increase was observed in mRNA levels of *Cyp17a1* and *Hsd3b2* ($P < 0.05$). On the other hand, in F1 (n = 3), there was only an upturn in mRNA levels of *Cyp17a1* ($P < 0.05$). In G2 (n = 5), only *Hsd3b2* mRNA levels increased ($P < 0.05$), while in F2 (n = 3), *Lhr* mRNA levels rose significantly ($P < 0.05$) and *Hsd3b2* was on the verge of being significantly upregulated. In G3 (n = 3), *Hsd3b2* was upregulated ($P < 0.05$) and CYP11A1 and *Lhr* were both borderline in terms of significant upregulation, but in G4 (n = 8), mRNA levels of *Lhr* and *Hsd3b2* were both significantly upregulated ($P < 0.05$).

Immunohistochemical analysis

Results from protein expression of LHR, ADRP, STAR, CYP11A1, CYP17A1, HSD3B1, HSD3B2, NOTCH1, CD13 and CD26 were compared after 8 days of *in vitro* culture versus Day 0 (D0; control) (Table I).

It is important to point out that on D0, there was a considerable proportion of isolated SCs that were positive for LHCGR and HSD3B1, and more than 10% positive for CYP17A1 (Table I). Interestingly, after *in vitro* culture, there was increased expression of most proteins involved in the steroidogenic pathway in all groups (Table I; Figs 4 and 5). Apart from G1 and F1, all other groups exhibited a significant ($P < 0.05$) upturn in the number of CD13-positive cells (Table I; Fig. 4). Moreover, after *in vitro* culture, we observed a higher number of CD26-positive cells compared to controls (D0) (Table I; Fig. 5). There was also a significant increase ($P < 0.05$) in NOTCH1-positive cells in G3 and G4 (Table I, Fig. 5).

Expression of CD13, a specific marker for the theca interna with steroidogenic activity, is presented in Supplementary Fig. S1. Positive and negative control tissue and human ovary for each marker are shown in Supplementary Figs S2 and S3.

Ultrastructural analysis

Results from transmission electron microscopy (TEM) showed a remarkable difference between cells before and after *in vitro* culture and between groups. Before *in vitro* culture (D0), cells appeared to be undifferentiated, with a high nucleus/cytoplasm ratio, few organelles, mostly round mitochondria with scarce cristae (immature mitochondria) and few endoplasmic reticulum cisternae (Fig. 6, D0).

Different culture conditions did not appear to affect cell health status, as cells had a normal appearance, with some at the proliferative stage. In all groups, they developed an endoplasmic reticulum and showed higher numbers of mitochondria and lipid droplets compared to D0 (Figs 6, 7 and 8). Similar to D0 findings, cells in G1 and F1 had a high nucleus/cytoplasm ratio, and nuclei exhibited loose chromatin and visible nucleoli, suggesting DNA transcription (Fig. 6, G1-a). While we only found round mitochondria in F1 (Fig. 6, F1), we observed round and elongated mitochondria (Fig. 6, G1-c) and gap junctions between cells in G1 (Fig. 6, G1-b and c: arrow heads). In both G1 and F1, some endoplasmic reticulum and lipid droplets were detected in examined cells (Fig. 6, G1-b and F1).

In G2 (Fig. 6, G2-a) and F2 (Fig. 7, F2-a), we found active cells with a low nucleus/cytoplasm ratio. Ultrastructural analysis of attached cells (G2) showed that they had a round, oval or somewhat undulated nucleus, rough and abundant smooth endoplasmic reticulum, Golgi apparatus, lipid droplets, oval and elongated mitochondria with tubular or vesicular cristae and lysosomes (Fig. 6, G2-a; Fig. 7, G2-b and c). Ultrastructural analysis of F2 cells revealed that floating structures contained three different cell types (Fig. 7, F2-a): (i) cells with elongated nuclei, well developed rough endoplasmic reticulum, Golgi apparatus, rod-shaped mitochondria with lamellar cristae, lipid droplets and free ribosomes (Fig. 7, F2-a: circle); (ii) cells ellipsoidal in shape with an oval nucleus, rough endoplasmic reticulum, Golgi apparatus, lipid droplets, elongated or oval mitochondria with lamellar or tubular cristae, a fairly developed smooth endoplasmic reticulum and lysosomes (Fig. 7, F2-a: four tails star; Fig. 8, F2-e); and (iii) cells with the same ultrastructure as described for attached cells in G2 with undulated nuclei (Fig. 7, F2-a: five tails star, b, c and d).

Cells in G3 also proved to be active, with a low nucleus/cytoplasm ratio, nuclei with loose chromatin and visible nucleoli (one or two)

Downloaded from https://academic.oup.com/humrep/article/35/12/2793/6015748 by Universite catholique de louvain user on 11 January 2021

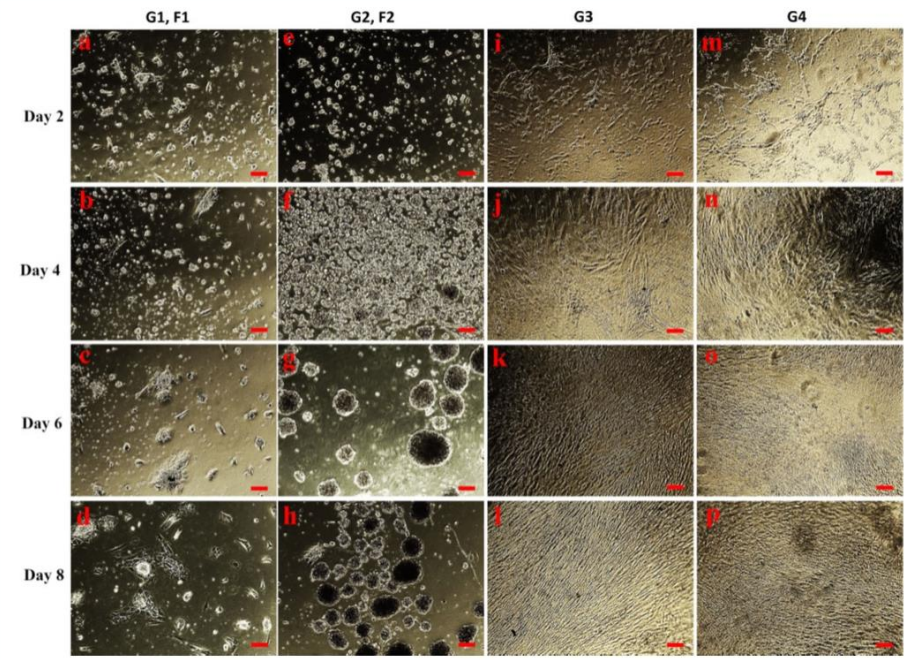


Figure 2. Stromal cells in *in vitro* culture. Ovarian cortical SCs in BM (G1, F1) at different time points (a, b, c, d). SCs in EM (G2, F2) at different time points (e, f, g, h). SCs in EM seeded onto an atelocollagen membrane (G3) at different time points (i, j, k, l). SCs in EM seeded onto one side of an atelocollagen membrane in co-culture with COV434 cells on the other side of the membrane (G4) at different time points (m, n, o, p). Scale bars: 100 μm. G1–G4 attached cells, F1, F2 floating cells.

(Fig. 8, G3-a). Ultrastructural evaluation of these cells showed cells similar to F2, but also the presence of a new cell type. This latter population presented with lamelliform microvilli, acentric nuclei, numerous lipid droplets, mitochondria with tubular cristae, well developed smooth and rough endoplasmic reticulum and Golgi apparatus (Fig. 8, G3-a and b).

G4 cells appeared to be less active than G3 cells, considering their low/medium nucleus/cytoplasm ratio (Fig. 8, G4-a). Their nuclei also showed loose chromatin and visible nucleoli (one or two) (Fig. 8, G4-a and b). Ultrastructural studies revealed the presence of a few cells similar to those found in F2, larger numbers of cells similar to G3, and a new group of cells with dense aggregates (Fig. 8, G4-c). Most cells in G4 exhibited an irregular rectangular shape with an eccentrically situated nucleus containing prominent nucleoli, mainly close to the nuclear membrane. Their Golgi apparatus had associated mitochondria, and they showed tubular endoplasmic reticulum, dense membrane-bound vesicular granules and many dense aggregates (Fig. 8, G4-a, b and c).

Secretion of DHEA and progesterone

Increasing patterns of secretion of DHEA and progesterone were observed by ELISA kits in different groups after 8 days of *in vitro* culture (Fig. 9). A linear trend was observed with time, showing a significant rise ($q < 0.001$) in DHEA concentrations in medium during the culture period in G1 ($n = 6$), G2 ($n = 5$), G3 ($n = 3$) and G4 ($n = 9$). A similar trend for progesterone levels also demonstrated a statistical increase ($q < 0.001$) in G2 ($n = 5$), G3 ($n = 3$) and G4 ($n = 9$), but G1 remained the same throughout the culture period. In co-culture conditions (G4), medium from the well, which was in contact with COV434 cells, contained no detectable amounts of DHEA or progesterone.

Statistical comparisons for progesterone levels between groups on Day 8 (D8) were as follows: G1 vs G2 ($q < 0.05$), G1 vs G3 ($q < 0.05$), G1 vs G4 ($q < 0.05$), G2 vs G3 ($q < 0.05$), G2 vs G4 ($q = 0.06$) and G3 vs G4 ($q = 0.22$).

Statistical comparisons for DHEA levels between groups on D8 were as follows: G1 vs G2 ($q = 0.33$), G1 vs G3 ($q = 0.09$), G1 vs G4

Downloaded from https://academic.oup.com/humrep/article/35/12/2793/6015748 by Universite catholique de louvain user on 11 January 2021

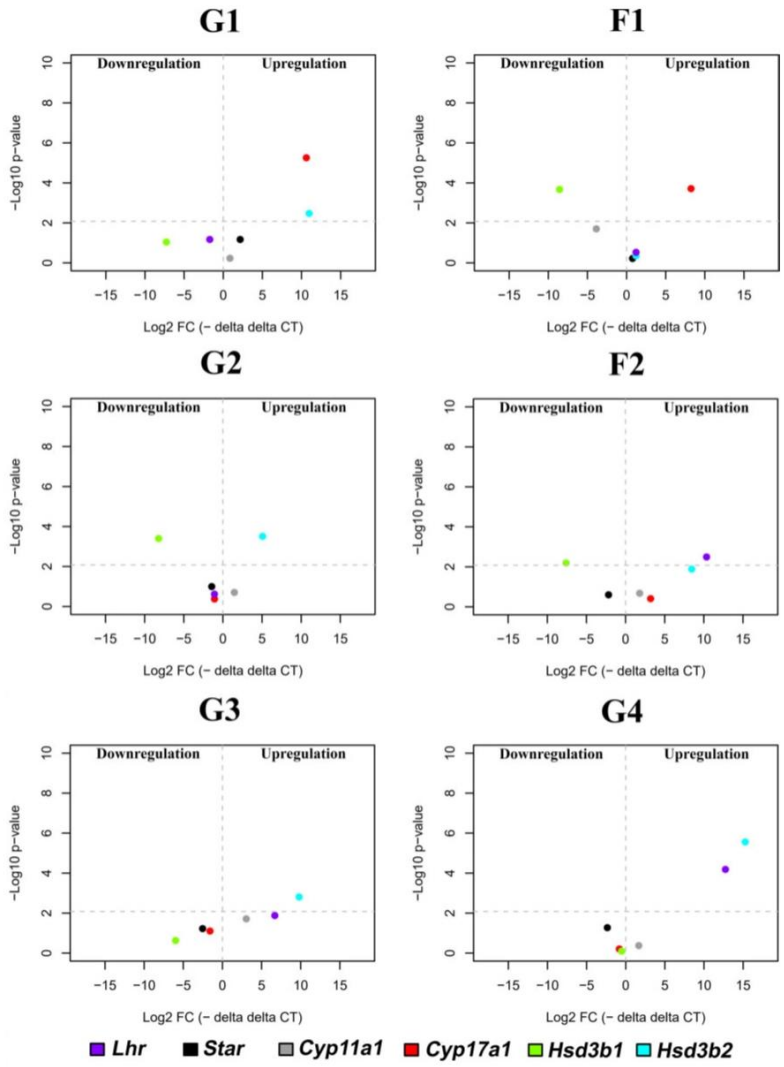


Figure 3. Quantitative real-time PCR results presented in volcano plots. mRNA expression for enzymes involved in steroidogenesis of theca/steroidogenic cells. Large magnitude fold changes (*x*-axis) and high statistical significance (-log10 of *P*-value, *y*-axis). The horizontal dashed line shows the position of $P = 0.05$, with dots above the line being $P < 0.05$ and dots below the line being $P > 0.05$. The vertical dashed line shows the boundary between down- and upregulation: downregulation on the left and upregulation on the right.

Downloaded from https://academic.oup.com/humrep/article/35/12/2793/6015748 by Universite catholique de louvain user on 11 January 2021

Table I Immunostaining of cells for different theca cell markers.

	Day 0	G1	F1	G2	F2	G3	G4
LHR	45.6%[a] (7481/16 397)	99%[b] (91/92)	36.1%[a] (129/357)		97.1%[b] (408/420)	90.5%[b] (247/273)	97.0%[b] (1156/1192)
STAR	0.2%[a] (1/570)	27%[b] (4/15)	82.2%[b] (693/758)		17.7%[b] (23/130)	6.3%[a] (78/1245)	26.8%[b] (82/306)
CYP11A1	0%[a] (0/331)	81.0[b] (191/236)	91.4%[b] (693/758)		99.1%[b] (114/115)	79.3%[b] (1153/1454)	97.5%[b] (2652/2720)
CYP17A1	16.7%[a] (139/833)	93.5%[b] (214/229)	64.1%[b] (397/619)	89%[b] (31/35)	79.0%[b] (729/923)	38.8%[a] (247/637)	99.4%[b] (2807/2823)
HSD3B1	47.5%[a] (95/200)	100%[b] (54/54)	98.8%[b] (163/165)		99.8%[b] (464/465)	98.9%[b] (178/180)	98.8%[b] (948/960)
HSD3B2	1.0%[a] (10/960)	74%[b] (29/39)	65.9%[b] (257/390)		24%[a] (20/85)	76.8%[b] (209/272)	94.8%[b] (346/365)
ADRP	0%[a] (0/1400)	93%[b] (51/55)	88.3%[b] (293/332)		99.2%[b] (124/125)	93.3%[b] (265/284)	97.7[b] (469/480)
CD13	0%[a] (0/10)	0%[a] (0/36)	1.6%[a] (6/377)	43%[b] (30/77)	21.1%[b] (76/360)	33.8%[b] (67/198)	24.5%[b] (111/453)
CD26	5.2%[a] (11/213)	47%[a] (34/72)	93.8%[b] (180/192)	100%[b] (10/10)	84.1%[b] (269/320)	76.5%[b] (130/170)	98.2%[b] (933/950)
NOTCH1	0.5%[a] (3/580)	4%[a] (2/47)	24.1%[a] (63/261)		12.2%[a] (22/181)	92.1%[b] (557/605)	95.6%[b] (717/750)

For each staining protocol values show mean percentage of positively stained cells (numbers in parentheses show number of positive cells out of the total number of cells counted).
[a,b]Indicate the statistical difference ($P < 0.05$) in each group after 8 days culture compared to Day 0 for every immunostaining.
ADRP, adipose differentiation-related protein; CD13, aminopeptidase-N; CD26, dipeptidyl peptidase IV; CYP11A1, cholesterol side-chain cleavage enzyme; CYP17A1, cytochrome P450 17A1; D0, Day 0; HSD3B1, hydroxy-delta-5-steroid dehydrogenase, 3 beta- and steroid delta-isomerase 1; HSD3B2, hydroxy-delta-5-steroid dehydrogenase, 3 beta- and steroid delta-isomerase 2; LHR, luteinizing hormone receptor; NOTCH1, Notch homolog 1, translocation-associated (drosophila); STAR, steroidogenic acute regulatory protein.

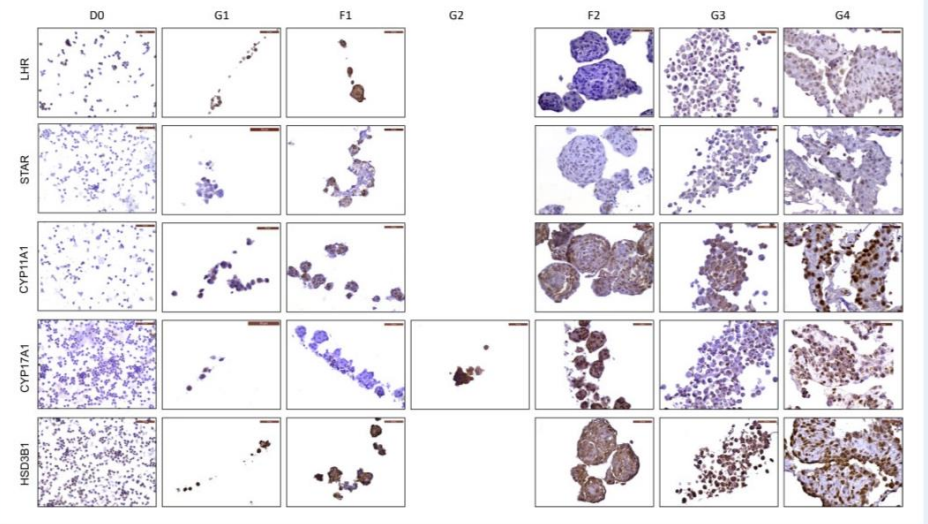


Figure 4. Immunohistochemistry of LHR, STAR, CYP11A1, CYP17A1 and HSD3B1 in cells on D0 (before culture), and G1, F1, G2, F2, G3 and G4 after 8 days of *in vitro* culture. Scale bars: 50 μm.

Downloaded from https://academic.oup.com/humrep/article/35/12/2793/6015748 by Universite catholique de louvain user on 11 January 2021

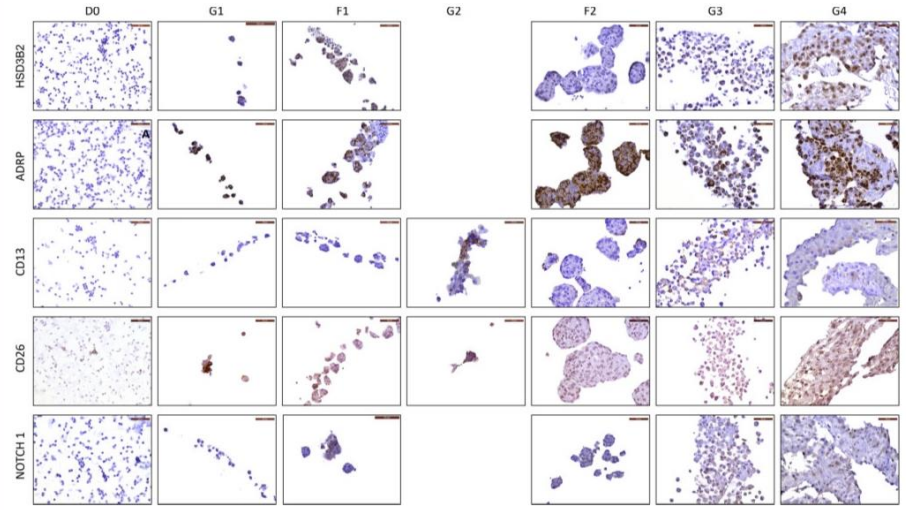


Figure 5. Immunohistochemistry of HSD3B2, ADRP, CD13, CD26 and NOTCH1 in cells on D0 (before culture), and G1, F1, G2, F2, G3 and G4 after 8 days of *in vitro* culture. Scale bars: 50 µm.

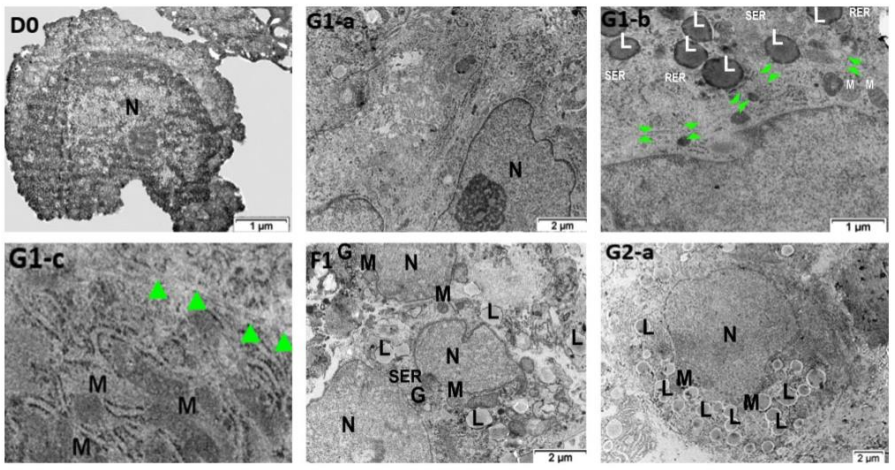


Figure 6. Transmission electron microscopy of cells before (D0) and after 8 days of *in vitro* culture. Cells before *in vitro* culture (D0). Ovarian cortical SCs in BM showing attached cells at the bottom of the well (G1—a, b and c) and floating spheroid structures (F1). SCs in EM showing attached cells at the bottom of the well (G2-a). G, Golgi apparatus; L, lipid droplets; M, mitochondria; N, nucleus; RER, rough endoplasmic reticulum; SER, smooth endoplasmic reticulum. G1-b and c: arrow heads: gap junctions.

Downloaded from https://academic.oup.com/humrep/article/35/12/2793/6015748 by Universite catholique de louvain user on 11 January 2021

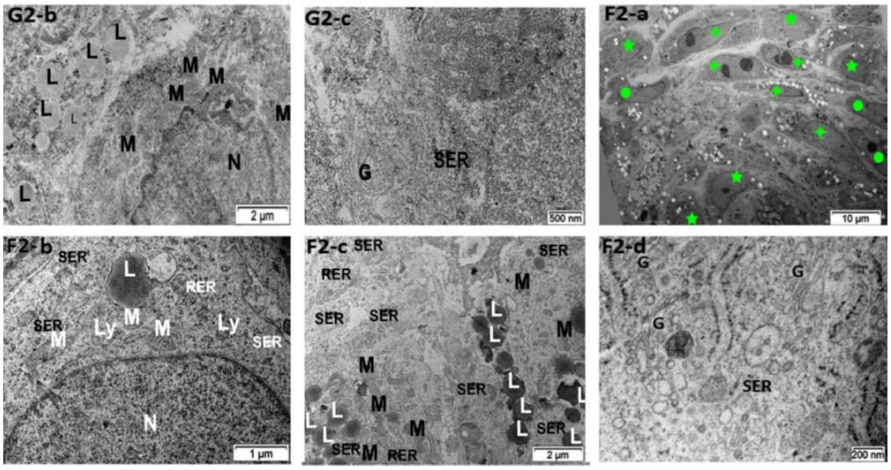


Figure 7. Transmission electron microscopy of cells after 8 days of *in vitro* culture. Ovarian cortical SCs in EM showing attached cells at the bottom of the well (G2—b and c) and floating spheroid structures (F2—a, b, c and d). Ly, lysosome. F2-a: circle: fibroblast; four tails star: transitional cells; five tails star: theca cells.

($q = 0.09$), G2 vs G3 ($q = 0.47$), G2 vs G4 ($q = 0.58$) and G3 vs G4 ($q = 0.58$).

Discussion

Since the main goal of our experiments was to obtain differentiated human TCs, we designed a study where we *in vitro*-cultured SCs isolated from the cortical layer of postmenopausal ovaries in medium enriched with growth factors thought to be involved in TC differentiation (Honda *et al.*, 2007; Liu *et al.*, 2015; Dalman *et al.*, 2018a,b). Since GCs have also been implicated in this process, we tested the co-culture approach with GCs (Orisaka *et al.*, 2006; Qiu *et al.*, 2013) as well. In all tested groups, we obtained large numbers of steroid-producing cells. At first, gene and protein expression patterns for proteins involved in the theca steroidogenic pathway appeared to indicate that virtually all cortical ovarian cells can differentiate into TCs, which would be in line with findings obtained in studies using bovine and caprine SCs (Orisaka *et al.*, 2006; Qiu *et al.*, 2013). However, in G1, the lack of CD13 immunostaining, a surface marker specific to TCs (Fujiwara *et al.*, 1992), showed that these cells were not TCs. On the other hand, ultrastructural analysis and the presence of CD13-positive cells confirmed that the TC population accounted for 21–43% of differentiated cells in the other groups (G2, G3 and G4). Interestingly, differentiation was not found to halt once cells were converted into TCs. In fact, just like in the human ovary, this process advances until TC luteinization and small luteal cell senescence, as evidenced by TEM. With the help of atelocollagen inserts, which improved cell attachment and proliferation and consequently their communication, TC differentiation was faster, so small luteal cells could be detected (G3 and G4). Addition of COV434 cells accelerated this process further, as older luteal cells with aggregates of luteal debris were also observed in G4. Luteal debris consists of small, dense, circular elements representing clumps of regressing luteal cells, as described by Fraser *et al.* (1999) and Adams and Hertig (1969).

G1 and F1 were both significantly positive for *Cyp17a1* mRNA and all studied proteins involved in the steroidogenic pathway. TEM images from the two different cell populations in the first group (G1 and F1) showed characteristics of steroid-producing cells: they were positive for all enzymes involved in the steroidogenic pathway and CD26, but negative for CD13 and NOTCH1. mRNA expression is not always consistent with the level of expressed proteins. The correlation can be as little as 40%, depending on the tissue and *in vitro* culture system (Vogel and Marcotte, 2012). There are many processes between transcription and translation and, as mentioned by Vogel and Marcotte (2012), protein stability is a big factor. The half-life of different proteins can range from minutes to days, while the degradation rate of mRNA would fall within a much tighter range (2–7 h for mammalian mRNA vs 48 h for protein) (Vogel and Marcotte, 2012). Moreover, the ultrastructure of these cells was different from TCs in the ovaries, which show steroid-secreting activity and are characterized by a round, oval or somewhat undulated nucleus, Golgi apparatus, rough endoplasmic reticulum, abundant smooth endoplasmic reticulum, lipid droplets, oval mitochondria with tubular or vesicular cristae and lysosomes

Downloaded from https://academic.oup.com/humrep/article/35/12/2793/6015748 by Universite catholique de louvain user on 11 January 2021

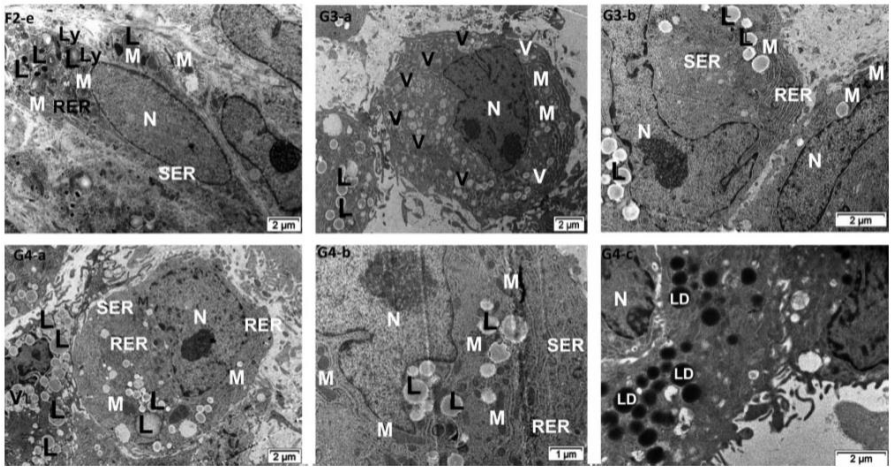


Figure 8. Transmission electron microscopy of cells after 8 days of *in vitro* culture. Floating spheroid structures (F2-e), ovarian cortical SCs in EM seeded onto an atelocollagen membrane (G3—a and b), and SCs in EM seeded onto one side of an atelocollagen membrane in co-culture with COV434 cells on the other side of the membrane (G4—a, b and c). LD, luteal debris; V, vacuole.

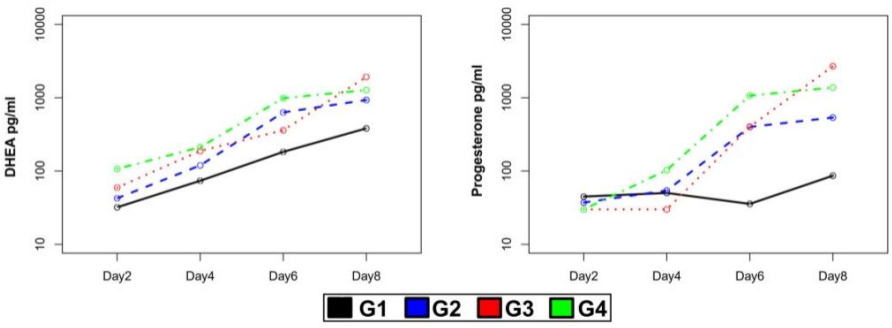


Figure 9. Enzyme-linked immunosorbent assays. Dehydroepiandrosterone levels on the left and progesterone levels on the right. Different time points for hormone measurement in the *x*-axis and logarithmic expression of hormones (pg/ml) in the *y*-axis. SCs in BM (G1). SCs in EM (G2) at different time points, SCs in EM seeded onto an atelocollagen membrane (G3) at different time points, SCs in EM seeded onto one side of an atelocollagen membrane in co-culture with COV434 cells on the other side of the membrane (G4) at different time points.

(Hiura *et al.*, 1981). On the other hand, the presence of gap junctions in attached cells in G1 and increasing secretion patterns of DHEA but not progesterone during *in vitro* culture are reported to be specific characteristics of ovarian interstitial steroid-producing cells (Dawson and McCabe, 1951; Semenova, 1969). According to Erickson *et al.* (1985), there are four types of interstitial cells in the ovary: primary (Gondos and Hobel, 1973), secondary (Kingsbury, 1939; Dawson and McCabe, 1951), theca (Peters, 1969) and hilar (Semenova, 1969).

Downloaded from https://academic.oup.com/humrep/article/35/12/2793/6015748 by Universite catholique de louvain user on 11 January 2021

Differentiation observed in G1 could be due to KSR, which contains mainly lipid-rich albumin (Kojima *et al.*, 2016), and these lipids could be responsible for DHEA synthesis. Indeed, in murine testicular explant culture, KSR was shown to increase testosterone production (Reda *et al.*, 2017). DHEA is the precursor of testosterone in testes and androstenedione in ovarian TCs (Bordini and Rosenfield, 2011).

Since TCs differentiate adjacent to developing follicles, it is assumed that once follicles start their growth, they secrete factors that stimulate TC differentiation (Magoffin and Magarelli, 1995; Honda *et al.*, 2007; Liu *et al.*, 2015). Ovarian interstitial cells develop and maintain a specialized phenotype in serum-free conditions, which is different from other types of cells in the ovary. It is clear that LH is the most important stimulating force in interstitial cells, inducing their differentiation both at morphological and biochemical levels (Erickson *et al.*, 1985). In addition to LH, there are other major factors that affect TC differentiation (Honda *et al.*, 2007). Using neonatal mouse ovaries, Honda *et al.* (2007) showed that purified putative theca stem cells were induced to differentiate into TCs *in vitro* under the influence of LH, IGF-1, SCF (also known as kit ligand), and conditioned medium from GCs. IGF-1 alone stimulated expression of LHRs (Magoffin and Weitsman, 1994) and steroidogenic enzymes. CYP11A1 and HSD3B, but not CYP17A1, was found to act synergistically with LH to increase expression of these enzymes (Magoffin and Weitsman, 1993a,b,c). In rats, a combination of IGF-1 and SCF increased expression of LHR, STAR, CY11A1, CYP17A1 and HSD3B, which provides strong evidence that these factors may act synergistically to regulate TC differentiation and steroid production (Huang *et al.*, 2001). bFGF has been shown to impact somatic cell mitosis, steroid synthesis, differentiation and apoptosis (Walters and Schallenberger, 1984; Tilly *et al.*, 1992; Lavranos *et al.*, 1994), while may influence theca development indirectly through stimulating SCF expression (Nilsson and Skinner, 2004). TGF-β superfamily members like bone morphogenetic proteins and growth differentiation factors, with vital roles in controlling follicle growth and development (Shimasaki *et al.*, 2004; Knight and Glister, 2006; Xia and Schneyer, 2009), are also involved in TC recruitment, proliferation and differentiation, which may or may not interact with gonadotropins (Young and McNeilly, 2010). By enriching the medium with growth factors purportedly involved in this process, as well as FSH and LH, we observed much lower concentrations of attached fibroblast-like cells and larger spheroid structures in G2 than in G1. Steroidogenic ultrastructural features of attached G2 cells and their undulated nucleus appeared to indicate that they had differentiated into TCs. Moreover, their membrane stained positive for CD13. ELISA results confirmed that these cells were actively secreting steroids; there was an increase in DHEA production from Day 2 (D2), while progesterone secretion started after four days of *in vitro* culture.

F2 structures were upregulated for *Lhr* and *Hsd3b2* and also expressed proteins and enzymes involved in the steroidogenic pathway of TCs. Ultrastructurally, these cells have three distinct features; some of them are fibroblast-like cells (Kingsbury, 1939) with elongated nuclei, others are transitional cells (Kingsbury, 1939) ellipsoidal in shape with an oval nucleus, and a further group resembles TCs with an undulated nucleus (Hiura *et al.*, 1981). Transitional cells are found halfway along the differentiation pathway of fibroblasts into TCs (Kingsbury, 1939).

Interestingly, our results from G2 and F2 show that being attached to a surface promoted a faster differentiation, demonstrating that substrate also has an impact on cell behavior (Kanta, 2015). This was confirmed in G3, where all cells remained firmly attached to the collagen membrane and differentiation reached the last stage, namely small luteal cells. Cells in G3 showed upregulation of *Lhr*, *Cyp11a1* and *Hsd3b2* at the mRNA level and expressed steroidogenic enzymes and CD13, CD26 and NOTCH1. Indeed, the ultrastructure of these cells showed the presence of small concentrations of fibroblasts, transitional cells and TCs and a large number of small luteal cells (Van Lennep and Madden, 1965), with lamelliform microvilli and an acentric nucleus together with other characteristics of steroidogenic cells (Ohara *et al.*, 1987). Our ELISA results show higher levels of secreted DHEA and progesterone in G3 medium compared to G2. Moreover, increasing DHEA levels from Day 2 of *in vitro* culture (D2) and progesterone secretion from Day 4 (D4) onwards also support our findings.

In G4, cells exhibited upregulated mRNA levels of *Lhr*, *Cyp11a1* and *Hsd3b2* and were positive for proteins and enzymes involved in the steroidogenic pathway of TCs, plus the three markers of steroidogenic/theca and luteal cells, CD13, CD26 and NOTCH1. Ultrastructural analysis revealed the presence of a few fibroblasts, transitional cells and TCs (Hiura *et al.*, 1981). However, most cells were ultrastructurally similar to small luteal cells. Conversely, luteal cells obtained from this group were somewhat different from luteal cells from G3, as they contained luteal debris, resembling older small luteal cells (Dawson and McCabe, 1951; Enders, 1962; Enders and Lyons, 1964; Green and Maqueo, 1965; Van Lennep and Madden, 1965; Blanchette, 1966; Adams and Hertig, 1969). We also observed a profuse agranular endoplasmic reticulum together with mitochondria containing tubular cristae, which is characteristic of many types of actively secreting steroid cells, including active human corpora lutea (Green and Maqueo, 1965; Van Lennep and Madden, 1965) and small luteal cells in different mammalian species (Enders, 1962; Enders and Lyons, 1964; Blanchette, 1966). According to Adams and Hertig (1969), a close association between tubular endoplasmic reticulum and mitochondria may be a morphological reflection of the conversion of cholesterol to progesterone.

Apart from growth factors, hormones and substrate, the presence of a GC line also plays a role in cell differentiation. Indeed, COV434 cells accelerate cell differentiation even further, as demonstrated by the presence of older small luteal cells with aggregates of luteal debris. Honda *et al.* (2007) also reported that while medium enriched with growth factors and hormones did lead to cell differentiation, fully mature TCs were only obtained after co-culture with GCs. It would be interesting to perform COV434 cell co-culture with BM in order to gain a better understanding of the role of GCs in TC differentiation.

Due to the similarity between bovine and human ovaries, we hypothesized that cortical SCs in general could differentiate into TCs (Orisaka *et al.*, 2006). However, we observed that while most cells became steroidogenic after *in vitro* culture, only a proportion of them were TCs, which indicates that there is a population of precursor TCs in human ovaries as in mouse ovaries (Liu *et al.*, 2015). More interestingly, such cells remain in human ovaries, even after menopause. Recently, Fan *et al.* (2019) showed a number of genes expressed by progenitor TCs, including NME2, APOD, APOC1, MEST, WFDC1, MATN2, PTCH1 and ACTA2 in the theca layer of antral follicles. In their study on progenitor TCs, Dalman *et al.* (2018a,b) differentiated theca stem cells from human small antral follicles and reported LHR, GLI2 and PTCH1 as markers of these cells. Since all these studies

Downloaded from https://academic.oup.com/humrep/article/35/12/2793/6015748 by Universite catholique de louvain user on 11 January 2021

were conducted in the theca layer where cells already received differentiation signals, further studies are needed to confirm the presence of progenitor TCs in fertile and postmenopausal human ovaries. The introduced markers could help to test the hypothesis of progenitor TCs and serve to identify these cells in postmenopausal ovaries.

In conclusion, we showed for the first time that human TCs can differentiate *in vitro* under the influence of different growth factors and hormones (Honda *et al.*, 2007; Liu *et al.*, 2015; Dalman *et al.*, 2018a,b). These cells closely resemble their ovarian counterparts when investigated by immunohistochemical, ultrastructural and functional analyses. Our results are a great step forward in the understanding of TC ontogenesis in human ovaries. Moreover, *in vitro*-generated human TCs can be used for studies on drug screening and exposure to endocrine-disrupting chemicals, as well as elucidating TC-associated pathologies, such as androgen-secreting tumors and polycystic ovary syndrome.

Supplementary data

Supplementary data are available at *Human Reproduction* online.

Data availability

The datasets generated and analysed during the current study are available from the corresponding author on reasonable request.

Acknowledgements

We are grateful to Mira Hryniuk for reviewing the English language of the manuscript and Dolores Gonzalez and Olivier Van Kerk for their technical assistance. We also thank Prof. Carolina M. Lucci (University of Brasília, Brazil) for her advice during cell ultrastructure analysis and all patients who donated ovarian tissue for research.

Authors' roles

P.A.: study design, experimental procedures, analysis, interpretation of data and manuscript preparation. M.M.D.: tissue supply and manuscript revision. J.A.: statistical analysis. A.C.: support for analysis of ultrastructural images. C.A.A.: experimental design, experimental procedures, interpretation of results and manuscript revision.

Funding

This study was supported by grants from the Fonds National de la Recherche Scientifique de Belgique (FNRS) (C.A.A. is an FRS-FNRS Research Associate; grant MIS #F4535 16 awarded to C.A.A.; grant 5/4/150/5 awarded to M.M.D.; grant ASP-RE314 awarded to P.A.) and Foundation Against Cancer (grant 2018-042 awarded to A.C.).

Conflict of interest

The authors declare no conflict of interests.

References

Adams EC, Hertig AT. Studies on the human corpus luteum. I. Observations on the ultrastructure of development and regression of the luteal cells during the menstrual cycle. *J Cell Biol* 1969;**41**:696–715.

Adib S, Valojerdi MR. Molecular assessment, characterization, and differentiation of theca stem cells imply the presence of mesenchymal and pluripotent stem cells in sheep ovarian theca layer. *Res Vet Sci* 2017;**114**:378–387.

Blanchette EJ. Ovarian steroid cells: II. The lutein cell. *J Cell Biol* 1966;**31**:517–542.

Bordini B, Rosenfield RL. Normal pubertal development: Part I: the endocrine basis of puberty. *Pediatr Rev* 2011;**32**:223–229.

Chiti MC, Dolmans M-M, Hobeika M, Cernogoraz A, Donnez J, Amorim CA. A modified and tailored human follicle isolation procedure improves follicle recovery and survival. *J Ovarian Res* 2017;**10**:71.

Dalman A, Totonchi M, Valojerdi MR. Establishment and characterization of human theca stem cells and their differentiation into theca progenitor cells. *J Cell Biochem* 2018a;**119**:9853–9865.

Dalman A, Totonchi M, Valojerdi MR. Human ovarian theca-derived multipotent stem cells have the potential to differentiate into oocyte-like cells *in vitro*. *Cell J* 2018b;**20**:527–536.

Dawson AB, McCabe M. The interstitial tissue of the ovary in infantile and juvenile rats. *J Morphol* 1951;**88**:543–571.

Edson MA, Nagaraja AK, Matzuk MM. The mammalian ovary from genesis to revelation. *Endocr Rev* 2009;**30**:624–712.

Enders AC. Observations on the fine structure of lutein cells. *J Cell Biol* 1962;**12**:101–113.

Enders AC, Lyons W. Observations on the fine structure of lutein cells: II. The effects of hypophysectomy and mammotrophic hormone in the rat. *J Cell Biol* 1964;**22**:127–141.

Erickson GF, Magoffin DA, Dyer CA, Hofeditz C. The ovarian androgen producing cells: a review of structure/function relationships. *Endocr Rev* 1985;**6**:371–399.

Fan X, Bialecka M, Moustakas I, Lam E, Torrens-Juaneda V, Borggreven N, Trouw L, Louwe L, Pilgram G, Mei H. Single-cell reconstruction of follicular remodeling in the human adult ovary. *Nature Commun* 2019;**10**:1–13.

Fraser H, Lunn S, Harrison D, Kerr JB. Luteal regression in the primate: different forms of cell death during naturaland gonadotropin-releasing hormone antagonist or prostaglandin analogue-induced luteolysis. *Biol Reprod* 1999;**61**:1468–1479.

Fujiwara H, Maeda M, Imai K, Fukuoka M, Yasuda K, Horie K, Takakura K, Taii S, Mori T. Differential expression of aminopeptidase-N on human ovarian granulosa and theca cells. *J Clin Endocrinol Metab* 1992;**74**:91–95.

Gondos B, Hobel C. Interstitial cells in the human fetal ovary. *Endocrinology* 1973;**93**:736–739.

Green JA, Maqueo M. Ultrastructure of the human ovary: I. The luteal cell during the menstrual cycle. *Am J Obstet Gynecol* 1965;**92**:946–957.

Hatzirodos N, Glister C, Hummitzsch K, Irving-Rodgers HF, Knight PG, Rodgers RJ. Transcriptomal profiling of bovine ovarian granulosa and theca interna cells in primary culture in comparison with their *in vivo* counterparts. *PLoS One* 2017;**12**:e0173391.

Downloaded from https://academic.oup.com/humrep/article/35/12/2793/6015748 by Universite catholique de louvain user on 11 January 2021

Havelock JC, Rainey WE, Carr BR. Ovarian granulosa cell lines. *Mol Cell Endocrinol* 2004;**228**:67–78.

Hiura M, Nogawa T, Fujiwara A. Electron microscopy of cytodifferentiation and its subcellular steroidogenic sites in the theca cell of the human ovary. *Histochemistry* 1981;**71**:269–277.

Honda A, Hirose M, Hara K, Matoba S, Inoue K, Miki H, Hiura H, Kanatsu-Shinohara M, Kanai Y, Kono T *et al.* Isolation, characterization, and *in vitro* and *in vivo* differentiation of putative thecal stem cells. *Proc Natl Acad Sci USA* 2007;**104**:12389–12394.

Huang CT, Weitsman SR, Dykes BN, Magoffin DA. Stem cell factor and insulin-like growth factor-I stimulate luteinizing hormone-independent differentiation of rat ovarian theca cells. *Biol Reprod* 2001;**64**:451–456.

Itami S, Yasuda K, Yoshida Y, Matsui C, Hashiura S, Sakai A, Tamotsu S. Co-culturing of follicles with interstitial cells in collagen gel reproduce follicular development accompanied with theca cell layer formation. *Reprod Biol Endocrinol* 2011;**9**:159.

Kanta J. Collagen matrix as a tool in studying fibroblastic cell behavior. *Cell Adh Migr* 2015;**9**:308–316.

Kingsbury B. Atresia and the interstitial cells of the ovary. *Am J Anat* 1939;**65**:309–331.

Knight PG, Glister CJR. TGF-B superfamily members and ovarian follicle development. *Reproduction* 2006;**132**:191–206.

Kojima K, Sato T, Naruse Y, Ogawa T. Spermatogenesis in explanted fetal mouse testis tissues. *Biol Reprod* 2016;**95**:63.

Lavranos TC, Rodgers HF, Bertoncello I, Rodgers RJ. Anchorage-independent culture of bovine granulosa cells: the effects of basic fibroblast growth factor and dibutyryl camp on cell division and differentiation. *Exp Cell Res* 1994;**211**:245–251.

Liu C, Peng J, Matzuk MM, Yao HH-C. Lineage specification of ovarian theca cells requires multicellular interactions via oocyte and granulosa cells. *Nat Commun* 2015;**6**:1–11.

Magoffin DA, Magarelli PC. Preantral follicles stimulate luteinizing hormone independent differentiation of ovarian theca-interstitial cells by an intrafollicular paracrine mechanism. *Endocr* 1995;**3**:107–112.

Magoffin DA, Weitsman SR. Effect of insulin-like growth factor-I on cholesterol side-chain cleavage cytochrome p450 messenger ribonucleic acid expression in ovarian theca-interstitial cells stimulated to differentiate *in vitro*. *Mol Cell Endocrinol* 1993a;**96**:45–51.

Magoffin DA, Weitsman SR. Insulin-like growth factor-I stimulates the expression of 3 beta-hydroxysteroid dehydrogenase messenger ribonucleic acid in ovarian theca-interstitial cells. *Biol Reprod* 1993b;**48**:1166–1173.

Magoffin DA, Weitsman SR. Differentiation of ovarian theca-interstitial cells *in vitro*: regulation of 17 alpha-hydroxylase messenger ribonucleic acid expression by luteinizing hormone and insulin-like growth factor-I. *Endocrinology* 1993c;**132**:1945–1951.

Magoffin DA, Weitsman SR. Insulin-like growth factor-I regulation of luteinizing hormone (LH) receptor messenger ribonucleic acid expression and LH-stimulated signal transduction in rat ovarian theca-interstitial cells. *Biol Reprod* 1994;**51**:766–775.

Nilsson EE, Skinner MK. Kit ligand and basic fibroblast growth factor interactions in the induction of ovarian primordial to primary follicle transition. *Mol Cell Endocrinol* 2004;**214**:19–25.

Ohara A, Mori T, Taii S, Ban C, Narimoto K. Functional differentiation in steroidogenesis of two types of luteal cells isolated from mature human corpora lutea of menstrual cycle. *J Clin Endocrinol Metab* 1987;**65**:1192–1200.

Orisaka M, Tajima K, Mizutani T, Miyamoto K, Tsang BK, Fukuda S, Yoshida Y, Kotsuji F. Granulosa cells promote differentiation of cortical stromal cells into theca cells in the bovine ovary. *Biol Reprod* 2006;**75**:734–740.

Peters H. The development of the mouse ovary from birth to maturity. *Eur J Endocrinol* 1969;**62**:98–116.

Qiu M, Liu J, Han C, Wu B, Yang Z, Su F, Quan F, Zhang Y. The influence of ovarian stromal/theca cells during *in vitro* culture on steroidogenesis, proliferation and apoptosis of granulosa cells derived from the goat ovary. *Reprod Dom Anim* 2014;**49**:170–176.

Qiu M, Quan F, Han C, Wu B, Liu J, Yang Z, Su F, Zhang Y. Effects of granulosa cells on steroidogenesis, proliferation and apoptosis of stromal cells and theca cells derived from the goat ovary. *J Steroid Biochem Mol Biol* 2013;**138**:325–333.

Reda A, Albalushi H, Montalvo SC, Nurmio M, Sahin Z, Hou M, Geijsen N, Toppari J, Söder O, Stukenborg J-B. Knock-out serum replacement and melatonin effects on germ cell differentiation in murine testicular explant cultures. *Ann Biomed Eng* 2017;**45**:1783–1794.

Semenova I. Adrenergic innervation of ovaries in Stein-Leventhal syndrome. *Vestn Akad Med Nauk SSSR* 1969;**24**:58–62.

Shimasaki S, Moore RK, Otsuka F, Erickson GF. The bone morphogenetic protein system in mammalian reproduction. *Endocr Rev* 2004;**25**:72–101.

Soares M, Sahrari K, Chiti MC, Amorim C, Ambroise J, Donnez J, Dolmans M-M. The best source of isolated stromal cells for the artificial ovary: medulla or cortex, cryopreserved or fresh? *Hum Reprod* 2015;**30**:1589–1598.

Tilly JL, Billig H, Kowalski KI, Hsueh A. Epidermal growth factor and basic fibroblast growth factor suppress the spontaneous onset of apoptosis in cultured rat ovarian granulosa cells and follicles by a tyrosine kinase-dependent mechanism. *Mol Endocrinol* 1992;**6**:1942–1950.

Van Lennep EW, Madden LM. Electron microscopic observations on the involution of the human corpus luteum of menstruation. *Z Zellforsch Mikrosk Anat* 1965;**66**:365–380.

Vandesompele J, De Preter K, Pattyn F, Poppe B, Van Roy N, De Paepe A, Speleman F. Accurate normalization of real-time quantitative RT-PCR data by geometric averaging of multiple internal control genes. *Genome Biol* 2002;**3**:RESEARCH0034.

Vitt UA, McGee EA, Hayashi M, Hsueh AJ. *In vivo* treatment with GDF-9 stimulates primordial and primary follicle progression and theca cell marker CYP17 in ovaries of immature rats. *Endocrinology* 2000;**141**:3814–3820.

Vogel C, Marcotte EM. Insights into the regulation of protein abundance from proteomic and transcriptomic analyses. *Nat Rev Genet* 2012;**13**:227–232.

Walters DL, Schallenberger E. Pulsatile secretion of gonadotrophins, ovarian steroids and ovarian oxytocin during the periovulatory phase of the oestrous cycle in the cow. *J Reprod Fertil* 1984;**71**:503–512.

Xia Y, Schneyer AL. The biology of activin: recent advances in structure, regulation and function. *J Endocrinol* 2009;**202**:1–12.

Downloaded from https://academic.oup.com/humrep/article/35/12/2793/6015748 by Universite catholique de louvain user on 11 January 2021

Yamada S, Fujiwara H, Honda T, Higuchi T, Nakayama T, Inoue T, Maeda M, Fujii S. Human granulosa cells express integrin α2 and collagen type IV: possible involvement of collagen type IV in granulosa cell luteinization. *Mol Hum Reprod* 1999;**5**:607–617.

Yang Z, Xiong H-R. *Culture Conditions and Types of Growth Media for Mammalian Cells Biomedical Tissue Culture*. Croatia: InTech, 2012, 3–18.

Young J, McNeilly AS. Theca: the forgotten cell of the ovarian follicle. *Reproduction* 2010;**140**:489–504.

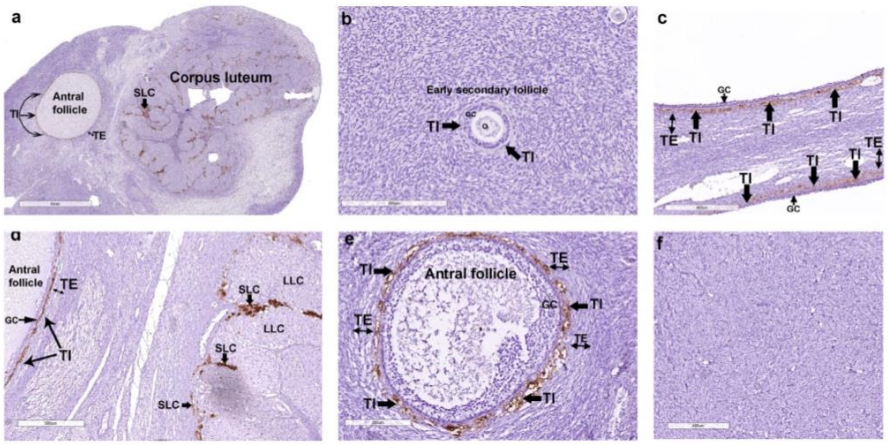
Zhang H, Vollmer M, De Geyter M, Litzistorf Y, Ladewig A, Dürrenberger M, Guggenheim R, Miny P, Holzgreve W, De Geyter C. Characterization of an immortalized human granulosa cell line (COV434). *Mol Hum Reprod* 2000;**6**:146–153.

Downloaded from https://academic.oup.com/humrep/article/35/12/2793/6015748 by Universite catholique de louvain user on 11 January 2021

Human Reproduction, pp. 1–1, 2020
doi:10.1093/humrep/deaa246

human reproduction

SUPPLEMENTARY DATA

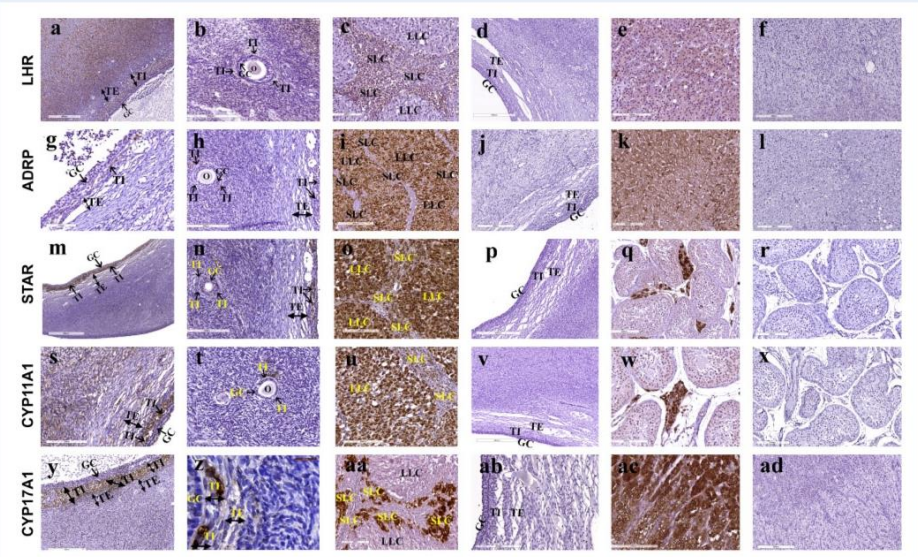


Supplementary Figure S1. Immunohistochemistry of CD13 in the human ovary. (**a**) A section of fertile human ovarian tissue containing an antral follicle and corpus luteum containing CD13-positive theca interna (TC) and small luteal cells (SLC) stained in brown respectively (black arrows). (**b**) Early secondary follicle (SF) with no expression of CD13 in the early formation of theca layer (black arrows). (**c**) Two antral follicles showing a CD13-positive theca layer stained in brown (black arrows). (**d**) Closer view of the antral follicle and corpus luteum, showing CD13 to only be expressed in the theca interna and small luteal cells (black arrows showing cells in brown). (**e**) CD13-positive theca interna cells (black arrow) in an antral follicle. (**f**) No expression of CD13 was observed in postmenopausal ovaries.

Human Reproduction, pp. 1–1, 2020
doi:10.1093/humrep/deaa246

human reproduction

SUPPLEMENTARY DATA

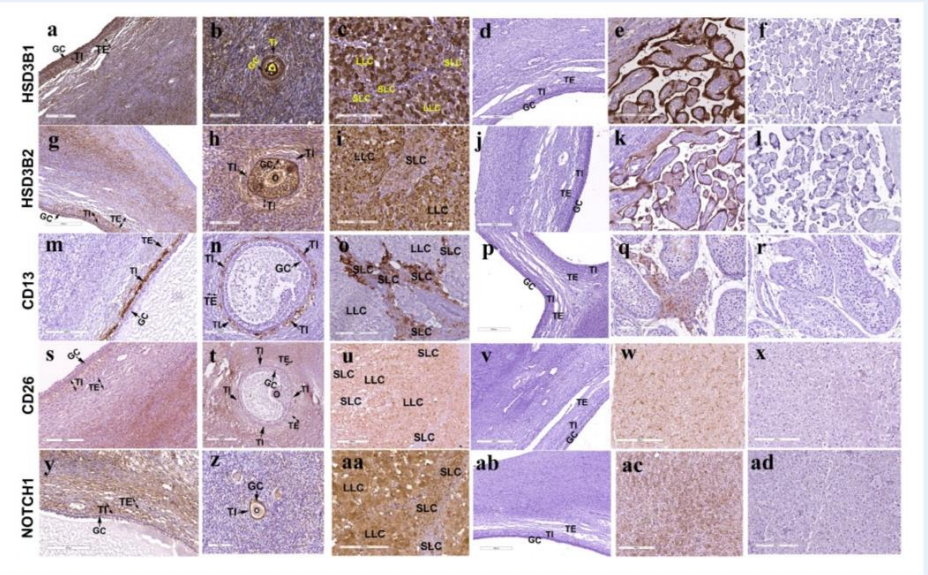


Supplementary Figure S2. Immunohistochemistry of LHCGR, ADRP, STAR, CYP11A1 and CYP17A1 on fertile human ovarian tissue and other human tissue serving as positive and negative controls. Antral follicles (a, g, m, s and y), secondary follicles (b, h, n, t and z), corpus luteum (c, i, o, u and aa), human ovary as a negative control, antral follicle (d, j, p, v and ab), human adrenal gland as a positive control (e and ac), human adrenal gland as a negative control (f and ad), human liver as a positive and negative control (k and l, respectively), human testis as a positive control (q and w) and human testis as a negative control (r and x). GC, granulosa cells; LLC, large luteal cells; O, oocyte; SLC, small luteal cells; TE, theca externa; TI, theca interna.

Human Reproduction, pp. 1–1, 2020
doi:10.1093/humrep/deaa246

human reproduction

SUPPLEMENTARY DATA



Supplementary Figure S3. Immunohistochemistry of HSD3B1, HSD3B2, ADRP, CD13, CD26 and NOTCH1 on fertile human ovarian tissue and other human tissue serving as positive and negative controls. Antral follicles (a, g, m, n, s, t and y), secondary follicles (b, h and z), corpus luteum (c, i, o, u and aa), human ovary as a negative control, antral follicle (d, j, p, v and ab), human placenta as a positive control (e and k), human placenta as a negative control (f and l), human testis as a positive control (q), human testis as a negative control (r), human liver tissue as a positive control (w and ac) and human liver tissue as a positive control (x and ad).

Human Reproduction, pp. 1–1, 2020
doi:10.1093/humrep/deaa246

human reproduction

SUPPLEMENTARY DATA

Supplementary Table SI Composition of enriched medium used for *in vitro* culture of isolated human ovarian cortical stromal cells (SCs).

Medium		Basic component	Abbreviation	Final concentration	Supplier
Enriched medium	Basic medium	Dulbecco's modified Eagle's medium/Ham's nutrient mixture F-12 with 1% l-alanyl-l-glutamine	DMEM/F-12	N/A	
		KnockOut™ serum replacement	KSR	10% (v/v)	Gibco
		Antibiotic-antimycotic	Anti-Anti	1% (v/v)	
		Insulin-transferrin-selenium	ITS	1% (v/v)	
		Recombinant human stem cell factor	SCF	100 ng/ml	
		Recombinant human bone morphogenic protein 6	BMP-6	20 ng/ml	
		Recombinant human transforming growth factor beta	TGF-β	20 ng/ml	
		Recombinant human hepatocyte growth factor	HGF	20 ng/ml	PeproTech EC, London, UK
		Recombinant human keratinocyte growth factor	KGF	20 ng/ml	
		Recombinant human insulin-like growth factor I	IGF-I	100 ng/ml	
		Recombinant Human fibroblast growth factor basic	bFGF	10 ng/ml	
		Recombinant human epidermal growth factor	EGF	20 ng/ml	
		Recombinant human growth differentiation factor 9	GDF-9	20 ng/ml	Sigma-Aldrich
		Follicle-stimulating hormone	FSH	100 ng/ml	Menopur; Ferring, Alst, Belgium
		Luteinizing hormone	LH	100 ng/ml	

BMP, bone morphogenetic protein; GDF, growth differentiation factor; KSR, KnockOut™ serum replacement.

Human Reproduction, pp. 1–1, 2020
doi:10.1093/humrep/deaa246

human reproduction

SUPPLEMENTARY DATA

Supplementary Table SII Probes used for qPCR analysis.

Gene name	Gene symbol	Reference	Company
LH receptor	*Lhr*	*Hs00174885-m1*	*Thermo Fisher, Scientific*
Steroidogenic acute regulatory protein	*Star*	*Hs00986559-g1*	*Thermo Fisher, Scientific*
Cytochrome P450 family 11 subfamily A member 1	*Cyp11a1*	*Hs00167984-m1*	*Thermo Fisher, Scientific*
Cytochrome P450 family 17 subfamily A member 1	*Cyp17a1*	*Hs01124136-m1*	*Thermo Fisher, Scientific*
Hydroxy-delta-5-steroid dehydrogenase, 3 beta- and steroid delta-isomerase 1	*Hsd3b1*	*Hs04194787-g1*	*Thermo Fisher, Scientific*
Hydroxy-delta-5-steroid dehydrogenase, 3 beta- and steroid delta-isomerase 2	*Hsd3b2*	*Hs00605123-m1*	*Thermo Fisher, Scientific*
Human RPLPO (large ribosomal protein) endogenous control (FAM™/MGB Probe, Non-Primer Limited)	*Rplpo*	*Hs99999902-m1*	*Thermo Fisher, Scientific*
E74-like ETS transcription factor 1	*Elf1*	*Hs00152844-m1*	*Thermo Fisher, Scientific*
Hypoxanthine phosphoribosyl transferase 1	*Hprt1*	*Hs99999909-m1*	*Thermo Fisher, Scientific*

Human Reproduction, pp. 1–1, 2020
doi:10.1093/humrep/deaa246

human reproduction

SUPPLEMENTARY DATA

Supplementary Table SIII Summary of immunohistochemical protocols applied to assess ovarian cortical stromal cells (SCs) differentiation.

Antigen	Antigen retrieval step	Antibody type	Dilution	Incubation	Positive control	What it should stain
LHR (PA5-21271; Thermo Fisher Scientific, Rockford, USA)	Tris EDTA buffer (pH 9.0) (20 min at 98°C)	Polyclonal (rabbit)	1:1000 in TBS + 5% BSA + 2% milk	RT 1 h	Adrenal gland	Theca and luteal cells (cytoplasm - membrane)
ADRP (SC-377429; Santa Cruz Biotechnology, Santa Cruz, USA)	Citrate buffer (pH 6.0) (75 min at 98°C)	Monoclonal (mouse)	1:200 in TBS + 1% NGS + 0.1% BSA	4°C O/N	Liver	Only luteal cells (cytoplasm - membrane)
STAR (AB133657; Abcam, Cambridge, UK)	Citrate buffer (pH 6.0) (75 min at 98°C)	Monoclonal (rabbit)	1:200 in TBS + 1% NGS + 0.1% BSA	4°C O/N	Testis	Theca and luteal cells (cytoplasm - outer mitochondrial membrane)
CYP11A1 (HPA016436; Sigma Aldrich/Merck, Darmstadt, Germany)	Tris EDTA buffer (pH 9.0) (20 min at 98°C)	Polyclonal (rabbit)	1:1000 in TBS + 10% NGS + 1% BSA	4°C O/N	Testis	Theca and luteal cells (cytoplasm - inner mitochondrial membrane)
CYP17A1 (ORB5948; Biorbyt, Cambridge, UK)	Tris EDTA buffer (pH 9.0) (20 min at 98°C)	Polyclonal (rabbit)	1:200 in TBS + 2.5% BSA + 1% milk	4°C O/N	Adrenal gland	Theca and luteal cells (cytoplasm - endoplasmic reticulum)
HSD3B1 (AB55268; Abcam)	Citrate buffer (pH 6.0) (75 min at 98°C)	Monoclonal (mouse)	1:100 in TBS + 1% NGS + 0.1% BSA	4°C O/N	Placenta	Theca and luteal cells (cytoplasm - endoplasmic reticulum)
HSD3B2 (GTX102813; Genetex, San Antonio, USA)	Citrate buffer (pH 6.0) (75 min at 98°C)	Polyclonal (rabbit)	1:500 in TBS + 1% NGS + 0.1% BSA	4°C O/N	Placenta	Theca and luteal cells (cytoplasm - endoplasmic reticulum)
NOTCH1 (SC-376403, Clone A-8, Santa Cruz Biotechnology)	Citrate buffer (pH 6.0) (75 min at 98°C)	Monoclonal (mouse)	1:100 in TBS + 1% NGS + 0.1% BSA	4°C O/N	Liver	Luteal cells (cytoplasmic - membrane)
CD13 (NCL-CD13-304; Leica Biosystems, UK)	Citrate buffer (pH 6.0) (75 min at 98°C)	Monoclonal (mouse)	1:100 in TBS + 1% NGS + 0.1% BSA	4°C O/N	Testis	Theca and luteal cells (cytoplasm - membrane)
CD26 (AM26442SU-L; OriGene Technologies, USA)	Citrate buffer (pH 6.0) (75 min at 98°C)	Monoclonal (mouse)	No diluent: ready to use	4°C O/N	Liver	Theca and luteal cells (cytoplasm - membrane)

ADRP, adipose differentiation-related protein; BSA, bovine serum albumin; CD13, aminopeptidase-N; CD26, dipeptidyl peptidase IV; CYP11A1, cholesterol side-chain cleavage enzyme; CYP17A1, cytochrome P450 17A1; HSD3B1, hydroxy-delta-5-steroid dehydrogenase, 3 beta- and steroid delta-isomerase 1; HSD3B2, hydroxy-delta-5-steroid dehydrogenase, 3 beta- and steroid delta-isomerase 2; LHR, LH receptor; NGS, normal goat serum; NOTCH1, Notch homolog 1, translocation-associated (drosophila); O/N, overnight; RT, room temperature; STAR, steroidogenic acute regulatory protein; TBS, tris-buffered saline.

Chapter 4:

Conclusions and perspectives

4.1 Conclusions

This thesis has made a substantial contribution to ongoing research into fertility restoration in women, especially in developing biological aspects of the transplantable engineered ovary.

4.1.1 Assessment of the steroidogenic pathway in human follicles

The classic "two-cell, two-gonadotropin" model describes the cooperation between theca and granulosa cells to ensure the production of estradiol (the most bioactive ovarian estrogenic steroid) during the follicular phase (Edson *et al.*, 2009). The theca cells possess all cellular receptors and enzymatic components required for *de novo* androgen production from circulating cholesterol. These androgens subsequently diffuse through the basement membrane and serve as substrates for the granulosa cells, which express the enzymes required to convert them to estradiol. Theca cell steroidogenesis is mainly under the control of LH, which activates the cAMP signaling pathway via a G protein-coupled receptor (Short, 1964). LH/cAMP induces the expression of the key steroidogenic enzymes StAR to translocate cholesterol from the outer mitochondrial membrane to the inner one where CYP11A1 is located and performs the first step of steroidogenesis by converting cholesterol to pregnenolone. This steroid is then converted mainly to androstenedione in most species via the successive actions of CYP17A1 and HSD3B residing in the smooth endoplasmic reticulum. Androstenediones will diffuse through the basement membrane to granulosa cells, where they

are then further transformed into estradiol by FSH-stimulated cells. The secretion of progesterone is essential for ovulation, embryonic implantation, and the maintenance of pregnancy. The chain of events leading to progesterone secretion begins with the preovulatory LH surge. The latter stimulates the granulosa and theca cells to undergo a terminal differentiation process called luteinization, which is characterized by growth arrest, tissue remodeling, angiogenesis, and changes in gene expression that will lead to the formation and function of the corpus luteum (Stocco *et al.*, 2007).

Our results on assessing proteins involved in theca cell steroidogenesis in the human ovary show steroid biosynthesis progress along with follicle development, and enzyme levels exhibit increasing expression patterns. And we can see in ''Figure 5 of Article 1'' the graphs on the staining index of LH, ADRP/ perilipin-2, StAR, CYP11A1, CYP17A1, and HSD3B1, and 2, show the increase during folliculogenesis, evidenced by their area covered and expression intensity (staining index). The graphs show the immunostaining quantification of different proteins at each follicle stage.

In the graphs, we see more than two-fold expression in the LH receptor, ADRP/ Perilipin-2, StAR, and CYP11A1. This was expected since just before ovulation and luteinization process, a huge surge in LH following by LH receptor happens, leading to a dramatic increase in progesterone production by luteinizing granulosa and theca cells (Richards, 1994). Luteal cells are supposed to convert cholesterol directly to progesterone solely by the action of CYP11A1 and HSD3B2 (Christenson and Devoto,

2003). However, the increase in HSD3B2 expression was not as dramatic as that of CYP11A1 when comparing corpus luteum and preovulatory follicles, which may be because the SI for HSD3B1 and 2 was already high in preovulatory follicles. Progesterone is the major steroid product of the newly formed corpus luteum and is essential for implantation of the embryo by supporting the uterine endometrium and maintenance of pregnancy. Luteal cells express high levels of StAR, CYP11A1, and HSD3B1 (rodents and most species) or HSD3B2 (humans) to produce high levels of steroids (Richards, 2001). It is also explainable why there is not a significant increase in CYP17A1 at the corpus luteum stage. It is because CYP11A1 in theca cells of growing follicles acts to convert cholesterol to pregnenolone. However, in luteal cells, the downregulation of CYP17A1 allows pregnenolone to be converted mainly to progesterone by HSD3B instead of being converted to DHEA (Niswender *et al.*, 2000).

4.1.2 Investigation of the presence of a precursor theca cell population in human ovaries

In mice, theca cell fate specification has already occurred at the time of birth as neonatal ovaries contain a specific theca stem/progenitor cell population expressing *Gli3* and *Ptch1*, which after differentiation into theca cells, express *Lhr* and *Gli2* (Honda *et al.*, 2007). The differentiated theca cells are resided in the ovarian mesenchyme and are separated from the oocyte-granulosa cell structure by a basement membrane (Edson *et al.*, 2009). The histological juxtaposition of theca cells to

granulosa cells leads to the hypothesis that recruitment of the theca cells from the ovarian stroma is regulated by the factor(s) produced by granulosa cells (Liu *et al.*, 2010). In the presence of GDF9 secreted by the oocyte, IHH and DHH ligand in granulosa cells are expressed and act in a paracrine manner on their downstream target in (progenitor) theca cells through PTCH1 receptor to induce and activate the transcription factors GLI1, GLI2, and GLI3 which are also potential markers for progenitor theca cells in mice (Honda *et al.*, 2007; Liu *et al.*, 2015; Russell *et al.*, 2007; Wijgerde *et al.*, 2005).

Our results from studying the GDF9-HH-GLI pathway in human fetal, prepubertal, fertile, and menopausal ovaries are presented in ''Article 2'', showing differences between humans and mice in this pathway. IHC on GDF9 showed its expression from the oocyte in the fetus, prepubertal and fertile follicles; meanwhile, its expression in the stromal cells of fertile and menopausal ovaries was also confirmed with qPCR analyses on *Gdf9* mRNA in menopausal ovaries. IHH, DHH, and SHH were always expressed throughout the ovaries during all the periods of life, not only limited to the follicles but also the stromal cells. qPCR analyses on *Ihh* showed the presence of its transcript in menopausal ovaries. PTCH1 receptor was also detected not only on theca cells but oocyte, granulosa cells, and the stroma of fertile and menopausal ovaries. GLI1, 2, and 3 are expressed throughout the ovary in all the periods of life, while there was no mRNA for Gli1 and 2 but Gli3 in the stromal cells of postmenopausal ovaries.

To conclude, our findings indicate that GLI1, GLI2, and GLI3 proteins do not appear to be specific markers for precursor theca cells in human ovaries because they are confined neither to a specific population of cells nor limited to the ovary age. Despite mouse, our results indicate that GLI proteins and PTCH receptors are involved in steroidogenesis as general rather than specific markers of theca cells. Our findings on the GDF9-HH-GLI pathway provide a basis for future investigations into human ovaries. They could be applied to define cell-specific responses to GDF9-HH-GLI signaling in human follicles and stromal cells, determining how this pathway modulates follicle development and steroidogenic function in ovaries from the fetal to the postmenopausal stage.

4.1.3 In vitro differentiation of human theca cells

While ovarian tissue cryopreservation followed by orthotropic reimplantation is a promising method to restore endocrine function and fertility in women and prepubertal girls needing immediate chemotherapy, it is not recommended to the patients who are remitted from the high risk of metastasis cancers due to the high chance of reseeding malignant cells, which can cause recurrence of the primary disease after transplantation (Dolmans *et al.*, 2013; Donnez and Dolmans, 2013; Donnez *et al.*, 2015). TEO could be a safe alternative to restore fertility in this group of women. TEO should consist of a proper 3D matrix, which should mimic the natural environment of the ovary, to support follicle growth and survival (Amorim and Shikanov, 2016; Chiti *et al.*, 2017a; Chiti *et al.*, 2015; Dolmans *et al.*, 2007; Dolmans *et al.*, 2008;

Donnez and Kim, 2011; Luyckx *et al.*, 2014; Rajabzadeh *et al.*, 2015; Shea *et al.*, 2014; Smith *et al.*, 2014; Soares *et al.*, 2015c; Vanacker *et al.*, 2014). However, this is not enough. Ovarian cells are also pivotal since they are responsible for vascularization in the ovarian tissue (Chiti *et al.*, 2015; Dath *et al.*, 2011; Luyckx *et al.*, 2014) and providing a complex bidirectional paracrine signaling with follicles (Donnez and Kim, 2011; Tagler *et al.*, 2011). One important remaining question is the presence of theca cells in the TEO. As human follicles are isolated at the primordial stage, there is no layer of theca cells around them.

In general, it is believed that once the follicle is activated at the primary stage, a change in the phenotype of granulosa cells from flattened to cuboidal is observable, and it starts to secrete different factors such as KL, bFGF, and KGF to recruit; and LH, GDF9, IGF and KL to differentiate theca cells from the ovarian stroma (Young and McNeilly, 2010). Theca cells start to appear at the later stage of secondary follicles and form a layer around the granulosa-oocyte structure (Young and McNeilly, 2010). They play an indispensable role in folliculogenesis by providing structural support for the follicle and androstenedione as a substrate for granulosa cells to convert it to estradiol (Edson *et al.*, 2009; Hirshfield, 1991; Nilsson and Skinner, 2001). Besides such important tasks for theca cells, less knowledge is available regarding their recruitment, growth, and differentiation due to the lack of access to their origin (Honda *et al.*, 2007; Liu *et al.*, 2015).

Since the main goal of our experiments was to obtain differentiated human theca cells for TEO, we designed a study where stromal cells

isolated from the cortical layer of postmenopausal ovaries were in vitro cultured in (I) basic medium (BM), which was composed of DMEM-F12, Knock-out serum, and antibiotics (Group 1 = G1), (II) enriched medium (EM), which contained BM supplemented with growth factors, FSH and LH (Group 2 = G2), (III) EM and a permeable membrane to favor cell attachment (Group 3 = G3), and (IV) EM and a permeable membrane in co-culture with COV434, a granulosa-cell line (Group 4 = G4). Since it has been proven that growth factors are involved in theca cell differentiation (Dalman *et al.*, 2018a; Honda *et al.*, 2007; Liu *et al.*, 2015; Young and McNeilly, 2010), and granulosa cells are implicated in this process, we tested the co-culture approach with the latter (Orisaka *et al.*, 2006; Qiu *et al.*, 2013) as well.

In all tested groups, we obtained large numbers of steroid-producing cells. Initially, results from gene and protein expression patterns for proteins involved in the theca steroidogenic pathway appeared to indicate that virtually all cortical ovarian cells can differentiate into theca cells, which would be in concordance with findings obtained in studies using bovine and goat stromal cells (Orisaka *et al.*, 2006; Qiu *et al.*, 2013). However, in G1, the lack of CD13 immunostaining, a surface marker specific to theca interna cells (Fujiwara *et al.*, 1992a), showed that these cells were not theca ones. On the other hand, based on ultrastructural analysis and CD13 immunostaining, theca cell population accounted for 21%-43% of differentiated cells in G2, G3, and G4. Interestingly, in G3 and G4, differentiation was not found to halt once cells were converted into theca ones, and just like in the human ovary, this process advances

until their luteinization and small luteal cell senescence, as evidenced by TEM. This occurred with the help of atelocollagen inserts, which improved cell attachment and proliferation, and consequently, their communication, leading to a faster differentiation, so small luteal cells could be detected. The addition of COV434 cells in G4 accelerated this process further, as older luteal cells with aggregates of luteal debris (Adams and Hertig, 1969; Fraser *et al.*, 1999) were also observed.

Since GLI1 does not appear to be a marker for precursor theca cells in the human ovary (Article 2), and due to its similarity to cow and goat counterpart, we hypothesized that cortical stromal cells, in general, can differentiate into theca cells (Orisaka *et al.*, 2006; Qiu *et al.*, 2013). Our data demonstrated that while most cells after in vitro culture became steroidogenic, only a proportion of them was theca cells. This indicates that similar to mice (Liu *et al.*, 2015), there is indeed a population of precursor theca cells in human ovaries. Another possibility is that theca cells are originated from mesenchymal stem cells present in the human ovary (Coffman *et al.*, 2019). Dalman *et al.* (2018a) reported isolated theca stem cells from the periphery of antral follicles could be differentiated into theca progenitor cells, osteocyte-, adipocyte- and chondrocyte-like cells in special culture media. Perhaps, what these authors called theca stem cells are indeed mesenchymal stem cells. Since they assessed isolated theca stem cells with CD29, CD44, CD73, CD90, and CD105, which are indeed markers for mesenchymal stem cells (Feng-Juan *et al.*, 2014; Maleki *et al.*, 2014; Moraes, 2018).

In our study, for the first time, it is shown that we can differentiate theca cells from cells isolated from human postmenopausal thanks to the presence of different growth factors and hormones in the in vitro culture medium (Dalman *et al.*, 2018a; Honda *et al.*, 2007; Liu *et al.*, 2015). These cells closely resemble their ovarian counterparts when investigated by immunohistochemical, ultrastructural, and functional analyses. We believe that our findings are a great step forward in understanding theca cell ontogenesis in human ovaries.

4.2 Perspectives and future research

While this study was able to demonstrate that human theca cells could be differentiated from cells present in the cortex of postmenopausal ovaries, which was an essential requirement for the success of the transplantable engineered ovary, it also conducted to two important questions:

4.2.1 What is the origin of theca cells in the human ovary?

Based on our findings, we hypothesize that theca cells differentiate from a subpopulation of cells present in the ovarian cortex. Since there is not a known specific marker that we could use to confirm our hypothesis, we have to differentiate them in a more controlled study attempting to uncover them by the origin and number of differentiated cells.

To confirm this, the first step is to divide the isolated ovarian cells into subpopulations. For instance, after isolation, cells could be sorted into four different groups using CD31 and CD34 markers:

1. CD34- and CD31-positive cells
2. CD34-negative and CD31-positive cells
3. CD34-positive and CD31-negative cells
4. CD34- and CD31-negative cells

The first two groups would be discarded as they represent endothelial cells and their precursor cells, which are very unlikely to differentiate into theca cells. The last two ones (mesenchymal stromal cells and their progenitor cells) will be kept for in vitro studies. Plating separately these two cell groups could provide us the first indication to confirm our hypothesis, presence of precursor, or show that similar to large animal models (Orisaka *et al.*, 2006; Qiu *et al.*, 2013), human theca cells differentiate potentially from all ovarian stromal ones. Cells would be in vitro culture using the enriched medium and collagen membrane described in "Article 4", as this appeared to be the fast way to differentiate them without the time-consuming step of plating COV434 cells (Article 4). In order to assess precisely when the cells start differentiating and calculate the precise proportion of cells that undergo this process, which would also help us to identify their origin, they would be in vitro cultured not only for 8 days but also during shorter periods (for instance, 2, 4, and 6 days).

Moreover, in vitro culture could be performed using a live cell imaging microscope. We could track individual cells through time, assess the

morphological heterogeneity of the population in the well, and investigate dry mass dynamics during biological processes such as differentiation. Since the water content of the cells causes the variations in surface integral of the optical phase in live cells, measuring the nonaqueous content or dry mass of living cells using the mentioned microscope provides an entirely non-invasive method (Popescu *et al.*, 2008). Using such a microscope in our experiment would also enable us to precisely segment lipid droplets, calculate their metrics, and investigate their dry mass dynamics. Differentiated cells could be identified with a fluorescent marker against CD13 during culture, which could allow for assessment of cell behavior and changes and their lipid droplets individually. CD13-positive cells could be sorted and have their proportion calculated. Finally, a comparison between differentiated cells and the ones from the group that originated them and theca cells collected from punctured follicles from IVF candidates (positive control) could be performed by single-cell analysis. This is a useful method in cellular biology that helps to study genomics, transcriptomics, proteomics, and metabolomics at the single-cell level (Habibi *et al.*, 2017; Wang and Bodovitz, 2010). We believe results from single-cell analyses would provide us invaluable data of genomic map of three studied groups and give us a clear view of which genes with what intensity are up-or down-regulated in the cells as well as the similarities and differences among original cells put in culture, differentiated ones at each time point and theca cells from IVF patients.

4.2.2 Can theca cells be differentiated in the transplantable engineered ovary?

Since the final goal is to develop a safe transplantable engineered ovary as an alternative to restore fertility for patients with high-risk category cancers, an in vivo experiment is mandatory. While cells have been shown to differentiate in vitro under the influence of proteins synthesized by the oocyte and granulosa cells in growing follicles, we need to ensure that this can occur in vivo under the influence of isolated follicles. To this end, we could repeat the grafting experiments in immunodeficient mice of our group (Chiti *et al.*, 2015; Chiti *et al.*, 2017b; Chiti *et al.*, 2017c; Luyckx *et al.*, 2014; Paulini *et al.*, 2016), encapsulating isolated human preantral follicles and ovarian cells in a fibrin matrix. However, instead of performing only one week of transplantation, we could leave the graft for longer periods (for instance, 1, 2, 4, and 6 weeks) in order to assess the influence of growing follicles on the recruitment and differentiation of theca cells and formation of a theca interna layer around them. After the different periods of grafting, theca cells could be identified using CD13 and their steroidogenic potential assessed using markers described in “Article 1”.

I. References

Accialini P, Hernández SF, Bas D, Pazos M, Irusta G, Abramovich D, Tesone M. A link between Notch and progesterone maintains the functionality of the rat corpus luteum. *Reproduction* 2015;149: 1-10.

Adams EC, Hertig AT. Studies on the human corpus luteum: I. observations on the ultrastructure of development and regression of the luteal cells during the menstrual cycle. *The Journal of cell biology* 1969;41: 696-715.

Adams J, Liu Z, Ren YA, Wun W-S, Zhou W, Kenigsberg S, Librach C, Valdes C, Gibbons W, Richards J. Enhanced inflammatory transcriptome in the granulosa cells of women with polycystic ovarian syndrome. *The Journal of Clinical Endocrinology & Metabolism* 2016;101: 3459-3468.

Adams SR, Harootunian AT, Buechler YJ, Taylor SS, Tsien RY. Fluorescence ratio imaging of cyclic AMP in single cells. *Nature* 1991;349: 694-697.

Adashi EY, Resnick CE, D'Ercole AJ, Svoboda ME, van Wyk JJ. Insulin-like growth factors as intraovarian regulators of granulosa cell growth and function. *Endocrine reviews* 1985;6: 400-420.

Adib S, Valojerdi MR. Molecular assessment, characterization, and differentiation of theca stem cells imply the presence of mesenchymal and pluripotent stem cells in sheep ovarian theca layer. *Research in Veterinary Science* 2017;114: 378-387.

Ahmed TA, Griffith M, Hincke M. Characterization and Inhibition of Fibrin Hydrogel–Degrading Enzymes During Development of Tissue Engineering Scaffolds. *Tissue engineering* 2007;13: 1469-1477.

Al-Alem L, Puttabyatappa M, Rosewell K, Brännström M, Akin J, Boldt J, Muse K, Curry Jr TE. Chemokine ligand 20: a signal for leukocyte recruitment during human ovulation? *Endocrinology* 2015;156: 3358-3369.

Al-Mehdi M. Fine structure and origin of interstitial tissue in the ovary of the pregnant rat. *Cells Tissues Organs* 1979;103: 245-251.

Alaminos M, Sánchez-Quevedo MaDC, Munoz-Ávila JI, Serrano D, Medialdea S, Carreras I, Campos A. Construction of a complete rabbit cornea substitute using a fibrin-agarose scaffold. *Investigative ophthalmology visual science* 2006;47: 3311-3317.

Amelkina O, Zschockelt L, Painer J, Serra R, Villaespesa F, Krause E, Jewgenow K, Braun BC. Progesterone, estrogen, and androgen receptors in the corpus luteum of the domestic cat, Iberian lynx (Lynx pardinus) and Eurasian lynx (Lynx lynx). *Theriogenology* 2016;86: 2107-2118.

Amorim CA. Artificial ovary *Gonadal tissue cryopreservation in fertility preservation*. 2016. Springer, pp. 175-192.

Amorim CA, Shikanov A. The artificial ovary: current status and future perspectives. *Future oncology* 2016;12: 2323-2332.

Amorim CA, Van Langendonckt A, David A, Dolmans M-M, Donnez J. Survival of human pre-antral follicles after cryopreservation of ovarian tissue, follicular isolation and in vitro culture in a calcium alginate matrix. *Human Reproduction* 2009;24: 92-99.

Aqmasheh S. Effects of mesenchymal stem cell derivatives on hematopoiesis and hematopoietic stem cells. *Advanced pharmaceutical bulletin* 2017;7: 165.

Attia GR, Dooley CA, Rainey WE, Carr BR. Transforming growth factor β inhibits steroidogenic acute regulatory (StAR) protein expression in human ovarian thecal cells. *Molecular and cellular endocrinology* 2000;170: 123-129.

Badylak SF, Brown BN, Gilbert TW, Daly KA, Huber A, Turner NJ. Biologic scaffolds for constructive tissue remodeling. *Biomaterials* 2011;32: 316.

Bagavandoss P. Temporal expression of tenascin-C and type I collagen in response to gonadotropins in the immature rat ovary. *Acta histochemica* 2014;116: 1125-1133.

Balestrini JL, Billiar KL. Equibiaxial cyclic stretch stimulates fibroblasts to rapidly remodel fibrin. *Journal of biomechanics* 2006;39: 2983-2990.

Barbieri RL, Makris A, Ryan K. Insulin stimulates androgen accumulation in incubations of human ovarian stroma and theca. *Obstetrics and gynecology* 1984;64: 73S-80S.

Barbieri RL, Makris A, Ryan KJ. Effects of insulin on steroidogenesis in cultured porcine ovarian theca. *Fertility sterility* 1983;40: 237-241.

Bassett DL. The changes in the vascular pattern of the ovary of the albino rat during the estrous cycle. *American Journal of Anatomy* 1943;73: 251-291.

Bedaiwy MA. Strategies for fertility preservation and gonadal protection during gonadotoxic chemotherapy and radiotherapy. *Middle East Fertil Soc J* 2005;10: 1-21.

Bergmann NM, West JL. Histogenesis in Three-Dimensional Scaffolds *Principles of Regenerative Medicine*. 2008. Burlington, Academic Press, pp. 686-703.

Berisha B, Schams D, Kosmann M, Amselgruber W, Einspanier R. Expression and tissue concentration of vascular endothelial growth factor, its receptors, and localization in the bovine corpus luteum during estrous cycle and pregnancy. *Biology of Reproduction* 2000;63: 1106-1114.

Berkholtz CB, Lai BE, Woodruff TK, Shea LD. Distribution of extracellular matrix proteins type I collagen, type IV collagen, fibronectin, and laminin in mouse folliculogenesis. *Histochemistry and cell biology* 2006;126: 583-592.

Besmer P. The kit ligand encoded at the murine Steel locus: a pleiotropic growth and differentiation factor. *Current opinion in cell biology* 1991;3: 939-946.

Birla RK, Borschel GH, Dennis RG, Brown DL. Myocardial engineering in vivo: formation and characterization of contractile, vascularized three-dimensional cardiac tissue. *Tissue engineering* 2005;11: 803-813.

Brasaemle DL. Thematic review series: adipocyte biology. The perilipin family of structural lipid droplet proteins: stabilization of lipid droplets and control of lipolysis. *Journal of lipid research* 2007;48: 2547-2559.

Bridges PJ, Cho J, Ko C. Endothelins in regulating ovarian and oviductal function. *Frontiers in bioscience* 2011;3: 145.

Briley SM, Jasti S, McCracken JM, Hornick JE, Fegley B, Pritchard MT, Duncan FE. Reproductive age-associated fibrosis in the stroma of the mammalian ovary. *Reproduction* 2016;152: 245.

Brown H, Russell D. Blood and lymphatic vasculature in the ovary: development, function and disease. *Human reproduction update* 2014;20: 29-39.

Brown HM, Robker RL, Russell DL. Development and hormonal regulation of the ovarian lymphatic vasculature. *Endocrinology* 2010;151: 5446-5455.

Bruns H, Kneser U, Holzhüter S, Roth B, Kluth J, Kaufmann PM, Kluth D, Fiegel HC. Injectable liver: a novel approach using fibrin gel as a matrix

for culture and intrahepatic transplantation of hepatocytes. *Tissue engineering* 2005;11: 1718-1726.

Bulun SE. *Williams Textbook of Endocrinology*. 13 edn, 2016.

Burden HW. Adrenergic innervation in ovaries of the rat and guinea pig. *American Journal of Anatomy* 1972;133: 455-461.

Burden HW, Irvin I, Lawrence jr E. The effects of denervation on the localization of ▵ 5-3β-hydroxysteroid dehydrogenase activity in the rat ovary during pregnancy. *Cells Tissues Organs* 1977;97: 286-290.

Cacioppo JA, Lin P-CP, Hannon PR, McDougle DR, Gal A, Ko C. Granulosa cell endothelin-2 expression is fundamental for ovulatory follicle rupture. *Scientific reports* 2017;7: 1-11.

Campbell B, Souza C, Skinner A, Webb R, Baird D. Enhanced response of granulosa and theca cells from sheep carriers of the FecB mutation in vitro to gonadotropins and bone morphogenic protein-2,-4, and-6. *Endocrinology* 2006;147: 1608-1620.

Capps ML, Lawrence IE, Burden HW. Ultrastructure of the cells of the ovarian interstitial gland in hypophysectomized rats. *Cell and Tissue Research* 1978;193: 433-442.

Care AS, Diener KR, Jasper MJ, Brown HM, Ingman WV, Robertson SA. Macrophages regulate corpus luteum development during embryo implantation in mice. *The Journal of clinical investigation* 2013;123: 3472-3487.

Carithers JR, Green JA. Ultrastructure of rat ovarian interstitial cells I. Normal structure and regressive changes following hypophysectomy. *Journal of ultrastructure research* 1972;39: 239-250.

Carroll J, Gosden RG. Physiology: Transplantation of frozen—thawed mouse primordial follicles. *Human Reproduction* 1993;8: 1163-1167.

Chapman RM. Effect of cytotoxic therapy on sexuality and gonadal function. In Oncology Si (ed). 1982. WALTER REED ARMY INST OF RESEARCH WASHINGTON DC, pp. 84-89.

Chiti C, Viswanath A, Vanacker J, Germain L, White L, Dolmans M, Des Rieux A, Amorim C. Hydrogel from bovine decellularized ovarian extracellular matrix supports mouse follicle survival in vitro *Front Bioeng Biotechnol Conference Abstract: 10th World Biomaterials Congress*. 2016, Montréal, Canada: Frontiers, pp. 17-22.

Chiti M, Dolmans M, Orellana R, Soares M, Paulini F, Donnez J, Amorim C. Influence of follicle stage on artificial ovary outcome using fibrin as a matrix. *Human Reproduction* 2015;31: 427-435.

Chiti MC, Dolmans M-M, Donnez J, Amorim C. Fibrin in reproductive tissue engineering: a review on its application as a biomaterial for fertility preservation. *Annals of biomedical engineering* 2017a;45: 1650-1663.

Chiti MC, Dolmans M-M, Hobeika M, Cernogoraz A, Donnez J, Amorim CA. A modified and tailored human follicle isolation procedure improves follicle recovery and survival. *Journal of ovarian research* 2017b;10: 71.

Chiti MC, Dolmans M-M, Lucci C, Paulini F, Donnez J, Amorim C. Further insights into the impact of mouse follicle stage on graft outcome in an artificial ovary environment. *MHR: Basic science of reproductive medicine* 2017c;23: 381-392.

Chiti MC, Dolmans M-M, Mortiaux L, Zhuge F, Ouni E, Shahri PAK, Van Ruymbeke E, Champagne S-D, Donnez J, Amorim CA. A novel fibrin-based artificial ovary prototype resembling human ovarian tissue in terms of architecture and rigidity. *Journal of assisted reproduction and genetics* 2018;35: 41-48.

Chiti MC, Dolmans M-M, Orellana R, Soares M, Paulini F, Donnez J, Amorim C. Influence of follicle stage on artificial ovary outcome using fibrin as a matrix. *Human Reproduction* 2015;31: 427-435.

Cho S-W, Kim I, Kim S-H, Rhie JW, Choi CY, Kim B-S. Enhancement of adipose tissue formation by implantation of adipogenic-differentiated preadipocytes. *Biochemical biophysical research communications* 2006;345: 588-594.

Christenson LK, Devoto L. Cholesterol transport and steroidogenesis by the corpus luteum. *Reproductive Biology and Endocrinology* 2003;1: 1-9.

Christenson LK, Gunewardena S, Hong X, Spitschak M, Baufeld A, Vanselow J. Research resource: preovulatory LH surge effects on

follicular theca and granulosa transcriptomes. *Molecular endocrinology* 2013;27: 1153-1171.

Chung Y-I, Ahn K-M, Jeon S-H, Lee S-Y, Lee J-H, Tae G. Enhanced bone regeneration with BMP-2 loaded functional nanoparticle–hydrogel complex. *Journal of controlled release* 2007;121: 91-99.

Clark BJ, Wells J, King SR, Stocco DM. The purification, cloning, and expression of a novel luteinizing hormone-induced mitochondrial protein in MA-10 mouse Leydig tumor cells. Characterization of the steroidogenic acute regulatory protein (StAR). *Journal of Biological Chemistry* 1994;269: 28314-28322.

Coffman LG, Pearson AT, Frisbie LG, Freeman Z, Christie E, Bowtell DD, Buckanovich RJ. Ovarian Carcinoma-Associated Mesenchymal Stem Cells Arise from Tissue-Specific Normal Stroma. *Stem Cells* 2019;37: 257-269.

Cohen-Fredarow A, Tadmor A, Raz T, Meterani N, Addadi Y, Nevo N, Solomonov I, Sagi I, Mor G, Neeman M. Ovarian dendritic cells act as a double-edged pro-ovulatory and anti-inflammatory sword. *Molecular endocrinology* 2014;28: 1039-1054.

Conti M, Chang R. Folliculogenesis, ovulation, and luteogenesis. *Endocrinology: adult and pediatric* 2015;7: 2179-2191.

Dalman A, Totonchi M, Valojerdi MR. Establishment and characterization of human theca stem cells and their differentiation into theca progenitor cells. *Journal of Cellular Biochemistry* 2018a;119: 9853-9865.

Dalman A, Totonchi M, Valojerdi MR. Human Ovarian Theca-Derived Multipotent Stem Cells Have The Potential to Differentiate into Oocyte-Like Cells In Vitro. *Cell Journal (Yakhteh)* 2018b;20: 527.

Dath C, Dethy A, Van Langendonckt A, Van Eyck A-S, Amorim C, Luyckx V, Donnez J, Dolmans M-M. Endothelial cells are essential for ovarian stromal tissue restructuring after xenotransplantation of isolated ovarian stromal cells. *Human reproduction* 2011;26: 1431-1439.

Dawson AB, McCabe M. The interstitial tissue of the ovary in infantile and juvenile rats. *Journal of Morphology* 1951;88: 543-571.

de Lambert G, Poirot C, Guérin F, Brugières L, Martelli H. Preservation of future fertility in pediatric patients with cancer. *Journal of visceral surgery* 2018;155: S41-S46.

Deanesly R. Origins and development of interstitial tissue in ovaries of rabbit and guinea-pig. *Journal of anatomy* 1972;113: 251.

Death AK, McGrath KC, Sader MA, Nakhla S, Jessup W, Handelsman DJ, Celermajer DS. Dihydrotestosterone promotes vascular cell adhesion molecule-1 expression in male human endothelial cells via a nuclear factor-κB-dependent pathway. *Endocrinology* 2004;145: 1889-1897.

Devoto L, Fuentes A, Kohen P, Céspedes P, Palomino A, Pommer R, Muñoz A, Strauss III JF. The human corpus luteum: life cycle and function in natural cycles. *Fertility and sterility* 2009;92: 1067-1079.

Dewailly D, Robin G, Peigne M, Decanter C, Pigny P, Catteau-Jonard S. Interactions between androgens, FSH, anti-Müllerian hormone and estradiol during folliculogenesis in the human normal and polycystic ovary. *Human reproduction update* 2016;22: 709-724.

Dhandayuthapani B, Yoshida Y, Maekawa T, Kumar DS. Polymeric scaffolds in tissue engineering application: a review. *International journal of polymer science* 2011;2011.

Di Marcotullio L, Ferretti E, Greco A, De Smaele E, Screpanti I, Gulino A. Multiple ubiquitin-dependent processing pathways regulate hedgehog/gli signaling: implications for cell development and tumorigenesis. *Cell cycle* 2007;6: 390-393.

Dietrich F, Lelkes PI. Fine-tuning of a three-dimensional microcarrier-based angiogenesis assay for the analysis of endothelial-mesenchymal cell co-cultures in fibrin and collagen gels. *Angiogenesis* 2006;9: 111-125.

Dolmans M-M, Luyckx V, Donnez J, Andersen CY, Greve T. Risk of transferring malignant cells with transplanted frozen-thawed ovarian tissue. *Fertility and sterility* 2013;99: 1514-1522.

Dolmans M-M, Marinescu C, Saussoy P, Van Langendonckt A, Amorim C, Donnez J. Reimplantation of cryopreserved ovarian tissue from patients with acute lymphoblastic leukemia is potentially unsafe. *Blood* 2010;116: 2908-2914.

Dolmans M-M, Martinez-Madrid B, Gadisseux E, Guiot Y, Yuan WY, Torre A, Camboni A, Van Langendonckt A, Donnez J. Short-term transplantation of isolated human ovarian follicles and cortical tissue into nude mice. *Reproduction* 2007;134: 253-262.

Dolmans M-M, Michaux N, Camboni A, Martinez-Madrid B, Van Langendonckt A, Annarita Nottola S, Donnez J. Evaluation of Liberase, a purified enzyme blend, for the isolation of human primordial and primary ovarian follicles. *Human Reproduction* 2006;21: 413-420.

Dolmans M-M, Yuan WY, Camboni A, Torre A, Van Langendonckt A, Martinez-Madrid B, Donnez J. Development of antral follicles after xenografting of isolated small human preantral follicles. *Reproductive biomedicine online* 2008;16: 705-711.

Dolmans M-M, Yuan WY, Camboni A, Torre A, Van Langendonckt A, Martinez-Madrid B, Donnez J. Development of antral follicles after xenografting of isolated small human preantral follicles. *Reproductive biomedicine online* 2008;16: 705-711.

Dong J, Albertini DF, Nishimori K, Kumar TR, Lu N, Matzuk MM. Growth differentiation factor-9 is required during early ovarian folliculogenesis. *Nature* 1996;383: 531-535.

Donnez J, Dolmans M-M. Fertility preservation in women. *Nature Reviews Endocrinology* 2013;9: 735.

Donnez J, Dolmans M-M. Fertility preservation in women. *New England Journal of Medicine* 2017;377: 1657-1665.

Donnez J, Dolmans M-M, Diaz C, Pellicer A. Ovarian cortex transplantation: time to move on from experimental studies to open clinical application. *Fertility and sterility* 2015;104: 1097-1098.

Donnez J, Dolmans MM. Fertility Preservation in Women. *N Engl J Med* 2017;377: 1657-1665.

Donnez J, Kim SS. *Principles and practice of fertility preservation*, 2011. Cambridge university press.

Dooley CA, Attia GR, Rainey WE, Moore DR, Carr BRJTJoCE, Metabolism. Bone morphogenetic protein inhibits ovarian androgen production. *The Journal of Clinical Endocrinology and Metabolism* 2000;85: 3331-3337.

Doshi SB, Agarwal A. The role of oxidative stress in menopause. *Journal of mid-life health* 2013;4: 140.

Drummond AE. The role of steroids in follicular growth. *Reproductive biology endocrinology* 2006;4: 16.

Dupont E, Labrie F, Luu-The V, Pelletier G. Immunocytochemical localization of 3 beta-hydroxysteroid dehydrogenase/delta 5-delta 4-isomerase in human ovary. *The Journal of Clinical Endocrinology Metabolism* 1992;74: 994-998.

Dyer C, Erickson GF. Norepinephrine amplifies human chorionic gonadotropin-stimulated androgen biosynthesis by ovarian theca-interstitial cells. *Endocrinology* 1985;116: 1645-1652.

Edson MA, Nagaraja AK, Matzuk MM. The Mammalian Ovary from Genesis to Revelation. *Endocrine Reviews* 2009;30: 624-712.

Edson MA, Nalam RL, Clementi C, Franco HL, DeMayo FJ, Lyons KM, Pangas SA, Matzuk MM. Granulosa cell-expressed BMPR1A and BMPR1B have unique functions in regulating fertility but act redundantly to suppress ovarian tumor development. *Molecular endocrinology* 2010;24: 1251-1266.

El-Hefnawy T, Zeleznik AJ. Synergism between FSH and activin in the regulation of proliferating cell nuclear antigen (PCNA) and cyclin D2 expression in rat granulosa cells. *Endocrinology* 2001;142: 4357-4362.

Elvin JA, Clark AT, Wang P, Wolfman NM, Matzuk MM. Paracrine actions of growth differentiation factor-9 in the mammalian ovary. *Molecular endocrinology* 1999;13: 1035-1048.

Elvin JA, Yan C, Wang P, Nishimori K, Matzuk MM. Molecular characterization of the follicle defects in the growth differentiation factor 9-deficient ovary. *Molecular endocrinology* 1999;13: 1018-1034.

Erickson G. The ovary: Basic principles and concepts. *Endocrinology and Metabolism* 1995;3rd edition: 973-1048.

Erickson GF. Primary cultures of ovarian cells in serum-free medium as models of hormone-dependent differentiation. *Molecular and cellular endocrinology* 1983;29: 21-49.

Erickson GF. The graafian follicle: a functional definition *Ovulation*. 2000. Springer, pp. 31-48.

Erickson GF, Magoffin DA, Dyer CA, Hofeditz C. The ovarian androgen producing cells: a review of structure/function relationships. *Endocrine reviews* 1985;6: 371-399.

Eyrich D, Brandl F, Appel B, Wiese H, Maier G, Wenzel M, Staudenmaier R, Goepferich A, Blunk T. Long-term stable fibrin gels for cartilage engineering. *Biomaterials* 2007;28: 55-65.

Fan H-Y, Liu Z, Johnson PF, Richards JS. CCAAT/enhancer-binding proteins (C/EBP)-α and-β are essential for ovulation, luteinization, and the expression of key target genes. *Molecular endocrinology* 2011;25: 253-268.

Fan H-Y, Liu Z, Shimada M, Sterneck E, Johnson PF, Hedrick SM, Richards JS. MAPK3/1 (ERK1/2) in ovarian granulosa cells are essential for female fertility. *Science* 2009;324: 938-941.

Farnworth PG, Stanton PG, Wang Y, Escalona R, Findlay JK, Ooi GT. Inhibins differentially antagonize activin and bone morphogenetic protein action in a mouse adrenocortical cell line. *Endocrinology* 2006;147: 3462-3471.

Feher J. *Female Reproductive Physiology*, 2012. Quantitative Human Physiology.

Feng-Juan L, Tuan RS, Cheung KMC, Leung VYL. Concise review: the surface markers and identity of human mesenchymal stem cells. *Stem cells* 2014;32: 1408-1419.

Feng C-W, Bowles J, Koopman P. Control of mammalian germ cell entry into meiosis. *Molecular and cellular endocrinology* 2014;382: 488-497.

Feng Y, Cui P, Lu X, Hsueh B, Billig FM, Yanez LZ, Tomer R, Boerboom D, Carmeliet P, Deisseroth K. CLARITY reveals dynamics of ovarian follicular architecture and vasculature in three-dimensions. *Scientific reports* 2017;7: 1-13.

Findlay JK. An update on the roles of inhibin, activin, and follistatin as local regulators of folliculogenesis. *Biology of reproduction* 1993;48: 15-23.

Fitzpatrick SL, Richards JS. Regulation of cytochrome P450 aromatase messenger ribonucleic acid and activity by steroids and gonadotropins in rat granulosa cells. *Endocrinology* 1991;129: 1452-1462.

Fleischer RT, Vollenhoven BJ, Weston GC. The effects of chemotherapy and radiotherapy on fertility in premenopausal women. *Obstetrical gynecological survey* 2011;66: 248-254.

Fournet N, Weitsman S, Zachow R, Magoffin D. Transforming growth factor-beta inhibits ovarian 17 alpha-hydroxylase activity by a direct noncompetitive mechanism. *Endocrinology* 1996;137: 166-174.

Fowler PA, Anderson RA, Saunders PT, Kinnell H, Mason JI, Evans DB, Bhattacharya S, Flannigan S, Franks S, Monteiro A. Development of steroid signaling pathways during primordial follicle formation in the human fetal ovary. *The Journal of Clinical Endocrinology and Metabolism* 2011;96: 1754-1762.

Franks S, Hardy K. Androgen action in the ovary. *Frontiers in endocrinology* 2018;9: 452.

Fraser H, Lunn S, Harrison D, Kerr JB. Luteal regression in the primate: different forms of cell death during naturaland gonadotropin-releasing hormone antagonist or prostaglandin analogue-induced luteolysis. *Biology of Reproduction* 1999;61: 1468-1479.

Fraser HM. Regulation of the ovarian follicular vasculature. *Reproductive Biology and Endocrinology* 2006;4: 18.

Freire AV, Ropelato MG, Rey RA. Development and Function of the Ovaries and Testes in the Fetus and Neonate *Maternal-Fetal and Neonatal Endocrinology*. 2020. Elsevier, pp. 625-641.

Fujiwara H, Maeda M, Imai K, Fukuoka M, Yasuda K, Horie K, Takakura K, Taii S, Mori T. Differential expression of aminopeptidase-N on human ovarian granulosa and theca cells. *The Journal of Clinical Endocrinology & Metabolism* 1992a;74: 91-95.

Fujiwara H, Maeda M, Imai K, Fukuoka M, Yasuda K, Takakura K, Mori T. Human luteal cells express dipeptidyl peptidase IV on the cell surface.

The Journal of Clinical Endocrinology & Metabolism 1992b;75: 1352-1357.

Fujiwara H, Ueda M, Hattori N, Mori T, Maeda M. A differentiation antigen of human large luteal cells in corpora lutea of the menstrual cycle and early pregnancy. *Biology of reproduction* 1996;54: 1173-1183.

Gago LA, Ginsburg KA. Premature Ovarian Failure. *Encyclopedia of Endocrine Diseases* 2004: 65-72.

Garcia-Ortiz JE, Pelosi E, Omari S, Nedorezov T, Piao Y, Karmazin J, Uda M, Cao A, Cole SW, Forabosco A. Foxl2 functions in sex determination and histogenesis throughout mouse ovary development. *BMC developmental biology* 2009;9: 36.

Gibson E, Mahdy H. Anatomy, Abdomen and Pelvis, Ovary *StatPearls [Internet]*. 2019. StatPearls Publishing.

Glister C, Kemp CF, Knight PG. Bone morphogenetic protein (BMP) ligands and receptors in bovine ovarian follicle cells: actions of BMP-4,-6 and-7 on granulosa cells and differential modulation of Smad-1 phosphorylation by follistatin. *Reproduction* 2004;127: 239-254.

Glister C, Richards SL, Knight PG. Bone morphogenetic proteins (BMP)-4,-6, and-7 potently suppress basal and luteinizing hormone-induced androgen production by bovine theca interna cells in primary culture: could ovarian hyperandrogenic dysfunction be caused by a defect in thecal BMP signaling? *Endocrinology* 2005;146: 1883-1892.

Glister C, Satchell L, Bathgate RA, Wade JD, Dai Y, Ivell R, Anand-Ivell R, Rodgers RJ, Knight PG. Functional link between bone morphogenetic proteins and insulin-like peptide 3 signaling in modulating ovarian androgen production. *Proceedings of the National Academy of Sciences* 2013;110: E1426-E1435.

Gosden R. Restitution of fertility in sterilized mice by transferring primordial ovarian follicles. *Human Reproduction* 1990;5: 117-122.

Gracia CR, Sammel MD, Freeman E, Prewitt M, Carlson C, Ray A, Vance A, Ginsberg JP. Impact of cancer therapies on ovarian reserve. *Fertility sterility* 2012;97: 134-140. e131.

Greve T, Clasen-Linde E, Andersen M, Andersen M, Rosendahl M, Ralfkiaer E, Yding Andersen C. No signs of viable malignant cells in frozen-thawed ovarian cortex intended for fertility preservation from patients with leukaemia. *Blood* 2012;22: 4311-4316.

Grummer R, Carroll D. A review of lipoprotein cholesterol metabolism: importance to ovarian function. *Journal of animal science* 1988;66: 3160-3173.

Gulino A, Di Marcotullio L, Ferretti E, De Smaele E, Screpanti I. Hedgehog signaling pathway in neural development and disease. *Psychoneuroendocrinology* 2007;32: S52-S56.

Guraya SS, Greenwald GS. A comparative histochemical study of interstitial tissue and follicular atresia in the mammalian ovary. *The Anatomical Record* 1964;149: 411-433.

Habibi I, Cheong R, Lipniacki T, Levchenko A, Emamian ES, Abdi A. Computation and measurement of cell decision making errors using single cell data. *PLoS computational biology* 2017;13: e1005436.

Hammond JM, Baranao JLS, Skaleris D, Knight AB, Romanus JA, Rechler MM. Production of insulin-like growth factors by ovarian granulosa cells. *Endocrinology* 1985;117: 2553-2555.

Hassanpour A, Talaei-Khozani T, Kargar-Abarghouei E, Razban V, Vojdani Z. Decellularized human ovarian scaffold based on a sodium lauryl ester sulfate (SLES)-treated protocol, as a natural three-dimensional scaffold for construction of bioengineered ovaries. *Stem cell research therapy* 2018;9: 1-13.

Hatzirodos N, Glister C, Hummitzsch K, Irving-Rodgers HF, Knight PG, Rodgers RJ. Transcriptomal profiling of bovine ovarian granulosa and theca interna cells in primary culture in comparison with their in vivo counterparts. *PLOS ONE* 2017;12: e0173391.

Havelock JC, Rainey WE, Bradshaw KD, Carr BR. The post-menopausal ovary displays a unique pattern of steroidogenic enzyme expression. *Human Reproduction* 2005;21: 309-317.

Hernandez E, Roberts Jr C, Leroith D, Adashi E. Rat ovarian insulin-like growth factor I (IGF-I) gene expression is granulosa cell-selective: 5′-untranslated mRNA variant representation and hormonal regulation. *Endocrinology* 1989;125: 572-574.

Hernandez ER, Hurwitz A, Payne DW, Dharmarajan A, Purchio AF, Adashi EY. Transforming growth factor-β 1 inhibits ovarian androgen production: gene expression, cellular localization, mechanisms (s), and site (s) of action. *Endocrinology* 1990;127: 2804-2811.

Hernandez F, Peluffo MC, Stouffer RL, Irusta G, Tesone M. Role of the DLL4-NOTCH system in PGF2alpha-induced luteolysis in the pregnant rat. *Biology of reproduction* 2011;84: 859-865.

Hild-Petito S, West NB, Brenner RM, Stouffer RL. Localization of androgen receptor in the follicle and corpus luteum of the primate ovary during the menstrual cycle. *Biology of reproduction* 1991;44: 561-568.

Hillier S. Gonadotropic control of ovarian follicular growth and development. *Molecular and cellular endocrinology* 2001;179: 39-46.

Hillier S, Yong E, Illingworth P, Baird D, Schwall R, Mason A. Effect of recombinant activin on androgen synthesis in cultured human thecal cells. *The Journal of Clinical Endocrinology and Metabolism* 1991;72: 1206-1211.

Hillier S, Yong E, Illingworth P, Baird D, Schwall R, Mason A. Effect of recombinant inhibin on androgen synthesis in cultured human thecal cells. *Molecular and Cellular Endocrinology* 1991;75: R1-R6.

Hirshfield AN. Development of follicles in the mammalian ovary *International review of cytology*. 1991. Elsevier, pp. 43-101.

Hirshfield AN. Overview of ovarian follicular development: considerations for the toxicologist. *Environmental molecular mutagenesis* 1997;29: 10-15.

Hiura M, Nogawa T, Fujiwara A. Electron microscopy of cytodifferentiation and its subcellular steroidogenic sites in the theca cell of the human ovary. *Histochemistry* 1981;71: 269-277.

Ho W, Tawil B, Dunn JC, Wu BM. The behavior of human mesenchymal stem cells in 3D fibrin clots: dependence on fibrinogen concentration and clot structure. *Tissue Engineering* 2006;12: 1587-1595.

Hojo M, Inokuchi S, Kidokoro M, Fukuyama N, Tanaka E, Tsuji C, Miyasaka M, Tanino R, Nakazawa H. Induction of vascular endothelial growth factor by fibrin as a dermal substrate for cultured skin substitute. *Plastic reconstructive surgery* 2003;111: 1638-1645.

Holtz AM, Peterson KA, Nishi Y, Morin S, Song JY, Charron F, McMahon AP, Allen BL. Essential role for ligand-dependent feedback antagonism of vertebrate hedgehog signaling by PTCH1, PTCH2 and HHIP1 during neural patterning. *Development* 2013;140: 3423-3434.

Honda A, Hirose M, Hara K, Matoba S, Inoue K, Miki H, Hiura H, Kanatsu-Shinohara M, Kanai Y, Kono T *et al.* Isolation, characterization, and in vitro and in vivo differentiation of putative thecal stem cells. *PNAS* 2007;104: 12389-12394.

Hsueh AJ, Kawamura K, Cheng Y, Fauser BC. Intraovarian control of early folliculogenesis. *Endocrine reviews* 2015;36: 1-24.

Huang CT, Weitsman SR, Dykes BN, Magoffin DA. Stem cell factor and insulin-like growth factor-I stimulate luteinizing hormone-independent differentiation of rat ovarian theca cells. *Biology of reproduction* 2001;64: 451-456.

Hummitzsch K, Hatzirodos N, Irving-Rodgers HF, Hartanti MD, Perry VE, Anderson RA, Rodgers RJ. Morphometric analyses and gene expression related to germ cells, gonadal ridge epithelial-like cells and granulosa cells during development of the bovine fetal ovary. *Plos one* 2019;14: e0214130.

Hyman JH, Tulandi T. Fertility preservation options after gonadotoxic chemotherapy. *Clinical Medicine Insights: Reproductive Health* 2013;7: CMRH. S10848.

Ingham P, Taylor A, Nakano Y. Role of the Drosophila patched gene in positional signalling. *Nature* 1991;353: 184-187.

Ingham PW, McMahon AP. Hedgehog signaling in animal development: paradigms and principles. *Genes & development* 2001;15: 3059-3087.

Irving-Rodgers HF, Hummitzsch K, Murdiyarso LS, Bonner WM, Sado Y, Ninomiya Y, Couchman JR, Sorokin LM, Rodgers RJ. Dynamics of extracellular matrix in ovarian follicles and corpora lutea of mice. *Cell and tissue research* 2010;339: 613-624.

Irving-Rodgers HF, Morris S, Collett RA, Peura TT, Davy M, Thompson JG, Mason HD, Rodgers RJ. Phenotypes of the ovarian follicular basal lamina

predict developmental competence of oocytes. *Human Reproduction* 2009;24: 936-944.

Itami S, Yasuda K, Yoshida Y, Matsui C, Hashiura S, Sakai A, Tamotsu S, Endocrinology. Co-culturing of follicles with interstitial cells in collagen gel reproduce follicular development accompanied with theca cell layer formation. *Reproductive Biology and Endocrinology* 2011;9: 159.

Joyce IM, Clark AT, Pendola FL, Eppig JJ. Comparison of recombinant growth differentiation factor-9 and oocyte regulation of KIT ligand messenger ribonucleic acid expression in mouse ovarian follicles. *Biology of reproduction* 2000;63: 1669-1675.

Juengel JL, Bibby AH, Reader KL, Lun S, Quirke LD, Haydon LJ, McNatty KP. The role of transforming growth factor-beta (TGF-beta) during ovarian follicular development in sheep. *Reproductive Biology and Endocrinology* 2004;2: 78.

K.Hughes C, L.Pate J. Luteolysis and the Corpus Luteum of Pregnancy *The Ovary*. 2019, pp. 269-292.

Kayani AR, Glister C, Knight PG. Evidence for an inhibitory role of bone morphogenetic protein (s) in the follicular-luteal transition in cattle. *Reproduction* 2009;137: 67.

Keros V, Xella S, Hultenby K, Pettersson K, Sheikhi M, Volpe A, Hreinsson J, Hovatta O. Vitrification versus controlled-rate freezing in

cryopreservation of human ovarian tissue. *Human reproduction* 2009;24: 1670-1683.

Khan I, Belanger A, Ida Chen Y-D, Gibori G. Influence of high-density lipoprotein on estradiol stimulation of luteal steroidogenesis. *Biology of reproduction* 1985;32: 96-104.

Kim J, Perez A, Nelson O, Zhou H, Shikanov A. Engineering artificial ovarian tissue using multi-arm poly (ethylene glycol) hydrogel *TISSUE ENGINEERING PART A*. 2015. MARY ANN LIEBERT, INC 140 HUGUENOT STREET, 3RD FL, NEW ROCHELLE, NY 10801 USA, pp. S29-S29.

Kim J, Perez AS, Claflin J, David A, Zhou H, Shikanov A. Synthetic hydrogel supports the function and regeneration of artificial ovarian tissue in mice. *NPJ Regenerative medicine* 2016;1: 1-8.

Kimmel AR, Brasaemle DL, McAndrews-Hill M, Sztalryd C, Londos C. Adoption of PERILIPIN as a unifying nomenclature for the mammalian PAT-family of intracellular lipid storage droplet proteins. *Journal of lipid research* 2010;51: 468-471.

Kingsbury B. Atresia and the interstitial cells of the ovary. *American Journal of Anatomy* 1939;65: 309-331.

Kipp JL, Kilen SM, Woodruff TK, Mayo KE. Activin regulates estrogen receptor gene expression in the mouse ovary. *Journal of Biological Chemistry* 2007;282: 36755-36765.

Knight PG, Glister C. Potential local regulatory functions of inhibins, activins and follistatin in the ovary. *Reproduction* 2001;121: 503-512.

Knight PG, Glister C. TGF-β superfamily members and ovarian follicle development. *Reproduction* 2006;132: 191-206.

Knight PG, Satchell L, Glister C. Intra-ovarian roles of activins and inhibins. *Molecular and cellular endocrinology* 2012;359: 53-65.

Ko C, Meidan R, Bridges PJ. Why two endothelins and two receptors for ovulation and luteal regulation? *Life sciences* 2012;91: 501-506.

Kovanci E, Rohozinski J, Simpson JL, Heard MJ, Bishop CE, Carson SA. Growth differentiating factor-9 mutations may be associated with premature ovarian failure. *Fertility and Sterility* 2007;87: 143-146.

Kreeger PK, Fernandes NN, Woodruff TK, Shea LD. Regulation of mouse follicle development by follicle-stimulating hormone in a three-dimensional in vitro culture system is dependent on follicle stage and dose. *Biology of reproduction* 2005;73: 942-950.

Kristensen SG, Rasmussen A, Byskov AG, Andersen CY. Isolation of pre-antral follicles from human ovarian medulla tissue. *Human Reproduction* 2011;26: 157-166.

Kuyama H, Uemura S, Yoshida A, Yamamoto M. Close relationship between the short round ligament and the ovarian prolapsed inguinal hernia in female infants. *Pediatric surgery international* 2019;35: 625-629.

Kwintkiewicz J, Giudice LC. The interplay of insulin-like growth factors, gonadotropins, and endocrine disruptors in ovarian follicular development and function *Seminars in reproductive medicine*. 2009. © Thieme Medical Publishers, pp. 043-051.

Laissue P, Christin-Maitre S, Touraine P, Kuttenn F, Ritvos O, Aittomaki K, Bourcigaux N, Jacquesson L, Bouchard P, Frydman R. Mutations and sequence variants in GDF9 and BMP15 in patients with premature ovarian failure. *European Journal of Endocrinology* 2006;154: 739-744.

Lambert dG, Poirot C, Guérin F, Brugières L, Martelli H. Preservation of future fertility in pediatric patients with cancer. *Journal of visceral surgery* 2018;155: S41-S46.

Lan Z-J, Krause M, Redding S, Li X, Wu G, Zhou H, Bohler H, Ko C, Cooney A, Zhou JJM *et al.* Selective deletion of Pten in theca-interstitial cells leads to androgen excess and ovarian dysfunction in mice. *Molecular and cellular endocrinology* 2017;444: 26-37.

Laronda MM, Jakus AE, Whelan KA, Wertheim JA, Shah RN, Woodruff TK. Initiation of puberty in mice following decellularized ovary transplant. *Biomaterials* 2015;50: 20-29.

LaVoie HA. Luteal Steroidogenesis. *In: Meidan R (eds) The Life Cycle of the Corpus Luteum*. 2017. Springer, Cham, pp. 37-55.

LaVoie HA, King SR. Transcriptional regulation of steroidogenic genes: STARD1, CYP11A1 and HSD3B. *Experimental biology and medicine* 2009;234: 880-907.

Lavranos TC, Rodgers HF, Bertoncello I, Rodgers RJ. Anchorage-independent culture of bovine granulosa cells: the effects of basic fibroblast growth factor and dibutyryl cAMP on cell division and differentiation. *Experimental cell research* 1994;211: 245-251.

Lawrence Jr IE, Burden HW. The autonomic innervation of the interstitial gland of the rat ovary during pregnancy. *American Journal of Anatomy* 1976;147: 81-93.

Lawrence Jr IE, Burden HW. The origin of the extrinsic adrenergic innervation to the rat ovary. *The Anatomical Record* 1980;196: 51-59.

Le Bouffant R, Guerquin M, Duquenne C, Frydman N, Coffigny H, Rouiller-Fabre V, Frydman R, Habert R, Livera G. Meiosis initiation in the human ovary requires intrinsic retinoic acid synthesis. *Human reproduction* 2010;25: 2579-2590.

Lebbe M, Woodruff TK. Involvement of androgens in ovarian health and disease. *Molecular human reproduction* 2013;19: 828-837.

Lee S, Kang D-W, Hudgins-Spivey S, Krust A, Lee E-Y, Koo Y, Cheon Y, Gye MC, Chambon P, Ko C. Theca-specific estrogen receptor-α knockout mice lose fertility prematurely. *Endocrinology* 2009;150: 3855-3862.

Lee WS, Yoon SJ, Yoon TK, Cha KY, Lee SH, Shimasaki S, Lee S, Lee KA. Effects of bone morphogenetic protein-7 (BMP-7) on primordial follicular growth in the mouse ovary. *Molecular Reproduction Development: Incorporating Gamete Research* 2004;69: 159-163.

Lenie S, Smitz J. Functional AR signaling is evident in an in vitro mouse follicle culture bioassay that encompasses most stages of folliculogenesis. *Biology of reproduction* 2009;80: 685-695.

Li R, Phillips DM, Mather JP. Activin promotes ovarian follicle development in vitro. *Endocrinology* 1995;136: 849-856.

Lierman S, Tilleman K, Cornelissen M, De Vos WH, Weyers S, T'Sjoen G, Cuvelier CA, De Sutter P. Follicles of various maturation stages react differently to enzymatic isolation: a comparison of different isolation protocols. *Reproductive biomedicine online* 2015;30: 181-190.

Lin H-K, Madihally SV, Palmer B, Frimberger D, Fung K-M, Kropp BP. Biomatrices for bladder reconstruction. *Advanced drug delivery reviews* 2015;82: 47-63.

Lin H-K, Madihally SV, Palmer B, Frimberger D, Fung K-M, Kropp BP. Biomatrices for bladder reconstruction. *Advanced drug delivery reviews* 2015;82: 47-63.

Liu C-F, Liu C, Yao HH-C. Building pathways for ovary organogenesis in the mouse embryo *Current topics in developmental biology*. 2010. Elsevier, pp. 263-290.

Liu C, Peng J, Matzuk MM, Yao HH-C. Lineage specification of ovarian theca cells requires multicellular interactions via oocyte and granulosa cells. *Nature communications* 2015;6: 1-11.

Liu C, Peng J, Matzuk MM, Yao HH. Lineage Specification of Ovarian Theca Cells Requires Multi-Cellular Interactions via Oocyte and Granulosa Cells. *Nature communications* 2015;6: 6934.

Liu C, Peng J, Matzuk MM, Yao HHC. Lineage specification of ovarian theca cells requires multicellular interactions via oocyte and granulosa cells. *Nature Communications* 2015;6: 6934.

Liu JY, Swartz DD, Peng HF, Gugino SF, Russell JA, Andreadis ST. Functional tissue-engineered blood vessels from bone marrow progenitor cells. *Cardiovascular research* 2007;75: 618-628.

Lobo MV, Huerta L, Arenas MI, Busto R, Lasunción MA, Martín-Hidalgo A. Hormone-sensitive lipase expression and IHC localization in the rat ovary, oviduct, and uterus. *Journal of Histochemistry & Cytochemistry* 2009;57: 51-60.

Londos C, Brasaemle D, Gruia-Gray J, Servetnick D, Schultz C, Levin D, Kimmel A. Perilipin: unique proteins associated with intracellular neutral lipid droplets in adipocytes and steroidogenic cells. 1995. Portland Press Ltd.

Lum L, Beachy PA. The Hedgehog response network: sensors, switches, and routers. *Science* 2004;304: 1755-1759.

Luyckx V, Dolmans M-M, Vanacker J, Legat C, Moya CF, Donnez J, Amorim CA. A new step toward the artificial ovary: survival and proliferation of isolated murine follicles after autologous transplantation in a fibrin scaffold. *Fertility and sterility* 2014;101: 1149-1156.

Luyckx V, Dolmans M-M, Vanacker J, Legat C, Moya CF, Donnez J, Amorim CAJF, sterility. A new step toward the artificial ovary: survival and proliferation of isolated murine follicles after autologous transplantation in a fibrin scaffold. *Fertility sterility* 2014;101: 1149-1156.

Luyckx V, Dolmans M-M, Vanacker J, Scalercio SR, Donnez J, Amorim CA. First step in developing a 3D biodegradable fibrin scaffold for an artificial ovary. *Journal of ovarian research* 2013;6: 83.

Ma Y, Andrisse S, Chen Y, Childress S, Xue P, Wang Z, Jones D, Ko C, Divall S, Wu S. Androgen receptor in the ovary theca cells plays a critical role in androgen-induced reproductive dysfunction. *Endocrinology* 2017;158: 98-108.

Macklon N, Fauser B. Follicle development during the normal menstrual cycle. *Maturitas* 1998;30: 181-188.

Macklon NS, Fauser BC. Follicle-stimulating hormone and advanced follicle development in the human. *Archives of medical research* 2001;32: 595-600.

Magoffin D, Erickson G. Primary culture of differentiating ovarian androgen-producing cells in defined medium. *Journal of Biological Chemistry* 1982;257: 4507-4513.

Magoffin DA, Weitsman SR. Differentiation of ovarian theca-interstitial cells in vitro: regulation of 17 alpha-hydroxylase messenger ribonucleic acid expression by luteinizing hormone and insulin-like growth factor-I. *Endocrinology* 1993a;132: 1945-1951.

Magoffin DA, Weitsman SR. Effect of insulin-like growth factor-I on cholesterol side-chain cleavage cytochrome P450 messenger ribonucleic acid expression in ovarian theca-interstitial cells stimulated to differentiate in vitro. *Molecular and cellular endocrinology* 1993b;96: 45-51.

Magoffin DA, Weitsman SR. Insulin-like growth factor-I stimulates the expression of 3β-hydroxysteroid dehydrogenase messenger ribonucleic acid in ovarian theca-interstitial cells. *Biology of Reproduction* 1993c;48: 1166-1173.

Magoffin DA, Weitsman SRJBor. Insulin-like growth factor-I regulation of luteinizing hormone (LH) receptor messenger ribonucleic acid expression and LH-stimulated signal transduction in rat ovarian theca-interstitial cells. 1994;51: 766-775.

Maleki M, Ghanbarvand F, Behvarz MR, Ejtemaei M, Ghadirkhomi E. Comparison of mesenchymal stem cell markers in multiple human adult stem cells. *International journal of stem cells* 2014;7: 118.

Man L, Lustgarten-Guahmich N, Kallinos E, Redhead-Laconte Z, Liu S, Schattman B, Redmond D, Hancock K, Zaninovic N, Schattman G. Comparison of Human Antral Follicles of Xenograft versus Ovarian

Origin Reveals Disparate Molecular Signatures. *Cell reports* 2020;32: 108027.

Manova K, Huang EJ, Angeles M, De Leon V, Sanchez S, Pronovost SM, Besmer P, Bachvarova RF. The expression pattern of the c-kit ligand in gonads of mice supports a role for the c-kit receptor in oocyte growth and in proliferation of spermatogonia. *Developmental biology* 1993;157: 85-99.

Manova K, Nocka K, Besmer P, Bachvarova RF. Gonadal expression of c-kit encoded at the W locus of the mouse. *Development* 1990;110: 1057-1069.

McNatty KP, Galloway SM, Wilson T, Smith P, Hudson NL, O'Connell A, Bibby AH, Heath DA, Davis GH, Hanrahan JP. Physiological effects of major genes affecting ovulation rate in sheep *Genetics Selection Evolution*. 2005. BioMed Central, pp. S25.

McNatty KP, Makris A, Degrazia C, Rapin O, Ryan KJ. The production of progesterone, androgens, and estrogens by granulosa cells, thecal tissue, and stromal tissue from human ovaries in vitro. *The Journal of Clinical Endocrinology & Metabolism* 1979;49: 687-699.

McNeilly A, Crawford J, Taragnat C, Nicol L, McNeilly J. The differential secretion of FSH and LH: regulation through genes, feedback and packaging. *Reproduction Supplement* 2003;61: 463-476.

McNeilly AS. Lactational control of reproduction. *Reproduction, Fertility and Development* 2001;13: 583-590.

Meirow D, Biederman H, Anderson RA, Wallace WHB. Toxicity of chemotherapy and radiation on female reproduction. *Clinical obstetrics gynecology* 2010;53: 727-739.

Meirow D, Dor J, Kaufman B, Shrim A, Rabinovici J, Schiff E, Raanani H, Levron J, Fridman E. Cortical fibrosis and blood-vessels damage in human ovaries exposed to chemotherapy. Potential mechanisms of ovarian injury. *Human reproduction* 2007;22: 1626-1633.

Meirow D, Hardan I, Dor J, Fridman E, Elizur S, Ra'anani H, Slyusarevsky E, Amariglio N, Schiff E, Rechavi G. Searching for evidence of disease and malignant cell contamination in ovarian tissue stored from hematologic cancer patients. *Human Reproduction* 2008;23: 1007-1013.

Meirow D, Nugent D. The effects of radiotherapy and chemotherapy on female reproduction. *Human reproduction update* 2001;7: 535-543.

Mesa JM, Zaporojan V, Weinand C, Johnson TS, Bonassar L, Randolph MA, Yaremchuk MJ, Butler PE. Tissue engineering cartilage with aged articular chondrocytes in vivo. *Plastic reconstructive surgery* 2006;118: 41-49.

Miller KD, Siegel RL, Lin CC, Mariotto AB, Kramer JL, Rowland JH, Stein KD, Alteri R, Jemal A. Cancer treatment and survivorship statistics, 2016. *CA: a cancer journal for clinicians* 2016;66: 271-289.

Mol A, van Lieshout MI, Dam-de Veen CG, Neuenschwander S, Hoerstrup SP, Baaijens FP, Bouten CV. Fibrin as a cell carrier in cardiovascular tissue engineering applications. *Biomaterials* 2005;26: 3113-3121.

Moraes D. What the relationship between CD90 e CD44 in Mesenchymal Stem Cells? *Cytotherapy* 2018;20: S47.

Mori H, Matsumoto K. Development of the secondary interstitial gland in the rabbit ovary. *Journal of Anatomy* 1973;116: 417.

Motro B, Bernstein A. Dynamic changes in ovarian c-kit and Steel expression during the estrous reproductive cycle. *Developmental Dynamics* 1993;197: 69-79.

Motro B, van der Kooy D, Rossant J, Reith A, Bernstein A. Contiguous patterns of c-kit and steel expression: analysis of mutations at the W and Sl loci. *Development* 1991;113: 1207-1221.

Mouloungui E, Zver T, Roux C, Amiot C. A protocol to isolate and qualify purified human preantral follicles in cases of acute leukemia, for future clinical applications. *Journal of ovarian research* 2018;11: 4.

Murphy MJ, Halow NG, Royer PA, Hennebold JD. Leukemia inhibitory factor is necessary for ovulation in female rhesus macaques. *Endocrinology* 2016;157: 4378-4387.

Murray A, Gosden R, Allison V, Spears N. Effect of androgens on the development of mouse follicles growing in vitro. *Reproduction* 1998;113: 27-33.

Murta D, Batista M, Silva E, Trindade A, Mateus L, Duarte A, Lopes-da-Costa L. Differential expression of Notch component and effector genes during ovarian follicle and corpus luteum development during the oestrous cycle. *Reproduction, Fertility and Development* 2015;27: 1038-1048.

Nair LS, Laurencin CT. Biodegradable polymers as biomaterials. *Progress in polymer science* 2007;32: 762-798.

Nakamura M, Minegishi T, Hasegawa Y, Nakamura K, Igarashi S, Ito I, Shinozaki H, Miyamoto K, Eto Y, Ibuki Y. Effect of an activin A on follicle-stimulating hormone (FSH) receptor messenger ribonucleic acid levels and FSH receptor expressions in cultured rat granulosa cells. *Endocrinology* 1993;133: 538-544.

Neilson D, Jones GS, Woodruff JD, GOLDBERG B. The innervation of the ovary. *Obstetrical & Gynecological Survey* 1970;25: 889-904.

Nicol L, Bishop SC, Pong-Wong R, Bendixen C, Holm L-E, Rhind SM, McNeilly AS. Homozygosity for a single base-pair mutation in the oocyte-specific GDF9 gene results in sterility in Thoka sheep. *Reproduction* 2009;138: 921.

Nicosia SV. Ovarian Changes During the Climacteric *Mastroianni L, Paulsen CA (eds) Aging, Reproduction, and the Climacteric*. 1986. Springer, Boston, MA, pp. 179-199.

Nieponice A, Maul TM, Cumer JM, Soletti L, Vorp DA. Mechanical stimulation induces morphological and phenotypic changes in bone

marrow-derived progenitor cells within a three-dimensional fibrin matrix. *Journal of biomedical materials research Part A* 2007;81: 523-530.

Nilsson E, Skinner MK. Cellular interactions that control primordial follicle development and folliculogenesis. *Journal of the Society for Gynecologic Investigation* 2001;8: S17-S20.

Nilsson E, Skinner MK. Cellular interactions that control primordial follicle development and folliculogenesis. *Journal of the Society for Gynecologic Investigation* 2001;8: S17-S20.

Nilsson EE, Skinner MK. Growth and differentiation factor-9 stimulates progression of early primary but not primordial rat ovarian follicle development. *Biology of reproduction* 2002;67: 1018-1024.

Nilsson EE, Skinner MK. Bone morphogenetic protein-4 acts as an ovarian follicle survival factor and promotes primordial follicle development. *Biology of reproduction* 2003;69: 1265-1272.

Nilsson EE, Skinner MK. Kit ligand and basic fibroblast growth factor interactions in the induction of ovarian primordial to primary follicle transition. *Molecular and cellular endocrinology* 2004;214: 19-25.

Niswender GD, Juengel JL, Silva PJ, Rollyson MK, McIntush EW. Mechanisms controlling the function and life span of the corpus luteum. *Physiological reviews* 2000;80: 1-29.

Nolan DJ, Ginsberg M, Israely E, Palikuqi B, Poulos MG, James D, Ding B-S, Schachterle W, Liu Y, Rosenwaks Z. Molecular signatures of tissue-specific microvascular endothelial cell heterogeneity in organ maintenance and regeneration. *Developmental cell* 2013;26: 204-219.

Ogawa T, Yogo K, Ishida N, Takeya T. Synergistic effects of activin and FSH on hyperphosphorylation of Rb and G1/S transition in rat primary granulosa cells. *Molecular and cellular endocrinology* 2003;210: 31-38.

Ohara A, Mori T, Tall S, Ban C, Narimoto K. Functional differentiation in steroidogenesis of two types of luteal cells isolated from mature human corpora lutea of menstrual cycle. *The Journal of Clinical Endocrinology & Metabolism* 1987;65: 1192-1200.

Oliver JE, Aitman TJ, Powell JF, Wilson CA, Clayton RN. Insulin-like growth factor I gene expression in the rat ovary is confined to the granulosa cells of developing follicles. *Endocrinology* 1989;124: 2671-2679.

Olofsson S-O, Boström P, Andersson L, Rutberg M, Perman J, Borén J. Lipid droplets as dynamic organelles connecting storage and efflux of lipids. *Biochimica et Biophysica Acta (BBA)-Molecular and Cell Biology of Lipids* 2009;1791: 448-458.

Orisaka M, Tajima K, Mizutani T, Miyamoto K, Tsang BK, Fukuda S, Yoshida Y, Kotsuji F. Granulosa cells promote differentiation of cortical stromal cells into theca cells in the bovine ovary. *Biology of reproduction* 2006;75: 734-740.

Otsuka F, Moore RK, Shimasaki S. Biological function and cellular mechanism of bone morphogenetic protein-6 in the ovary. *Journal of Biological Chemistry* 2001;276: 32889-32895.

Ouni E, Vertommen D, Amorim CA. The Human Ovary and Future of Fertility Assessment in the Post-Genome Era. *International journal of molecular sciences* 2019;20: 4209.

Ouni E, Vertommen D, Chiti MC, Dolmans M-M, Amorim CA. A draft map of the human ovarian proteome for tissue engineering and clinical applications. *Molecular & Cellular Proteomics* 2019;18: S159-S173.

Padmanabhan V, McNeilly AS. Is there an FSH-releasing factor? *Reproduction* 2001;121: 21-30.

Pangas SA, Saudye H, Shea LD, Woodruff TK. Novel approach for the three-dimensional culture of granulosa cell–oocyte complexes. *Tissue engineering* 2003;9: 1013-1021.

Parenteau-Bareil R, Gauvin R, Berthod F. Collagen-based biomaterials for tissue engineering applications. *Materials* 2010;3: 1863-1887.

Park Y, Maizels ET, Feiger ZJ, Alam H, Peters CA, Woodruff TK, Unterman TG, Lee EJ, Jameson JL, Hunzicker-Dunn M. Induction of cyclin D2 in rat granulosa cells requires FSH-dependent relief from FOXO1 repression coupled with positive signals from Smad. *Journal of Biological Chemistry* 2005;280: 9135-9148.

Parrott JA, Skinner MK. Direct actions of kit-ligand on theca cell growth and differentiation during follicle development. *Endocrinology* 1997;138: 3819-3827.

Parrott JA, Skinner MK. Thecal cell-granulosa cell interactions involve a positive feedback loop among keratinocyte growth factor, hepatocyte growth factor, and Kit ligand during ovarian follicular development. *Endocrinology* 1998;139: 2240-2245.

Parrott JA, Skinner MK. Kit ligand actions on ovarian stromal cells: effects on theca cell recruitment and steroid production. *Molecular reproduction and development* 2000;55: 55-64.

Paulini F, Vilela JM, Chiti MC, Donnez J, Jadoul P, Dolmans M-M, Amorim CA. Survival and growth of human preantral follicles after cryopreservation of ovarian tissue, follicle isolation and short-term xenografting. *Reproductive biomedicine online* 2016;33: 425-432.

Picton HM, Gosden RG. In vitro growth of human primordial follicles from frozen-banked ovarian tissue. *Molecular and cellular endocrinology* 2000;166: 27-35.

Popescu G, Park Y, Lue N, Best-Popescu C, Deflores L, Dasari RR, Feld MS, Badizadegan K. Optical imaging of cell mass and growth dynamics. *American Journal of Physiology-Cell Physiology* 2008;295: C538-C544.

Poretsky L, Grigorescu F, Seibel M, Moses A, Flier J. Distribution and characterization of insulin and insulin-like growth factor I receptors in

normal human ovary. *The Journal of Clinical Endocrinology Metabolism* 1985;61: 728-734.

Pors S, Ramlose M, Nikiforov D, Lundsgaard K, Cheng J, Andersen CY, Kristensen S. Initial steps in reconstruction of the human ovary: survival of pre-antral stage follicles in a decellularized human ovarian scaffold. *Human Reproduction* 2019;34: 1523-1535.

Prodoehl MJ, Irving-Rodgers HF, Bonner WM, Sullivan TM, Micke GC, Gibson MA, Perry VE, Rodgers RJ. Fibrillins and latent TGFβ binding proteins in bovine ovaries of offspring following high or low protein diets during pregnancy of dams. *Molecular and cellular endocrinology* 2009;307: 133-141.

Qiu M, Quan F, Han C, Wu B, Liu J, Yang Z, Su F, Zhang Y. Effects of granulosa cells on steroidogenesis, proliferation and apoptosis of stromal cells and theca cells derived from the goat ovary. *The Journal of steroid biochemistry and molecular biology* 2013;138: 325-333.

Quattropani SL. Morphogenesis of the ovarian interstitial tissue in the neonatal mouse. *The Anatomical record* 1973;177: 569-583.

Rajabzadeh AR, Eimani H, Koochesfahani HM, Shahvardi A-H, Fathi R. Morphological study of isolated ovarian preantral follicles using fibrin gel plus platelet lysate after subcutaneous transplantation. *Cell Journal (Yakhteh)* 2015;17: 145.

Ramshaw JA, Peng YY, Glattauer V, Werkmeister JA. Collagens as biomaterials. *Journal of Materials Science: Materials in Medicine* 2009;20: 3.

Ren Y, Cowan RG, Harman RM, Quirk SM. Dominant activation of the hedgehog signaling pathway in the ovary alters theca development and prevents ovulation. *Molecular Endocrinology* 2009;23: 711-723.

Ren Y, Cowan RG, Migone FF, Quirk SM. Overactivation of hedgehog signaling alters development of the ovarian vasculature in mice. *Biology of reproduction* 2012;86: 174, 171-115.

Rennels EG. Influence of hormones on the histochemistry of ovarian interstitial tissue in the immature rat. *American Journal of Anatomy* 1951;88: 63-107.

Reynaud K, Cortvrindt R, Smitz J, Driancourt MA. Effects of kit ligand and anti-kit antibody on growth of cultured mouse preantral follicles. *Molecular Reproduction Development: Incorporating Gamete Research* 2000;56: 483-494.

Rice BF, Savard K. Steroid hormone formation in the human ovary: IV. Ovarian stromal compartment: formation of radioactive steroids from Acetate-1-14C and action of gonadotropins. *The Journal of Clinical Endocrinology & Metabolism* 1966;26: 593-609.

Richards JS. Hormonal control of gene expression in the ovary. *Endocrine reviews* 1994;15: 725-751.

Richards JS. Perspective: the ovarian follicle—a perspective in 2001. *Endocrinology* 2001;142: 2184-2193.

Richards JS, Liu Z, Shimada M. *Knobil and Neill's Physiology of Reproduction*. 4 edn, 2015.

Richards JS, Ren YA, Candelaria N, Adams JE, Rajkovic A. Ovarian follicular theca cell recruitment, differentiation, and impact on fertility: 2017 update. *Endocrine reviews* 2017;39: 1-20.

Rico C, Dodelet-Devillers A, Paquet M, Tsoi M, Lapointe E, Carmeliet P, Boerboom D. HIF1 activity in granulosa cells is required for FSH-regulated Vegfa expression and follicle survival in mice. *Biology of Reproduction* 2014;90: 135, 131-137.

Rivkees SA, Crawford JD. The relationship of gonadal activity and chemotherapy-induced gonadal damage. *Jama* 1988;259: 2123-2125.

Robker RL, Russell DL. A Primate-Specific Mediator of Ovulation? 2016. Oxford University Press, pp. 4209-4211.

Rojas J, Chávez-Castillo M, Olivar LC, Calvo M, Mejías J, Rojas M, Morillo J, Bermúdez V. Physiologic course of female reproductive function: a molecular look into the prologue of life. *Journal of pregnancy* 2015;2015.

Rosendahl M, Andersen MT, Ralfkiær E, Kjeldsen L, Andersen MK, Andersen CYJF, sterility. Evidence of residual disease in cryopreserved ovarian cortex from female patients with leukemia. *Fertility sterility* 2010;94: 2186-2190.

Rowe SL, Lee S, Stegemann JP. Influence of thrombin concentration on the mechanical and morphological properties of cell-seeded fibrin hydrogels. *Acta biomaterialia* 2007;3: 59-67.

Russell MC, Cowan RG, Harman RM, Walker AL, Quirk SM. The hedgehog signaling pathway in the mouse ovary. *Biology of reproduction* 2007;77: 226-236.

Russell MC, Cowan RG, Harman RM, Walker AL, Quirk SM. The Hedgehog Signaling Pathway in the Mouse Ovary1. *Biology of Reproduction* 2007;77: 226-236.

Sadler TW. *Langman's Medical Embryology*. 8 edn, 2000. Lippincott Williams & Wilkins, Philadelphia, PA.

Sargent KM, Lu N, Clopton DT, Pohlmeier WE, Brauer VM, Ferrara N, Silversides DW, Cupp AS. Loss of vascular endothelial growth factor A (VEGFA) isoforms in granulosa cells using pDmrt-1-Cre or Amhr2-Cre reduces fertility by arresting follicular development and by reducing litter size in female mice. *PloS one* 2015;10.

Schams D, Steinberg V, Steffl M, Meyer HH, Berisha B. Expression and possible role of fibroblast growth factor family members in porcine antral follicles during final maturation. *Reproduction* 2009;138: 141-149.

Schmidt VM, Isachenko V, Rappl G, Rahimi G, Hanstein B, Morgenstern B, Mallmann P, Isachenko E. Comparison of the enzymatic efficiency of Liberase TM and tumor dissociation enzyme: effect on the viability of

cells digested from fresh and cryopreserved human ovarian cortex. *Reproductive Biology and Endocrinology* 2018;16: 1-14.

Seal B, Otero T, Panitch A. Polymeric biomaterials for tissue and organ regeneration. *Materials Science Engineering: R: Reports* 2001;34: 147-230.

Sen A, Hammes SR. Granulosa cell-specific androgen receptors are critical regulators of ovarian development and function. *Molecular Endocrinology* 2010;24: 1393-1403.

Sen A, Prizant H, Light A, Biswas A, Hayes E, Lee H-J, Barad D, Gleicher N, Hammes SR. Androgens regulate ovarian follicular development by increasing follicle stimulating hormone receptor and microRNA-125b expression. *Proceedings of the National Academy of Sciences* 2014;111: 3008-3013.

Sese N, Cole M, Tawil B. Proliferation of human keratinocytes and cocultured human keratinocytes and fibroblasts in three-dimensional fibrin constructs. *Tissue Engineering Part A* 2011;17: 429-437.

Shea LD, Woodruff TK, Shikanov A. Bioengineering the ovarian follicle microenvironment. *Annual review of biomedical engineering* 2014;16: 29-52.

Shi J, Yoshino O, Osuga Y, Koga K, Hirota Y, Hirata T, Yano T, Nishii O, Taketani Y. Bone morphogenetic protein-6 stimulates gene expression of follicle-stimulating hormone receptor, inhibin/activin β subunits, and

anti-Müllerian hormone in human granulosa cells. *Fertility and sterility* 2009;92: 1794-1798.

Shikone T, Yamoto M, Kokawa K, Yamashita K, Nishimori K, Nakano R. Apoptosis of human corpora lutea during cyclic luteal regression and early pregnancy. *The Journal of Clinical Endocrinology & Metabolism* 1996;81: 2376-2380.

Shikone T, Yamoto M, Nakano R. Follicle-stimulating hormone induces functional receptors for basic fibroblast growth factor in rat granulosa cells. *Endocrinology* 1992;131: 1063-1068.

Shimasaki S, Moore RK, Otsuka F, Erickson GF. The bone morphogenetic protein system in mammalian reproduction. *Endocrine reviews* 2004;25: 72-101.

Shimasaki S, Zachow RJ, Li D, Kim H, Iemura S-i, Ueno N, Sampath K, Chang RJ, Erickson GF. A functional bone morphogenetic protein system in the ovary. *Proceedings of the National Academy of Sciences* 1999;96: 7282-7287.

Shimizu T, Jiang J-Y, Sasada H, Sato E. Changes of messenger RNA expression of angiogenic factors and related receptors during follicular development in gilts. *Biology of Reproduction* 2002;67: 1846-1852.

Short R. Ovarian Steroid Synthesis and Secretion In Vivo. *Recent progress in hormone research* 1964;20: 303.

Shukovski L, Dyson M, Findlay JK. The effects of follistatin, activin and inhibin on steroidogenesis by bovine thecal cells. *Molecular and cellular endocrinology* 1993;97: 19-27.

Skinner MK. *Encyclopedia of reproduction*. 2 edn, 2018. Academic Press.

Slee RB, Hillier SG, Largue P, Harlow CR, Miele G, Clinton M. Differentiation-dependent expression of connective tissue growth factor and lysyl oxidase messenger ribonucleic acids in rat granulosa cells. *Endocrinology* 2001;142: 1082-1089.

Smith RM, Shikanov A, Kniazeva E, Ramadurai D, Woodruff TK, Shea LD. Fibrin-mediated delivery of an ovarian follicle pool in a mouse model of infertility. *Tissue Engineering Part A* 2014;20: 3021-3030.

Soares M. Fertility preservation and leukemia: cellular components of the artificial ovary and disease retransmission through the graft. 2015a. UCL-Université Catholique de Louvain.

Soares M, Sahrari K, Amorim CA, Saussoy P, Donnez J, Dolmans M-M. Evaluation of a human ovarian follicle isolation technique to obtain disease-free follicle suspensions before safely grafting to cancer patients. *Fertility sterility* 2015b;104: 672-680. e672.

Soares M, Sahrari K, Chiti MC, Amorim C, Ambroise J, Donnez J, Dolmans M-M. The best source of isolated stromal cells for the artificial ovary: medulla or cortex, cryopreserved or fresh? *Human reproduction* 2015c;30: 1589-1598.

Soares M, Saussoy P, Maskens M, Reul H, Amorim CA, Donnez J, Dolmans MM. Eliminating malignant cells from cryopreserved ovarian tissue is possible in leukaemia patients. *British journal of haematology* 2017;178: 231-239.

Soares M, Saussoy P, Sahrari K, Amorim CA, Donnez J, Dolmans M-M. Is transplantation of a few leukemic cells inside an artificial ovary able to induce leukemia in an experimental model? *Journal of assisted reproduction and genetics* 2015d;32: 597-606.

Solano ME, Sander VA, Ho H, Motta AB, Arck PC. Systemic inflammation, cellular influx and up-regulation of ovarian VCAM-1 expression in a mouse model of polycystic ovary syndrome (PCOS). *Journal of reproductive immunology* 2011;92: 33-44.

Solovyeva EV, Hayashi M, Margi K, Barkats C, Klein C, Amsterdam A, Hsueh AJ, Tsafriri A. Growth differentiation factor-9 stimulates rat theca-interstitial cell androgen biosynthesis. *Biology of reproduction* 2000;63: 1214-1218.

Sonmezer M, Oktay K. Fertility preservation in female patients. *Human reproduction update* 2004;10: 251-266.

Souza C, Campbell B, McNeilly A, Baird D. Effect of bone morphogenetic protein 2 (BMP2) on oestradiol and inhibin A production by sheep granulosa cells, and localization of BMP receptors in the ovary by immunohistochemistry. *Reproduction* 2002;123: 363-369.

Spears N, Lopes F, Stefansdottir A, Rossi V, De Felici M, Anderson R, Klinger F. Ovarian damage from chemotherapy and current approaches to its protection. *Human reproduction update* 2019;25: 673-693.

Spicer L, Voge J, Allen D. Insulin-like growth factor-II stimulates steroidogenesis in cultured bovine thecal cells. *Molecular and cellular endocrinology* 2004;227: 1-7.

Spicer LJ, Aad PY, Allen DT, Mazerbourg S, Payne AH, Hsueh AJ. Growth differentiation factor 9 (GDF9) stimulates proliferation and inhibits steroidogenesis by bovine theca cells: influence of follicle size on responses to GDF9. *Biology of Reproduction* 2008;78: 243-253.

Spicer LJ, Chamberlain CS. Influence of cortisol on insulin-and insulin-like growth factor 1 (IGF-1)-induced steroid production and on IGF-1 receptors in cultured bovine granulosa cells and thecal cells. *Endocrine* 1998;9: 153-161.

Spicer LJ, Sudo S, Aad PY, Wang LS, Chun S-Y, Ben-Shlomo I, Klein C, Hsueh AJ. The hedgehog-patched signaling pathway and function in the mammalian ovary: a novel role for hedgehog proteins in stimulating proliferation and steroidogenesis of theca cells. *Reproduction* 2009;138: 329-339.

Sriraman V, Sinha M, Richards JS. Progesterone receptor-induced gene expression in primary mouse granulosa cell cultures. *Biology of reproduction* 2010;82: 402-412.

Stewart R, Spicer L, Hamilton T, Keefer B. Effects of insulin-like growth factor I and insulin on proliferation and on basal and luteinizing hormone-induced steroidogenesis of bovine thecal cells: involvement of glucose and receptors for insulin-like growth factor I and luteinizing hormone. *Journal of Animal Science* 1995;73: 3719-3731.

Stocco C, Telleria C, Gibori G. The molecular control of corpus luteum formation, function, and regression. *Endocrine reviews* 2007;28: 117-149.

Stocco DM, Clark BJ. Regulation of the acute production of steroids in steroidogenic cells. *Endocrine reviews* 1996;17: 221-244.

Strauss JF, Williams CJ. Ovarian Life Cycle *Yen and Jaffe's Reproductive Endocrinology*. 2019. Elsevier, pp. 167-205.e169.

Stringer JM, Western PS. A step toward making human oocytes. *Nature Biotechnology* 2019;37: 24-25.

Sun J, Tan H. Alginate-based biomaterials for regenerative medicine applications. *Materials* 2013;6: 1285-1309.

Sun T, Chan MLH, Quek C-H, Yu H. Improving mechanical stability and density distribution of hepatocyte microcapsules by fibrin clot and gold nano-particles. *Journal of biotechnology* 2004;111: 169-177.

Sun Y-C, Sun X-F, Dyce PW, Shen W, Chen H. The role of germ cell loss during primordial follicle assembly: a review of current advances. *International journal of biological sciences* 2017;13: 449.

Suuronen E, Muzakare L, Doillon C, Kapila V, Li F, Ruel M, Griffith M. Promotion of angiogenesis in tissue engineering: developing multicellular matrices with multiple capacities. *The International journal of artificial organs* 2006;29: 1148-1157.

Svensson K-G, Owman C, Sjöberg N-O, Sporrong B, Walles B. Ultrastructural evidence for adrenergic innervation of the interstitial gland in the guinea pig ovary. *Neuroendocrinology* 1975;17: 40-47.

Szołtys M, Słomczyńska M, Galas J, Duda M, Sakiewicz A. Expression of androgen receptor and 3β-hydroxysteroid dehydrogenase in corpora lutea during pregnancy in the rat. *Reproduction, Fertility and Development* 2007;19: 356-365.

Tagler DJ, Shea LD, Woodruff TK. Contributions of ovarian stromal cells to follicle culture *Principles and Practice of Fertility Preservation*. 2011. Cambridge University Press.

Taipale J, Cooper M, Maiti T, Beachy P. Patched acts catalytically to suppress the activity of Smoothened. *Nature* 2002;418: 892-896.

Talbott H, Davis JS. Lipid droplets and metabolic pathways regulate steroidogenesis in the corpus luteum *The life cycle of the corpus luteum*. 2017. Springer, pp. 57-78.

Telfer E, Torrance C, Gosden R. Morphological study of cultured preantral ovarian follicles of mice after transplantation under the kidney capsule. *Reproduction* 1990;89: 565-571.

Telfer EE, McLaughlin M, Ding C, Thong KJ. A two-step serum-free culture system supports development of human oocytes from primordial follicles in the presence of activin. *Human Reproduction* 2008;23: 1151-1158.

Tessmar JK, Göpferich AM. Customized PEG-derived copolymers for tissue-engineering applications. *Macromolecular bioscience* 2007;7: 23-39.

Thomas FH, Armstrong DG, Telfer EE. Activin promotes oocyte development in ovine preantral follicles in vitro. *Reproductive Biology and Endocrinology* 2003;1: 76.

Tilly JL, Billig H, Kowalski KI, Hsueh A. Epidermal growth factor and basic fibroblast growth factor suppress the spontaneous onset of apoptosis in cultured rat ovarian granulosa cells and follicles by a tyrosine kinase-dependent mechanism. *Molecular Endocrinology* 1992;6: 1942-1950.

Tingen CM, Kiesewetter SE, Jozefik J, Thomas C, Tagler D, Shea L, Woodruff TK. A macrophage and theca cell-enriched stromal cell population influences growth and survival of immature murine follicles in vitro. *Reproduction* 2011;141: 809.

Torrealday S, Kodaman P, Pal L. Premature Ovarian Insufficiency-an update on recent advances in understanding and management. *F1000Research* 2017;6.

Turner EC, Hughes J, Wilson H, Clay M, Mylonas KJ, Kipari T, Duncan WC, Fraser HM. Conditional ablation of macrophages disrupts ovarian vasculature. *Reproduction* 2011;141: 821-831.

Van Dorp W, Mulder RL, Kremer LC, Hudson MM, Van Den Heuvel-Eibrink MM, Van Den Berg MH, Levine JM, Van Dulmen-Den Broeder E, Di Iorgi N, Albanese A. Recommendations for premature ovarian insufficiency surveillance for female survivors of childhood, adolescent, and young adult cancer: a report from the International Late Effects of Childhood Cancer Guideline Harmonization Group in collaboration with the PanCareSurFup Consortium. *Journal of Clinical Oncology* 2016;34: 3440.

Van Wezel I, Umapathysivam K, Tilley W, Rodgers R. Immunohistochemical localization of basic fibroblast growth factor in bovine ovarian follicles. *Molecular and Cellular Endocrinology* 1995;115: 133-140.

Vanacker J, Dolmans M-M, Luyckx V, Donnez J, Amorim CA. First transplantation of isolated murine follicles in alginate. *Regenerative medicine* 2014;9: 609-619.

Vanacker J, Luyckx V, Dolmans M-M, Des Rieux A, Jaeger J, Van Langendonckt A, Donnez J, Amorim CA. Transplantation of an alginate–matrigel matrix containing isolated ovarian cells: first step in developing a biodegradable scaffold to transplant isolated preantral follicles and ovarian cells. *Biomaterials* 2012;33: 6079-6085.

Vanorny DA, Mayo KE. The role of Notch signaling in the mammalian ovary. *Reproduction* 2017;153: R187-R204.

Vernon R, Spicer L. Effects of basic fibroblast growth factor and heparin on follicle-stimulating hormone-induced steroidogenesis by bovine granulosa cells. *Journal of animal science* 1994;72: 2696-2702.

Wallace WHB, Anderson RA, Irvine DS. Fertility preservation for young patients with cancer: who is at risk and what can be offered? *The lancet oncology* 2005;6: 209-218.

Wang D, Bodovitz S. Single cell analysis: the new frontier in 'omics'. *Trends in biotechnology* 2010;28: 281-290.

Wang J, Roy SK. Growth differentiation factor-9 and stem cell factor promote primordial follicle formation in the hamster: modulation by follicle-stimulating hormone. *Biology of reproduction* 2004;70: 577-585.

Warne G, Fairley K, Hobbs JB, Martin F. Cyclophosphamide-induced ovarian failure. *New England Journal of Medicine* 1973;289: 1159-1162.

Wei L-H, Chou C-H, Chen M-W, Rose-John S, Kuo M-L, Chen S-U, Yang Y-SJTJoCE, Metabolism. The role of IL-6 trans-signaling in vascular leakage: implications for ovarian hyperstimulation syndrome in a murine model. *The Journal of Clinical Endocrinology & Metabolism* 2013;98: E472-E484.

Weinand C, Pomerantseva I, Neville CM, Gupta R, Weinberg E, Madisch I, Shapiro F, Abukawa H, Troulis MJ, Vacanti JP. Hydrogel-β-TCP scaffolds and stem cells for tissue engineering bone. *Bone* 2006;38: 555-563.

Welt C, Sidis Y, Keutmann H, Schneyer A. Activins, inhibins, and follistatins: from endocrinology to signaling. A paradigm for the new millennium. *Experimental biology and medicine* 2002;227: 724-752.

West-Farrell ER, Xu M, Gomberg MA, Chow YH, Woodruff TK, Shea LD. The mouse follicle microenvironment regulates antrum formation and steroid production: alterations in gene expression profiles. *Biology of reproduction* 2009;80: 432-439.

Wiater E, Vale W. Inhibin is an antagonist of bone morphogenetic protein signaling. *Journal of Biological Chemistry* 2003;278: 7934-7941.

Wijgerde M, Ooms M, Hoogerbrugge JW, Grootegoed JA. Hedgehog signaling in mouse ovary: Indian hedgehog and desert hedgehog from granulosa cells induce target gene expression in developing theca cells. *Endocrinology* 2005;146: 3558-3566.

Williams CJ, Erickson GF. Morphology and physiology of the ovary *Endotext [Internet]*. 2012. MDText. com, Inc.

Wong AH, Zhou D, Rini JM. The X-ray crystal structure of human aminopeptidase N reveals a novel dimer and the basis for peptide processing. *Journal of Biological Chemistry* 2012;287: 36804-36813.

Woodruff TK, Shea LD. A new hypothesis regarding ovarian follicle development: ovarian rigidity as a regulator of selection and health. *Journal of assisted reproduction and genetics* 2011;28: 3-6.

Wu S, Divall S, Nwaopara A, Radovick S, Wondisford F, Ko C, Wolfe A. Obesity-induced infertility and hyperandrogenism are corrected by deletion of the insulin receptor in the ovarian theca cell. *Diabetes* 2014;63: 1270-1282.

Wu X, Chen L, Brown CA, Yan C, Matzuk MM. Interrelationship of growth differentiation factor 9 and inhibin in early folliculogenesis and ovarian tumorigenesis in mice. *Molecular endocrinology* 2004;18: 1509-1519.

Xia Y, Schneyer AL. The biology of activin: recent advances in structure, regulation and function. *The Journal of endocrinology* 2009;202: 1.

Xu M, Kreeger PK, Shea LD, Woodruff TK. Tissue-engineered follicles produce live, fertile offspring. *Tissue engineering* 2006;12: 2739-2746.

Yamamoto N, Christenson LK, McAllister JM, Strauss III JFJTJoCE, Metabolism. Growth differentiation factor-9 inhibits 3′ 5′-adenosine monophosphate-stimulated steroidogenesis in human granulosa and theca cells. *The Journal of Clinical Endocrinology and Metabolism* 2002;87: 2849-2856.

Yamamoto S, Konishi I, Nanbu K, Komatsu T, Mandai M, Kuroda H, Matsushita K, Mori T. Immunohistochemical localization of basic fibroblast growth factor (bFGF) during folliculogenesis in the human ovary. *Gynecological Endocrinology* 1997;11: 223-230.

Yang M, Fortune J. Testosterone stimulates the primary to secondary follicle transition in bovine follicles in vitro. *Biology of Reproduction* 2006;75: 924-932.

Yoon DM, Fisher JP. Natural and synthetic polymeric scaffolds *Biomedical Materials*. 2009. Springer, pp. 415-442.

Yoshino T, Saito D. Epithelial-to-mesenchymal transition–based morphogenesis of dorsal mesentery and gonad *Seminars in cell & developmental biology*. 2019. Elsevier, pp. 105-112.

Young J, McNeilly AS. Theca: the forgotten cell of the ovarian follicle. *Reproduction* 2010;140: 489-504.

Young JM, McNeilly AS. Theca: the forgotten cell of the ovarian follicle. *Reproduction* 2010;140: 489-504.

Zhao J, Taverne MA, van der Weijden GC, Bevers MM, van den Hurk R. Effect of activin A on in vitro development of rat preantral follicles and localization of activin A and activin receptor II. *Biology of reproduction* 2001;65: 967-977.

Ziegler Dd, Fraisse T, Candolle Gd, Vulliemoz N, Bellavia M, Colamaria S. Roles of FSH and LH during the follicular phase: insight into natural cycle IVF. *Reproductive biomedicine online* 2007;15: 507-513.

Zsebo KM, Wypych J, McNiece IK, Lu HS, Smith KA, Karkare SB, Sachdev RK, Yuschenkoff VN, Birkett NC, Williams LR. Identification, purification,

and biological characterization of hematopoietic stem cell factor from buffalo rat liver-conditioned medium. *Cell* 1990;63: 195-201.

II. Other publications during the thesis

i. First-author article

Journal of Assisted Reproduction and Genetics (2020) 37:2545–2553
https://doi.org/10.1007/s10815-020-01901-8

REPRODUCTIVE PHYSIOLOGY AND DISEASE

Assessing and validating housekeeping genes in normal, cancerous, and polycystic human ovaries

P. Asiabi[1] · J. Ambroise[2] · C. Giachini[3] · M. E. Coccia[3] · B. Bearzatto[2] · M. C. Chiti[1] · M. M. Dolmans[1,4] · C. A. Amorim[1]

Received: 31 March 2020 / Accepted: 23 July 2020 / Published online: 30 July 2020
© Springer Science+Business Media, LLC, part of Springer Nature 2020

Abstract
Purpose Housekeeping genes (HKGs), reference or endogenous control genes, are vital to normalize mRNA levels between different samples. Since using inappropriate HKGs can lead to unreliable results, selecting the proper ones is critical for gene expression studies. To this end, normal human ovaries, as well as those from patients diagnosed with ovarian endometrioid adenocarcinoma (OEA), ovarian mucinous adenocarcinoma (OMA), ovarian serous papillary carcinoma (OSPC), and polycystic ovary syndrome (PCOS), were used to identify the most suitable housekeeping genes.
Methods RNA was isolated from 5 normal human ovaries (52–79 years of age), 9 cancerous ovaries (3 OEA, 3 OMA, 3 OSPC; 49–75 years of age), and 4 PCOS ovaries (18–35 years of age) in women undergoing hysterectomy. cDNA was synthesized using a whole transcriptome kit, and quantitative real-time PCR was performed using TaqMan array 96-well plates containing 32 human endogenous controls in triplicate.
Results Among 32 HKGs studied, RPS17, RPL37A, PPIA, 18srRNA, B2M, RPLP0, RPLP30, HPRT1, POP4, CDKN1B, and ELF1 were selected as the best reference genes.
Conclusions This study confirms recent investigations demonstrating that conventional HKGs, such as GAPDH and beta-actin, are not suitable reference genes for specific pathological conditions, emphasizing the importance of determining the best HKGs on a case-by-case basis and according to tissue type. Our results have identified reliable HKGs for studies of normal human ovaries and those affected by OEA, OMA, OSPC, or PCOS, as well as combined studies of control subjects vs. each cancer or PCOS group.

Keywords Housekeeping/reference/endogenous control genes · Gene expression · Ovarian endometrioid adenocarcinoma (OEA) · Ovarian mucinous adenocarcinoma (OMA) · Ovarian serous papillary carcinoma (OSPC) · Polycystic ovary syndrome (PCOS)

Electronic supplementary material The online version of this article (https://doi.org/10.1007/s10815-020-01901-8) contains supplementary material, which is available to authorized users.

✉ C. A. Amorim
christiani.amorim@uclouvain.be

[1] Pôle de Recherche en Gynécologie, Institut de Recherche Expérimentale et Clinique, Université Catholique de Louvain, Avenue Mounier 52, bte B1.52.02, 1200 Brussels, Belgium

[2] Centre de Technologies Moléculaires Appliquées, Institut de Recherche Expérimentale et Clinique, Université Catholique de Louvain, 1200 Brussels, Belgium

[3] Department of Clinical and Experimental Biomedical Sciences, University of Florence, 50134 Florence, Italy

[4] Gynecology Department, Cliniques Universitaires Saint-Luc, 1200 Brussels, Belgium

Introduction

Transcriptional regulation is a key factor in cellular responses, so analysis of gene expression profiles has become an essential part of biomedical research [1]. Real-time quantitative polymerase chain reaction (qPCR) is the current method of choice for specific and highly sensitive expression profiling of selected groups of target genes. However, despite being a powerful technique, data normalization remains problematic. At present, use of the so-called housekeeping genes (HKGs), endogenous control genes or reference genes, is the gold standard to normalize mRNA fractions of interest. HKGs are often used to correct sample-to-sample variations, including the amount and integrity of materials, enzymatic efficiency, cDNA sample loading, and differences between tissues or cells in overall transcription activity [2, 3].

By definition, HKGs selected for normalization should not be influenced by experimental or biological conditions, and their own expression levels should be identical in tumors and adjacent healthy sites. A growing number of studies show that expression levels of commonly used HKGs are affected by experimental conditions or vary in pathological states, particularly cancer, highlighting the risk of blind use of classic HKGs [4–7]. Although GAPDH and beta-actin are widely used, they are not suitable HKGs in many cases involving cell proliferation, differentiation, metabolic changes, hypoxia, and cancer [8–13]. Since no universal reference gene has yet been detected, the choice of HKG(s) should be validated in each investigated condition. To this end, bioinformatic tools like NormFinder, BestKeeper, and geNorm have been developed [3, 14, 15].

Regarding the incidence of polycystic ovary syndrome (PCOS) and ovarian cancers, it is assumed that PCOS elevates ovarian cancer risk through increased androgen exposure [16, 17], so gene analyses for early diagnosis are highly recommended [17]. In order to obtain reliable results from qPCR, it is essential to use the correct reference gene(s). With this in mind, our study set out to assess 32 HKGs in healthy ovarian tissue as a control group, ovarian endometrioid adenocarcinoma (OEA), ovarian mucinous adenocarcinoma (OMA), ovarian serous papillary carcinoma (OSPC), and PCOS groups individually, all 5 groups together, and healthy ovaries vs. pathological cases.

Materials and methods

Source of ovaries and ethical approval

Biopsies of ovarian tissue were removed from five healthy women to investigate the presence of ovarian metastasis. However, all of them proved to be free of any pathology. Moreover, samples of OEA ($n = 3$), OMA ($n = 3$), and OSPC ($n = 3$) were obtained from the anatomic pathology laboratory of Saint-Luc's Hospital. Use of human ovarian tissue was approved by the Institutional Review Board of the Université Catholique de Louvain on November 28, 2016 (IRB reference 2012/23MAR/125, registration number B403201213872). The tissue was frozen in Tissue-Tek® O.C.T.™ compound (Sakura, Netherlands) and cut with the Microm HM 560 microtome (Thermo Fisher, USA) into 5-μm sections (Table 1). Four PCOS samples (Table 1) were procured from anovulatory patients resistant to clomiphene, who had undergone laparoscopy to remove benign ovarian cysts and assess previous ovarian resection. At the moment of surgery, biopsies of the ovarian tissue (far from the cysts) were collected for this study. Samples were acquired as snap-frozen tissue in cryotubes filled with RNAlater™-ICE frozen tissue transition solution (Invitrogen, USA) from the assisted reproduction technology center of the Careggi University Hospital in Florence, Italy (ethical approval n. 11314_bio).

RNA extraction and cDNA synthesis

Tissue fragments were placed in lysing matrix Z tubes (MP Biomedicals, USA) containing 2 mm yttria-stabilized zirconium beads with 600 μl RLT Plus buffer from the AllPrep DNA/RNA micro kit (QIAGEN, Germany) with 1% 2-mercaptoethanol (Sigma-Aldrich, Germany). Samples were lysed by bead beating for two 30-s cycles at 6 m/s in FastPrep lysing matrix Z tubes. A cooling step on ice (40-s cycles) was performed between the two bead beatings. Tubes containing the lysates were then centrifuged for 3 min at 14,000*g*. Supernatant was collected and RNA was extracted according to the manufacturer's instructions. Briefly, the supernatant with RLT Plus and 2-mercaptoethanol was first passed through the DNA column to selectively bind genomic DNA. After centrifugation at 8000*g* for 30 s, the eluate containing RNA was mixed with 70% ethanol, before placing inside a RNeasy MinElute spin column and centrifuging at 8000*g* for 30 s. At this point, the eluate was discarded and the column was then washed once each with RW1 and RPE1 buffers, respectively, provided by the kit, with centrifugation after each washing step (8000*g* for 30 s). Eighty percent ethanol was added to the column, followed by centrifugation (8000*g* for 2 min), before finally eluting the RNA in 14 μl RNase-free water.

Isolated RNA concentrations were measured using the Qubit 4 fluorometer (Thermo Fisher Scientific, USA) and the Qubit RNA broad range assay kit. Since part of our samples were cryostat slices of OCT-embedded frozen tissue [18], the QuantiTect whole transcriptome kit (QIAGEN, Germany) was used to synthesize and amplify cDNA from 20 ng of isolated RNA. This kit does not amplify small RNA molecules, such as tRNAs or miRNAs, or degraded RNA. In fact, RNA transcripts should be longer than 500 nucleotides. Synthesized cDNA concentrations were measured using the Qubit 4 fluorometer (Thermo Fisher Scientific) and Qubit dsDNA broad range assay kit (Thermo Fisher Scientific) to be sure of loading 25 ng of cDNA in each well.

Quantitative real-time PCR

Expression levels of 32 commonly used candidates for HKGs (Table 2) [19, 20] were studied using predesigned TaqMan array 96-well fast plates for human endogenous controls (Applied Biosystems, CA, USA). Each TaqMan® gene expression assay consisted of a fluorogenic carboxyfluorescein (FAM™) dye-labeled minor groove binder (MGB) probe and two amplification primers (forward and reverse) provided in a

Table 1 Description of study groups, ovarian tissue origin, and biopsy storage conditions

Groups	Tissue type	Patient age	Code	Tissue size	Tissue condition
G1	Healthy ovarian tissue (controls)	59	1	10 fragments of 5 μm each	Frozen in OCT*
		61	2	10 fragments of 5 μm each	Frozen in OCT*
		68	3	10 fragments of 5 μm each	Frozen in OCT*
		52	4	10 fragments of 5 μm each	Frozen in OCT*
		79	5	10 fragments of 5 μm each	Frozen in OCT*
G2	Endometrioid adenocarcinoma	73	6	10 fragments of 5 μm each	Frozen in OCT*
		49	7	10 fragments of 5 μm each	Frozen in OCT*
		73	8	10 fragments of 5 μm each	Frozen in OCT*
G3	Mucinous adenocarcinoma	42	9	10 fragments of 5 μm each	Frozen in OCT*
		53	10	10 fragments of 5 μm each	Frozen in OCT*
		56	11	10 fragments of 5 μm each	Frozen in OCT*
G4	Serous papillary carcinoma	73	12	10 fragments of 5 μm each	Frozen in OCT*
		75	13	10 fragments of 5 μm each	Frozen in OCT*
		61	14	10 fragments of 5 μm each	Frozen in OCT*
G5	Polycystic ovary syndrome	35	15	0.2 cm × 0.2 cm × 0.2 cm	Snap-frozen**
		18	16	0.2 cm × 0.2 cm × 0.3 cm	Snap-frozen**
		26	17	0.3 cm × 0.3 cm × 0.5 cm	Snap-frozen**
		35	18	0.3 cm × 0.3 cm × 0.3 cm	Snap-frozen**

*OCT: optimal cutting temperature compound

**Snap-frozen at − 80 °C

pre-formulated 20X mix; 1X final concentrations were 250 nM for the probe and 900 nM for each primer. Each assay is estimated to have an amplification efficiency of 100 10% (Thermo Fisher Scientific) [20]. A single 96-well plate was used for each individual sample. Ten microliters of pyrogen together with DNAse- and RNAse-free diethyl pyrocarbonate (DEPC) water (Invitrogen, USA) containing 25 ng cDNA was added to each well, followed by 10 μl TaqMan gene expression Master Mix (Thermo Fisher, Lithuania) in a total volume of 20 μl. For every study group, all the reactions for reference genes were performed at least in triplicate both biologically and technically. Standard cycling conditions were as follows: 2 min at 50 °C, 10 min at 95 °C, 50 cycles of 15 s at 95 °C, and 1 min at 60 °C. Thermal cycling and fluorescence detection were performed using the StepOnePlus Real-Time PCR system (Applied Biosystems).

Data analysis

To analyze our data, the bioinformatic tool geNorm was used. The geNorm algorithm was developed by Vandesompele et al. [3] and is considered the gold standard for determining the most stable set and number of HKGs to use for accurate relative quantification. An advantage of the geNorm algorithm is that it is only slightly affected by the expression intensity of candidate genes [2, 3]. In a first step, the average of qPCR technical triplicates was computed for each target gene. If a single technical replicate out of three was undetermined, it was removed from downstream analysis, as previously recommended [21]. Because the variability of the technical replicates sharply increased when the *Ct* value exceeded 35 (Supplementary Fig. 1), samples with $Ct > 35$ were withdrawn before HKG selection. The "selectHKs" function of the NormqPCR program was then used to pick out the most stable HKGs by applying the geNorm algorithm. GeNorm uses mean pairwise variation for a given reference gene candidate compared with other candidates (M-value) and excludes the least stable genes before repeating the analysis, until only the most stable genes are left [3]. Since an appropriate reference gene should have an M-value below 0.5 or 1.0 in homogeneous and heterogeneous cell/tissue sample sets respectively, and we were working with cortex and medulla adjacent to the cortex, the threshold for the M-value in this study was set at < 1 [22]. As all samples in this study belong to 5 distinct groups (G1: normal human ovary; G2: OEA; G3: OMA; G4: OSPC; and G5: PCOS), selection of the best HKGs was done on samples from each group individually and all groups together, before being applied to samples from G1 vs. G2, G1 vs. G3, G1 vs. G4, and G1 vs. G5 (Figs. 1, 2, and 3).

Results

We analyzed a predesigned human endogenous control panel consisting of 32 primers, one in each well in triplicate, top identify the most stable HKGs.

Table 2 Assay ID, gene symbol, and name of 32 investigated predesigned HKGs in 96 plates in triplicate

Target	Assay ID	Gene symbol	Gene name
1	Hs99999901_s1	18S rRNA	Eukaryotic 18S rRNA
2	Hs99999903_m1	ACTB	Actin; beta
3	Hs99999906_m1	PGK1	Phosphoglycerate kinase 1
4	Hs00824723_m1	UBC	Ubiquitin C
5	Hs00201226_m1	CASC3	Cancer susceptibility candidate 3
6	Hs00206469_m1	PUM1	Pumilio homolog 1 (drosophila)
7	Hs00245445_m1	ABL1	C-Abl oncogene 1; non-receptor tyrosine kinase
8	Hs00198357_m1	POP4	Ribonuclease P protein subunit p29
9	Hs99999905_m1	GAPDH	Glyceraldehyde-3-phosphate dehydrogenase
10	Hs99999907_m1	B2M	Beta-2-microglobulin
11	Hs99999902_m1	RPLP0	Ribosomal protein; large; P0
12	Hs00237047_m1	YWHAZ	Tyrosine 3-monooxygenase/tryptophan 5-monooxygenase activation protein
13	Hs00355782_m1	CDKN1A	Cyclin-dependent kinase inhibitor 1A
14	Hs00197826_m1	PSMC4	Proteasome (prosome; macropain) 26S subunit
15	Hs00152844_m1	ELF1	E74-like factor 1 (ETS domain transcription factor)
16	Hs01102345_m1	RPL37A	Ribosomal protein L37a
17	Hs99999909_m1	HPRT1	Hypoxanthine phosphoribosyltransferase 1
18	Hs00609297_m1	HMBS	Hydroxymethylbilane synthase
19	Hs99999910_m1	TBP	TATA box-binding protein
20	Hs99999904_m1	PPIA	Peptidylprolyl isomerase A (cyclophilin A)
21	Hs00153277_m1	CDKN1B	Cyclin-dependent kinase inhibitor 1B (p27; Kip1)
22	Hs00426752_m1	EIF2B1	Eukaryotic translation inhibition factor 2B
23	Hs02596862_g1	MT-ATP6	Mitochondrially encoded ATP synthese 6
24	Hs00265497_m1	RPL30	Ribosomal protein L30
25	Hs99999908_m1	GUSB	Glucuronidase; beta
26	Hs00183533_m1	IPO8	Importin 8
27	Hs99999911_m1	TFRC	Transferrin receptor (p90; CD71)
28	Hs00172187_m1	POLR2A	Polymerase (RNA) II (DNA directed) polypeptide A
29	Hs00169255_m1	GADD45A	Growth arrest and DNA damage-inducible
30	Hs00362795_g1	PES1	Pescadillo ribosomal biogenesis factor 1
31	Hs00608519_m1	MRPL19	Mitochondrial ribosomal protein L19
32	Hs00734303_g1	RPS17	Ribosomal protein S17

1. The most stable HKGs per group

In five samples of normal human ovary (G1), 5 HKGs were suggested, namely beta 2-microglobulin (B2M), ribosomal protein L30 (RPL30), ribosomal protein P0 (RPLP0), peptidylprolyl isomerase A (cyclophilin A) (PPIA), and ribosomal protein L37a (RPL37A) (Fig. 1G1). In three OEA samples, 6 HKGs, namely pescadillo ribosomal biogenesis factor 1 (PES1), ribosomal protein S17-like (RPS17), B2M, RPL37A, PPIA, and eukaryotic 18s rRNA (18S rRNA), were endorsed (Fig. 1G2). In three OMA samples, RPL37A, RPLP0, and RPS17 were the most stable HKGs respectively (Fig. 1G3). In three OSPC samples, 6 HKGs emerged, namely B2M, PPIA, RPL30, RPLP0, RPL37A, and RPS17 (Fig. 1G4). Finally, in four PCOS samples, B2M, RPL30, PPIA, and RPLP0 ranged from the most to the least stable HKGs in the set threshold (Fig. 1G5).

2. The most stable HKGs in all groups

Among 18 investigated samples, RPL37A and RPS17 were shown to be the most stable HKGs (Fig. 2).

3. The most stable HKGs in the control group vs. OEA, OMA, OSPC, and PCOS subjects

In the study of five healthy control ovarian tissue fragments vs. three OEA samples, RPL37A, RPS17, and PPIA showed the least variation among all investigated HKGs. On the other hand, in an analysis of the five controls vs. three OMA

samples, RPL37A and RPS17 showed the best stability to be chosen as HKGs. Controls vs. three OSPC samples identified B2M, RPL30, PPIA, and RPLP0 as having the least variation. Finally, in a comparison of the five controls vs. four PCOS samples, RPL37A and RPS17 were the most stable HKGs out of all 32 studied genes (Fig. 3).

Discussion

Although qPCR is recommended as an accurate method to investigate precise gene expression levels with high sensitivity [23, 24] in basic research, molecular medicine, and biotechnology [25], it is crucial to use the right HKGs to normalize data [26, 27]. In this study, we conducted extensive analysis of human ovarian tissue in an attempt to recommend specific use of optimal HKGs for this tissue. Due to tissue specificity for HKGs [4–7], we evaluated a panel of 32 HKGs in 18 samples from normal human ovaries as controls, PCOS ovaries, and three types of ovarian cancer, namely OEA, OMA, and OSPC. In each experiment, we introduced HKGs with an M-value less than 1 [22], and as it decreased, there was less variation in chosen gene expression in the different analyses. Our results suggest RPL37A, PPIA, and RPS17 to be the most stable HKGs in expression levels in the human ovary. RPL37A was also provided by Siemens Healthcare Diagnostics (Cologne, Germany) for use by Sinn et al. [28] in their studies on patients with high-stage, high-grade serous adenocarcinomas, consistent with the general population of ovarian cancer patients in their study. Looking into the literature and HKG studies in human ovaries, our findings on PPIA appear to corroborate those of Yan-Li et al. [29], who suggested PPIA as a reference gene in postmenopausal ovaries and serous ovarian cancer subtypes. PPIA was also proposed as a reference gene in native and vitrified/thawed human ovarian tissue by Nikishin et al. [30]. Both geNorm and NormFinder found PPIA to be a reliable reference gene in studies by Li et al. [29] on serous ovarian cancer. Sharan et al. [31] recommended that a combination of PPIA and either GAPDH, ACTB, HPRT, or TBP, or appropriate combinations of two or three of these genes, be used to verify results from different studies on various human cancers. RPS17 along with 18S rRNA was suggested as a reliable HKG in Wharton's jelly–derived mesenchymal stem cells (WJ-MSCs) that were undergoing transduction and differentiation by Borkowska et al. [32]. Our results also indicate that RPLP0, B2M, RPL30, 18S rRNA, and PES1 may be suitable HKGs in human ovary studies. RPLP0 encodes ribosomal protein components of the 60S subunit, and Nikishin et al. [30] considered RPLP0 to be the most stable reference gene in human native and vitrified/thawed ovarian tissue. In another study, Shen et al. [33] demonstrated that the RPLP0 gene may prove

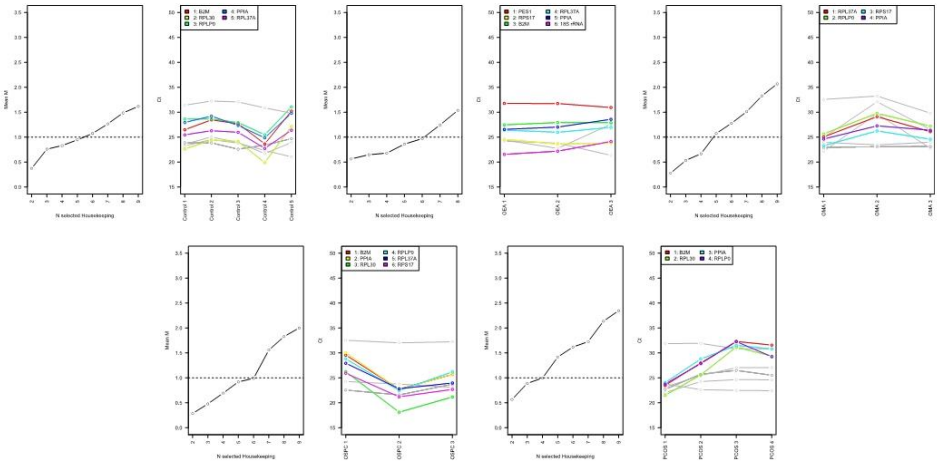


Fig. 1 geNorm analyses in each studied group. G1 is healthy control ovarian tissue, G2 is ovarian endometrioid adenocarcinoma (OEA), G3 is ovarian mucinous adenocarcinoma (OMA), G4 is ovarian serous papillary carcinoma (OSPC), and G5 is polycystic ovary syndrome (PCOS). In each group, in the graph on the left, the X-axis represents the codes of the studied genes and the Y-axis the M-value. In the graph on the right, the X-axis represents the studied samples and the Y-axis the *Ct* value of the genes. The legend reports only HKGs selected by geNorm. The lower the M-value, the more stable the HKG, as shown below. G1: B2M > RPL30 > RPLP0 > PPIA > RPL37AG2: PES1 > RPS17 > B2M > RPL37A > PPIA > 18S rRNAG3: RPL37A > RPLP0 > RPS17 > PPIAG4: B2M > PPIA > RPL30 > RPLP0 > RPL37A > RPS17G5: B2M > RPL30 > PPIA > RPLP0

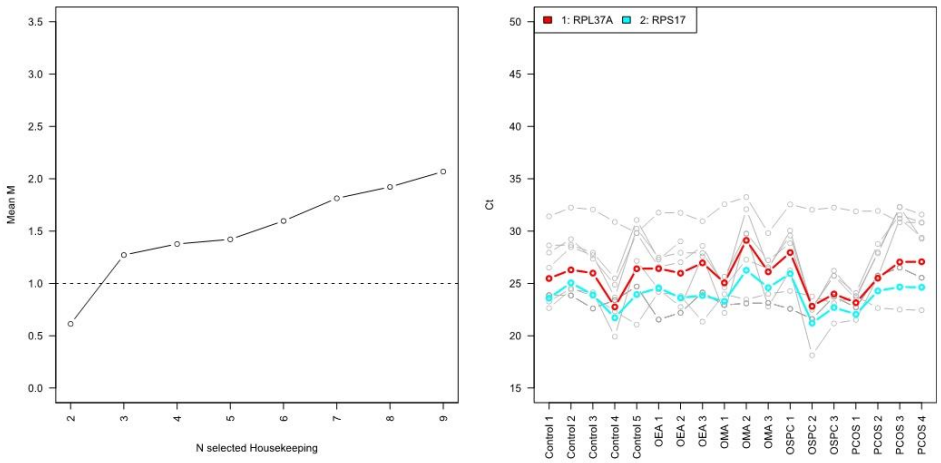


Fig. 2 geNorm analyses in all groups together (18 samples), including control samples, ovarian endometrioid adenocarcinoma (OEA), ovarian mucinous adenocarcinoma (OMA), ovarian serous papillary carcinoma (OSPC), and polycystic ovary syndrome (PCOS). The graph on the left represents the codes of the studied genes (X-axis) and their mean value (Y-axis). The graph on the right represents the studied groups (X-axis) and *Ct* values (Y-axis). The legend reports only the HKGs selected by geNorm. The most stable HKGs in all groups were RPL37A > RPS17

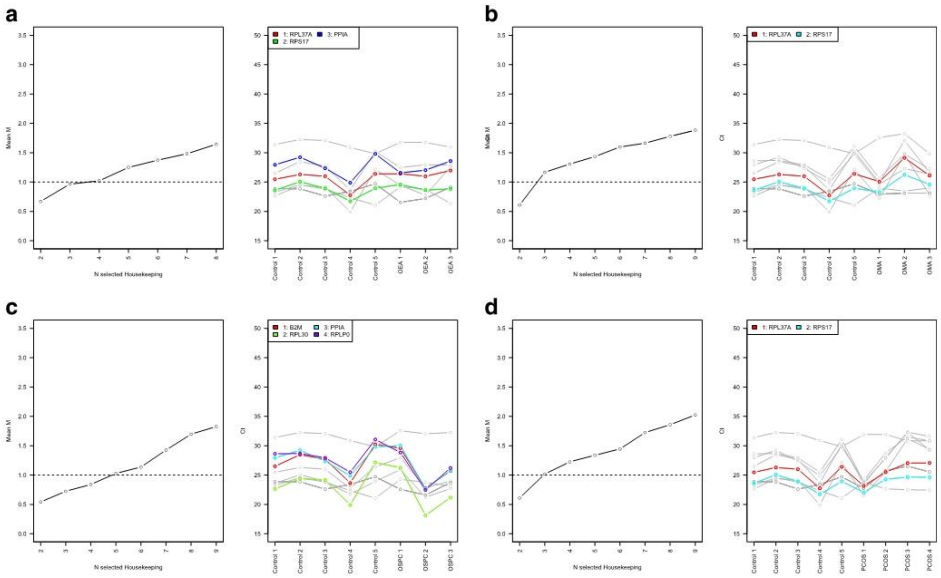


Fig. 3 geNorm analyses in control samples (G1) vs. G2, G3, G4, and G5. **a** G1 vs. OEA: RPL37A > RPS17 > PPIA. **b** G1 vs. OMA: RPL37A > RPS17. **c** G1 vs. OSPC: B2m > RPL30 > PPIA > RPLP0. **d** G1 vs. PCOS: RPL37A > RPS17. In each comparison, the graph on the left represents the codes of the studied genes (X-axis) and their mean value (Y-axis). The graph on the right represents the studied groups (X-axis) and *Ct* values (Y-axis). The legend reports only the HKGs selected by geNorm

Table 3 Summary of the selected HKGs with an M-value < 1 in all studied groups

	B2M	RPL30	RPLP0	PPIA	RPL37A	RPS17	18S rRNA	PES1
Control	*	*	*	*	*			
OEA	*			*	*	*	*	*
OMA			*	*	*	*		
OSPC	*	*	*	*	*	*		
PCOS	*	*	*	*				
All					*	*		
Control vs. OEA				*	*	*		
Control vs. OMA					*	*		
Control vs. OSPC	*	*	*	*				
Control vs. PCOS					*	*		
Frequency out of 10	5	4	5	7	8	7	1	1

Control normal human ovary, *OEA* ovarian endometrioid adenocarcinoma, *OMA* ovarian mucinous adenocarcinoma, *OSPC* ovarian serous papillary carcinoma, *PCOS* polycystic ovary syndrome. Frequency out of ten referring to the repetition of each gene in a total of ten experiments. Beta-2-microglobulin (B2M), ribosomal protein L30 (RPL30), ribosomal protein, large, P0 (RPLP0), peptidylprolyl isomerase A (cyclophilin A) (PPIA), ribosomal protein L37a (RPL37A), ribosomal protein S17-like (RPS17), eukaryotic 18s rRNA (18S rRNA), and pescadillo ribosomal biogenesis factor 1 (PES1)

reliable to normalize gene expression in human cervical tissue. RPLP0 together with RPL4 and HSPCB are also recommended for normalization in all ovarian-related research [34]. B2M was reported by Ofinran et al. [35] as an appropriate reference gene in human ovarian cancer, borderline ovarian cancer, and normal ovarian tissue. RPL30 was recommended as a suitable HKG in a study of the Scandinavian population, including borderline ovarian tumors [36]. Our findings on 18S rRNA as an applicable HKG in ovarian cancer are consistent with other studies on human ovarian cancer [34, 37]. PES1, to our knowledge, has not been stablished as a reliable HKG in human ovary, but has been used as an HKG in human lung cancer [38]. Li et al. [39] showed that PES1 differentially regulates the expression balance of ERα and ERβ and may play a crucial role in ovarian cancer.

While our data could have been reinforced by more extensive sampling, human ovarian tissue remains a precious material to be used in research, particularly when it comes from reproductive-age women. Similar to our study, Ofinran et al. [35] also used ovarian tissue fragments to represent the whole ovary. Such practice was also performed by Aithal and Rajeswari [40], who collected brain samples from paraffin-embedded blocks. Furthermore, it is important to bear in mind that sample sizes comparable or smaller than ours have been described in studies in different human tissues [2, 20, 40–43].

It is also important to stress that there are other factors that could play a role in our findings, such as age difference between control and PCOS groups, and menstrual cycle stage at the moment of ovarian biopsy collection. Moreover, we did not evaluate genome-wide transcript expression. However, it is important to bear in mind that, among the 32 most popular HKGs, we obtained quite similar gene results in different types of investigations.

In conclusion, our study showed RPL37A, PPIA, RPS17, RPLP0, B2M, RPL30, 18S rRNA, and PES1 to be the most suitable HKGs out of the 32 investigated reference genes in 18 samples from individual studies in normal human ovaries, OEA, OMA, OSPC, and PCOS samples, all groups together and control tissue vs. patient groups (Table 3). On the other hand, as there is also disease specificity for HKGs in the same tissue, we propose particular HKGs for some common ovarian pathologies, like the 3 types of ovarian cancer and PCOS. Our results can be used to provide a good starting point for developing primers to use or be selected in gene array studies in order to ensure generation of accurate and robust data in the same tissue conditions in different gene expression studies.

Acknowledgments We are grateful to Mira Hryniuk for reviewing the English language of the manuscript and Dolores Gonzalez and Olivier Van Kerk for their technical assistance. We are also thankful to Professor Etienne Marbaix for his kind collaboration and providing ovarian control and cancerous samples.

Authors' contributions P. A.: study design, experimental procedures, analysis, interpretation of data, and manuscript preparation. J. A.: statistical analysis. C. G. and M. E. C.: PCOS tissue supply. B. B.: manuscript revision. M. C. C.: PCOS tissue supply and manuscript revision. M. M. D.: manuscript preparation and revision. C. A. A.: experimental design, experimental procedures, interpretation of results, and manuscript revision.

Funding information This study was supported by grants from the Fonds National de la Recherche Scientifique de Belgique (FNRS) (C. A. Amorim is an FRS-FNRS Research Associate; grant MIS #F4535 16 awarded to C. A. Amorim; grant 5/4/150/5 awarded to M. M. Dolmans; grant ASP-RE314 awarded to P. Asiabi; FNRS-PDR Convention T.0077.14 and EOS grant 30443682).

Compliance with ethical standards

Conflict of interest The authors declare that they have no conflict of interest.

Ethical approval Use of human ovarian tissue was approved by the Institutional Review Board of the Université Catholique de Louvain on November 28, 2016 (IRB reference 2012/23MAR/125, registration number B403201213872).

Four PCOS samples came from the assisted reproduction technology center of the Careggi University Hospital in Florence, Italy (Ethical approval n. 11314_bio).

References

1. Matys V, Fricke E, Geffers R, Gössling E, Haubrock M, Hehl R, et al. TRANSFAC®: transcriptional regulation, from patterns to profiles. Nucleic Acids Res. 2003;31(1):374–8.
2. Almeida TA, Quispe-Ricalde A, Montes de Oca F, Foronda P, Hernández MM. A high-throughput open-array qPCR gene panel to identify housekeeping genes suitable for myometrium and leiomyoma expression analysis. Gynecol Oncol. 2014;134(1):138–43.
3. Vandesompele J, et al. *Accurate normalization of real-time quantitative RT-PCR data by geometric averaging of multiple internal control genes*. Genome Biol. 2002;3(7):research0034. 1.
4. Hendriks-Balk MC, Michel MC, Alewijnse AE. Pitfalls in the normalization of real-time polymerase chain reaction data. Basic Res Cardiol. 2007;102(3):195–7.
5. Rocha-Martins M, Njaine B, Silveira MS. Avoiding pitfalls of internal controls: validation of reference genes for analysis by qRT-PCR and Western blot throughout rat retinal development. PLoS One. 2012;7(8):e43028.
6. Thellin O, Zorzi W, Lakaye B, de Borman B, Coumans B, Hennen G, et al. Housekeeping genes as internal standards: use and limits. J Biotechnol. 1999;75(2–3):291–5.
7. Guénin S, et al. Normalization of qRT-PCR data: the necessity of adopting a systematic, experimental conditions-specific, validation of references. J Exp Bot. 2009;60(2):487–93.
8. Selvey S, Thompson EW, Matthaei K, Lea RA, Irving MG, Griffiths LR. β-Actin—an unsuitable internal control for RT-PCR. Mol Cell Probes. 2001;15(5):307–11.
9. Ruan W, Lai M. Actin, a reliable marker of internal control? Clin Chim Acta. 2007;385(1–2):1–5.
10. Caradec J, et al. 'Desperate house genes': the dramatic example of hypoxia. Br J Cancer. 2010;102(6):1037.
11. Caradec J, Sirab N, Revaud D, Keumeugni C, Loric S. Is GAPDH a relevant housekeeping gene for normalisation in colorectal cancer experiments? Br J Cancer. 2010;103(9):1475–6.
12. Mansur NR, Meyer-Siegler K, Wurzer JC, Sirover MA. Cell cycle regulation of the glyceraldehyde3phosphate dehydrogenaseluracil DNA glycosylase gene in normal human cells. Nucleic Acids Res. 1993;21(4):993–8.
13. Vilà MR, et al. Increased glyceraldehyde-3-phosphate dehydrogenase expression in renal cell carcinoma identified by RNA-based, arbitrarily primed polymerase chain reaction. Cancer. 2000;89(1):152–64.
14. Andersen CL, Jensen JL, Ørntoft TF. Normalization of real-time quantitative reverse transcription-PCR data: a model-based variance estimation approach to identify genes suited for normalization, applied to bladder and colon cancer data sets. Cancer Res. 2004;64(15):5245–50.
15. Pfaffl MW, Tichopad A, Prgomet C, Neuvians TP. Determination of stable housekeeping genes, differentially regulated target genes and sample integrity: BestKeeper–excel-based tool using pair-wise correlations. Biotechnol Lett. 2004;26(6):509–15.
16. Risch HA. Hormonal etiology of epithelial ovarian cancer, with a hypothesis concerning the role of androgens and progesterone. J Natl Cancer Inst (JNCI). 1998;90(23):1774–86.
17. Jiao J, Sagnelli M, Shi B, Fang Y, Shen Z, Tang T, et al. Genetic and epigenetic characteristics in ovarian tissues from polycystic ovary syndrome patients with irregular menstruation resemble those of ovarian cancer. BMC Endocr Disord. 2019;19(1):30.
18. Dupasquier S, Delmarcelle AS, Marbaix E, Cosyns JP, Courtoy PJ, Pierreux CE. Validation of housekeeping gene and impact on normalized gene expression in clear cell renal cell carcinoma: critical reassessment of YBX3/ZONAB/CSDA expression. BMC Mol Biol. 2014;15(1):9.
19. Bustin SA, Benes V, Garson JA, Hellemans J, Huggett J, Kubista M, et al. The MIQE Guidelines: Minimum Information for Publication of Quantitative Real-Time PCR Experiments. Clin Chem. 2009;55(4):611–22.
20. Ayakannu T, Taylor AH, Willets JM, Brown L, Lambert DG, McDonald J, et al. Validation of endogenous control reference genes for normalizing gene expression studies in endometrial carcinoma. Mol Hum Reprod. 2015;21(9):723–35.
21. Pabinger S, Rödiger S, Kriegner A, Vierlinger K, Weinhäusel A. A survey of tools for the analysis of quantitative PCR (qPCR) data. Biomol Detect Quantif. 2014;1(1):23–33.
22. Hellemans J, Mortier G, de Paepe A, Speleman F, Vandesompele J. qBase relative quantification framework and software for management and automated analysis of real-time quantitative PCR data. Genome Biol. 2007;8(2):R19.
23. Gachon C, Mingam A, Charrier B. Real-time PCR: what relevance to plant studies? J Exp Bot. 2004;55(402):1445–54.
24. Kozera B, Rapacz M. Reference genes in real-time PCR. J Appl Genet. 2013;54(4):391–406.
25. Rebouças EL, et al. Real time PCR and importance of housekeepings genes for normalization and quantification of mRNA expression in different tissues. Braz Arch Biol Technol. 2013;56(1):143–54.
26. Suzuki T, Higgins PJ, Crawford DR. Control selection for RNA quantitation. Biotechniques. 2000;29(2):332–7.
27. Radonić A, Thulke S, Mackay IM, Landt O, Siegert W, Nitsche A. Guideline to reference gene selection for quantitative real-time PCR. Biochem Biophys Res Commun. 2004;313(4):856–62.
28. Sinn BV, Darb-Esfahani S, Wirtz RM, Faggad A, Weichert W, Buckendahl AC, et al. Vascular endothelial growth factor C mRNA expression is a prognostic factor in epithelial ovarian cancer as detected by kinetic RT-PCR in formalin-fixed paraffin-embedded tissue. Virchows Arch. 2009;455(6):461–7.
29. Li Y-L, Ye F, Hu Y, Lu WG, Xie X. Identification of suitable reference genes for gene expression studies of human serous ovarian cancer by real-time polymerase chain reaction. Anal Biochem. 2009;394(1):110–6.
30. Nikishin DA, Filatov MA, Kiseleva MV, Bagaeva TS, Konduktorova VV, Khramova YV, et al. Selection of stable expressed reference genes in native and vitrified/thawed human ovarian tissue for analysis by qRT-PCR and Western blot. J Assist Reprod Genet. 2018;35(10):1851–60.
31. Sharan R, et al. Consensus reference gene (s) for gene expression studies in human cancers: end of the tunnel visible? Cell Oncol. 2015;38(6):419–31.
32. Borkowska P, Zielińska A, Paul-Samojedny M, Stojko R, Kowalski J. Evaluation of reference genes for quantitative real-time PCR in Wharton's jelly-derived mesenchymal stem cells after lentiviral transduction and differentiation. Mol Biol Rep. 2020;47(2):1107–15.

33. Shen Y, Li Y, Ye F, Wang F, Lu W, Xie X. Identification of suitable reference genes for measurement of gene expression in human cervical tissues. Anal Biochem. 2010;405(2):224–9.
34. Fu J, Bian L, Zhao L, Dong Z, Gao X, Luan H, et al. Identification of genes for normalization of quantitative real-time PCR data in ovarian tissues. Acta Biochim Biophys Sin. 2010;42(8):568–74.
35. Ofinran O, Bose U, Hay D, Abdul S, Tufatelli C, Khan R. Selection of suitable reference genes for gene expression studies in normal human ovarian tissues, borderline ovarian tumours and ovarian cancer. Mol Med Rep. 2016;14(6):5725–31.
36. Kolkova Z, Arakelyan A, Casslén B, Hansson S, Kriegova E. Normalizing to GADPH jeopardises correct quantification of gene expression in ovarian tumours–IPO8 and RPL4 are reliable reference genes. J Ovarian Res. 2013;6(1):60.
37. Yang L, He J, Huang S, Zhang X, Bian Y, He N, et al. Activation of hedgehog signaling is not a frequent event in ovarian cancers. Mol Cancer. 2009;8(1):112.
38. Sharungbam GD, Schwager C, Chiblak S, Brons S, Hlatky L, Haberer T, et al. Identification of stable endogenous control genes for transcriptional profiling of photon, proton and carbon-ion irradiated cells. Radiat Oncol. 2012;7(1):70.
39. Li J, Zhuang Q, Lan X, Zeng G, Jiang X, Huang Z. PES1 differentially regulates the expression of ERα and ERβ in ovarian cancer. IUBMB Life. 2013;65(12):1017–25.
40. Aithal MG, Rajeswari N. Validation of housekeeping genes for gene expression analysis in glioblastoma using quantitative real-time polymerase chain reaction. Brain Tumor Res Treat. 2015;3(1):24–9.
41. Nazet U, Schröder A, Grässel S, Muschter D, Proff P, Kirschneck C. Housekeeping gene validation for RT-qPCR studies on synovial fibroblasts derived from healthy and osteoarthritic patients with focus on mechanical loading. PLoS One. 2019;14(12):e0225790.
42. Biade S, Marinucci M, Schick J, Roberts D, Workman G, Sage EH, et al. Gene expression profiling of human ovarian tumours. Br J Cancer. 2006;95(8):1092–100.
43. Caracausi M, Piovesan A, Antonaros F, Strippoli P, Vitale L, Pelleri MC. Systematic identification of human housekeeping genes possibly useful as references in gene expression studies. Mol Med Rep. 2017;16(3):2397–410.

Publisher's note Springer Nature remains neutral with regard to jurisdictional claims in published maps and institutional affiliations.

ii. Co-authored article

Journal of Assisted Reproduction and Genetics (2018) 35:41–48
https://doi.org/10.1007/s10815-017-1091-3

FERTILITY PRESERVATION

A novel fibrin-based artificial ovary prototype resembling human ovarian tissue in terms of architecture and rigidity

Maria Costanza Chiti[1] · Marie-Madeleine Dolmans[1,2] · Lucie Mortiaux[3] · Flanco Zhuge[3] · Emna Ouni[1] · Parinaz Asiabi Kohneh Shahri[1] · Evelyne Van Ruymbeke[3] · Sophie-Demoustier Champagne[3] · Jacques Donnez[4] · Christiani Andrade Amorim[1]

Received: 20 July 2017 / Accepted: 14 November 2017 / Published online: 13 December 2017
© Springer Science+Business Media, LLC, part of Springer Nature 2017

Abstract

Purpose The aim of this study is to optimize fibrin matrix composition in order to mimic human ovarian tissue architecture for human ovarian follicle encapsulation and grafting.

Methods Ultrastructure of fresh human ovarian cortex in age-related women ($n = 3$) and different fibrin formulations (F12.5/T1, F30/T50, F50/T50, F75/T75), rheology of fibrin matrices and histology of isolated and encapsulated human ovarian follicles in these matrices.

Results Fresh human ovarian cortex showed a highly fibrous and structurally inhomogeneous architecture in three age-related patients, but the mean SD of fiber thickness (61.3 to 72.4 nm) was comparable between patients. When the fiber thickness of four different fibrin formulations was compared with human ovarian cortex, F50/T50 and F75/T75 showed similar fiber diameters to native tissue, while F12.5/T1 was significantly different (p value < 0.01). In addition, increased concentrations of fibrin exhibited enhanced storage modulus with F50/T50, resembling physiological ovarian rigidity. Excluding F12.5/T1 from further analysis, only three remaining fibrin matrices (F30/T50, F50/T50, F75/T75) were histologically investigated. For this, frozen-thawed fragments of human ovarian tissue collected from 22 patients were used to isolate ovarian follicles and encapsulate them in the three fibrin formulations. All three yielded similar follicle recovery and loss rates soon after encapsulation. Therefore, based on fiber thickness, porosity, and rigidity, we selected F50/T50 as the fibrin formulation that best mimics native tissue.

Conclusions Of all the different fibrin matrix concentrations tested, F50/T50 emerged as the combination of choice in terms of ultrastructure and rigidity, most closely resembling human ovarian cortex.

Keywords Human ovarian tissue microstructure · Scanning electron microscopy · Fibrin matrix · Porosity · Isolated follicles · Artificial ovary

✉ Marie-Madeleine Dolmans
marie-madaleine.dolmans@uclouvain.be

Maria Costanza Chiti
maria.chiti@clouvain.be

Lucie Mortiaux
luciemortiaux@gmail.com

Flanco Zhuge
flanco.zhuge@uclouvain.be

Emna Ouni
emna.ouni@uclouvain.be

Parinaz Asiabi Kohneh Shahri
parinaz.asiabi@uclouvain.be

Evelyne Van Ruymbeke
evelyne.vanruymeke@uclouvain.be

Sophie-Demoustier Champagne
sophie.demoustier@uclouvain.be

Jacques Donnez
jacque.donnez@gmail.com

Christiani Andrade Amorim
christiani.amorim@uclouvain.be

[1] Pôle de Recherche en Gynécologie, Institut de Recherche Expérimentale et Clinique, Université Catholique de Louvain, Avenue Mounier 52, bte. B1.52.02, 1200 Brussels, Belgium

[2] Gynecology Department, Cliniques Universitaires Saint-Luc, 1200 Brussels, Belgium

[3] Institute of Condensed Matter and Nanosciences, Bio and Soft Matter, Université Catholique de Louvain, Croix du Sud 1, 1348 Louvain-la-Neuve, Belgium

[4] Society for Research into Infertility, Brussels, Belgium

Introduction

Ovarian tissue cryopreservation and transplantation after cancer remission is a promising fertility restoration strategy that has already led to more than 100 live births worldwide [1–3]. Nevertheless, cancer patients at high risk of ovarian involvement cannot undergo ovarian tissue transplantation after being cured because of reasonable concerns about disease recurrence [4–7]. With a view to offering these women future alternatives allowing them to conceive, in recent years, we have been developing a transplantable artificial ovary. Conceptually, the artificial ovary requires cryopreservation of ovarian tissue before initiation of cancer treatment, followed by follicle isolation and encapsulation inside an artificial matrix, before grafting to the patient with the goal of restoring her endocrine and reproductive functions [8]. Despite encouraging results showing that a safe and efficient follicle isolation procedure is now feasible for human application [9–12], creating the appropriate scaffold to encapsulate and temporarily support human follicles after grafting remains a challenge [13].

Many different matrices have already been tested [14–21], with a fibrin-based scaffold emerging as the elective choice for construction of an artificial ovary prototype [22]. Since the majority of studies in this field have been conducted with mouse follicles, it is vital to investigate the right combination of fibrinogen and thrombin (F/T) to use in humans. These two components are the principal constituents of fibrin and key players in controlling the porosity and rigidity of the scaffold, and hence the ability to encapsulate and graft human follicles. Previous studies [23, 24] have suggested that while a fibrin matrix with low concentrations of fibrinogen and thrombin (F12.5/T1) is suitable for encapsulation and grafting of mouse secondary follicles, it may lack adequate stiffness to support primordial-primary follicles. This hypothesis was subsequently confirmed by Paulini et al. [21] using a scaffold with higher concentrations of fibrinogen and thrombin (F50/T10) to encapsulate and graft human primordial-primary follicles [21]. However, in order to design an artificial matrix that mimics the physiological ovarian environment, it is first necessary to gather more knowledge on the physical structure of the native human ovary.

Our study therefore aims to investigate human ovarian tissue microstructure in order to identify the fibrin formulation that best resembles the natural milieu of the human ovary in terms of architecture, porosity, and rigidity.

Materials and methods

Experimental design

Fresh human ovarian cortex samples ($n = 3$) were obtained from three age-related women (28–34 years of age) after laparoscopic surgery for benign gynecological disease after gaining informed consent. These biopsies and four different fibrin clot formulations (F12.5/T1, F30/T50, F50/T50, F75/T75) were analyzed by scanning electron microscopy (SEM) to assess and compare their ultrastructure. Fibrin matrices were also investigated for storage or elastic modulus (G') in order to evaluate their stiffness. Based on the significant difference in fiber thickness and porosity between F12.5/T1 and human ovarian cortex, as well as our previous unpublished findings on human follicles [25], we excluded F12.5/T1 from subsequent histological analysis. Frozen cryovials of ovarian cortex from different patients ($n = 22$) were then collected from the ovarian tissue bank, thawed and processed for follicle isolation, as previously described in one of our recently submitted papers [26]. Once isolated, preantral follicles (between 14 and 50) were embedded in the three remaining fibrin clot formulations (F30/T50, F50/T50, F75/T75) in order to compare follicle recovery and loss rates after fibrin encapsulation.

Ethics

Use of human ovarian tissue was approved by the Institutional Review Board of the Université Catholique de Louvain on 2 June, 2014 (IRB reference 2012/23MAR/125, registration number B403201213872). After obtaining informed consent, fragments of ovarian tissue were collected from patients affected by mesothelial cysts, rectovaginal nodules without associated ovarian endometriomas, and pelvic inflammatory disease.

Fibrin clot reconstitution

Reconstitution and dilution of the two components (fibrinogen and thrombin) of the fibrin sealant kit (Tissucol, Baxter, Lessines, Belgium) and fibrin clot formation were previously described by Paulini et al. [21]. Fibrinogen (100 mg/mL) was diluted in saline solution (0.9% NaCl) to obtain four concentrations, 12.5, 30, 50, and 75 mg/mL, and thrombin (500 IU/mL) in 40 mmol/L $CaCl_2$ to achieve concentrations of 1, 50, and 75 IU/mL. For fibrin polymerization, 100 μL of the appropriate fibrinogen concentration was mixed once with 100 μL of the corresponding thrombin concentration and incubated at 37 °C for 15 or 45 min depending on the F/T combination. The samples were then fixed in Karnovsky solution (2.5% glutaraldehyde [Agar Scientific, Brussels, Belgium] and 4% paraformaldehyde in 0.1 M phosphate-buffered saline [PBS]) for 24 h or immediately processed for rheological investigations.

Morphological analysis of human ovarian cortex and different fibrin matrices

Ovarian biopsies were immediately transported on ice to the laboratory in minimal essential medium plus Glutamax™

(MEM; Gibco, Invitrogen, Merelbeeke, Belgium). The medulla was removed with surgical scissors and the cortex fixed in Karnovsky solution for 24 h. After fixation, the ovarian fragments and four different fibrin matrices were immersed overnight in a solution of 30% glycerol in 0.1 M PBS (4 °C), plunged into liquid nitrogen, and cryofractured. The samples were washed in fresh 0.1 M PBS three times for 5 min each, before post-fixation with a solution of 2% osmium tetroxide (OsO_4) in 0.1 M PBS in the dark. After 1 h, the washing step was repeated three times, as previously described. The samples were then dehydrated with a graded series of ethanol (30–100%), dried to the critical point, coated with gold film (Cressington sputter coater 208HR), and analyzed by SEM (JSM-7600F, JEOL) set at 15-keV electron beam energy.

Rheological analysis of the mechanical properties of different fibrin formulations

In order to measure the rigidity of the four different fibrin matrices, their linear viscoelastic properties were investigated by small-amplitude oscillatory shear rheology using an MCR 301 (Anton Paar, Germany) rheometer. Temperature was controlled by a convection oven operating under air. Measurements were obtained at 37 °C using 8-mm parallel-plate geometry. Sandpaper was fixed to the lower plate to avoid slipping and ensure good adhesion of the samples to the steel surface. Each fibrin formulation was analyzed and compared for G'.

Thawing of frozen ovarian cortex and follicle isolation

Cryovials of frozen ovarian cortex from different patients (n = 22) were thawed and processed for follicle isolation, as recently described [26]. Briefly, after mechanical tissue dissociation, the ovarian tissue was incubated in 10 mL of PBS with Ca^{2+} and Mg^{2+} (Gibco, Thermo Fisher Scientific, Ghent, Belgium) in the presence of 0.28 Wünsch units/mL Liberase DH (Roche Diagnostics) and 8 Kunitz units/mL DNase I (Roche Diagnostics, Brussels, Belgium) in a water bath (37 °C) for up to 90 min with gentle agitation and pipetted every 15 min. The enzymatic digestion step was halted by adding a similar volume of PBS + 10% heat-inactivated fetal bovine serum. Fully isolated follicles were retrieved with the help of a stereomicroscope and 130-μm micropipette by two operators.

Follicle encapsulation and histological analysis

Because of the considerable difference in fiber thickness and porosity between human ovarian cortex and the F12.5/T1 combination encountered after SEM analysis, this fibrin formulation was not further investigated for follicle encapsulation. Only the three remaining F/T combinations were used to embed human follicles for histological analysis. For follicle encapsulation, a droplet of 12 μL fibrinogen (30, 50, and 75 mg/mL) was deposited on a glass petri dish, to which between 14 and 50 isolated preantral follicles were added (3 μL). The droplet was then mixed with 15 μL thrombin (50 and 75 IU/mL) and incubated at 37 °C for 15 min. After polymerization, the fibrin clot was gently detached, covered with 2% melted agarose (UltraPure, Thermo Fisher Scientific, Ghent, Belgium) and immediately fixed in 4% formalin [27]. After 24 h of fixation, the clots were embedded in paraffin for histology. Each fibrin clot was cut into 5-μm serial sections and every second section was stained with hematoxylin and eosin to count and compare the encapsulated follicles and follicular structures. Follicles were identified by a surrounding basal lamina and GCs with a central oocyte. Follicular structures were defined as groups of cells organized in round formations with no visible oocyte.

Statistical analysis

The Kruskal-Wallis test was applied to compare fiber thickness between ovarian tissue samples and fibrin matrices, and follicle recovery and loss rates after fibrin encapsulation. A p value < 0.05 was considered statistically significant. All statistical analyses were performed with GraphPad Prism 7 software (GraphPad, La Jolla, USA). Dunn's multiple comparison test was also conducted post hoc.

Results

Microstructure of human ovarian cortex and fibrin matrices

The overall architecture of ovarian tissue showed no significant difference in fiber density or fiber organization between patients (Fig. 1). Indeed, all ovarian cortex fragments were found to be highly fibrous and structurally inhomogeneous. A visible cluster of primordial-primary follicles is shown in Fig. 1c. There was also no significant difference in mean SD fiber thickness (61.3 to 72.4 nm) between patients.

As illustrated in Fig. 2, all fibrin formulations exhibited a fibrillary structure and more homogeneous organization of their filaments than did human ovarian tissue. Moreover, when F/T concentrations were raised, we observed an increase in the number of fibers, and hence fibrin consistency. On the other hand, the porosity of fibrin networks as well as fiber diameter decreased at higher F/T concentrations (Table 1). When mean SD fiber thickness was compared with human ovarian tissue, a significant difference was observed only with F12.5/T1 ($p < 0.01$), while F50/T50 and F75/T75 showed very similar fiber thickness values to ovarian cortex (Fig. 2).

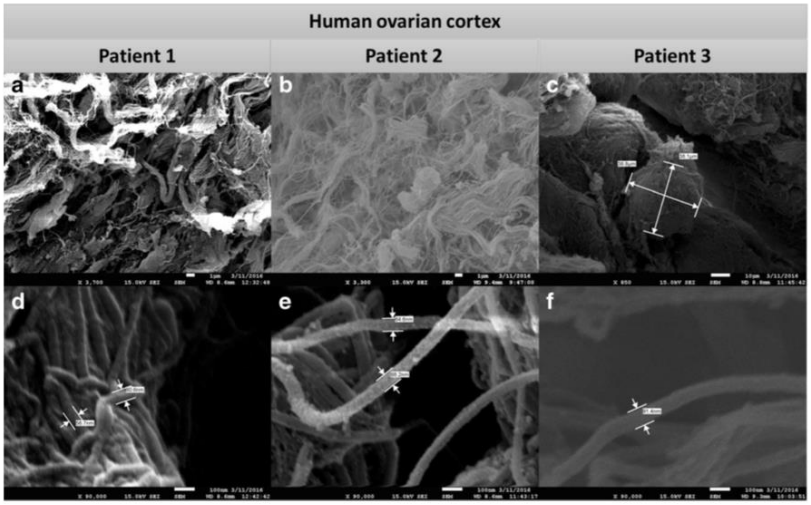


Fig. 1 SEM analysis of fresh human ovarian cortex. No significant difference was found between ovarian tissue fragments from the three patients. Patients 1 (**a**) and 2 (**b**) show heterogeneous distribution of collagen fibers. In patient 3, we can observe a cluster of primordial-primary follicles (one of them marked with crossed white arrows) of 38 μm (**c**). Fiber thickness (white arrows and bars) was measured in ovarian samples from all patients (**d**–**f**)

Viscoelastic properties of different fibrin formulations

As previously mentioned, four different fibrin matrices (F12.5/T1, F30/T50, F50/T50, F75/T75) were investigated for G'. Dynamic oscillatory shear measurements were taken at 37 °C in order to characterize the viscoelastic response of the samples. First, strain sweep tests were conducted at a frequency of 1 rad/s to determine the limits of the linear regime of deformation. Based on these results, the amplitude of deformation used in frequency sweep tests was fixed at 0.4% for all samples to ensure measurements within the linear regime. In all samples, experimental storage moduli showed fully elastic behavior (namely with G' almost independent of the frequency of oscillatory shear flow). Corresponding values of the storage moduli (140, 1100, 3800, and 9300 Pa) are presented in Fig. 3 for all four concentrations. Higher F/T concentrations gave rise to increased G', resulting from more cross-linking points within the systems, yielding a more rigid fibrin matrix.

Follicle encapsulation and histological analysis

After follicle isolation, a total of 696 follicles were retrieved and encapsulated in the three selected fibrin formulations: 216, 228, and 252 follicles were placed in F30/T50 ($n = 7$ clots), F50/T50 ($n = 7$ clots), and F75/T75 ($n = 7$ clots) fibrin clots, respectively, and processed for hematoxylin and eosin staining. Then, to evaluate whether fibrin matrix concentrations would influence follicle recovery and loss, we counted and compared the number of follicles detected in the three different fibrin formulations. As shown in Table 2, mean follicle recovery and loss rates ranged between 44 and 47% and 29 and 39%, respectively. However, when mean SD values of follicles found and lost were compared, no statistical difference was noted between the three fibrin formulations shortly after encapsulation (Table 2). Figure 4 shows isolated follicles encapsulated in the different fibrin scaffold concentrations.

Discussion

With a view to creating a transplantable artificial ovary, our aim was to optimize fibrin scaffold composition [16, 21, 23, 24] for human follicle encapsulation and grafting.

Human ovarian cortex and fibrin matrix microstructure

One of the key aspects in the design of the artificial ovary is a supporting matrix [8]. Among all different matrices used in in vivo studies [14–21, 28], a fibrin-based scaffold appears to be the best choice [22]. However, our previous studies have demonstrated that while a fibrin matrix with low concentrations of fibrinogen and thrombin (F12.5/T1) may well be

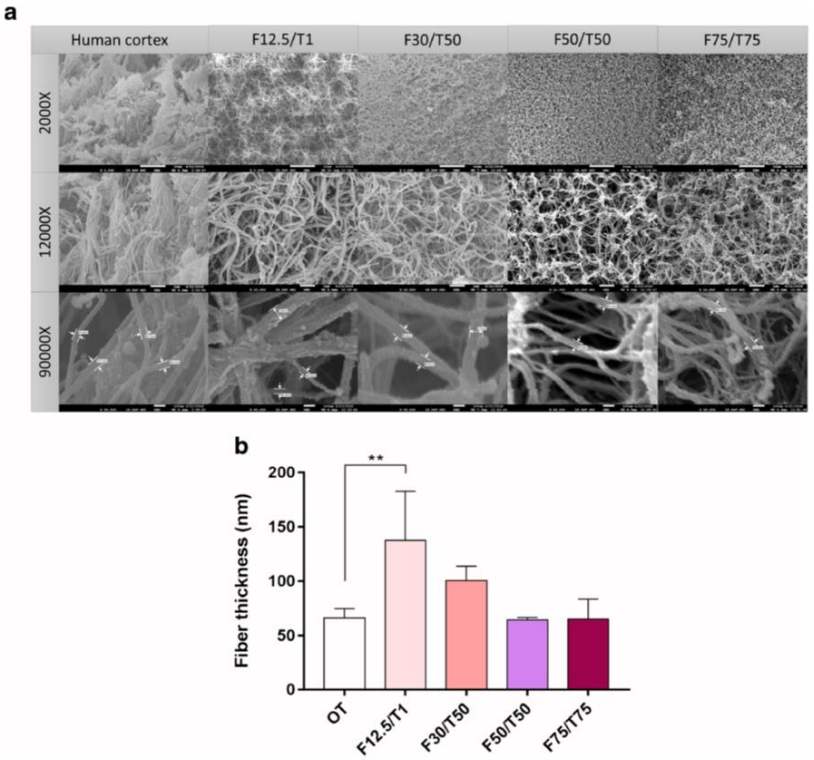


Fig. 2 Ultrastructure of human ovarian cortex and different fibrin formulations. SEM image of human ovarian cortex and fibrin matrix formulations at different magnifications (× 2000; × 12,000; × 90,000) (**a**). Graphic representation of fiber thickness in human ovarian tissue (OT) and four fibrin formulations (**b**)

suitable for encapsulation and grafting of mouse secondary follicles, it could lack the required stiffness to support human primordial-primary follicles [16, 23, 24]. This hypothesis was reinforced when we observed that human preantral follicles showed better survival rates with higher F/T concentrations (F50/T10) [21]. We therefore decided to conduct a more in-depth analysis of the ultrastructure of human ovarian cortex and compare our findings with different fibrin formulations based on in vivo studies from the existing literature [22].

Table 1 Fibrin fiber thickness according to different fibrin formulations. Increased F/T concentrations exhibited decreased fiber thickness

Fiber thickness (mean SD)	
F12.5/T1	137.5 45.5 nm
F30/T50	100.8 13.2 nm
F50/T50	64.5 2.3 nm
F75/T75	65.4 18.4 nm

Indeed, our goal was to identify the fibrin formulation that most closely mimics physiological ovarian cortex architecture.

In the present study, we demonstrated that fragments of ovarian cortex collected from women of similar age have a generally similar architecture, with a very dense, fibrous, and inhomogeneous structure characterized by interlaced collagen fibers of comparable thickness. It has been proved that collagen fibrils, which constitute one of the most abundant components of the ovarian extracellular matrix [29, 30], tend to increase in number [31] and diameter with age [32]. We showed that conducting a comparative analysis between human ovarian cortex microstructure and fibrin formulations is an efficient way of identifying a supporting scaffold that best resembles the architecture of the human ovary, achieving optimal porosity to encapsulate and transplant follicles. Considering the vast physiological differences that exist between rodent

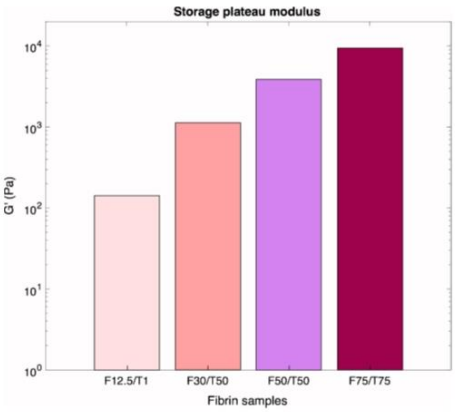


Fig. 3 Graphic representation of fibrin rigidity (storage modulus G') according to different fibrin formulations. The stiffness (G') of fibrin matrices was positively correlated with increased concentrations of fibrinogen and thrombin

and primate ovaries [33], use of mouse follicles for the design of an artificial ovary prototype, as suggested by Laronda et al. [19], may not necessarily be translatable to humans, so caution should be exercised. Hence, in our study, we considered human ovarian tissue architecture as the reference standard for creation of the artificial ovary prototype. Importantly, the great difference found between F12.5/T1 and ovarian tissue ultrastructure may also explain the low human follicle recovery rates encountered in our previous study, when preantral follicles were encapsulated in F12.5/T1 and grafted to mice [25]. Indeed, some fibrin matrix combinations exhibited a less dense and compact structure, with more homogeneous and organized distribution of fibrin fibers than human ovarian cortex. In addition, an inverse correlation was found between F/T concentrations, fiber thickness, and pore size, as documented in other reports [34–36]. Interestingly, when F/T concentrations were increased to F50/T50 and F75/T75, the formulations exhibited fiber thickness comparable to human ovarian cortex. This led us to hypothesize that these combinations may mimic the physiological environment of human follicles more closely, making them good candidates for the artificial ovary prototype. However, another important feature to consider in the development of a transplantable artificial ovary is the rigidity of the matrix. It has been previously demonstrated that ovary stiffness [37], hence also that of the artificial ovary prototype [21, 38], may influence follicle behavior. We therefore decided to investigate the storage modulus of the four selected fibrin matrices and compare it with that of human ovarian tissue [39]. As expected, increased concentrations of fibrinogen and thrombin yielded higher G' levels, and consequently greater rigidity, in line with earlier reports from the literature [36, 40]. Nevertheless, only F50/T50 showed similar rigidity to human ovarian tissue [39].

Table 2 Follicle recovery rates, follicular structures, and follicle loss after fibrin matrix encapsulation. Follicle recovery rates, follicular structures, and follicle loss with different fibrin formulations were compared shortly after encapsulation

Fibrin formulation	Follicle recovery		Follicular structures		Follicle loss	
F30/T50 ($n = 7$)	46	21%a	26	17%b	38	21%c
F50/T50 ($n = 7$)	44	24% a	18	11%b	39	20%c
F75/T75 ($n = 7$)	47	22%a	23	14%b	29	30%c

Different letters in each column (a, b, c) indicate significant differences ($p < 0.05$)

Follicle encapsulation

Based on the great difference encountered between human ovarian cortex and F12.5/T1 ultrastructure, as well as previously discouraging findings with human follicles encapsulated in F12.5/T1 and subsequently grafted [25], we excluded this fibrin formulation from further histological investigations. From the other three fibrin combinations, around 50% of follicles were recovered soon after fibrin polymerization, which is consistent with earlier studies using human follicles [21]. However, a non-negligible percentage of follicle loss was found with all fibrin formulations, as previously stated for mouse follicles [24]. Taking into account that most follicles are normally located at the border of the fibrin clot, this loss may be partially explained by retraction of the fibrin matrices after fixation and dehydration, which typically occurs during histological processing. In the context of future clinical application, it should be borne in mind that the fibrin clot needs to be grafted to the patient as soon as it is created.

General conclusion

In conclusion, among all the different fibrin matrix concentrations tested, F50/T50 appears to be the combination of choice in terms of ultrastructure and rigidity, most closely resembling human ovarian cortex. Such findings are essential to help us standardize fibrin matrix architecture.

Acknowledgments The authors thank Patricia Meijers for her collaboration and scientific advice on fibrin in the project. They also thank Mira Hryniuk, BA, for reviewing the English language of the manuscript and Delphine Magnin, Dolores Gonzalez, and Olivier Van Kerk for their technical assistance. This study was supported by grants from the Fonds National de la Recherche Scientifique de Belgique (FNRS) awarded to C. A. Amorim as a research associate for the FRS-FNRS and M.M. Dolmans (grant 5/4/150/5), Fonds Spéciaux de Recherche, Fondation St Luc,

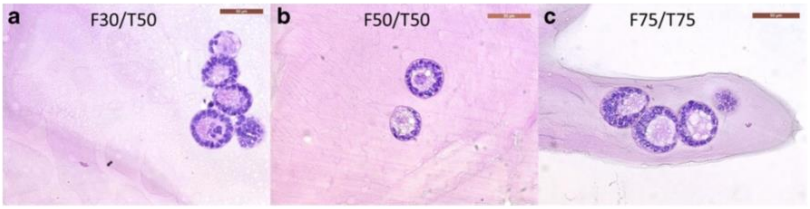


Fig. 4 Histology of isolated human follicles in different fibrin formulations. Follicles encapsulated in F30/T50 (**a**), F50/T50 (**b**), and F75/T75 (**c**). Scale bar 50 μm

Foundation Against Cancer, and Wallonie-Bruxelles International, and donations from the Ferrero family.

Compliance with ethical standards

Conflict of interest The authors declare that they have no conflict of interest.

References

1. Donnez J, Dolmans MM. Ovarian cortex transplantation: 60 reported live births brings the success and worldwide expansion of the technique towards routine clinical practice. J Assist Reprod Genet. 2015;32(8):1167–70.
2. Anderson RA, Wallace WHB, Telfer EE. Ovarian tissue cryopreservation for fertility preservation: clinical and research perspectives. Human Reproduction Open. 2017;2017(1):hox001-hox.
3. Jensen AK, Macklon KT, Fedder J, Ernst E, Humaidan P, Andersen CY. 86 successful births and 9 ongoing pregnancies worldwide in women transplanted with frozen-thawed ovarian tissue: focus on birth and perinatal outcome in 40 of these children. J Assist Reprod Genet. 2017;34(3):325–36.
4. Smitz J, Dolmans MM, Donnez J, Fortune JE, Hovatta O, Jewgenow K, et al. Current achievements and future research directions in ovarian tissue culture, in vitro follicle development and transplantation: implications for fertility preservation. Hum Reprod Update. 2010;16(4):395–414.
5. Dolmans MM, Luyckx V, Donnez J, Andersen CY, Greve T. Risk of transferring malignant cells with transplanted frozen-thawed ovarian tissue. Fertil Steril. 2013;99(6):1514–22.
6. Donnez J, Dolmans MM. Fertility preservation in women. Nat Rev Endocrinol. 2013;9(12):735–49.
7. Soares M, Saussoy P, Maskens M, Reul H, Amorim CA, Donnez J, et al. Eliminating malignant cells from cryopreserved ovarian tissue is possible in leukaemia patients. Br J Haematol. 2017;178(2):231–239.
8. Amorim CA. Artificial ovary. In: Suzuki N, Donnez J. Gonadal tissue cryopreservation in fertility preservation. Tokyo: Springer; 2016. p. 175–192.
9. Kristensen SG, Rasmussen A, Byskov AG, Andersen CY. Isolation of pre-antral follicles from human ovarian medulla tissue. Human reproduction (Oxford, England). 2011;26(1):157–66.
10. Vanacker J, Camboni A, Dath C, Van Langendonckt A, Dolmans MM, Donnez J, et al. Enzymatic isolation of human primordial and primary ovarian follicles with Liberase DH: protocol for application in a clinical setting. Fertil Steril. 2011;96(2):379–83.e3.
11. Lierman S, Tilleman K, Cornelissen M, De Vos WH, Weyers S, T'Sjoen G, et al. Follicles of various maturation stages react differently to enzymatic isolation: a comparison of different isolation protocols. Reprod BioMed Online. 2015;30(2):181–90.
12. Soares M, Sahrari K, Amorim CA, Saussoy P, Donnez J, Dolmans MM. Evaluation of a human ovarian follicle isolation technique to obtain disease-free follicle suspensions before safely grafting to cancer patients. Fertil Steril. 2015;104(3):672–80.e2.
13. Amorim CA, Shikanov A. The artificial ovary: current status and future perspectives. Future oncology (London, England). 2016;12(20):2323–32.
14. Dolmans MM, Martinez-Madrid B, Gadisseux E, Guiot Y, Yuan WY, Torre A, et al. Short-term transplantation of isolated human ovarian follicles and cortical tissue into nude mice. Reproduction (Cambridge, England). 2007;134(2):253–62.
15. Vanacker J, Dolmans MM, Luyckx V, Donnez J, Amorim CA. First transplantation of isolated murine follicles in alginate. Regen Med. 2014;9(5):609–19.
16. Luyckx V, Dolmans MM, Vanacker J, Legat C, Fortuno Moya C, Donnez J, et al. A new step toward the artificial ovary: survival and proliferation of isolated murine follicles after autologous transplantation in a fibrin scaffold. Fertil Steril. 2014;101(4):1149–56.
17. Kniazeva E, Hardy AN, Boukaidi SA, Woodruff TK, Jeruss JS, Shea LD. Primordial follicle transplantation within designer biomaterial grafts produce live births in a mouse infertility model. Sci Rep. 2015;5:17709.
18. Laronda MM, Jakus AE, Whelan KA, Wertheim JA, Shah RN, Woodruff TK. Initiation of puberty in mice following decellularized ovary transplant. Biomaterials. 2015;50:20–9.
19. Laronda MM, Rutz AL, Xiao S, Whelan KA, Duncan FE, Roth EW, et al. A bioprosthetic ovary created using 3D printed microporous scaffolds restores ovarian function in sterilized mice. Nat Commun. 2017;8:15261.
20. Kim J, Perez AS, Claflin J, David A, Zhou H, Shikanov A. Synthetic hydrogel supports the function and regeneration of artificial ovarian tissue in mice. Npj Regenerative Medicine. 2016;1:16010.
21. Paulini F, Vilela JM, Chiti MC, Donnez J, Jadoul P, Dolmans MM, et al. Survival and growth of human preantral follicles after cryopreservation of ovarian tissue, follicle isolation and short-term xenografting. Reprod BioMed Online. 2016;33(3):425–32.
22. Chiti MC, Dolmans MM, Donnez J, Amorim CA. Fibrin in reproductive tissue engineering: a review on its application as a biomaterial for fertility preservation. Ann Biomed Eng. 2017;45(7):1650–1663.
23. Chiti MC, Dolmans MM, Orellana R, Soares M, Paulini F, Donnez J, et al. Influence of follicle stage on artificial ovary outcome using fibrin as a matrix. Human reproduction (Oxford, England). 2016;31(2):427–35.
24. Chiti MC, Dolmans MM, Lucci CM, Paulini F, Donnez J, Amorim CA. Further insights into the impact of mouse follicle stage on graft outcome in an artificial ovary environment. Mol Hum Reprod. 2017;23(6):381–392.
25. Amorim CA. The ovarian follicle microenviroment and the artificial ovary. Shanghai: 4th World Congress of International Society for Fertility Preservation; 2015.

26. Chiti MC. A modified and tailored human follicle isolation procedure improve follicle survival in an artificial ovary prototype after short term xenografting. J Ovarian Res. 2017;10(1):71.
27. Fox CH, Johnson FB, Whiting J, Roller PP. Formaldehyde fixation. The journal of histochemistry and cytochemistry : official journal of the Histochemistry Society. 1985;33(8):845–53.
28. Smith RM, Shikanov A, Kniazeva E, Ramadurai D, Woodruff TK, Shea LD. Fibrin-mediated delivery of an ovarian follicle pool in a mouse model of infertility. Tissue Eng A. 2014;20(21–22):3021–30.
29. Rodgers RJ, Irving-Rodgers HF, Russell DL. Extracellular matrix of the developing ovarian follicle. Reproduction (Cambridge, England). 2003;126(4):415–24.
30. Cho A, Howell VM, Colvin EK. The extracellular matrix in epithelial ovarian cancer—a piece of a puzzle. Front Oncol. 2015;5:245.
31. Herraiz S, Diaz-Garcia C, Pellicer A. Ovarian tissue cryopreservation: slow freezing. In: Suzuki N, Donnez J, editors. Gonadal tissue cryopreservation in fertility preservation. Tokyo: Springer Japan; 2016. p. 53–77.
32. Armstrong CG, Mow VC. Variations in the intrinsic mechanical properties of human articular cartilage with age, degeneration, and water content. J Bone Joint Surg Am. 1982;64(1):88–94.
33. Chaffin CL, Vandevoort CA. Follicle growth, ovulation, and luteal formation in primates and rodents: a comparative perspective. Experimental biology and medicine (Maywood, NJ). 2013;238(5):539–48.
34. Wolberg AS. Thrombin generation and fibrin clot structure. Blood Rev. 2007;21(3):131–42.
35. Kim BS, Sung HM, You HK, Lee J. Effects of fibrinogen concentration on fibrin glue and bone powder scaffolds in bone regeneration. J Biosci Bioeng. 2014;118(4):469–75.
36. Germain L, De Berdt P, Vanacker J, Leprince J, Diogenes A, Jacobs D, et al. Fibrin hydrogels to deliver dental stem cells of the apical papilla for regenerative medicine. Regen Med. 2015;10(2):153–67.
37. Woodruff TK, Shea LD. A new hypothesis regarding ovarian follicle development: ovarian rigidity as a regulator of selection and health. J Assist Reprod Genet. 2011;28(1):3–6.
38. Choi JK, Agarwal P, Huang H, Zhao S, He X. The crucial role of mechanical heterogeneity in regulating follicle development and ovulation with engineered ovarian microtissue. Biomaterials. 2014;35(19):5122–8.
39. Wood CD, Vijayvergia M, Miller FH, Carroll T, Fasanati C, Shea LD, et al. Multi-modal magnetic resonance elastography for noninvasive assessment of ovarian tissue rigidity in vivo. Acta Biomater. 2015;13:295–300.
40. Duong H, Wu B, Tawil B. Modulation of 3D fibrin matrix stiffness by intrinsic fibrinogen-thrombin compositions and by extrinsic cellular activity. Tissue Eng A. 2009;15(7):1865–76.

iii. Co-authored book chapter

AMORIM CA, **ASIABI P**, OUNI E, VILELA J, CAMBONI A, CHITI MC. Transplantation of isolated follicles and the engineered ovary. IN: Female and Male Fertility Preservation. Grynberg M, Patrizio P (Eds). Springer Nature. Switzerland. 2020, *in press*.

CHAPTER 30

TRANSPLANTATION OF ISOLATED FOLLICLES AND THE ENGINEERED OVARY

Christiani A. Amorim, Parinaz Asiabi, Emna Ouni, Janice Vilela, Alessandra Camboni, Maria C. Chiti

Université Catholique de Louvain, Institut de Recherche Expérimentale et Clinique, Pôle de Recherche en Gynécologie, Avenue Mounier 52, bte. B1.52.02, 1200 Brussels, Belgium

1. Abstract

For over a decade, increasing numbers of research groups all over the world have focused their efforts on development of a transplantable engineered ovary. With the growing incidence of curable cancer among young girls and women and greater awareness of the need to safeguard fertility, the number of patients who can benefit from this strategy has also been rising, as having the possibilities of other applications. However, this scenario is still quite far from a clinical setting. Indeed, development of an engineered ovary has proved to be very challenging and our lack of knowledge of human ovaries makes this task even more difficult. While studies in mice have proved the feasibility of the concept, demonstrating the ability of engineered ovary prototypes to restore both endocrine and reproductive functions, new discoveries about human ovaries and their follicle populations show discrepancies between mammalian species. These relate to ovarian extracellular matrix composition and stiffness, and follicle development. Therefore, in this chapter, we will highlight progress that has already been made in constructing a transplantable engineered ovary and discuss possible future directions.

Key-words: Preantral follicles, ovary, leukemia, fertility preservation, transplantable engineered ovary, cancer

2. Introduction

Cancer is one of the major health issues worldwide, and the first or second leading cause of death depending on the world area investigated. Indeed, the International Agency for Research on Cancer estimated that in 2018, more than 276,000 people under 44 years were diagnosed with cancer in Europe (1). Incidence rates are significantly higher in females (65%) than males (35%) in these younger age groups (Fig. 1). However, thanks to vast improvements in cancer treatments, 5-year survival rates are now 65% in adults, and as high as 83% in children (2). Taking into account the known gonadotoxicity of some cancer treatments and increasing numbers of cancer survivors, fertility preservation is becoming a clinical and moral duty in oncological practice.

While most cancer patients can choose among different fertility preservation strategies, prepubertal patients and women who cannot delay the start of their chemo- or

radiotherapy have had to rely on ovarian tissue cryopreservation followed by orthotopic reimplantation once cured (3). Despite successful outcomes reported with this approach, including more than 130 live births to date (3), it cannot be universally applied. Indeed, in certain types of cancer, malignant cells may be present in the ovaries, so transplantation of frozen-thawed ovarian tissue fragments is not advised (4). Although most malignant tumors in reproductive-age subjects do not metastasize to the ovaries, hematological malignancies like leukemia and Burkitt's lymphoma, as well as neuroblastoma, carry a high risk of ovarian metastasis (5). Leukemia is the most common cancer in Europe among young girls up to 19 years of age, and the seventh most prevalent in women of reproductive age (20-44 years old), representing 5% of all cancer cases in women. Thanks to early diagnosis and improved treatments, almost 50% of patients survive (1). Burkitt's lymphoma accounts for around half of all malignant non-Hodgkin's lymphomas in children (6), with an estimated annual incidence of 3,000 girls aged between 0 and 14 years (1). Fortunately, around 85% of patients survive after treatment (6). Neuroblastoma represents around 10% of solid tumors in children under 15 years of age, affecting one in every 70,000 (7). In patients aged over one year, 5-year survival rates can reach 95% for some localized tumors (7).

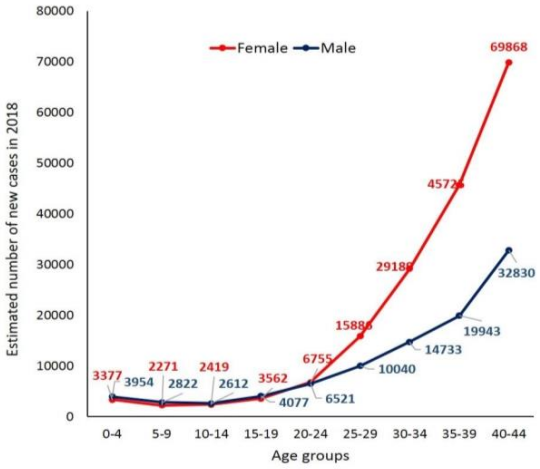


Figure 1. Estimated number of new cancer cases and age-specific incidence rates (1).

Since studies have shown that cancer cells are able to resist the freeze-thawing procedure and spread in the host after xenotransplantation (8), autografting of cryopreserved tissue can potentially lead to recurrence of the disease in affected patients. Sadly, there are no currently available options for fertility restoration in these women. However, there are two main approaches under development: *in vitro* growth of preantral follicles followed by *in vitro* maturation of their oocytes (see Chapter 29), or transplantation of isolated preantral follicles, also known as the engineered ovary. In the last decade, the idea of engineering an ovary has been gaining ground and increasing numbers of research teams worldwide have been concentrating their efforts on developing this strategy. The aim of this chapter is therefore to discuss the latest

advances in the field and future directions of this emerging fertility restoration approach.

3. Transplantable engineered ovary concept

By definition, the transplantable engineered ovary has the essential role of replacing the natural organ, thereby allowing complete folliculogenesis, with production of fertilizable mature oocytes and secretion of sex hormones. In order to construct a tissue-engineered ovary, we need to consider three essential points: (i) safe isolation of a large number of preantral follicles; (ii) presence of different populations of ovarian cells; and (iii) creation of a three-dimensional (3D), biodegradable matrix to encapsulate isolated follicles and cells, and protect them during and after grafting.

In practice, after patient remission, fragments of her frozen ovarian tissue would be thawed for further follicle isolation. In the meantime, a second ovarian biopsy would be taken from the patient after her cancer treatment for cell isolation. In this way, we could ensure that only ovarian cells would be added to the transplantable engineered ovary, as all malignant cells would have been destroyed by chemo- or radiotherapy. Isolated preantral follicles and ovarian cells would then be encapsulated inside the matrix and transplanted back to the patient.

4. Are isolated follicles able to survive and resume folliculogenesis after transplantation?

The follicle is the functional unit of the ovary and has two main functions: it is responsible for hormone production and providing the ideal environment for oocyte growth and development. Follicles are present in the ovary at different stages: primordial, primary, secondary and antral. Preantral follicles (primordial, primary and secondary) represent 90-95% of all follicles but, of this number, only 0.1% will go on to develop to the antral stage, while the rest will undergo atresia. Why so few follicles are destined to ovulate remains a mystery. However, it is known that not only follicle themselves, but also surrounding ovarian cells and extracellular matrix (ECM) play a role in the process.

Isolation of preantral follicles potentially allows us to safely use these structures in the transplantable engineered ovary, as they are enclosed inside a basement membrane that prevents their granulosa cells and oocyte coming into contact with capillaries, white blood cells and nerve processes (9). However, they cannot survive alone, as demonstrated in some *in vitro* culture studies. Indeed, while isolated mouse follicles enclosed in a collagen gel matrix were able to survive *in vitro* for at least two weeks, when they grew to multilayer stages, they showed signs of degeneration and no antrum or theca cell formation (10, 11). On the other hand, when isolated mouse follicles were transplanted together with ovarian cells, they successfully reached the antral stage in three days, with blood vessels appearing after five days and theca cells six days post-grafting (11). After 10 days, 16 oocytes were recovered for *in vitro* fertilization and 12 developed up to the 2-cell embryo stage (11).

After incorporating mouse ovarian tissue digests (isolated follicles and ovarian cells) in plasma clots, Gosden (12) transplanted them to the ovarian bursa of sterile mice. These constructs were able to restore fertility in their hosts, as pregnancies and offspring were

obtained after mating. Following graft removal, this author found ovary-like structures, with follicles at different stages of development. Carroll and Gosden (13) subsequently repeated the experiment using frozen-thawed ovaries and obtained similar results.

After isolation of follicles from human tissue, encapsulation of preantral follicles in plasma clots and xenotransplantation to immunodeficient mice, Dolmans et al. (14, 15) also reported follicle survival and growth. Moreover, stroma-like tissue of human origin was formed, suggesting the presence of isolated human stromal cells in the constructs. Indeed, when retrieving isolated follicles, we may inadvertently pick up isolated cells too (16). The constructs were found to be well vascularized already one week after xenografting (14) and, like in mice (12, 13), ovary-like tissue was observed (14, 15).

Based on these pioneering studies, we can confirm that preantral follicles are able to survive and resume growth after isolation and transplantation, but they need to be transplanted along with their accompanying ovarian cells and encapsulated in a 3D matrix.

5. How can we improve survival and growth of isolated follicles after transplantation?

The pioneering studies mentioned above revealed the basic requirements for survival of isolated follicles after transplantation. In recent years, numerous experiments have investigated matrix materials and cell populations for development of the transplantable engineered ovary.

5.1. Matrix materials: from polymers to decellularized ovarian tissue

One of the key steps in the development of the transplantable engineered ovary is finding the right matrix material to encapsulate isolated ovarian preantral follicles. Different hydrogels have been used for transplantation of isolated follicles in an attempt to enhance efficacy (11, 12, 17-22). Despite great advances, we still not identified the best matrix material to support complete human folliculogenesis. Indeed, our knowledge of human ovarian tissue remains incomplete, and great differences emerged when murine and human follicles were transplanted inside an engineered ovary prototype (23). Therefore, in this section, we will first briefly mention the general features of a 3D matrix for isolated preantral follicles, and then discuss the main findings obtained from murine and human ovarian follicles in various *in vivo* studies. Irrespective of the nature of the matrix (biological, synthetic or hybrid), there are other crucial points to consider before selecting one material over another. First of all, we must look at biocompatibility and biodegradability, features that are normally closely interconnected. Greater biocompatibility and biodegradability have been demonstrated with natural polymers (collagen, gelatin, alginate, fibrin, decellularized ECM) than synthetic ones (poly(ethylene glycol) [PEG]) because cell metalloproteinases cleave them without producing toxic compounds that may affect cell survival (24, 25). Indeed, broader application of biological matrices rather than synthetic scaffolds is documented in the literature (26). In addition, natural hydrogels like collagen or fibrin provide better cell adhesion than their synthetic counterparts thanks to the presence of peptides containing arginine-glycine-aspartate (RGD) sequences involved in integrin binding on cell surfaces. The architecture of the hydrogel's structure, as well as its viscoelastic properties and biochemical constitution, are also key elements. The composition and

porosity of the network will determine not only the rate at which nutrients, gas and metabolic waste move through the hydrogel, but also how follicle survival and development are affected. A recent study (27) showed how the controlled microporous geometry of the applied scaffold impacted mouse follicle survival, growth and maturation *in vitro*. The ovarian environment is indeed highly dynamic. Unlike any other cellular complex in the body, human ovarian follicles, once activated, increase in size up to 600X during growth and release various proteases essential to modifying their surrounding ovarian ECM and generating a more acquiescent milieu for their complete development. A hydrogel's viscoelastic properties are therefore key parameters to consider in the choice of matrix material. In this context, the ideal matrix should be rigid enough to mimic the stiffness of the collagen-rich ovarian cortex in the first few days post-transplantation, but then provide enough elasticity to allow complete follicle growth and protease degradation. A more challenging goal is mimicking the native biochemical ovarian environment. A recent study (23) was able to distinguish 1,508 different proteins in the human ovary, with more than 80 of them derived from the ovarian ECM. Although our knowledge of the biochemical composition of ovarian tissue is still in its infancy, complete characterization of the ovarian follicle microenvironment is vital to design a bioengineered ovary ressembling native tissue.

5.1.1. Animal studies

After groundbreaking studies on transplantation of isolated mouse follicles by Gosden's group (11-13), several decades passed before new attempts were made to graft these structures. Laronda et al. (27) developed a gelatin-based matrix using a 3D bioprinter, selecting specific architecture to maximize follicle-matrix interaction. When mouse ovarian follicles were grafted inside this matrix, restoration of fertility was achieved, demonstrating the importance of the architecture of the supporting scaffold for complete follicle development in mice.

Alginate-based matrices showed encouraging results with murine and non-human primate follicles after *in vitro* culture (28), but efficiency was diminished in *in vivo* studies. Vanacker et al. (18, 29) were the first to encapsulate and transplant isolated mouse preantral follicles in alginate. Although these follicles were able to grow to the antral stage, poor matrix degradation and revascularization were noted one week after autotransplantation. Both softer and more rigid alginate remain a good choice for culture of isolated murine (30) and human (31-33) follicles respectively, but new hydrogels are needed for follicle transplantation. In this context, fibrin matrices have found broader application. Unlike the previously mentioned natural matrix materials, this protein has shown numerous advantages. First of all, it was already being applied in diverse surgical settings. Moreover, thanks to the combination of its two main constituents, namely thrombin and fibrinogen, fibrin formulations and architecture could be adjusted according to the desired application (34). Indeed, softer fibrin formulations (made from lower fibrinogen and thrombin concentrations) were found to be optimal for mouse ovarian follicle transplantation (17, 35, 36), also leading to restoration of endocrine and reproductive functions when vascular endothelial growth factor (VEGF) was crosslinked to the matrix and gradually released after transplantation (19).

To date, only one synthetic hydrogel has been tested as a material for the engineered ovary. A combined PEG-vinyl sulfone (PEG-VS) matrix, with integrin-binding peptides

like RGD crosslinking PEG-VS with protease-sensitive peptides, was used to encapsulate partially isolated mouse preantral follicles before transplantation to mice (37). After 30 days, multiple antral follicles, corpora lutea and reduced follicle-stimulating hormone levels were observed, demonstrating that PEG-VS was able to support folliculogenesis and steroidogenesis. Furthermore, on day 60, around 60% of primordial and primary follicles were still detected in the graft, proving selective follicle recruitment over time (37).

An emerging new generation of matrices is now being derived from decellularized ovarian ECM. Ideally, allogeneic (22, 38) or even xenogeneic cell-free matrices retain the natural architecture of native tissue and, to a variable extent, most of the physiological components inside the native ECM. A few studies have reported decellularization of murine (39), porcine (40), bovine (38) and human (22, 38, 41) ovarian tissue. It is important to stress that decellularization protocols have been shown to affect matrix composition differently, changing concentrations of collagen, glycosaminoglycans (GAGs) and elastic fibers (39). When rodent ovarian cells were seeded in such a matrix, they were able to survive, proliferate, synthesize estradiol (38, 40) and even induce puberty in mice after grafting (38). This matrix was also successfully tested in the context of isolated mouse follicle transplantation (22).

5.1.2. Human studies

While fertility restoration using an engineered ovary prototype has already been proved in mice (12, 13, 19, 27), studies in humans have been rather more challenging (14, 20-22, 31). One of the main reasons is the physiological difference in folliculogenesis and the ovaries between rodents and humans. Extrapolating data from murine models to humans is therefore unreliable and disappointing.

To transplant isolated human preantral follicles, plasma clots (14, 15) were replaced by a fibrin matrix, as it was shown to have highly variable composition and fast degradation rates, but it led to follicle loss and irregular results after transplantation. Moreover, due to its very delicate structure, it could potentially be damaged during laparoscopic surgery.

Although softer fibrin formulations have been successfully used to transplant isolated mouse follicles (17, 35), our experience has shown that isolated human follicles require a stiffer fibrin matrix. After xenografting them inside a fibrin matrix containing increased fibrinogen and thrombin concentrations, follicle recovery rates were 20-35% (20, 21), comparable to results of xenografting of human ovarian tissue (42).

As in rodents, decellularized ovarian ECM has also been tested as an alternative to transplant isolated human preantral follicles. However, when a whole ovary or fragments of ovarian tissue are decellularized (38, 41), we obtained a heterogeneous tissue architecture with small and very large pores that were once occupied by different-sized follicles (Fig. 2). For this reason, routine cell seeding protocols to repopulate the matrix (43) cannot be applied. Instead, it is necessary to resort to different strategies that may actually defeat the purpose of one of the best features of decellularized matrices, namely structure. Indeed, when Pors et al. (22) created scalpel-made pockets in decellularized human ovarian ECM to insert isolated human follicles, they did not find any follicles after transplantation to mice. Positive results were achieved only when isolated follicles were embedded in Matrigel before being poured onto the constructs

(22), which demonstrates the need for another material to be used alongside decellularized ovarian ECM. It is, however, important to bear in mind that use of Matrigel, which is not approved in clinical practice, may also have positively influenced these findings.



Figure 2. Decellularized human ovary (41).

Another strategy to take advantage of the biochemical cues of ovarian ECM is its application in the form of decellularized hydrogels. Studies have revealed that these hydrogels can promote *de novo* formation of functional tissue (44), as they retain their biological characteristics and encourage tissue regeneration (45). After the decellularization process, numerous ECM proteins from native tissue can be found in the hydrogel (45), as well as cytokines stored in tissues or cells (46), which may promote tissue growth as they are released into regenerating tissue during hydrogel remodeling (45). We recently developed a decellularized bovine ovarian ECM hydrogel (47), in which ovarian follicles and cells could easily be seeded. Our preliminary results showed that after 10 days of *in vitro* culture, preantral follicles remained viable in the hydrogels (47).

5.2. Ovarian cells and their role in the transplantable engineered ovary

While the main players in the creation of a transplantable engineered ovary are isolated preantral follicles, the co-presence of cells may be fundamental to achieving complete folliculogenesis and improving ovarian regeneration. Indeed, several studies have pointed out that the number and spatial distribution of ovarian cells in an engineered ovary appear to play a key role in follicle development (48-50).

5.2.1. Ovarian stromal cells

Initial studies by Gosden's group (11-13) provided the first evidence of the role of ovarian stromal cells in the transplantable engineered ovary. These cells were needed for ovarian tissue reconstitution and possibly had an impact on follicle development. Indeed, stromal cells can synthesize numerous factors that regulate primordial follicle activation (51). In turn, granulosa cells and oocytes from growing primary follicles will

secrete growth factors to recruit and differentiate cells from the ovarian stromal compartment into theca cells (52, 53) essential for further follicle development.

Autologous stromal cells can be easily isolated from fresh or frozen-thawed ovarian tissue biopsies (54). The safest option is to harvest them from ovarian samples collected after patient disease remission, namely after cancer treatment, so there is no risk of malignant cell contamination of the engineered ovary. However, it is possible that some patients may not have any remaining ovarian tissue to collect these cells. In such cases, stromal cells can be retrieved from tissue samples cryopreserved before chemo- or radiotherapy. Cells can be isolated after follicle pick-up (20, 21), but a purging step is required to avoid any possible malignant cell contamination (55, 56). Soares (57) compared stromal cells collected from fresh ovarian tissue procured from patients after cancer treatment to frozen-thawed ovarian samples. This author did not observe any difference in the cells from the two groups in terms of survival (57). Moreover, isolated ovarian stromal cells can successfully proliferate after transplantation inside different matrices (17, 18, 20, 21, 29, 35, 57-59), and have been shown to contribute to matrix degradation and ECM synthesis (Fig. 3).

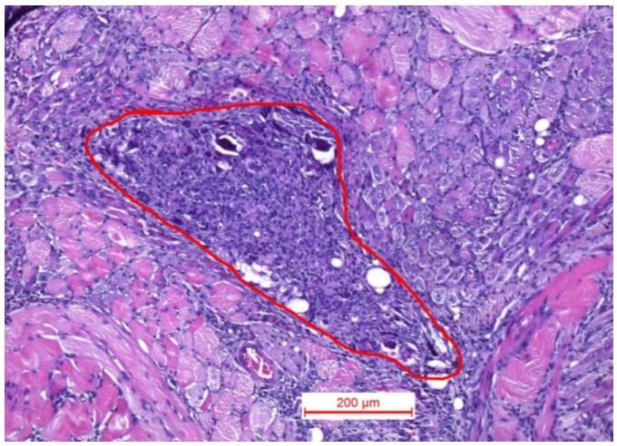


Figure 3. Isolated human ovarian stromal cells after encapsulation in a fibrin matrix (outlined in red) and 7 days of xenotransplantation to immunodeficient mouse.

5.2.2. Ovarian endothelial cells

Our first evidence that endothelial cells isolated from ovarian tissue play a significant role in the engineered ovary came from the study by Dath et al. (59). After comparing grafts containing isolated stromal cells with or without endothelial cells, they observed a large grafted area showing an impressive number of vessels as early as one week after transplantation (59) (Fig. 4). Soares et al. (54) subsequently assessed the influence of endothelial cell concentrations on vessel area and demonstrated a positive correlation between the number of grafted isolated cells and vascularization after 7 days of xenografting to immunodeficient mice (54). As endothelial cell concentrations are quite

low in ovarian cortex, we could consider isolating these cells from the medullary layer, as suggested by Soares et al. (54).

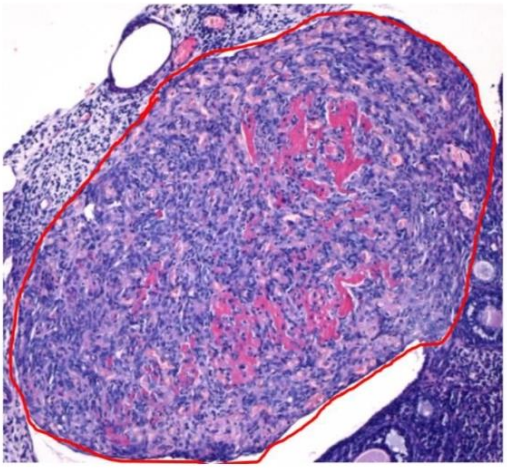


Figure 4. Isolated human ovarian stromal and endothelial cells after encapsulation in plasma clots (outlined in red) and 7 days of xenotransplantation to immunodeficient mouse.

While vascularization in the transplantable engineered ovary can initially be induced by the presence of isolated endothelial cells encapsulated in the matrix, it is important to stress that the number of vessels may also be influenced by growing follicles (60). Indeed, when isolated mouse secondary follicles were transplanted separately from small primordial and primary follicles, the grafts exhibited a greater vessel surface area and more vessels (60), possibly due to expression of angiogenic factors like VEGF by these growing follicles (61).

6. Deconstructing the native human ovary to construct an engineered ovary

6.1. Ovarian matrisome

Ovarian follicles and cells are inherently surrounded by a complex meshwork of proteins forming the ECM, which is destroyed by isolation procedures. Therefore, in order to develop a transplantable bioengineered ovary that offers an environment in which isolated human follicles can survive and grow, it is necessary to provide them with a biomimetic ECM. While numerous attempts by various research teams have demonstrated the feasibility of this concept (17, 18, 29, 34), they also revealed that developing an engineered ovary requires more than simple use of biomaterials and application of tissue engineering strategies. Indeed, an essential requirement for replicating the complexity of a functional ovary is a comprehensive understanding of the composition, architecture and plasticity of the human ovarian ECM, something we do not

yet have. Thus, deconstructing the microenvironment of ovarian cells and follicles is a prerequisite to constructing a bioinspired engineered ovary.

Proteomics is a powerful tool that can be used to scrutinize the composition of the ovarian ECM without a priori knowledge, in contrast to targeted studies using specific antibodies (62). Very recently, proteomics was used to characterize the composition of human ovarian tissue in reproductive-age subjects and develop the first draft map of the human ovarian matrisome (23). The matrisome is essentially an extended description of the ECM (63), including not only all structural ECM components, but also proteins able to regulate and remodel the ECM. It can be categorized as follows:

- Core matrisome proteins:
    - ECM glycoproteins
    - Collagens
    - Proteoglycans
- ECM-associated proteins:
    - ECM-affiliated proteins, namely proteins showing biochemical and architectural analogy with ECM proteins or known to be associated
    - ECM regulators, namely proteins responsible for ECM turnover
    - Secreted factors, namely secreted proteins interacting with core ECM proteins.

Ouni et al.'s study shows the human ovarian matrisome to be composed of: 49% collagen, 7% proteoglycans, 15% glycoproteins, 18% ECM-affiliated proteins, 10% ECM regulators and 1% secreted factors (23). Indeed, around 100 proteins make up the ovarian matrisome, so the task of developing a bioinspired engineered matrix is quite challenging. Selection criteria need to focus on key proteins whose presence is absolutely required in the engineered ovary. Only comparative studies between different age groups can elucidate specific features of the reproductive-age ovary that make it more inclined to follicle survival and development than its younger and older counterparts.

Understanding the composition of the ovarian matrisome is not enough to be able to construct a biomimetic ovary. It is also crucial to bear in mind that ovarian follicles are exceptional in that they can grow to around 600X their size during folliculogenesis (for instance, human follicles grow from 30 μm at the primordial stage to 18–24 mm when they are ready to ovulate). It is therefore important to explore the intrinsic elasticity of the human ovary. In contrast to proteomics, very few studies have investigated the elasticity of human ovarian tissue (64, 65). However, only recently, Ouni et al. (unpublished results) revealed the true elastic system components that confer intrinsic mechanical features to biological tissues, including collagen, known as the provider of tensile strength to tissue. On the other hand, elastin, elastin microfibril interface-located protein 1 (EMILIN-1), fibrillin-1 and GAGs are known to temper the rigidity of collagen by providing recoil and elasticity. This study revealed some interesting spatiotemporal changes to elastic ECM deposition and turnover, dictating the mechanical features of the human ovary in the course of a woman's lifetime. This is consistent with the emerging hypothesis related to the mechanobiology of the human ovary and dynamic reciprocity that exists between ovarian cells and their microenvironment (66-68).

Ouni et al.'s study also shed light on follicle-specific ECM composition, dependent on follicle stage and age. These data will prove very useful in developing the bioengineered ovary. Indeed, they emphasize the importance of encapsulating each type of isolated follicle in an appropriate biomaterial that must replicate the corresponding functional perifollicular ECM and respect ovarian tissue heterogeneity (69) to guarantee its biomimicry.

Another facet of the ovarian matrisome that needs to be investigated is its microarchitecture and ultrastructure. Indeed, it is essential to respect native tissue porosity and fiber organization because they are involved in nutrient and oxygen transport (70). Moreover, fibrous matrisome proteins provide cells with external stimuli and instructive cues to influence gene expression, cell behavior and morphology, as evidenced by emerging publications on this subject (71-73). Proof of the involvement of matrisome ultrastructure in dictating cell phenotype is how collagen alignment has been used as a prognostic signature for survival in human breast carcinoma (74). However, in the context of the ovary, these data are still lacking. Novel analytical techniques must therefore be applied to conduct in-depth studies of the ovarian microarchitecture and produce a map of the ultrastructural features of reproductive-age tissue and follicle stage niche.

Increasing evidence today points to different roles of the matrisome, particularly the ovarian matrisome, beyond its apparent primary function of physical support. Knowing that biodegradable matrices cannot replicate the complexity of a given microenvironment, decellularization has emerged as the ultimate means of creating more efficient biomimetic scaffolds (75). However, it is worth mentioning that decellularization methods rely on use of harsh physical, enzymatic and chemical procedures (for example, sodium dodecyl sulfate) (22, 76) that can deplete the decellularized scaffold and erase key matrisome elements. Therefore, without comparing the properties of such matrices against a reference of the native human ovarian matrisome, it is impossible to monitor their reliability to reproduce the ovarian cell microenvironment.

In contrast to most tissue engineering strategies relying on the presence of generic ECM components (collagen, fibrin, laminin, etc.) as indicators of the success of their biomimetic constructs, deconstructing the natural human ovary seeks to map the ovarian matrisome with its multiple facets. The aim is to build a reliable reference of its unique features, which will serve as a roadmap for developing a more closely biomimetic matrix tailored to human ovarian cells and follicles, and applicable in the field of fertility preservation.

6.2. Subpopulations of ovarian cells

While it is known that human ovaries contain a vast majority of stromal cells, followed by endothelial cells (77), it was only recently that in-depth characterization of cell populations was undertaken in human ovarian tissue (78, 79). In their study analyzing the ovarian cortical layer, Wagner et al. (78) not only identified other subpopulations of cells, but also reported their proportions; stromal, endothelial and perivascular cells correspond to around 83%, 5% and 10% of cells in the ovarian cortex respectively, while macrophages and T-cells account for around 0.5%. These findings are extremely important for development of an engineered ovary. For instance, macrophages play a role in matrix remodeling and synthesize growth factors and cytokines (80). Moreover,

M1 macrophages appear to be implicated in folliculogenesis in mouse ovaries (81), while M2 macrophages are involved in tissue repair through synthesis of anti-inflammatory cytokines, such as VEGF and transforming growth factor beta (82). Interestingly, these authors did not find a population of germline stem cells, which was a rather contentious finding by Tilly's group (83, 84). Analysis of the inner cortical layer of human ovaries revealed clusters of stromal, endothelial, theca, immune, smooth muscle and granulosa cells (79). Most importantly, Fan et al. (79) reported several types of these cells.

As these cell populations are essential to folliculogenesis, ECM synthesis, tissue remodeling, vascularization and other such processes, it is vital to ensure that they are present in the transplantable engineered ovary. Information generated by such studies is also crucial to evaluating the constructs after transplantation and understanding our findings.

6.2.1. Theca cells

Theca cells have been poorly investigated compared to granulosa cells and oocytes, but their role in folliculogenesis is undeniable. Indeed, if they were not included in engineered ovaries, follicles could not develop beyond the secondary stage and, consequently, ovarian function and fertility would never be restored.

Theca cells start to appear at the later stage of secondary follicles and form a layer around granulosa-oocyte structures (85). They play an indispensable role in folliculogenesis by providing structural support for follicles, and androstenedione as a substrate for granulosa cells to convert to estradiol (86-88). Besides such key tasks for theca cells, we have limited knowledge about their recruitment, growth and differentiation due to a lack of information concerning their origin (53, 89). A few studies using murine models have shown the presence of a subpopulation of ovarian cells, called theca progenitor stem cells, that are recruited to differentiate into theca cells under the influence of factors secreted by oocytes and granulosa cells (53, 89). Honda et al. (53) studied neonatal mouse ovaries and reported that theca progenitor stem cells express GLI family zinc finger 3 (GLI3) and protein patched homolog 1 (Ptch1) as markers, and can differentiate into theca cells in the presence of factors issuing from oocytes and granulosa cells. After differentiation, these cells express luteinizing hormone receptor (LHR), GLI2 and Ptch2. Liu et al. (89) found that there are two origins of theca progenitor cells in embryonic mouse gonads: (i) Wilm's tumor 1-positive mesenchymal cells intrinsic to the ovary, which differentiate into theca cells after birth, giving rise to theca fibroblasts, perivascular smooth muscle cells and interstitial ovarian cells; and (ii) GLI1-positive cells, which migrate from the mesonephros to the ovary and become steroidogenic androgen-producing cells inside the ovary. In large animal models, like cows (52) and goats (90), ovarian cortical stromal cells can differentiate into theca cells in the presence of granulosa cells by expressing cytochrome P450 17A1 (CYP17A1) and LHR as markers, as well as and androstenedione (52, 91), but there are no studies confirming the presence of a subpopulation of theca precursor cells in human ovaries. However, Fan et al. (79) detected a theca cell population in human ovaries that they termed common progenitor theca cells, which progress to theca interna or externa cells, but these findings still need to be confirmed. Moreover, these cells were found surrounding small antral follicles, in the inner cortical layer, while recruitment and differentiation of theca cells take place during the early primary/secondary stage of

follicle development. One may therefore wonder if these cells surround follicles right from the start or are spread throughout the ovarian cortex.

In a study using isolated bovine cortical stromal cells, Orisaka et al. (52) reported that cells can differentiate into theca cells under stimuli provided by granulosa cells *in vitro*, as evidenced by the steroidogenic markers they assessed. Subsequent to these intriguing results, Asiabi et al. (unpublished data) isolated stromal cells from the cortical layer of postmenopausal ovaries and *in vitro*-cultured them using a medium supplemented with growth factors presumed to be involved in theca cell differentiation. After 8 days of *in vitro* culture, up to 43% of cells differentiated into theca interna cells. Moreover, a modest proportion of small luteal cells was also identified. These findings indicate the presence of theca precursor cells spread throughout the cortical layer, which remain in the human ovary throughout its lifetime. *In vivo*, factors used by Asiabi et al. (unpublished data) are synthesized by granulosa cells and oocytes from growing follicles. We can therefore hypothesize that once isolated follicles and ovarian cells are transplanted along with the 3D matrix, these follicles can induce recruitment and differentiation of theca cells.

7. Conclusions

Pioneering studies into murine and human follicles (11-15) have demonstrated the feasibility of grafting isolated follicles, but recent findings indicate that this approach can be improved through utilization of a transplantable engineered ovary. Over the last years, we have shown that human preantral follicles can be safely isolated in large numbers by adapting the isolation protocol according to ovarian tissue type (16, 21, 92, 93). We have also learned that in order to restore ovarian function and fertility, ovarian cells need to be incorporated into the engineered ovary. Indeed, we witnessed their impact on the formation of ovary-like tissue, with vascularization and synthesis of the ECM (21, 35, 54, 59, 60). Under the influence of growing follicles, a subpopulation of these cells can be recruited to differentiate into theca cells (Asiabi et al., unpublished data). Taking advantage of insights acquired from single-cell analysis of human ovarian cortex (78, 79), we know it is possible to enrich the engineered ovary with specific subpopulations of ovarian cells to enhance tissue remodeling, or release growth factors that can positively affect folliculogenesis or synthesis of elastic proteins, for instance. Regarding the 3D matrix to be used to encapsulate and transplant isolated follicles and cells, numerous biomaterials have been tested (11, 14, 27, 28, 34, 36, 37). While they offer good mechanical support for follicles, they do not possess the biomechanical and biochemical cues normally present in the ovarian ECM. In recent years, investigations have shed new light on the composition and structure of human ovaries (23, 65), showing that the complexity of the ovarian ECM is impossible to replicate with a polymer. On the other hand, we may get closer to our goal with the use of decellularized ovarian matrices (22, 38-41, 43, 47). However, studies are still in their infancy and it is not yet possible to determine if this type of structure will be the matrix of choice for the engineered ovary.

Definitions

- Decellularization: a procedure first developed by Prof Stephen F. Badylak, where cells from a given tissue or organ are destroyed and removed, leaving only the

extracellular matrix scaffold. The purpose of this procedure is to create matrices to be used in tissue engineering and regenerative medicine approaches.

- Folliculogenesis: a process describing the activation and growth of ovarian primordial follicles up to preovulatory stage.
- Tissue engineering: an interdisciplinary field that uses the combination of cells, materials, biochemical and physicochemical factors and engineering with the goal of replacing, repairing, or improve tissues and organs in the body.

Take home messages

- Human preantral follicles can be safely isolated in large numbers.
- Survival and development of isolated ovarian preantral follicles is feasible.
- Ovarian cells have an important role in transplantable engineered ovary, as they aid in the scaffold degradation, synthesis of extracellular matrix and vascularization.
- A subpopulation of ovarian cells is able to differentiate into theca cells, which are essential for follicle development.
- Current biomaterials used to transplant isolated follicles and cells do not possess the biomechanical and biochemical cues normally present in the ovarian ECM.
- New studies have start revealing the complexity of the ovarian ECM in terms of composition and microarchitecture, which are crucial for the development of a 3D matrix for the transplantable engineered ovary.

10. Key readings

Papers underlined in the reference list are key readings in this topic.

References

1. Observatory GC. Cancer Today: International Agency for Research on Cancer 2019 [updated March, 2019; cited 2020 February 3]. Available from: http://gco.iarc.fr/today/online-analysis-table?v=2018&mode=cancer&mode_population=continents&population=900&populations=900&key=asr&sex=0&cancer=39&type=0&statistic=5&prevalence=0&population_group=0&ages_group%5B%5D=0&ages_group%5B%5D=8&nb_items=5&group_cancer=1&include_nmsc=1&include_nmsc_other=1.
2. Siegel RL, Miller KD, Jemal A. Cancer statistics, 2018. CA Cancer J Clin. 2018;68(1):7-30.
3. Donnez J, Dolmans MM. Fertility Preservation in Women. N Engl J Med. 2017;377(17):1657-65.
4. Dolmans MM, Masciangelo R. Risk of transplanting malignant cells in cryopreserved ovarian tissue. Minerva Ginecol. 2018;70(4):436-43.
5. Sonmezer M, Oktay K. Fertility preservation in female patients. Hum Reprod Update. 2004;10(3):251-66.

6. Orphanet. Burkitt lymphoma 2010 [updated February 2010; cited 2020 February 3]. Available from: https://www.orpha.net/consor/cgi-bin/Disease_Search.php?lng=EN&data_id=3747&Disease_Disease_Search_diseaseGroup=Burkitt-lymphoma&Disease_Disease_Search_diseaseType=Pat&Disease(s)/group%20of%20diseases=Burkitt-lymphoma&title=Burkitt%20lymphoma&search=Disease_Search_Simple.
7. Orphanet. Neuroblastoma 2009 [updated March 2009; cited 2020 February 3]. Available from: https://www.orpha.net/consor/cgi-bin/Disease_Search.php?lng=EN&data_id=548&Disease_Disease_Search_diseaseGroup=Neuroblastoma&Disease_Disease_Search_diseaseType=Pat&Disease(s)/group%20of%20diseases=Neuroblastoma&title=Neuroblastoma&search=Disease_Search_Simple.
8. Dolmans MM, Marinescu C, Saussoy P, Van Langendonckt A, Amorim C, Donnez J. Reimplantation of cryopreserved ovarian tissue from patients with acute lymphoblastic leukemia is potentially unsafe. Blood. 2010;116(16):2908-14.
9. Rodgers RJ, Irving-Rodgers HF, Russell DL. Extracellular matrix of the developing ovarian follicle. Reproduction. 2003;126(4):415-24.
10. Torrance C, Telfer E, Gosden RG. Quantitative study of the development of isolated mouse pre-antral follicles in collagen gel culture. J Reprod Fertil. 1989;87(1):367-74.
11. Telfer E, Torrance C, Gosden RG. Morphological study of cultured preantral ovarian follicles of mice after transplantation under the kidney capsule. J Reprod Fertil. 1990;89(2):565-71.
12. Gosden RG. Restitution of fertility in sterilized mice by transferring primordial ovarian follicles. Hum Reprod. 1990;5(5):499-504.
13. Carroll J, Gosden RG. Transplantation of frozen-thawed mouse primordial follicles. Hum Reprod. 1993;8(8):1163-7.
14. Dolmans MM, Martinez-Madrid B, Gadisseux E, Guiot Y, Yuan WY, Torre A, et al. Short-term transplantation of isolated human ovarian follicles and cortical tissue into nude mice. Reproduction. 2007;134(2):253-62.
15. Dolmans MM, Yuan WY, Camboni A, Torre A, Van Langendonckt A, Martinez-Madrid B, et al. Development of antral follicles after xenografting of isolated small human preantral follicles. Reprod Biomed Online. 2008;16(5):705-11.
16. Soares M, Saussoy P, Sahrari K, Amorim CA, Donnez J, Dolmans MM. Is transplantation of a few leukemic cells inside an artificial ovary able to induce leukemia in an experimental model? J Assist Reprod Genet. 2015;32(4):597-606.
17. Luyckx V, Dolmans MM, Vanacker J, Legat C, Fortuno Moya C, Donnez J, et al. A new step toward the artificial ovary: survival and proliferation of isolated murine follicles after autologous transplantation in a fibrin scaffold. Fertil Steril. 2014;101(4):1149-56.
18. Vanacker J, Dolmans MM, Luyckx V, Donnez J, Amorim CA. First transplantation of isolated murine follicles in alginate. Regen Med. 2014;9(5):609-19.
19. Kniazeva E, Hardy AN, Boukaidi SA, Woodruff TK, Jeruss JS, Shea LD. Primordial Follicle Transplantation within Designer Biomaterial Grafts Produce Live Births in a Mouse Infertility Model. Sci Rep. 2015;5:17709.
20. Paulini F, Vilela JM, Chiti MC, Donnez J, Jadoul P, Dolmans MM, et al. Survival and growth of human preantral follicles after cryopreservation of ovarian tissue,

follicle isolation and short-term xenografting. Reprod Biomed Online. 2016;33(3):425-32.
21. Chiti MC, Dolmans MM, Hobeika M, Cernogoraz A, Donnez J, Amorim CA. A modified and tailored human follicle isolation procedure improves follicle recovery and survival. J Ovarian Res. 2017;10(1):71.
22. Pors SE, Ramlose M, Nikiforov D, Lundsgaard K, Cheng J, Andersen CY, et al. Initial steps in reconstruction of the human ovary: survival of pre-antral stage follicles in a decellularized human ovarian scaffold. Hum Reprod. 2019;34(8):1523-35.
23. Ouni E, Vertommen D, Chiti MC, Dolmans MM, Amorim CA. A Draft Map of the Human Ovarian Proteome for Tissue Engineering and Clinical Applications. Mol Cell Proteomics. 2019;18(Suppl 1):S159-S73.
24. Yoon DM, Fisher JP. Natural and synthetic polymeric scaffolds. In: Narayan R, editor. Biomedical Materials. Berlin, Germany: Springer; 2009. p. 415-42.
25. Caliari SR, Burdick JA. A practical guide to hydrogels for cell culture. Nat Methods. 2016;13(5):405-14.
26. Amorim CA, Shikanov A. The artificial ovary: current status and future perspectives. Future Oncol. 2016;12(20):2323-32.
27. Laronda MM, Rutz AL, Xiao S, Whelan KA, Duncan FE, Roth EW, et al. A bioprosthetic ovary created using 3D printed microporous scaffolds restores ovarian function in sterilized mice. Nat Commun. 2017;8:15261.
28. Vanacker J, Amorim CA. Alginate: A Versatile Biomaterial to Encapsulate Isolated Ovarian Follicles. Ann Biomed Eng. 2017;45(7):1633-49.
29. Vanacker J, Luyckx V, Dolmans MM, Des Rieux A, Jaeger J, Van Langendonckt A, et al. Transplantation of an alginate-matrigel matrix containing isolated ovarian cells: first step in developing a biodegradable scaffold to transplant isolated preantral follicles and ovarian cells. Biomaterials. 2012;33(26):6079-85.
30. Filatov MA, Khramova YV, Semenova ML. In Vitro Mouse Ovarian Follicle Growth and Maturation in Alginate Hydrogel: Current State of the Art. Acta Naturae. 2015;7(2):48-56.
31. Amorim CA, Van Langendonckt A, David A, Dolmans MM, Donnez J. Survival of human pre-antral follicles after cryopreservation of ovarian tissue, follicular isolation and in vitro culture in a calcium alginate matrix. Hum Reprod. 2009;24(1):92-9.
32. Camboni A, Van Langendonckt A, Donnez J, Vanacker J, Dolmans MM, Amorim CA. Alginate beads as a tool to handle, cryopreserve and culture isolated human primordial/primary follicles. Cryobiology. 2013;67(1):64-9.
33. Vanacker J, Luyckx V, Amorim C, Dolmans MM, Van Langendonckt A, Donnez J, et al. Should we isolate human preantral follicles before or after cryopreservation of ovarian tissue? Fertil Steril. 2013;99(5):1363-8 e2.
34. Chiti MC, Dolmans MM, Donnez J, Amorim CA. Fibrin in Reproductive Tissue Engineering: A Review on Its Application as a Biomaterial for Fertility Preservation. Ann Biomed Eng. 2017;45(7):1650-63.
35. Chiti MC, Dolmans MM, Orellana R, Soares M, Paulini F, Donnez J, et al. Influence of follicle stage on artificial ovary outcome using fibrin as a matrix. Hum Reprod. 2016;31(2):427-35.
36. Smith RM, Shikanov A, Kniazeva E, Ramadurai D, Woodruff TK, Shea LD. Fibrin-mediated delivery of an ovarian follicle pool in a mouse model of infertility. Tissue Eng Part A. 2014;20(21-22):3021-30.

37. Kim J, Perez AS, Claflin J, David A, Zhou H, Shikanov A. Synthetic hydrogel supports the function and regeneration of artificial ovarian tissue in mice. NPJ Regen Med. 2016;1.
38. Laronda MM, Jakus AE, Whelan KA, Wertheim JA, Shah RN, Woodruff TK. Initiation of puberty in mice following decellularized ovary transplant. Biomaterials. 2015;50:20-9.
39. Alshaikh AB, Padma AM, Dehlin M, Akouri R, Song MJ, Brannstrom M, et al. Decellularization of the mouse ovary: comparison of different scaffold generation protocols for future ovarian bioengineering. J Ovarian Res. 2019;12(1):58.
40. Liu WY, Lin SG, Zhuo RY, Xie YY, Pan W, Lin XF, et al. Xenogeneic Decellularized Scaffold: A Novel Platform for Ovary Regeneration. Tissue Eng Part C Methods. 2017;23(2):61-71.
41. Hassanpour A, Talaei-Khozani T, Kargar-Abarghouei E, Razban V, Vojdani Z. Decellularized human ovarian scaffold based on a sodium lauryl ester sulfate (SLES)-treated protocol, as a natural three-dimensional scaffold for construction of bioengineered ovaries. Stem Cell Res Ther. 2018;9(1):252.
42. Nisolle M, Casanas-Roux F, Marbaix E, Jadoul P, Donnez J. Transplantation of cultured explants of human endometrium into nude mice. Hum Reprod. 2000;15(3):572-7.
43. Mirzaeian L, Eivazkhani F, Hezavehei M, Moini A, Esfandiari F, Valojerdi MR, et al. Optimizing The Cell Seeding Protocol to Human Decellularized Ovarian Scaffold: Application of Dynamic System for Bio-Engineering. Cell J. 2020;22(2):227-35.
44. Badylak SF, Brown BN, Gilbert TW, Daly KA, Huber A, Turner NJ. Biologic scaffolds for constructive tissue remodeling. Biomaterials. 2011;32(1):316-9.
45. Hoganson DM, Owens GE, O'Doherty EM, Bowley CM, Goldman SM, Harilal DO, et al. Preserved extracellular matrix components and retained biological activity in decellularized porcine mesothelium. Biomaterials. 2010;31(27):6934-40.
46. Voytik-Harbin SL, Brightman AO, Kraine MR, Waisner B, Badylak SF. Identification of extractable growth factors from small intestinal submucosa. J Cell Biochem. 1997;67(4):478-91.
47. Chiti MC, Viswanath A, Vanacker J, Germain L, White LJ, Dolmans MM, et al., editors. Hydrogel from bovine decellularized ovarian extracellular matrix supports mouse follicle survival in vitro. 10th World Biomaterials Congress; 2016 17-22 May 2016; Montréal, Canada: Frontiers.
48. Da Silva-Buttkus P, Marcelli G, Franks S, Stark J, Hardy K. Inferring biological mechanisms from spatial analysis: prediction of a local inhibitor in the ovary. Proc Natl Acad Sci U S A. 2009;106(2):456-61.
49. Hornick JE, Duncan FE, Shea LD, Woodruff TK. Multiple follicle culture supports primary follicle growth through paracrine-acting signals. Reproduction. 2013;145(1):19-32.
50. Gaytan F, Morales C, Leon S, Garcia-Galiano D, Roa J, Tena-Sempere M. Crowding and Follicular Fate: Spatial Determinants of Follicular Reserve and Activation of Follicular Growth in the Mammalian Ovary. PLoS One. 2015;10(12):e0144099.
51. Knight PG, Glister C. TGF-beta superfamily members and ovarian follicle development. Reproduction. 2006;132(2):191-206.
52. Orisaka M, Tajima K, Mizutani T, Miyamoto K, Tsang BK, Fukuda S, et al. Granulosa cells promote differentiation of cortical stromal cells into theca cells in the bovine ovary. Biol Reprod. 2006;75(5):734-40.

53. Honda A, Hirose M, Hara K, Matoba S, Inoue K, Miki H, et al. Isolation, characterization, and in vitro and in vivo differentiation of putative thecal stem cells. Proc Natl Acad Sci U S A. 2007;104(30):12389-94.
54. Soares M, Sahrari K, Chiti MC, Amorim CA, Ambroise J, Donnez J, et al. The best source of isolated stromal cells for the artificial ovary: medulla or cortex, cryopreserved or fresh? Hum Reprod. 2015;30(7):1589-98.
55. Schroder CP, Timmer-Bosscha H, Wijchman JG, de Leij LF, Hollema H, Heineman MJ, et al. An in vitro model for purging of tumour cells from ovarian tissue. Hum Reprod. 2004;19(5):1069-75.
56. Mouloungui E, Zver T, Roux C, Amiot C. A protocol to isolate and qualify purified human preantral follicles in cases of acute leukemia, for future clinical applications. J Ovarian Res. 2018;11(1):4.
57. Soares M. Fertility preservation and leukemia: cellular components of the artificial ovary and disease retransmission through the graft. Brussels: Université Catholique de Louvain; 2015.
58. Luyckx V, Dolmans MM, Vanacker J, Scalercio SR, Donnez J, Amorim CA. First step in developing a 3D biodegradable fibrin scaffold for an artificial ovary. J Ovarian Res. 2013;6(1):83.
59. Dath C, Dethy A, Van Langendonckt A, Van Eyck AS, Amorim CA, Luyckx V, et al. Endothelial cells are essential for ovarian stromal tissue restructuring after xenotransplantation of isolated ovarian stromal cells. Hum Reprod. 2011;26(6):1431-9.
60. Chiti MC, Dolmans MM, Lucci CM, Paulini F, Donnez J, Amorim CA. Further insights into the impact of mouse follicle stage on graft outcome in an artificial ovary environment. Mol Hum Reprod. 2017;23(6):381-92.
61. Kaczmarek MM, Schams D, Ziecik AJ. Role of vascular endothelial growth factor in ovarian physiology - an overview. Reprod Biol. 2005;5(2):111-36.
62. Ouni E, Vertommen D, Amorim CA. The Human Ovary and Future of Fertility Assessment in the Post-Genome Era. Int J Mol Sci. 2019;20(17).
63. Naba A, Clauser KR, Ding H, Whittaker CA, Carr SA, Hynes RO. The extracellular matrix: Tools and insights for the "omics" era. Matrix Biol. 2016;49:10-24.
64. Wood CD, Vijayvergia M, Miller FH, Carroll T, Fasanati C, Shea LD, et al. Multi-modal magnetic resonance elastography for noninvasive assessment of ovarian tissue rigidity in vivo. Acta Biomater. 2015;13:295-300.
65. Chiti MC, Dolmans MM, Mortiaux L, Zhuge F, Ouni E, Shahri PAK, et al. A novel fibrin-based artificial ovary prototype resembling human ovarian tissue in terms of architecture and rigidity. J Assist Reprod Genet. 2018;35(1):41-8.
66. Woodruff TK, Shea LD. A new hypothesis regarding ovarian follicle development: ovarian rigidity as a regulator of selection and health. J Assist Reprod Genet. 2011;28(1):3-6.
67. Kawamura K, Cheng Y, Suzuki N, Deguchi M, Sato Y, Takae S, et al. Hippo signaling disruption and Akt stimulation of ovarian follicles for infertility treatment. Proc Natl Acad Sci U S A. 2013;110(43):17474-9.
68. Thorne JT, Segal TR, Chang S, Jorge S, Segars JH, Leppert PC. Dynamic reciprocity between cells and their microenvironment in reproduction. Biol Reprod. 2015;92(1):25.
69. Choi JK, Agarwal P, Huang H, Zhao S, He X. The crucial role of mechanical heterogeneity in regulating follicle development and ovulation with engineered ovarian microtissue. Biomaterials. 2014;35(19):5122-8.

70. Kelleher CM, Vacanti JP. Engineering extracellular matrix through nanotechnology. J R Soc Interface. 2010;7 Suppl 6:S717-29.
71. Janson IA, Putnam AJ. Extracellular matrix elasticity and topography: material-based cues that affect cell function via conserved mechanisms. J Biomed Mater Res A. 2015;103(3):1246-58.
72. Alkmin S, Brodziski R, Simon H, Hinton D, Goldsmith RH, Patankar M, et al. Migration dynamics of ovarian epithelial cells on micro-fabricated image-based models of normal and malignant stroma. Acta Biomater. 2019;100:92-104.
73. Li Y, Xiao Z, Zhou Y, Zheng S, An Y, Huang W, et al. Controlling the Multiscale Network Structure of Fibers To Stimulate Wound Matrix Rebuilding by Fibroblast Differentiation. ACS Appl Mater Interfaces. 2019;11(31):28377-86.
74. Conklin MW, Eickhoff JC, Riching KM, Pehlke CA, Eliceiri KW, Provenzano PP, et al. Aligned collagen is a prognostic signature for survival in human breast carcinoma. Am J Pathol. 2011;178(3):1221-32.
75. Crapo PM, Gilbert TW, Badylak SF. An overview of tissue and whole organ decellularization processes. Biomaterials. 2011;32(12):3233-43.
76. White LJ, Taylor AJ, Faulk DM, Keane TJ, Saldin LT, Reing JE, et al. The impact of detergents on the tissue decellularization process: A ToF-SIMS study. Acta Biomater. 2017;50:207-19.
77. Asiabi P, Chiti MC, Amorim CA. Isolation and characterization of the human ovarian cell population for transplantation into an artificial ovary. Anim Reprod. 2019;16(1):39-44.
78. Wagner M, Yoshihara M, Douagi I, Damdimopoulos A, Panula S, Petropoulos S, et al. Single cell map of the human ovarian cortex. 2019:791343.
79. Fan X, Bialecka M, Moustakas I, Lam E, Torrens-Juaneda V, Borggreven NV, et al. Single-cell reconstruction of follicular remodeling in the human adult ovary. Nat Commun. 2019;10(1):3164.
80. Wu R, Van der Hoek KH, Ryan NK, Norman RJ, Robker RL. Macrophage contributions to ovarian function. Hum Reprod Update. 2004;10(2):119-33.
81. Ono Y, Nagai M, Yoshino O, Koga K, Nawaz A, Hatta H, et al. CD11c+ M1-like macrophages (MPhis) but not CD206+ M2-like MPhi are involved in folliculogenesis in mice ovary. Sci Rep. 2018;8(1):8171.
82. Sica A, Erreni M, Allavena P, Porta C. Macrophage polarization in pathology. Cell Mol Life Sci. 2015;72(21):4111-26.
83. Martin JJ, Woods DC, Tilly JL. Implications and Current Limitations of Oogenesis from Female Germline or Oogonial Stem Cells in Adult Mammalian Ovaries. Cells. 2019;8(2).
84. Woods DC, Tilly JL. Isolation, characterization and propagation of mitotically active germ cells from adult mouse and human ovaries. Nat Protoc. 2013;8(5):966-88.
85. Young JM, McNeilly AS. Theca: the forgotten cell of the ovarian follicle. Reproduction. 2010;140(4):489-504.
86. Edson MA, Nagaraja AK, Matzuk MM. The mammalian ovary from genesis to revelation. Endocr Rev. 2009;30(6):624-712.
87. Hirshfield AN. Development of follicles in the mammalian ovary. Int Rev Cytol. 1991;124:43-101.
88. Nilsson E, Skinner MK. Cellular interactions that control primordial follicle development and folliculogenesis. J Soc Gynecol Investig. 2001;8(1 Suppl Proceedings):S17-20.

89. Liu C, Peng J, Matzuk MM, Yao HH. Lineage specification of ovarian theca cells requires multicellular interactions via oocyte and granulosa cells. Nat Commun. 2015;6:6934.
90. Qiu M, Quan F, Han C, Wu B, Liu J, Yang Z, et al. Effects of granulosa cells on steroidogenesis, proliferation and apoptosis of stromal cells and theca cells derived from the goat ovary. J Steroid Biochem Mol Biol. 2013;138:325-33.
91. Vitt UA, McGee EA, Hayashi M, Hsueh AJ. In vivo treatment with GDF-9 stimulates primordial and primary follicle progression and theca cell marker CYP17 in ovaries of immature rats. Endocrinology. 2000;141(10):3814-20.
92. Soares M, Sahrari K, Amorim CA, Saussoy P, Donnez J, Dolmans MM. Evaluation of a human ovarian follicle isolation technique to obtain disease-free follicle suspensions before safely grafting to cancer patients. Fertil Steril. 2015;104(3):672-80 e2.
93. Soares M, Saussoy P, Maskens M, Reul H, Amorim CA, Donnez J, et al. Eliminating malignant cells from cryopreserved ovarian tissue is possible in leukaemia patients. Br J Haematol. 2017;178(2):231-9.